Characterizing the specificity of T follicular helper cell repertoire in human peripheral blood and tonsil samples



Elena Brenna

St Anne's College

University of Oxford

A thesis submitted for the degree of

Doctor of Philosophy

Trinity 2018

Table of Contents

List of Figures **5**

Abbreviations **8**

Abstract **12**

1 Introduction **13**

1.1 The immune system: general overview 13
1.1.1 The innate immune system 13
1.1.2 The adaptive immune system 14
1.2 Secondary lymphoid organs 15
1.3 T cell development and T cell receptor generation 17
1.3.1 T cell development 18
1.3.2 The T cell receptor (TCR) 21
1.4 Activation and heterogeneity of $CD4^+$ T cells 25
1.4.1 $CD4^+$ T cell heterogeneity and plasticity 27
1.4.2 $CD4^+$ T cell memory 32
1.5 T follicular helper cells and differentiation 34
1.6 Germinal centre formation 39
1.7 Immunological synapses between T and B cells 43
1.8 Circulating and memory Tfh cells 46
1.8.1 Circulating Tfh cells 46
1.8.2 Memory Tfh cells 47
1.8.3 Circulating Tfh cell function and relationship with lymphoid organs 49
1.9 T cell response to Influenza virus 55
1.10 Research questions and objectives 57

2 Materials and methods **61**

2.1 Cohorts and ethics 61
2.2 Media preparation 62
2.3 Peripheral blood and tonsil tissues processing 63
2.3.1 PBMC separation 63
2.3.2 Mononuclear cells from tonsil (MNC-T) separation 64
2.3.3 Preparation of feeder cells 66
2.4 Flow cytometry analysis and sorting strategy 67
2.5 Peptide pools, matrices and antigen screening 70
2.6 Repertoire analysis 73
2.6.1 T cell library technique 73
2.6.2 T cell receptor Vβ repertoire staining 74
2.7 Cytokine detection and phenotype analysis 75
2.8 Antigen-specific T cell clone technique 77
2.9 Human Leukocyte Antigen (HLA) type and restriction 79

2.9.1 HLA type on DNA extraction 79
2.9.2 Determination of HLA restriction of T cell clones 80
2.10 T cell receptor sequencing 81
2.10.1 Clonotyping of antigen-specific $CD4^+$ T cell clones 81
2.10.2 Deep T cell receptor sequencing of bulk $CD4^+$ T cell populations 84
2.11 T and B cell co-culture 86
2.12 Synaptic transfer on silica bead lipid bilayer 87
2.13 Enzyme-Linked Immunosorbent Assay 89
2.14 Statistical analysis 91

3 Results I: phenotypic profile of T follicular helper cell populations in peripheral blood and tonsils 93

3.1 Background and rationale 93
3.2 Surface marker, transcription factor and cytokine production profile of Tfh cells from blood and tonsils 95
3.3 Evaluation of the utility of the library method for repertoire analysis of circulating Tfh cell populations 105
3.4 Media optimisation for tonsil cell culture and cytokine receptors profiling of tonsil and blood cells during expansion 108
3.5 Conclusions 117

4 Results II: comparison of T cell receptor repertoire in circulating and tonsillar Tfh and non-Tfh cells 121

4.1 Background and rational 121
4.2 T cell receptor Vβ profile by flow cytometry 124
4.3 Comparison of T cell receptor sequences repertoire between circulating and tonsillar Tfh cells 127
4.4 Comparison of T cell receptor sequences repertoire between Tfh and non-Tfh cells 138
4.5 Conclusions 147

5 Results III: characterising the specificity of circulating Tfh and non-Tfh cells using Haemagglutinin protein 151

5.1 Background and rational 151
5.2 Influenza strains comparison 153
5.3 Precursor frequency and specificity for Haemagglutining in circulating Tfh and non-Tfh cells 156
5.4 Haemagglutinin-specific Tfh cell clones generation and peptide specificity 160
5.5 T cell receptor sequencing of HA-specific T cell clones and comparison with $CD4^+$ T cell repertoire from tonsil tissue 168
5.6 Conclusions 177

6 Results IV: T and B cell contact and observation of immunological synapses 179

6.1 Background and rational 179
6.2 Synaptic microvesicle transfers on silica bead lipid bilayer from circulating Tfh and non-Tfh cells 183
6.3 Determination of avidity and HLA restriction of antigen-specific Tfh and non-Tfh cell clones generation 193
6.4 T and B cell co-culture 201
6.5 Conclusions 209

7 Discussion 212

8 Supplemental material 225

8.1 Flow cytometry antibody list 225
8.1 Overlapping peptides 226

Bibliography 230

Acknowledgements 259

List of Figures

Figure 1.1 Sequential stages of T cell development in the thymus. 21

Figure 1.2 Structure and diversity of the T cell receptor αβ. 25

Figure 1.3 $CD4^+$ T cell helper subsets. 33

Figure 1.4 The germinal centre reaction. 42

Figure 1.5 Immunological synapses. 45

Figure 1.6 Three model hypotheses about Tfh memory heterogeneity. 55

Figure 2.1 General media reagents 62

Figure 2.2 List of reagents used for different media conditions. 63

Figure 2.3 Tonsil processing and flow cytometry staining comparison. 66

Figure 2.4 Gating strategy for T cell analysis. 68

Figure 2.5 List of optimized flow cytometry panels used within this thesis. 69

Figure 2.6 Antigens and controls. 71

Figure 2.7 Example of T cell clones mapping results. 72

Figure 2.8 Intracellular cytokine staining and transcription factor gating. 77

Figure 2.9 Gating strategy for antigen-enrichment. 79

Figure 2.10 Primer sequences. 82

Figure 2.11 TCR alpha (α) and beta (β) chains amplification. 83

Figure 2.12 Plate of confirmation gel. 83

Figure 2.13 Sorting strategy of $CD4^+$ populations for TCR deep-sequencing. 85

Figure 2.14 Example of the gating strategy for synaptic transfer analysis. 89

Figure 3.1 Blood and tonsil lymphocyte composition. 101

Figure 3.2 $CD4^+$ T cell subsets compared from blood and tonsil. 102

Figure 3.3 Tfh markers comparison between blood and tonsil $CD4^+$ T cell subsets. 103

Figure 3.4 Cytokine production profiles of blood and tonsil $CD4^+$ T cell populations. 105

Figure 3.5 TCR Vβ repertoire maintenance in blood $CD4^+$ T cell subsets after culture. 107

Figure 3.6 Media optimisation using naïve and memory $CD4^+$ T cells from peripheral blood. 113

Figure 3.7 Media check on $CD4^+$ T cells from tonsils. 114

Figure 3.8 Serum media optimisation in tonsils: gating and culture growth. 115

Figure 3.9 Serum media optimisation in tonsils: proliferation capacity. 116

Figure 3.10 Surface marker expression profile of T cell subsets during culture. .. 117

Figure 4.1 TCR Vβ profile between tonsil and blood by flow cytometry. 127

Figure 4.2 Number, count and efficiency of the TCR Vβ CDR3 sequenced from $CD4^+$ T cells. 133

Figure 4.3 Network visualisation of shared clonotypes between tonsil and blood $CD4^+$ T cell memory populations. 135

Figure 4.4 Cumulative clonotype sharing between tonsil and blood $CD4^+$ memory T cells. 136

Figure 4.5 Weighted analysis of the repertoire overlap between blood and tonsil populations. 138

Figure 4.6 Repertoire comparison of circulating Tfh versus non-Tfh cells in peripheral blood. 143

Figure 4.7 Repertoire comparison of tonsillar Tfh versus non-Tfh cells. 145

Figure 4.8 Weighted analysis of the repertoire overlap of tonsillar Tfh populations and repertoire diversity in blood and tonsils. 146

Figure 4.9 Repertoire overlap in 4 matched-tonsil and blood donors. 150

Figure 5.1 Alignment of Haemagglutinin (HA) protein from Wisconsin and California Influenza A strains. 155

Figure 5.2 Haemagglutinin-specificity in $CD4^+$ memory circulating Tfh and non-Tfh cells. 160

Figure 5.3 HA-specific $CD4^+$ T cell clones generation and Influenza antibody titre detection. 165

Figure 5.4 Peptide specificity of $CD4^+$ T cell memory clones and HLA type. 166

Figure 5.5 Peptide specificity in Tfh-Th1, Tfh-Th2 and ROM clones..... 167

Figure 5.6 αβTCR sequencing of HA-specific clones from donors 242 and 243. 174

Figure 5.7 Comparison of αβTCR sequences from HA-specific T cell clones with tonsil and blood repertoire in donor 242. 175

Figure 5.8 Comparison of αβTCR sequences from HA-specific T cell clones with tonsil and blood repertoire from donor 243. 176

Figure 6.1 Cell culture growth and cytokine profile during culture. 189

Figure 6.2 Microvesicle transfer of Tfh and non-Tfh cells after anti-CD3/anti-CD28 expansion. 191

Figure 6.3 Microvesicle transfer of Tfh and non-Tfh cells after co-culture with autologous B cells. 192

Figure 6.4 Generation of HA-specific T cell clones and determination of the peptide avidity. 199

Figure 6.5 HLA restriction of HA-specific T cell clones and monomer check. ... 201

Figure 6.6 Tfh and non-Tfh cell co-culture with naïve and memory B cells..... 207

Figure 6.7 High and low avidity Tfh-Th1 clones provide different help to total B cells in co-culture. 209

Figure 7.1 Graphical abstract..... 224

Figure 8.1 Flow cytometry antibody list. 226

Figure 8.2 List of peptides overlapping the entire HA/Wisconsin protein. 228

Figure 8.3 List of peptides overlapping the entire HA/California protein. 229

Abbreviations

AHR	Aryl hydrocarbon receptor
AID	Activation-induced cytidine deaminase
AIRE	Autoimmune regulator
APC	Antigen presenting cell
Ascl	Achaeta-scute homologue
Bcl	B cell lymphoma
BCR	B cell receptor
BFA	Brefeldin A
BLC	B lymphocyte chemoattractant
Bp	Base pair
BSLB	Beads-supported lipid bilayer
BST2	Bone marrow stromal cell antigen 2
CCL	Chemokine ligand
CCR	Chemokine receptor
CD	Cluster of differentiation
CDR	Complementarity-determining region
CLIP	Class II associated invariant-chain peptide
CM	Complete medium
CPM	Count per minute
cTfh	Circulating T follicular helper
CTLA-4	Cytotoxic T-lymphocyte-associated protein 4
CTLL	Cytotoxic T lymphocyte line
CXCL	CXC chemokine ligand
CXCR	CXC chemokine receptor
DC	Dendritic cell
DMSO	Dimethyl sulfoxide
DN	Double negative
DNA	Deoxyribonucleic acid
DP	Double positive
DZ	Dark zone

EC50	Half maximal (50%) effector concentration
EDTA	Ethylenediaminetetraacetic acid
ELISA	Enzyme-linked immunosorbent assay
ELISpot	Enzyme-linked immunospot
ETP	Early T cell precursor
FACS	Fluoroscence-activated cell sorting
FBS	Fetal bovine serum
FDC	Follicular dendritic cells
FMO	Fluorocrome minus one
FSC-A/H	Forward scatter-area/height of cells
GC	Germinal centre
GM-CSF	Granulocyte macrophage-colony stimulating factor
HA	Haemagglutinin
HBSS	Hank's balance salt solution
HIV	Human immunodeficiency virus
HLA	Human leukocyte antigen
HSA	Human serum albumin
HS	Human serum
HSC	Haematopoietic multipotent stem cells
ICAM	Intracellular cell adhesion molecule
ICOS	Inducible T cell co-stimulator
ICOSL	Inducible T cell co-stimulator ligand
ICS	Intracellular cytokine staining
IFN	Interferon
Ig	Immunoglobulin
IL	Interleukin
ILC	Innate lymphoid cell
IS	Immune synapse
ISP	Immature single-positive T cell
LFA	Lymphocyte function-associated antigen
LMPP	Lymphoid-primed multipotent precursor
LN	Lymph node

LZ	Light zone
MACS	Magnetic cell sorter
MALT	Mucosal-associated lymphoid tissues
MFI	Median fluorescent intensity
MHC	Major histocompatibility complex
MNC-T	Mononuclear cells from tonsil
mRNA	Messenger ribonucleic acid
NGS	Next generation sequencing
NK	Natural killer
PBMC	Peripheral blood mononuclear cells
PBS	Phosphate-buffered saline
PCC	Pigeon cytochrome C
PCR	Polymerase chain reaction
PD-1	Programmed cell death-1
PD-1L	Programmed cell death-1 ligand
PHA	Phytohemagglutinin
PMA	Phorbol 12-myristate 13-acetate
PRR	Pattern recognition receptor
PSGL	P-selectin glycoprotein ligand
Rag/RAG	Recombination-activating gene
RhCMV	Rhesus Cytomegalovirus
RNA	Ribonucleic acid
ROM	Rest of memory
ROR	Retinoic acid-related orphan receptor
RPMI	Roswell Park Memorial Institute medium
RSS	Recombination signal sequence
SCF	Stem cell factor
SD	Standard deviation
SEB	Staphylococcal enterotoxin B
SEM	Standard error of the mean
SFU	Spot forming unit
SHM	Somatic hypermutation

SIV	Simian immunodeficiency virus
SLB	Supported lipid bilayer
SP	Single positive
SSC-A/H	Side scatter -area/height of cells
SSM	Subcapsular sinus macrophages
STAT	Signal transducer and activator of transcription
TCF	T cell factor
Tcm	T central memory
TCR	T cell receptor
TdT	Terminal deoxynucleotidyltransferase
Tem	T effector memory
Tfh	T follicular helper
Tfr	T follicular regulatory
TGF	Transforming growth factor
Th	T helper
TIRFM	Total internal reflection fluorescent microscopy
TIV	Trivalent Influenza vaccine
TNF	Tumor necrosis factor
TREC	T cell receptor excision circle
Treg	T regulatory
V-D-J	Variable-Determining-Joining

Abstract

Title: Characterizing the specificity of T follicular helper cell repertoire in human peripheral blood and tonsil samples

College: St Anne's college
Name of the candidate: Elena Brenna
Programme of study: Doctor of Philosophy in Clinical Medicine
Date of submission: September 2018

T follicular helper cells (Tfh) are specialized $CD4^+$ T cells, primarily localized in germinal centers (GCs) in secondary lymphoid organs. These cells play a key role in supporting B cell responses and selection of affinity maturated antibodies. The majority of research to date on human Tfh cells has been restricted to circulating Tfh-like cells (cTfh) from peripheral blood because of difficulties in obtaining secondary lymphoid organs. However, the relationship between Tfh cells in lymph nodes (follicular Tfh) and cTfh cells as well as their distinctiveness from the $CXCR5^-$ memory $CD4^+$ T cell compartment are still unclear. By using donor-matched blood and tonsil samples, this project aimed to investigate the relationship between peripheral and follicular Tfh cells and also between Tfh and non-Tfh cell populations.

Phenotypic analyses characterized and identified populations of blood (Tfh-Th1, Tfh-Th2 and ROM) and tonsil (Tfh-GC, Tfh-Th1, Tfh-Th2 and ROM) cells to be compared. Targeted sequence-based analysis of the T cell receptor (TCR) showed a repertoire overlap between peripheral Tfh subsets and tonsillar Tfh cells as well as the distinction between Tfh and the rest of $CD4^+$ memory T cells. This was also confirmed in an antigen-specific system by comparing the peptide specificity and TCR repertoires of influenza virus haemagglutinin (HA) responsive Tfh and non-Tfh cells. Tfh and non-Tfh cell clones were also generated and their avidity characterized for use in Tfh and B cell co-cultures assays and for high resolution investigation of molecule trafficking in immune synapses. Correlation between peripheral and tonsillar compartments as well as distinction between Tfh and non-Tfh cells will inform the evaluation of Tfh responses in future clinical studies.

1 Introduction

1.1 The immune system: general overview

The immune system is a highly organised and specialised collection of cells and molecules that protects against infectious agents and other damage. To achieve this important role, the immune system recognises external pathogens, delivers targeted effector functions to kill the foreign entity and self-regulates this effector response to prevent excessive immune activation and tissue damage. Primarily a feature of the adaptive immune system following exposure to antigen, a long lived "memory" is generated, that ensures rapid and highly effective immune response upon a re-exposure to a previous immunogen (Murphy, 2012).

1.1.1 The innate immune system

During the encounter with an infectious agent, physical and chemical barriers form the initial defence and then the complement system as well as cells from the innate immune system recognize and phagocytose and/or destroy the foreign agent (Aderem and Underhill, 1999; Hornef et al., 2002). The innate immune system, which has an ancient origin in evolution (Fujita, 2002), comprises anatomical barriers, neutrophils, eosinophils, macrophages, dendritic cells (DCs), natural killer cells (NK) and a variety of soluble mediators such as cytokines, chemokines and complement proteins. The non-antigen-specific role of the innate immune system enables an immediate initial response via the recognition of microorganisms through a limited repertoire of pattern recognition receptors (PRRs), which are specific for

conserved molecules across bacteria, virus or parasites (Murphy, 2012). An essential role of the innate activation is to induce and tailor a more specific and targeted response of the adaptive immune system by capturing and presenting the antigen on the surface.

1.1.2 The adaptive immune system

The adaptive immune system comprises of T and B lymphocytes, which are the critical players of cell-mediated and humoral responses respectively. T lymphocytes recognize a specific antigen via T cell receptor (TCR) and are divided into $CD4^+$ and $CD8^+$ cells, depending on the co-receptor expressed on the surface. CD8 is carried by cytotoxic cells, while CD4 by helper and effector T cells (Mittrücker et al., 2014). $CD4^+$ T cells functions include cytokine production and B cell help (Sallusto, 2016; Samji and Khanna, 2017).

B cells recognize a foreign antigen via B cell receptor (BCR) and mediate humoral immunity through differentiation to effector plasma cells that secrete antibodies. Effector functions of antibodies are to neutralize microbes and toxins, to opsonise and phagocytose microbes, to promote cytotoxicity, mediate antibody-dependent cytotoxicity, activate complement and to internalize pathogens, as well as to enhance inflammation. In addition, antibodies generated following the initial encounter with a pathogen typically play a key role in eradicating and containing future infections with the same microbe (Heyman, 2000).

The effector phase that follows the recognition of an infectious element is characterized by the activation of both innate and adaptive responses, which cooperate for the elimination of a specific agent. This phase must be combined with

an opposing regulatory response that preserves the integrity of the immune system itself and avoids excessive inflammation, autoimmunity and hypersensitivity (Abbas and Lichtman, 2001). Immunological tolerance is a fundamental process, always present in the immune system, and it involves elimination of self-specific lymphocytes during thymic selection or peripheral inactivation every time a lymphocyte encounters a self-peptide presented by cells in the tissues on the classical MHC class I/II molecules. Functional inactivation of the lymphocyte response can also be induced by co-inhibitory signals, such as CTLA-4 that binds to CD80/CD86 and, instead of activation, promotes a non-response or anergy. During an immune response T regulatory cells (Treg, see section 1.4) with suppressive functions also contribute to constraining immunopathological responses (Josefowicz et al., 2012; Linsley et al., 1994; Vandermerwe et al., 1997).

During the final phase of an immune response, most of the effector lymphocytes are eliminated by apoptosis, but a few antigen-specific cells become part of the immunological memory to protect the individual against pathogens already encountered. The generation of T and B long-lived memory cells is a unique characteristic of the adaptive response and is fundamental for the efficacy of vaccination and re-encountered pathogens (Hammarlund et al., 2003; Lanzavecchia and Sallusto, 2009; Murphy, 2012).

1.2 Secondary lymphoid organs

The immune system is a complex network of specialized tissues, comprised of primary and secondary lymphoid organs where cells traffic between via blood and

lymph, with effector cells and elements capable of protecting from infectious agents and damage from dead or dying cells (Abbas and Lichtman, 2001). The primary lymphoid organs are the bone marrow and the thymus, where naïve T and B lymphocytes mature. Secondary lymphoid organs are lymph nodes, spleen, tonsils and mucosal/bronchus-associated lymphoid tissues (MALT and BALT), where the interaction between foreign antigens and the adaptive immune components is promoted. Secondary lymphoid organs are organised along the lymphatic system and located at convergence points of the lymphatic vessels (VanDePavert and Mebius, 2010).

Together with adenoids, palatine tonsils are lymphoglandular bodies localized on the back side of the throat that contribute to the first fundamental lymphoid barrier of the respiratory tract (VanKempen M.J.P. et al., 2007). Tonsils represent one of the major line of defence against viral and microbial pathogens and the tissue structure is anatomically and functionally organized into a crypt epithelium that covers tonsillar organs and increases the surface area, a cortical B-cell follicular area where follicular germinal centres are formed, an interfollicular or paracortical area mainly populated by T cells and a medullary area where the efferent lymphatic vessel generates (VanKempen M.J.P. et al., 2007). Because of the position and the anatomy of the crypt epithelium, developed to block any foreign agent, tonsils are often chronically infected and tonsillectomy is a common surgical procedure to avoid recurrent infections. $CD4^+$ and $CD8^+$ T cells as well as dendritic cells (DC) *ex vivo* isolated from tonsillar tissues are functional and have been previously used in immunological assays (Sada-Ovalle et al., 2012; Summers et al., 2001).

Lymphoid organs collect lymphatic fluids from the other organs and tissues, essential for the detection and the transport of the antigens via DCs and antigen presenting cells (APC). Peripheral blood is essential for the circulation of both naïve and effector lymphocytes through different tissues and it is connected with the lymphatic system at the peripheral tissues and in the lymphoid organs. It is the most accessible tissue and therefore commonly analysed in clinic to detect systemic and pathological markers (Abbas and Lichtman, 2001).

1.3 T cell development and T cell receptor generation

The bone marrow is the place where cells from the lymphoid lineage, such as T cells, B cells, innate lymphoid cells (ILCs) and natural killer cells (NK), originate from a common lymphoid progenitor, derived itself from the haematopoietic multipotent stem cell (HSC). While B lymphocyte development continues in the bone marrow, T lymphocytes migrate to the thymus to undergo maturation and antigen-receptor gene rearrangement and selection. Pre-T cells in the thymus receive specific signals from stromal cells providing ligands that activate the Notch signalling pathway, fundamental to trigger a T cell rather than a B cell commitment (Rothenberg, 2014). T lymphocyte progenitors in the thymus give rise to both α:β and γ:δ cells, which can be distinguished by different T cell receptor (TCR) chains. T cells that acquired α:β TCR further develop into classical CD4 and CD8 T cells, while γ:δ TCR promote a distinct lineage of innate-like lymphocytes (Vantourout and Hayday, 2013).

1.3.1 T cell development

Development of T cells occurs with the successive expression of specific transcription factors, such as Notch signalling together with GATA-3 and TCF-1, followed by BCL1 1b expression, elements determining commitment to the DN (double negative) phases (Ikawa, 2010; Rothenberg, 2014). T cell development is also guided in different localized areas of the thymus: the central medulla, the cortico-medullary junction, a peripheral cortex and a sub-capsular zone. Successive stages of early T cell development in different thymic microenvironments are illustrated (**Figure 1.1**). The early T cell precursor (ETP), which reaches the thymus from the blood, gives rise to four DN stages characterized by the absence of both CD4 and CD8 receptors and differential expression of CD25 (α-chain of the IL-2 receptor), CD44 and Kit (receptor for stem cell factor, SCF) (Koch and Radtke, 2011; Rothenberg et al., 2008). In the medulla the first stage, DN1, cells express a high level of CD44 and Kit and as they mature and migrate to the cortex they upregulate CD25, entering in the DN2 phase. The rearrangement of the β and γδ loci of the TCR is initiated in this phase, accompanied by a downregulation of CD44 and Kit and the induction of genes involved in the β-selection, such as *Rag-1/2* (recombination-activating gene 1/2). The step to the DN3 phase is crucial, since only cells with a productive β-chain rearrangement that paired an invariant pre-T-cell receptor α-chain to form a pre-T-cell receptor (pre-TCR) will survive (Von Boehmer, 2005; Borowski et al., 2004): the expression of a pre-TCR induces ligand-independent dimerization between two different pre-TCR, which leads to cell proliferation and causes phosphorylation and subsequent degradation of the enzyme RAG-2. Formation of a functional β:pre-TCR complex therefore ensures allelic

exclusion at the β locus by arresting a further β-chain gene rearrangement (Von Boehmer et al., 1998; Dudley et al., 1994). This phenomenon is fundamental for the identification of a unique Vβ-chain TCR for each T cell clonotype. The pre-TCR, also expressed on the surface together with the CD3 molecule, provides intracellular proliferation signals, which induce the DN4 phase in the sub-capsular zone and moreover the expression of both CD4 and CD8 receptors, double positive phase (DP). If instead a γδ TCR is expressed before the β locus rearrangement, the T cell is committed to a γδ lineage, fails to express CD4 and CD8 and migrates to the periphery without any selection (Hayday et al., 1999; Xiong and Raulet, 2007).

During the DP phase the α-chain locus rearrangement begins and in this process a single functional β-chain can be associated with different α-chains rearranged from both chromosomes, however because of the self-HLA molecule selection in this phase, it is unusual that both α-chains produce functional paired αβ TCR with same β-chain (Padovan et al., 1993; Petrie et al., 1993). DP thymocytes then undergo positive and negative selection before becoming single-positive (SP) T cells and exiting the thymus. Productive αβ TCR is tested first for interaction with self-peptide:self-HLA complexes expressed by cortical epithelial and stromal cells: binding within an affinity range promotes survival signals and proliferation, whilst T cells with receptors that fail to bind die. This positive selection promotes the development of a SP T cell, either $CD4^+$ or $CD8^+$ T cell that can respond to the same self HLA molecule bound to a set of foreign peptides (Marrack et al., 2008; Zerrahn et al., 1997). Subsequently SP T cells migrate to the medulla where negative selection occurs: cells with strong binding to a self-peptide:self-HLA complex, expressed by

thymic epithelial cells and DCs, undergo apoptosis. Negative selection is essential to prevent the formation of TCRs that are highly reactive to self-peptides and would therefore result in the generation of autoreactive T cells and autoimmune responses. Thymic epithelial cells play a crucial role in presenting self-peptides during this phase, through the expression of AIRE protein (autoimmune regulator): AIRE expressed ectopically in these cells activates a process called "promiscuous gene expression" that enables the presentation of self-antigens (Koh et al., 2008; Org et al., 2008).

A small population of SP $CD4^+$ T cells is characterized by a strong TCR signals to self-antigens, but not enough to induce apoptosis. This signal induces the expression of the transcription factor FoxP3 and the commitment to the lineage of natural regulatory T cells (nTreg) and expression of CD25 and CTLA-4 on the surface (Zheng and Rudensky, 2007). Of the initial double positive lymphocytes, only 2% of the cells survive the double selection process and become mature lymphocytes that form the T cell repertoire in the periphery.

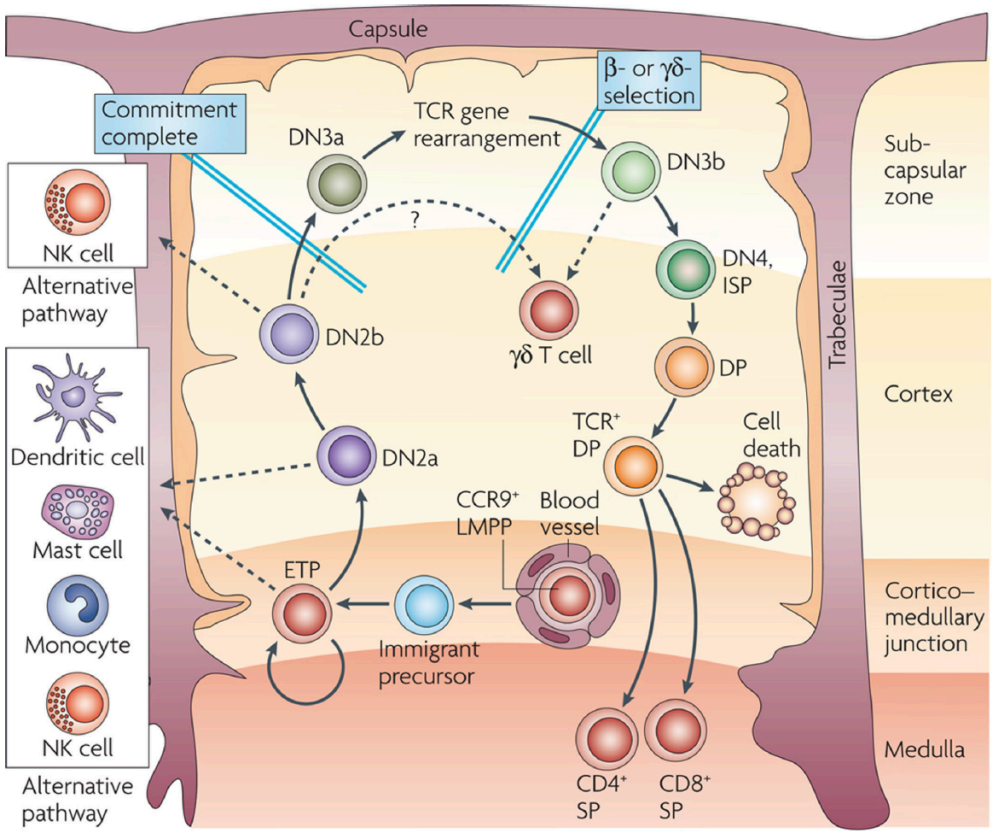


Figure 1.1 Sequential stages of T cell development in the thymus.

Schematic view of the T cell development pathways in different regions of the thymus. LMPP= lymphoid-primed multipotent precursor; ETP= early T cell precursor; DN2a to DN4= various stages of double-negative T cells; ISP= immature single-positive T cell; DP= double-positive T cell; SP= single-positive T cell (Reprinted by permission from Springer Nature: Nature Review of Immunology, Launching the T-Lineage Developmental Programme. Rothenberg et al., 2008)**.**

1.3.2 The T cell receptor (TCR)

The TCR is composed of an α and a β chain. The α locus contains the variable (V) and the joining (J) regions, while the β locus in addition to those, also contains additional diversity (D) segments (**Figure 1.2 a, b**) (Davis and Bjorkman, 1988). Both α and β chains contain a constant (C) region that does not undergo rearrangement. VJ and VDJ segments contribute to encoding the hypervariable

complementarity-determining regions (CDRs). CDR1 and CDR2 loops are encoded by the V genes from both chains, while the CDR3 region, which is the most variable loop of the TCR, is derived from the thymic recombination of the VJ junction region from the α chain and from the VDJ junction region of the β chain (**Figure 1.2 c, d**) (Nikolich-Žugich et al., 2004).

The wide diversity of the TCR repertoire is possible because of TCR recombination, also called V(D)J recombination, where TCR genetic segments are joined and generated (Schatz and Spanopoulou, 2005). Before this process the α and β loci present several V, J and D segments, which will be selected and modified during the rearrangement. The coding regions V (3'), D (from both sides) and J (5') gene segments are preceded by recombination signal sequences (RSSs) consisting of a conserved sequence of 7 nucleotides, a non-conserved spacer of 12bp or 23bp (base pair), followed by a conserved 9 nucleotides rich in AT (Adenine and Thymine) (Schatz and Spanopoulou, 2005). These sequences are important because they are recognized by enzymes that mediate the recombination between the segments of genes in order to obtain a VDJ for the β and a VJ segment for the α chains respectively. During the β-chain recombination the D and J segments are rearranged first and coupled with a V segment afterwards. RAG (recombination-activating gene) 1-2 recombinases are the main enzyme catalysers in the process of recognizing RSSs and cleave at the side of each coding segment. The alternation of 12bp and 23bp RSSs, which cause either one or two turns of the DNA helix, is crucial for RAG 1-2 enzymes to recognize and join the segments and it ensures the order of V-D and D-J recombination segments (Kavaler et al., 1984; Kurosawa et al., 1981; Sakano et al., 1981). The process generates T cell receptor excision circles (TRECs),

which are circular products of DNA which can be used as markers for T cells that have recently emigrated from the thymus (Kong et al., 1999). In addition to the DNA breaks, the lymphoid-specific enzyme deoxynucleotidyl transferase (TdT) adds non-germline nucleotides to the V-D, D-J and V-J junctions, creating a unique segment of TCR for each recombination arrangement (Cabaniols et al., 2001). Finally, DNA-modifying enzymes are recruited to mediate ligation of the ends of broken DNA strands and generate a linear sequence of DNA that will encode the TCR (Schatz and Spanopoulou, 2005).

The theoretical number of possible TCR αβ rearrangements is ~10^{14}, but calculations and experimental data estimate the diversity of naïve αβT cells at $2.5x10^{7}$ and 100-fold less for the memory repertoire (Arstila et al., 1999; Davis and Bjorkman, 1988; Nikolich-Žugich et al., 2004). Considering the average number of 10^{11} total T cells in human, each T cell clone must be expanded multiple times and the composition of the T cell repertoire is unique for each individual (Arstila et al., 1999). The wide diversity of T and B cell receptors (TCR and BCR) gene rearrangement allows the recognition of an extremely broad range of pathogens that may be encountered during a lifetime. This T cell receptor variety in an individual is called the repertoire and it is usually well established before puberty (Davis and Bjorkman, 1988). However, considering the vast number of different epitope-length peptides possible or present in nature, the low frequency of each T cell clone specific for a single existing peptide could not sustain an efficient and rapid immune response. It is therefore an acceptable hypothesis that in order to respond to the plethora of foreign peptides being presented by HLA molecules, T cells must have a certain degree of cross-reactivity and so recognize more than one peptide per clonotype (Mason,

1998). TCR cross reactivity has been described experimentally for both $CD4^+$ and $CD8^+$ T cells by different groups (Birnbaum et al., 2014; Campion et al., 2014; Selin et al., 2004; Su et al., 2013). Also of course, all peripheral T cells must have a low affinity for a self-peptide antigen presented by self HLA that enabled positive selection in the thymus.

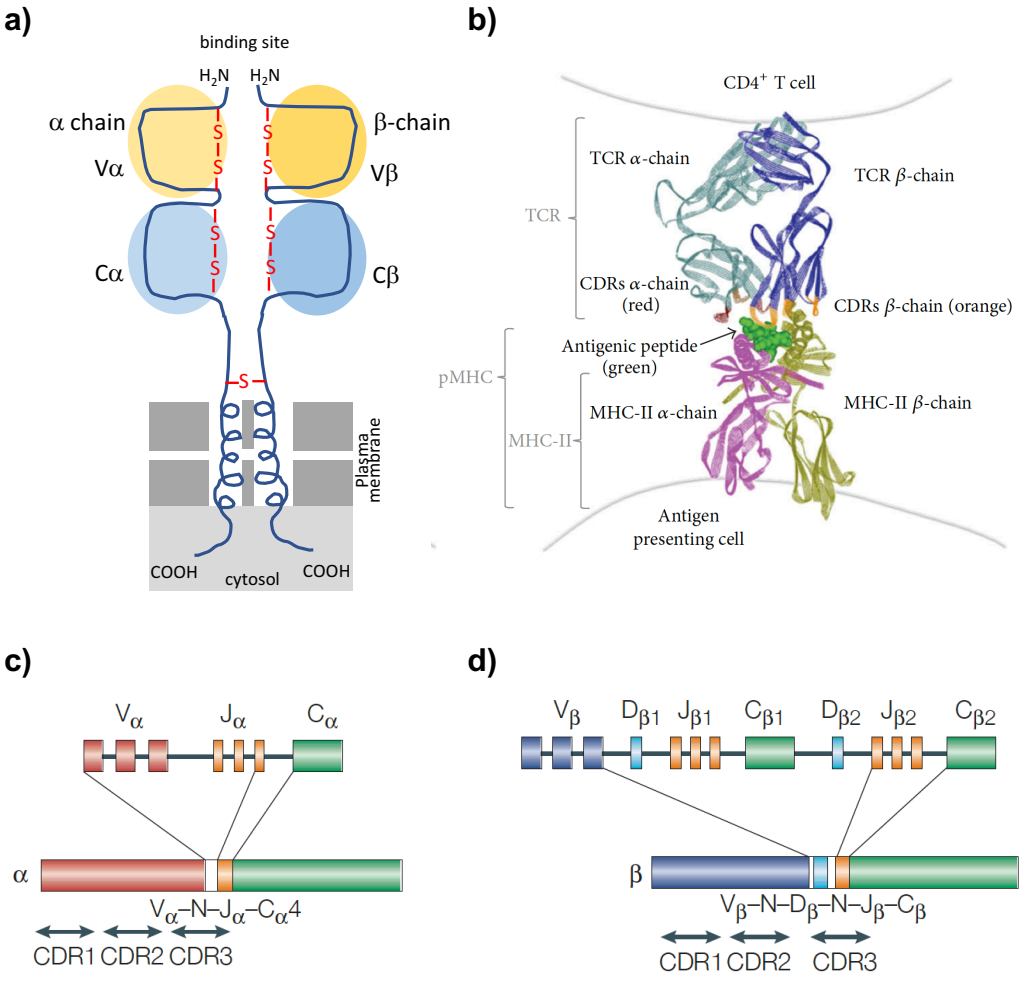


Figure 1.2 Structure and diversity of the T cell receptor αβ.

Schematic structure of the TCRαβ: (**a**) α and β chains are bound by a disulphide bridge and the extracellular domain is comprised of 2 constants (C_α, C_β) and 2 variable (V_α, V_β) regions. (**b**) The molecular structure illustrates the TCR (light blue=α, dark blue=β) binding the peptide-MHC-II complex (purple=α, yellow=β), with the antigenic peptide in green. A functional rearranged TCRαβ is shown: CDR1, CDR2 and CDR3 are generated by the recombination of the (**c**) V-J regions of the α chain and the (**d**) V-D-J regions of the β chain. TCR diversity is enhanced by the addition or deletion of nucleotides (N) between the junctions and mainly characterized by the CDR3 regions. (Figure adapted from Alberts et al., 2008 (a); González et al., 2013 (b); Figure (c, d) adapted by permission from Springer Nature: Nature Review of Immunology, The many important facets of T-cell repertoire diversity. Nikolich-Žugich et al., Copyright 2004).

1.4 Activation and heterogeneity of $CD4^+$ T cells

T cells that enter into the blood stream after being matured in the thymus and that have not yet encountered their specific antigen are called naïve. Naïve T cells traffic through lymph nodes, and are temporarily kept in the paracortical T cell zone by the expression of CCR7, which binds the chemokine CCL21 and other soluble factors produced by stromal cells (Cyster, 2000; Förster et al., 1999).

$CD8^+$ T cells are typically HLA class I restricted, therefore they can recognise cells from the self that all express HLA I, although recent studies have shown a very unusual restriction of $CD8^+$ T cells for MHC class II in rhesus macaques after RhCMV-SIV vaccination (Hansen et al., 2013; Murphy, 2012). Whereas, $CD4^+$ T cells are typically class II restricted and therefore interact with a more limited

number of cell types, primarily within the immune system, that express MHC II (Blum et al., 2013).

Professional antigen presenting cells (pAPC), specialized in capturing and presenting the antigen to T cells, are dendritic cells (DC), B cells and macrophages (Itano and Jenkins, 2003). DCs patrol peripheral tissues, the blood stream and secondary lymphoid organs, where these cells can take up antigens from endogenous cells, for example after an apoptotic event, or from exogenous sources such as pathogens, and process them for cross-presentation by the MHC class I pathway. $CD8^+$ T cells can then be cross-primed by DCs and recognize the antigen by TCR-MHC class I interaction (Blum et al., 2013; Heath et al., 2001). DCs can also take up endogenous or exogenous antigens, process them into peptides internally and present them on MHC class II molecules to $CD4^+$ T cells, which recognize the peptide via their TCRs.

Naïve $CD4^+$ T cells bind to APC through nonspecific adhesion molecules, including LFA-1 (lymphocyte function-associated antigen), which binds ICAM-1 and ICAM-2 (intracellular cell adhesion molecule) on the APC. This transient binding is necessary to stabilize the interaction between T cells and APC and to enable testing of specific TCRs that bind to the peptide-HLA-class-II (Garcia et al., 1996; Katz et al., 1973). When TCR binds to HLA-peptide the T cell is activated and this contact interface is called immune synapse (Dustin, 2008). Three different signals are crucial for this interaction: activation of the T cell through the engagement of the TCR and promotion of the TCR signalling; co-stimulatory factors, such as CD28 and inducible co-stimulator, ICOS (on the T cell) binding respectively B7 (CD80/CD86) and ICOSL (on the APC) to promote T cell survival and to amplify activation

intracellular pathways; finally cytokines produced by the APC and also present in the environment are important for $CD4^+$ T cell differentiation and function (Gonzalo et al., 2001; Lanzavecchia, 1999). This activation leads the T cells to undergo clonal expansion and differentiation to effector functions.

1.4.1 $CD4^+$ T cell heterogeneity and plasticity

After antigen-specific activation $CD4^+$ T cells differentiate into effector cells, they acquire the capacity to migrate to specific peripheral tissues through the expression of homing surface markers and to produce a range of cytokines that enhance a specific effector response, through the activation of multiple immune parameters (Sallusto and Lanzavecchia, 2009). Depending on the peptide signals, the co-stimulatory factors and the cytokines in the milieu, $CD4^+$ T cells can acquire different phenotypic and effector profiles and therefore functions to better accomplish the specific immune response against a certain pathogen. A brief summary of this heterogeneity is summarised in the description of the principal $CD4^+$ T cell subsets considered so far (**Figure 1.3**):

- The Th1 (T helper 1) cell phenotype is determined by IL-12 and IFN-γ in the environment, which induce the expression of the transcription factor TBET through STAT4 and STAT1-dependent pathways (Rogge et al., 1997; Szabo et al., 2000). Th1 cells characteristically produce IFN-γ and TNF-α and express on their surface the homing receptors CXCR3 and CCR5, which guide the T cells to inflamed tissues where their soluble chemokine ligands are produced (Djuretic et al., 2007; Groom and Luster, 2011a). Th1 cells defend the host from

intracellular bacteria and viruses, by cytokine production and by helping activation of specific $CD8^+$ T cells (Sallusto and Lanzavecchia, 2009). The importance of Th1 cells in response to virus infections is well-established: several studies have shown that $CD4^+$ T cells responding to different viruses have a Th1 phenotype (Moore et al., 1995; Palladino et al., 1991; Yang et al., 2013; Zielinski et al., 2011), and have demonstrated their contribution to virus control (Belz et al., 2002; Graham et al., 1994; Tamura et al., 1996).

- The Th2 (T helper 2) cell phenotype is driven by IL-4 in the milieu, which through STAT6 and other pathways induces the expression of several transcription factors important for Th2 differentiation, one of which is GATA-3 (Kaplan et al., 1996; Zheng and Flavell, 1997). The signature cytokines produced by Th2 cells are mainly IL-4, IL-5 and IL-13, but the Th2 phenotype is also characterized by the expression of surface homing markers such as CCR4, CCR3 and CRTh2 (Rivino et al., 2004; Sallusto et al., 1998). Th2 effectors protect against parasites and helminths, through promoting responses mediated by eosinophils, mast cells and IgE-producing B cells (Allen and Sutherland, 2014).

- The Th17 (T helper 17) cell phenotypes are induced under different influences of IL-6, TGF-β1, IL-23 and IL-β1 (Acosta-Rodriguez et al., 2007; Tuomela et al., 2012). Subsets of Th17 cells in respect to their effector function and microbe specificity have been described and their development depends on the combination of differentiation factors that are present in the priming milieu (Aschenbrenner et al., 2018; Zielinski et al., 2012). Expression of RORγt in

combination with other transcription factors such as STAT3, BATF, IRF-4, SOX5, and c-MAF, induce the production of IL-17A and IL-17F in addition to other effector and regulatory cytokines including IL-21, IL-22, GM-CSF and IL-10 (Ciofani et al., 2013; Tanaka et al., 2014). Th17 cells are enriched in $CCR6^{+}CCR4^{+}$ cells and are particularly important in defending the host against infection from fungi and extracellular bacteria (Acosta-Rodriguez et al., 2007; Annunziato et al., 2007; Puel et al., 2011). Recently a mixed phenotype of Th1/Th17 cells induced by *Mycobacterium tuberculosis* has been described and named Th1* (Lindestam Arlehamn et al., 2013). These cells express CXCR3 as well CCR6 and express both TBET and RORγt transcription factors (Lindestam Arlehamn et al., 2013).

- Th22 (T helper 22) cells include IL-22-producing T cells (Trifari et al., 2009). Th22 cells have been identified by the expression of CCR4 and CCR10 (induced in skin-draining secondary lymphoid organs) on their surface and therefore play a critical role in the skin health, homeostasis and immunity (Liu et al., 2009; Nograles et al., 2009). RORγt and T-BET have been shown to regulate the differentiation of this T cell subset in mouse models, but several aspects of Th22 cells function and differentiation are still under investigation (Duhen et al., 2009; Plank et al., 2017; Wolk et al., 2006).

- Tfh (T follicular helper) cells, are a specialized subset of $CD4^{+}$ T cells that provide help to B cells and play a key role in supporting B cell somatic hypermutation and selection of affinity maturated antibodies in germinal centers (Kim et al.,

2001; Schaerli et al., 2000). Tfh cells express the chemokine receptor CXCR5, which enables them to migrate into germinal centres (Breitfeld et al., 2000). The function and differentiation processes of Tfh cells are explained more in detail in the following sections.

- Treg (T regulatory) cells are divided into two groups: natural Treg (nTreg) and induced Treg (iTreg). Natural Treg cells differentiate in the thymus, while iTreg can differentiate from naïve $CD4^+$ T cells in the periphery upon exposure to TGF-β and with FoxP3 induction (Chen et al., 2003). Treg cells have an important immune-suppression function, achieved through mechanisms including the production of IL-10, TGF-β and IL-35 and the expression of the co-inhibitory receptor CTLA-4, which binds CD80 and CD86 on the APC and negatively modulates the response (Linsley et al., 1994; Vandermerwe et al., 1997). Treg cells also express the IL2-Rα (CD25) at a high level, which contributes to the regulatory function by sequestering the important T cell proliferation and survival factor IL-2 (Josefowicz et al., 2012). A regulatory population of T cells has been described which specifically locates in the germinal centre: T follicular regulatory cells (Tfr). Tfr cells express FoxP3 and CTLA-4 and present similar inhibitory characteristics to canonical Treg but also have similarities to T follicular helper cells, expressing CXCR5, PD-1 and Bcl-6, and inhibit an excessive germinal centre reaction, especially over-activation of Tfh cells (Chung et al., 2011; Linterman et al., 2012). Although several aspects of Tfr differentiation are still not clear, Tfr cells can differentiate from Tregs and also

from $CD4^+$ naïve T cells (Botta et al., 2017; Linterman et al., 2012; Sage and Sharpe, 2016).

The heterogeneity of $CD4^+$ T cell populations is further enhanced by a high level of flexibility and plasticity (Caza and Landas, 2015). The "fate" of a primed T cell clone can therefore change during its lifespan and depending on the environment one cell might acquire different phenotypes and functions over time (O'Shea et al., 2010). Several studies have demonstrated $CD4^+$ T cell flexibility on the basis of cytokine production and differentiated Th2, Th17 or Th22 cells can acquire different phenotypes in presence of certain stimuli in the environment (Chen et al., 2007; Hegazy et al., 2010; Plank et al., 2017; Veldhoen et al., 2008; Wilson et al., 2007). This process was elegantly demonstrated recently in human by Becattini et al.: the same T cell clonotypes (using TCRβ deep-sequencing comparison) were found in different subsets of T helper cells. In particular *Candida albicans*-specific clonotypes derived from Th17 cells were found in Th1* and Th2 subsets and *in vitro* priming experiments also showed that a single naïve T cell can generate multiple fates from the same antigen-stimulation (Becattini et al., 2014). Although this plastic and heterogeneous scenario might not focus on a specific and unique response generation, induction of a different spectrum of memory T cells could provide a broader and more diverse protection where necessary and ultimately benefit the survival of the organism.

1.4.2 $CD4^+$ T cell memory

When the acute immune response is resolved, 90% of the effector T cells undergo controlled cell death by apoptosis, but a minor fraction of antigen-specific cells will differentiate into $CD4^+$ memory cells, which can be reactivated again following encounter of the same antigen (Hataye et al., 2006).

Memory is an important characteristic of the adaptive immune system that allows a fast and effective immune response once re-challenged with the same antigen (Pepper and Jenkins, 2011). Two main populations of memory T cells can be distinguished: central memory (T_{CM}) and effector memory (T_{EM}) T cells, defined by the expression of homing receptors and the different functions (Pepper and Jenkins, 2011; Reinhardt et al., 2001; Sallusto et al., 1999, 2004). The expression of CCR7 and CD62L, in common with naïve T cells, leads the T_{CM} cells to be localized mainly in secondary lymphoid organs, while T_{EM} cells are found in peripheral tissues and present an immediate effector function after activation (Campbell et al., 1997). However, both T_{CM} and T_{EM} cells can be identified in peripheral blood (Sallusto et al., 1999). The lymphocyte common antigen CD45, a phosphatase expressed in all leucocytes, is present in different isoforms (Altin and Sloan, 1997) and in particular CD45RA and CD45RO isoforms are differently expressed by naïve versus memory T cells (Michie et al., 1992). Naïve T cells express CD45RA whilst both T_{CM} and T_{EM} are $CD45RA^-CD45RO^+$. However, some of the T_{EM} cells can re-acquire the expression CD45RA: they are called "terminally differentiated" effector memory (T_{EMRA}) and are tissue-infiltrating T cells increased in number during a chronic immune activation state (Derhovanessian et al., 2011; Valmori et al., 2002; Willinger et al., 2005). T_{CM} and $T_{EM,}$ when stimulated under polarizing conditions, acquire the

ability to differentiate into a particular subset of T helper cell depending on the presence of different soluble molecules in the environment (Sallusto et al., 2004).

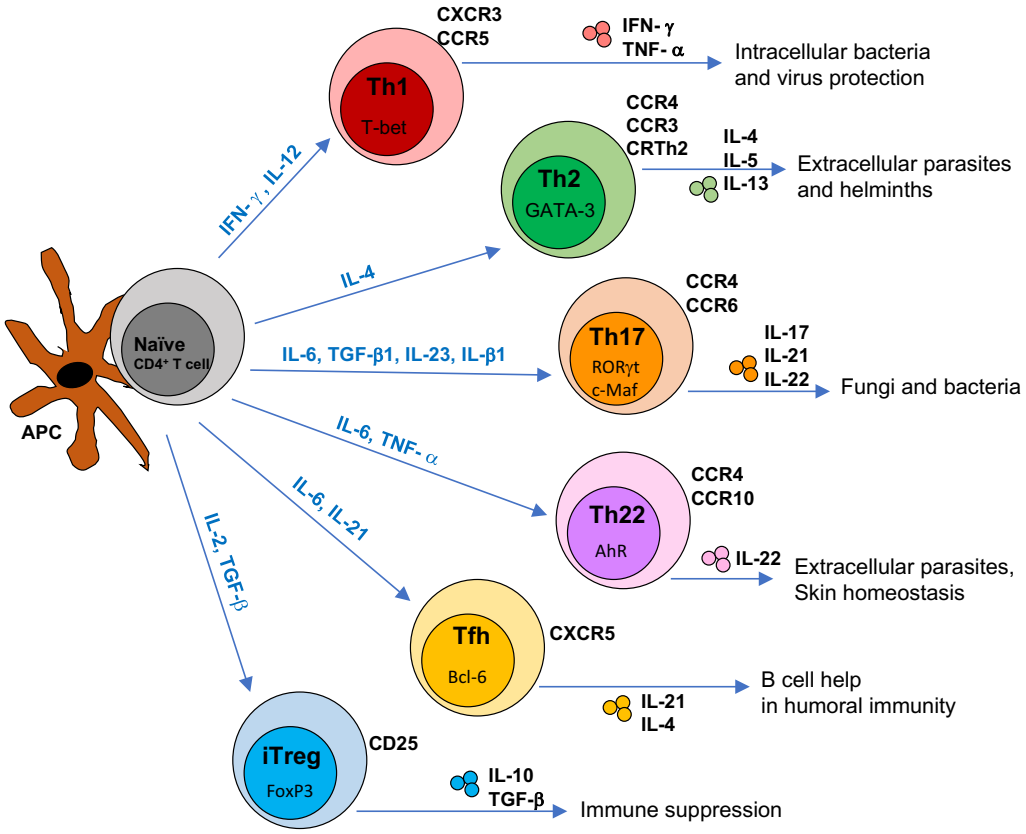


Figure 1.3 CD4⁺ T cell helper subsets.

Upon priming by an antigen presenting cell (APC) a naïve CD4⁺ T cell, depending on signals and cytokines in the environment, differentiates into distinct effector and regulatory phenotypes. The schematic figure illustrates for each subset (Th1, Th2, Th17, Th22, Tfh, iTreg), the cytokines involved in the differentiation process, transcription factors induced, surface markers expressed, effector cytokines produced after differentiation and function (Figure adapted from Tripathi and Lahesmaa, 2014).

1.5 T follicular helper cells and differentiation

The essential contact between B and T cells to induce long-lived antibody response was a fundamental observation made 50 years ago (Claman et al., 1966; Mitchell and Miller, 1968a, 1968b; Nossal et al., 1968). During the following 50 years the importance of a cognate T and B cell interaction for the production of high affinity antibodies has been well described, as well as the role of CD40-CD40L interaction (Armitage et al., 1992; Clark and Ledbetter, 1986; Crotty, 2015; Liu et al., 1989). Initially it was thought that most $CD4^+$ T cells, or at least Th2 cells, could help B cells but, the identification of a specific subpopulation of $CD4^+$ T cells particularly committed to interact with and support B cells was an important new concept discovered around 2000. Breitfeld et al., and a few other research groups (Kim et al., 2001; Schaerli et al., 2000), published findings of a novel subpopulation of $CD4^+$ T helper cells that express CXCR5. However it was Breitfeld who coined the term Tfh, stating "As these cells show all characteristics required for efficient B cell help within lymphoid follicles, we suggest calling these cells follicular B helper T cells (Tfh)" (Breitfeld et al., 2000). The expression of CXCR5 is indeed fundamental for the migration of these cells to the B cell border, into B cell follicles and germinal centres, since it binds CXCL13, also known as B lymphocyte chemoattractant (BLC), a chemokine required for the development of most secondary lymphoid organs (Ansel et al., 2000). In combination with CXCR5, the co-receptor PD-1 (programmed cell death 1) is also a marker expressed by Tfh cell populations (Dorfman et al., 2006; Haynes et al., 2007). PD-1 is a co-receptor associated with inhibitory signals and its function is to dephosphorylate the TCR components by recruiting SHP1 and SHP2 (Src-homology 2 domain-containing protein tyrosine phosphatases, PTPs) (Lorenz,

2009; Okazaki and Honjo, 2006; Sheppard et al., 2004). The role of PD-1 has been implicated in inducing and maintaining peripheral tolerance by switching off autoreactive T cells and prevent tissue damage (Okazaki and Honjo, 2006).

As described above, $CD4^+$ naïve T cells primed by antigen-presenting DC receive a Th1, Th2 or Th17 signal which causes them to differentiate into effector T cells and exit the lymph node migrating to the site of infection or inflammation. Tfh cell differentiation is a multifactorial process, which involves not only TCR engagement and the presence of specific cytokines in the environment, but also a unique interaction with antigen-specific B cells. The description of the differentiation processes of these cells remains controversial despite many years of research. This controversy is exacerbated by the different *in vivo* or *in vitro* models used to study it and the multiple factors involved. Although a few aspects remain unclear, I will review important elements that have been confidently described in the literature. Three spatial-temporal steps of Tfh differentiation can be distinguished: a priming phase with DC where TCR engagement, cytokines and surface homing-markers play a fundamental role; cognate interaction with B cells at the follicle border leading to greater commitment to the Tfh lineage and migration into the B cell follicle, followed by further interactions with B cells; finally the Tfh effector phase in the germinal centre reaction (Crotty, 2014; Vinuesa et al., 2005).

Throughout all the three differentiation phases the importance of the transcription factor "B cell CLL/lymphoma 6" (Bcl-6) has been identified as a critical regulator of Tfh cell commitment, development and function (Johnston et al., 2009; Nurieva et al., 2009; Yu et al., 2009). Bcl-6 promotes Tfh differentiation in part also by suppressing other important T helper cells transcriptional regulators, such as T-bet,

RORγt, GATA-3 (Nurieva et al., 2009; Yu et al., 2009) and it is antagonized by Blimp-1 (Johnston et al., 2009). Before its role in T cells, Bcl-6 was first studied in B cells. Bcl-6 was shown to be required for germinal centre differentiation and it is considered an oncogene in B-cell derived lymphoma (Ci et al., 2008; Klein and Dalla-Favera, 2008).

During the early priming phase TCR signals and cytokines in the environment initiate the acquisition of a pre-Tfh state, driving a surface marker phenotype necessary for the $CD4^+$ T cell to migrate from the T cell zone to the B cell border (Crotty, 2014). This phenotype consists of the downregulation of CCR7 and PSGL1 (both markers that bind to extracellular matrix signals in the T cell area) (Haynes et al., 2007; Poholek et al., 2010a) and the upregulation of CXCR5 and ICOS, which drive the T cell to the B cell border and bind respectively CXCL13 and ICOSL (Choi et al., 2011; Heissmeyer and Vogel, 2013). The initiation of CXCR5 expression is regulated by the transcription factor achaeta-scute homologue 2 (Ascl-2) (Liu et al., 2014). Both *in vivo* and *in vitro* mouse models propose that IL-21 and IL-6 strongly influence the early differentiation of Tfh cells although the presence of cytokines alone is not sufficient for Tfh differentiation (Linterman et al., 2010; Nurieva et al., 2008, 2009). IL-21 signalling is required for GC formation and for T and B cell maintenance, but normal Tfh cells were also found in the absence of IL-21 and IL-6 (Poholek et al., 2010b; Zotos et al., 2010). The importance of cytokines such as TGF-β, IL-23 and IL-12 in Tfh differentiation in humans, supports the hypothesis of shared properties between Th17 and Tfh in the early developmental steps and it leaves open speculation regarding the identity of these two populations (Schmitt et al., 2014). While IL-2 is an early potent inhibitor of Tfh phenotype (Ballesteros-Tato

et al., 2012; Johnston et al., 2012), recent studies have shown the importance of inducible costimulatory (ICOS) signalling for the early differentiation phase during DC priming and for the subsequent migration to B cell follicles (Choi et al., 2011; Xu et al., 2013). In addition to cytokines and external stimuli from the environment, the $CD4^+$ T cell fate is also influenced by the quality and quantity of the TCR signalling during priming and by the strength and the affinity of the TCR for the antigen (Germain and Stefanová, 1999; Malherbe et al., 2004; Tubo and Jenkins, 2016). Canonical $CD4^+$ T helper 1 and 2 cell differentiation is strictly dependent on the nature and the dose of the antigen (Constant et al., 1995; Hosken et al., 1995; VanPanhuys et al., 2014). The role of TCR affinity in Tfh cell differentiation is a little more controversial: studies using pigeon cytochrome C (PCC) in a mouse model showed that high affinity TCR are preferentially selected for residential follicular T effector function (Tfh-GC) during the acute response (Fazilleau et al., 2007, 2009), however this observation was not confirmed in a persistent viral infection model (Ploquin et al., 2011). Different from other $CD4^+$ T helper cell subsets, Tfh cell development requires a constant presence of antigen, and therefore a persistent TCR stimulation, which might also be important during priming with a DC (Baumjohann et al., 2013; Cirelli and Crotty, 2017; Deenick et al., 2010). However, the molecular mechanisms underlying the effect of TCR signals on T cell differentiation remain unclear (Tubo and Jenkins, 2016). Recently it has shown that a stronger TCR signalling leads the naïve cells to differentiate into IL-2-producing Tfh cells. In contrast, a lower TCR signalling enhances the differentiation of effector T cells that do not produce IL-2 and therefore require external IL-2 to accomplish their role (DiToro et al., 2018).

The distinct $CXCR5^{+}ICOS^{+}CCR7^{-}PSGL1^{-}$ phenotype acquired after the early priming phase, allows the "pre-Tfh" or "Tfh-like" cell to migrate to the B cell border, where it interacts with antigen-specific B cells via cognate peptide:HLA class II molecule ligation and other co-stimulatory molecules. This contact is essential for both Tfh and B cell survival and maturation: Tfh cells undergo maturation and enter into the B cell follicle; B cells undergo affinity maturation and somatic hypermutation. Tfh and B cells take part in the germinal centre responses, which constitutes the third stage of differentiation (Obst et al., 2005; Yarke et al., 2008).

During the germinal centre reaction Tfh cells acquire a "Tfh-GC effector phenotype", expressing at a high level CXCR5, PD-1, Maf, SAP and Bcl-6 (Crotty, 2011; Kroenke et al., 2012). Tfh-GC effector function is promoted by a prolonged peptide:HLA presentation by germinal centre B cells, but different experimental models still leave open discussion regarding the nature of the antigen in question (Tubo and Jenkins, 2016).

Studies in human tonsils compared the phenotypic and functional profile of different populations of memory $CD4^{+}$ T cells based on the expression of CXCR5 (Ma et al., 2009; Yu et al., 2009). Tfh-GC cells ($CXCR5^{hi}CD45RA^{-}$), were the highest producers of IL-21 and IL-4 and lowest producers of IFN-γ and IL-17A after a general PMA and ionomycin stimulation, compared to other memory $CD4^{+}$ T cell populations ($CXCR5^{lo}CD45RA^{-}$ and $CXCR5^{inter}CD45RA^{-}$ (Ma et al., 2009; Yu et al., 2009). During the GC reaction effector Tfh-GC cells, by producing IL-4 and IL-21 and via CD40L-CD40 contact, induce B cell survival and class-switching and contribute to the selection of high affinity B cells after BCR rearrangement (Avery et al., 2008; Casamayor-Palleja et al., 1995; Liu et al., 1989). IL-10 promotes plasma

cell differentiation (Arpin et al., 1995), however Tfh cells produce low levels of this cytokine (Chtanova et al., 2004; Ma et al., 2009).

1.6 Germinal centre formation

Germinal centres (GC) are dynamic structures localized in secondary lymphoid organs in the cortical B-cell follicular area where, after an immune challenge and Tfh cell contact, B cells undergo intense proliferation, BCR (B cell receptor) rearrangement and differentiation into plasma or memory cells (Bannard and Cyster, 2017). The GC is where long-lived memory and plasma B cells originate and therefore Tfh cells play a crucial role in generating an effective and long-term response to pathogens (Klein et al., 1998; Lanzavecchia and Sallusto, 2009; Victora and Nussenzweig, 2012). The generation of high affinity antibodies produced by B cells during a GC reaction is made possible by two phenomena occurring during BCR rearrangement: class-switch recombination, which places the original somatic heavy-chain of non-class-switched antibodies (IgM and IgD) onto an alternative C region generating a range of antibodies (eg. IgG1, IgG2, IgE, IgA); and somatic hypermutation, which introduces point mutations into the variable region to modifies the affinity of the antibody for the antigen (Jung et al., 1993). The secondary diversification of the BCR rearrangement is a complex process, mediated by multiple factors and initiated by the enzyme AID (activation-induced cytidine deaminase) (Revy et al., 2000; Sakano et al., 1980).

In the lymph nodes naïve B cells, usually identified as $IgM^{+}IgD^{+}CD27^{-}$, directly recognize antigen complexes via the BCR, signalling through which is enhanced by

co-receptors such as CD19, CD21 and CD81. Activation of B cells through the BCR by antigen complexes, initially captured from subcapsular sinus macrophages (SSM) and also from follicular dendritic cells (FDC), leads to BCR microclustering and subsequently the internalization of the antigen in an affinity-dependent manner (Spillane and Tolar, 2018). B cells and SSM are reciprocally dependent on one another, as each of them produce soluble factors essential for the maintenance and function of the other (Moseman et al., 2012). Antigen internalized by B cells is processed and presented on the surface with HLA class II molecules (Heesters et al., 2016). Upregulation of CCR7 on the activated B cell surface enables the migration of these cells to the border of the T cell zone in the lymph node, where they contact an antigen-specific T follicular helper cell (Tfh), already primed by a DC (Förster et al., 1999; Gatto et al., 2011). At the T cell border, B cells receive co-stimulatory signals from the Tfh cell such as ICOS, CD40L and CD28 that mediate signals via ICOSL, CD40L and CD80/CD86 respectively (Linterman et al., 2014; Noelle et al., 1992; Okada et al., 2005). Moreover, specialized NKT cells localized at the follicular border represent the first resource of IL-4 necessary for B cell survival (Gaya et al., 2018). After this first contact, class-switched B cells can take either an extra-follicular route and become plasma cells with low level of hypermutation, or form tight clusters of B cells and take part in the follicular pathway and the germinal centre reaction (**Figure 1.4**). The extra-follicular pathway gives rise to short-lived plasma cells secreting antigen-specific antibodies within days after antigen encounter and it is localized in the medullary cords of lymph nodes (MacLennan et al., 2003; Vinuesa et al., 2005).

During the follicular pathway, B cells selected after T cell contact enter into the dark zone (DZ) of the GC, where they undergo somatic hypermutation (SHM) and proliferation. After a few cycles, B cells exit the DZ and migrate to the light zone (LZ), where the rearranged BCR is tested for its affinity for the antigen (Heesters et al., 2014; Spillane and Tolar, 2018; Victora et al., 2010). If the affinity for the antigen is high enough to enable efficient capture of antigen from FDCs and good presentation of antigenic peptides with MHC class II, B cells are able to receive cognate help from Tfh cells, which deliver survival signals via CD40L ligation of CD40; otherwise they undergo apoptosis (Mesin et al., 2016). Tfh-GC cells in the LZ also produce cytokines such as IL-21 and IL-4, which not only induce B cell survival and proliferation but also antibody class-switching (Avery et al., 2008; Casamayor-Palleja et al., 1995; Liu et al., 1989). The movement of B cells between the DZ and LZ is influenced by the expression of the receptors CCR6 and CXCR4 on the B cell surface: CCR6 is upregulated in the LZ and binds to CCL20, expressed in lymphoid tissues after immune challenge, while CXCR4 is expressed by B cells in the DZ, since it binds to CXCL12, highly produced by localized stroma cells in the region (Hargreaves et al., 2001; Reimer et al., 2017; Wiede et al., 2013). B cells surviving the LZ selection can then re-enter the DZ for other cycles of SHM, or they can exit the GC and become efficient antibody-producing plasma cells or memory B cells (Heesters et al., 2014). Recent studies have also associated early expression of CCR6 with low-affinity memory B cell precursors in the GC (Ise et al., 2018; Suan et al., 2017).

The role of Tfh-GC cells in the GC reaction is fundamental for initial B cell selection and for affinity maturation. The GC also has available an important regulatory

counterpart, mediated by T follicular regulatory cells (Tfr). Tfr cells in addition to follicular markers such as CXCR5, PD-1, ICOS and Bcl-6, also express regulatory molecules including FoxP3 and CTLA4 (Chung et al., 2011; Linterman et al., 2012; Wollenberg et al., 2011). Although the complete regulatory mechanism is still poorly understood, Tfr cells are thought to limit the GC response and to regulate an excessive Tfh and B cell activation and proliferation by competing with CD28 to mediate a suppressive response (Vinuesa et al., 2005; Wang et al., 2015).

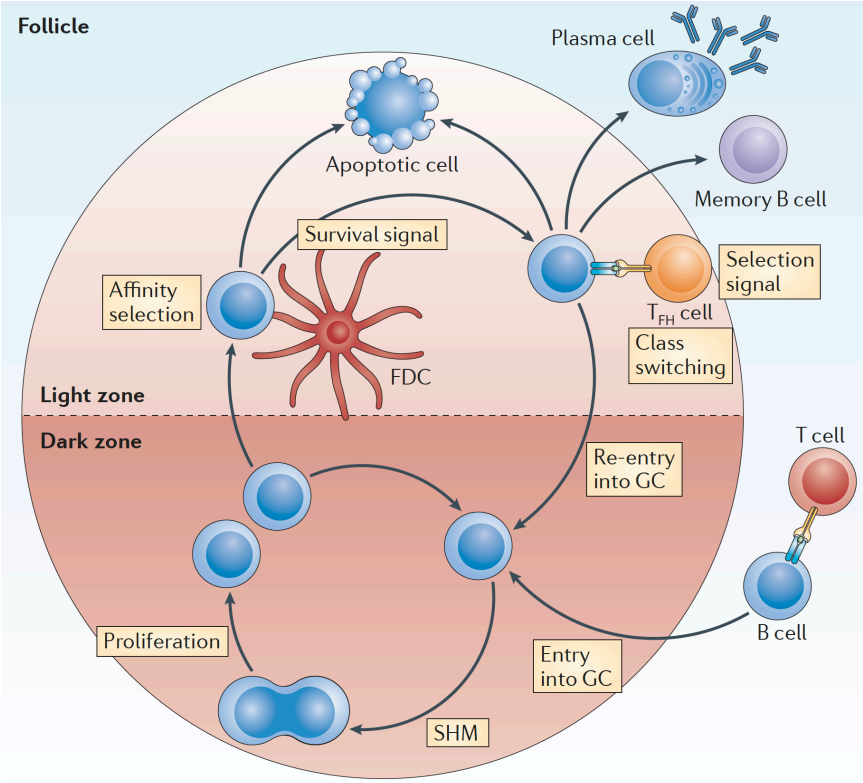


Figure 1.4 The germinal centre reaction.

Schematic view of the germinal centre reaction during an immune response. SHM=somatic hypermutation, FDC=follicular dendritic cells, GC=germinal centre (Reprinted by permission from Copyright Clearance Center: Springer Nature, Nature Review of Immunology, Follicular dendritic cells: dynamic antigen libraries. Heesters et al., 2014).

1.7 Immunological synapses between T and B cells

As described above, cell-cell interactions between DC and Tfh cells and later between Tfh and B cells are critical steps during the process of an effective immune response against antigens and for high affinity antibody production. These contacts, generally described between T cells and APC, are often called immune synapses (IS) (**Figure 1.5**) and they are controlled by multiple factors grouped into antigen recognition signals, adhesion molecules, co-stimulatory and co-inhibitory signals. LFA-1 and ICAM-1 interactions help in a non-antigen specific manner to facilitate the interaction between T cell and APC, while the actual antigen-specific interaction is driven by TCR and peptide:HLA complex (pHLA) (Garcia et al., 1996; Katz et al., 1973). During a T cell-APC interaction, the phosphatase CD45 on the surface of the T cell that is co-expressed with the CD3-TCR in the resting state, becomes segregated from the TCR by steric effects, as its size is too large for it to be accommodated at the IS where the T cell and APC come into close contact (Davis and van der Merwe, 2006). The absence of phosphatases allows the phosphorylation of the TCR by the associated kinase Lck, followed by the triggering of TCR signalling inside the T cell (Davis and van der Merwe, 2006).

In addition to TCR-pHLA, the cognate signal between T and APCs is amplified by CD40L and CD40 and is regulated by PD-1-PD-1L interactions (Casamayor-Palleja et al., 1995; Cubas et al., 2013). As already described, ICOS-ICOSL interaction during T-B interaction plays an important role not only in the segregation and early differentiation of Tfh cells, but also in reinforcing the signal during ISs and the B cell activation at the follicle border (Choi et al., 2011). All together, these co-stimulatory signals induce B cell survival and differentiation (Rush and Hodgkin, 2001).

This topic has previously been difficult to study due to the limited technology availability, however recent artificial models combining immunofluorescence with purified molecules on substrates, have helped the visualization of IS formation and have revealed the presence of extracellular vesicle trafficking throughout this close interface (Dustin, 2014a).

It is well-known that extracellular vesicles are important for the transfer of information in different tissues (Andaloussi et al., 2013). Extracellular vesicles generated from the plasma membrane are called ectosomes or microvesicles and they have a 50 to 1000 nm size (Pilzer et al., 2005). Microvesicles are formed by the outward budding and fission of the cell membrane and they have been found to be released in the IS between a T cell and an APC (Hess et al., 1999; Mittelbrunn et al., 2011). Ectosome release has some similarities with HIV budding, for instance the role of Tetherin (BST2 or CD317) in the formation of the extracellular bodies (Edgar et al., 2016; Gould et al., 2003), and synaptic ectosomes are known to elicit Ca^{2+} flux inside the APC via peptide:HLA signalling (Choudhuri et al., 2014). Recent findings describe how TCR segregate to one side of the LFA-1 enriched membrane and the invaginations of these microclusters form microvesicles containing TCR-pHLA, which are precisely released inside the APC/B cells to induce internal signalling and activation (Choudhuri et al., 2014) (**Figure 1.5 b**).

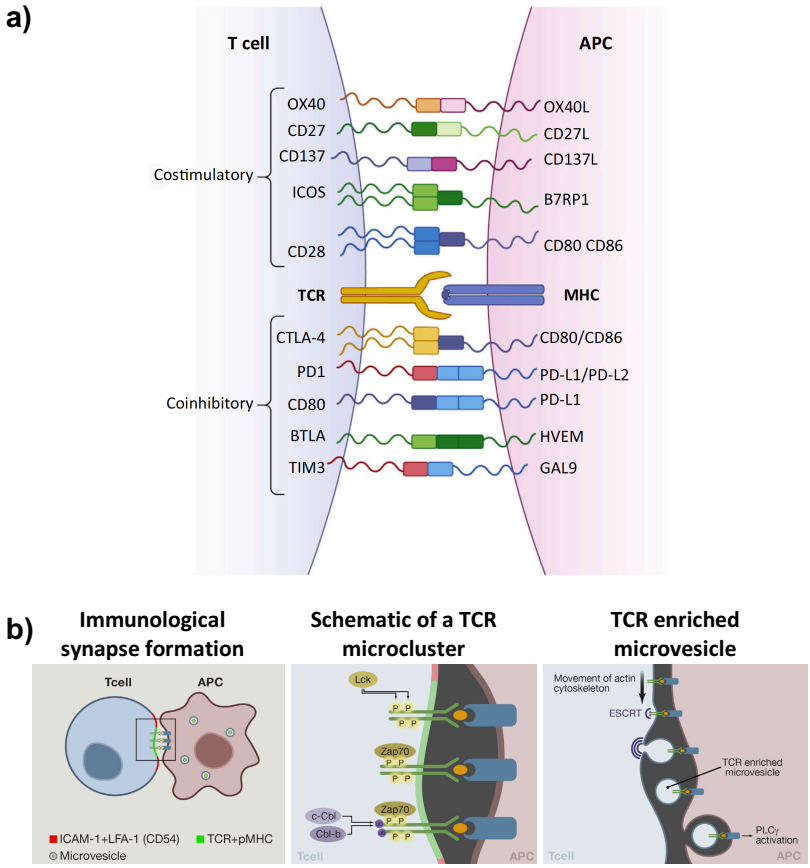


Figure 1.5 Immunological synapses.

(**a**) Schematic abstract of the signals occurring between a T cell and an antigen-presenting cells (APC), grouped into co-stimulatory and co-inhibitory signals. (**b**) TCR-enriched microvesicle formation in the immunological synapse is illustrated in the figure. (Figure (**a**) reprinted from Trends Mol. Med. *21*,. Pico de Coaña et al., 2015. Checkpoint blockade for cancer therapy: Revitalizing a suppressed immune system. 482–491. Copyright 2015 with permission from Elsevier; Figure (**b**) adapted from Dustin, 2014b).

1.8 Circulating and memory Tfh cells

1.8.1 Circulating Tfh cells

The name T "follicular" helper cells is indicative of the location of Tfh cells in the B cell follicle. This designation however does not preclude the presence of these Tfh $CD4^+$ T cells in other compartments, such as the peripheral blood or tissues. The majority of research to date on human Tfh has been restricted to peripheral blood because of difficulties in obtaining secondary lymphoid organs. Interestingly different populations of $CD4^+CXCR5^+$ T cells have been described in peripheral blood, termed "circulating Tfh" (cTfh), which represent a small frequency of the total memory $CD4^+$ T cells (Morita et al., 2011). Precise identification of cTfh cells within circulating $CD4^+CXCR5^+$ T cells is difficult, as canonical Tfh markers like PD-1 and ICOS are expressed at a much lower frequency in cTfh *ex vivo* compared to Tfh-GC cells from mice or human tonsils (He et al., 2013). Moreover, cTfh do not express Bcl-6 and in different studies cTfh cells are defined as either only $CXCR5^+$ or $CXCR5^+PD\text{-}1^{+/-}ICOS^{+/-}$ (Bentebibel et al., 2016; Morita et al., 2011). Despite discrepancies in cTfh definition, it is accepted that cTfh cells ($CXCR5^+$) promote Ig class-switching and plasmablast formation in co-cultures with naïve and memory B cells (Bentebibel et al., 2013; He et al., 2013; Locci et al., 2016; Morita et al., 2011). Based on the chemokine receptors CXCR3 and CCR6, different subsets of memory $CXCR5^+$ cTfh have been identified: Tfh Th1-like ($CXCR3^+CCR6^-$), Tfh Th2-like ($CXCR3^-CCR6^-$) and Tfh Th17-like ($CXCR3^-CCR6^+$). The names Th1-, Th2- and Th17-like are designated based upon the similarities of these subsets with canonical $CD4^+$ helper T cells Th1, Th2 and Th17. The diversity of cTfh phenotypes is also

evidenced by the differences in cytokine production and transcription factor expression observed when cTfh cells are co-cultured with naïve B cells (Morita et al., 2011):

- Tfh Th1-like: IFN-γ and T-bet expression
- Tfh Th2-like: IL-4, IL-5, IL-13, IL-21 and GATA-3 expression
- Tfh Th17-like: IL-17A, IL-21, IL-22 and RORγt expression

Depending on the antigenic stimulus used in the co-culture in different studies and how cTfh cells were identified, some of the above subsets showed a better ability to help B cells *in vitro* (Boswell et al., 2014; Locci et al., 2013). For example, using the super-antigen Staphylococcal enterotoxin B (SEB) in T and B cell co-cultures, Tfh Th2- and Th17-like cells were shown have a better capacity to help naïve B cells to become plasmablasts than Tfh Th1-like cells (Boswell et al., 2014; He et al., 2013; Locci et al., 2013). However, provision of cognate help to induce memory B cells to produce influenza-specific antibody was primarily mediated by Tfh Th1-like cells, identified as $CXCR5^+ICOS^+CXCR3^+$ (Bentebibel et al., 2013).

1.8.2 Memory Tfh cells

The role of circulating memory $CD4^+$ Tfh cells is still a highly-discussed topic in the field (Hale and Ahmed, 2015). After an immune response, a fraction of $CD4^+$ T helper 1, 2 and 17 cells survive as resting memory cells, maintaining the phenotype acquired during the initial priming to rapidly re-activate the same effector phenotype during a subsequent second challenge (Sallusto et al., 2010). During the immune effector phase, Tfh cells contribute to the production of long-lived memory B cells and therefore long-lived neutralizing antibodies, ready to provide protection on a

second encounter with the same pathogen (Victora and Nussenzweig, 2012). Generation of memory Tfh cells would then be unnecessary if the primary immune response was efficient. However, Tfh ($CXCR5^+$) memory cells promote an accelerated effective memory B cell response in the follicle after a second antigenic encounter as well as faster antibody-class switching (Macleod et al., 2011), which is important to facilitate rapid pathogen control if a second infection with the same pathogen is initiated, and also to enable antibody evolution if infection with an antigenically cross-reactive but different pathogen occurs. Other follow-up studies supported this hypothesis by describing generation of memory Tfh cells partially surviving after a primary immune response. Memory Tfh cells were shown to maintain CXCR5 expression, but to lose effector and activation markers such as PD-1, ICOS and Bcl-6 (Liu et al., 2012). A subsequent immune challenge then drove memory Tfh cells to a second effector Tfh phenotype with the ability to promote the generation of GC B cells (Fazilleau et al., 2007; Hale et al., 2013; Herati et al., 2017). The description of memory Tfh cells, that in the presence of memory and naïve B cells reactivate their follicular and "helping" function *in vitro*, is in line with the theory that memory Tfh cells are important to promote a rapid B cell memory response during a secondary challenge (Chevalier et al., 2011; Locci et al., 2013; Morita et al., 2011). A maintained reservoir of memory cTfh cells was also confirmed by an elegant study of successive influenza vaccinations, where oligoclonal Tfh cell responses were found many years later in memory cTfh cells (identified as PD-$1^+CXCR5^+ICOS^-CD38^-$) (Herati et al., 2017). The identity of memory cTfh cells is still unclear as well as the distinction between memory Tfh cells and other canonical memory T cells. Although cTfh show B cell helper functions

(unlike non-Tfh cells), it is still unclear whether cTfh cells might originate from $CXCR5^-$ memory $CD4^+$ T cells or whether they comprise a distinct population.

1.8.3 Circulating Tfh cell function and relationship with lymphoid organs

There is an obvious discrepancy between the classical effector Tfh-GC cell phenotype in the lymphoid organs and the different memory resting Tfh profiles found in the periphery. As described in detail above, effector Tfh-GC mainly produce IL-21 and IL-4 but do not produce IL-17A or IFN-γ, suggesting that effector Tfh cells do not present a heterogeneous profile, as observed for canonical T helper cells (eg. Th1, Th2, Th17). So how are peripheral Th1-, Th2- and Th17-like Tfh subsets generated? and are they or derivatives thereof involved in mediating effector functions? or if not, what is their role?

A few studies have shown a predominance of Tfh-Th1 cells during viral immune responses in humans and macaques (Bentebibel et al., 2013; Velu et al., 2016), although elicitation of Tfh-Th1 effector cells has been reported to be associated with a less efficient germinal centre response and suboptimal antibody production (Bowyer et al., 2018; Cubas et al., 2015; Obeng-Adjei et al., 2015; Ryg-Cornejo et al., 2016). The majority of recent studies agree on commitment of naïve $CD4^+$ T cells after viral challenge into the generation of two distinct lineages of Tfh-GC and Th1 cells (non-Tfh), which become effector and later memory cells (Boyden et al., 2012; Hale et al., 2013; Schmitt et al., 2016; Snell et al., 2016; Zander et al., 2017). This dual response against viral pathogens would allow at the same time the generation of both a Th1 effector response to act at the site of infection (driven by anti-viral IFN-

γ production) and a Tfh-GC response to promote the production of virus-specific antibodies. These findings are in line with the increase of cTfh CXCR3$^-$ cells after an immune response (Locci et al., 2013) and with the notion that Tfh CXCR3$^-$ contribute to a better and a more efficient humoral helper response (Hansen et al., 2017; Obeng-Adjei et al., 2015). This would also explain why cTfh CXCR3$^-$ is the subset in the periphery that best correlates with Tfh-GC cells both phenotypically and in gene expression profile studies (Locci et al., 2013). Other studies also described the important role of Tfh-Th17 in HIV infection (Boswell et al., 2014), but in a few studies a high level of Tfh-Th17 cells correlated with a pathological autoimmune scenario (Li et al., 2012; Yang et al., 2017).

Finally, it is well-known that antibody class-switch recombination directly depends on the cytokines in the environment: IL-5 induces IgA production, IFN-γ induces IgG3 and IgG2a, IL-4 induces IgE and TGF-β influences IgG2b production. The cytokines can be produced in part by T helper cells during B cell differentiation but also by other cells in the environment (Murphy, 2012; Reinhardt et al., 2009; Stavnezer, 1996). These findings suggest a requirement for Tfh heterogeneity after priming, in order to promote a high range of different types of specific antibodies during B cell contact.

Professor Shane Crotty has hypothesized different models to explain the discrepancy of the heterogeneous memory response combined with the unique features of non-heterogeneous effector Tfh-GC (Crotty, 2018) (**Figure 1.6**):

- The model of "imprinted partial plasticity" supports the idea that during priming by DC, the Tfh cell receives precise stimuli to acquire an initial skewed phenotype, for instance a Th1 profile. Tfh cells further differentiate

to effector Tfh-GC cells and downregulate most of these acquired Th1-program genes (such as *cxcr3*, *ifng* and *t-bet*). However, it is possible that the Th1-priming remains imprinted in the cell, hence when the Tfh-GC transit to the periphery and becomes a memory cell, it will re-express the initial Tfh/Th1 phenotype (**Figure 1.6 a**).

- The "de novo plasticity" model hypothesizes that a non-imprinted Tfh-GC cell is induced to become Th1, Th2 or Th17 from signals in the environment during its transit to become a memory cell, after mediating effector function (**Figure 1.6 b**).
- Heterogeneous memory Tfh cells could instead derive from mantle Tfh, so be generated during the early stage of the response just after being primed by a DC but before migrating into the follicle (**Figure 1.6 c**).

Thus, the ontogeny of heterogeneous subsets of memory circulating Tfh cells is still unknown, and this question goes in parallel with another important issue, which is the relationship between circulating and follicular Tfh cells. Given the importance of Tfh cell function for a specific humoral immune effector and memory response, evaluation of Tfh responses is crucial for the design of a productive vaccine in humans. Although minimally invasive techniques have been recently been developed to collect small number of cells from peripheral lymph nodes, such as fine needle aspirates (Diamantis et al., 2009; Havenar-Daughton et al., 2016; Prasad et al., 1996; Tatovic et al., 2015), methods that can detect peripheral markers to reflect the activity of Tfh cells in the germinal centre are needed and would be far more feasible to carry out on a large scale and would therefore be immensely valuable in clinical trials.

It is technically challenging and also problematic to compare circulating and germinal centre Tfh cells in humans. Firstly, the scarcity of matched secondary lymphoid organ and peripheral blood samples, second the additional difficulty and rarity of obtaining lymphoid organs and peripheral blood after a specific immune challenge and finally the limitations of the techniques and the parameters used currently to compare and identify Tfh cells in different compartments. Therefore, there are very few cohorts with matched lymph node and peripheral blood samples. A few studies have compared the phenotype and function of Tfh cells from secondary lymphoid organs and peripheral blood, although have not used donor-matched blood and lymphoid tissue samples (Chevalier et al., 2011; He et al., 2013). As described above, $CXCR5^{+}PD\text{-}1^{+}$ cells in the peripheral blood were the subset that showed the best ability to provide help to B cells, producing class-switched antibodies *in vitro* in different antigen systems (Chevalier et al., 2011; He et al., 2013; Morita et al., 2011). The capacity to help B cell class-switching however does not necessarily confirm a direct correlation between circulating and follicular Tfh cells during an immune response, especially given the ability of different memory Tfh cell subsets in the circulation to re-acquire Tfh function in the presence of B cells in assays *in vitro* (Bentebibel et al., 2013; Boswell et al., 2014). A limitation of considering only T cell phenotype and function is that they are variable features of $CD4^{+}$ T cells, which are known to be influenced by the stimuli in the environment and so the same cell type could express a different profile in different compartments and cell culture conditions (Sallusto et al., 2018).

Only two studies to date, have compared circulating and follicular Tfh cells using approaches that involve gene expression profiling or TCR repertoire analysis, rather

than phenotyping (Heit et al., 2017; Locci et al., 2013). In the interesting study by Locci et al. the gene expression profile of different $CD4^+$ T cell populations from infant tonsils was compared with that of peripheral blood populations from adult donors and $CXCR3^-$ cTfh were found to have the most similar gene expression profile to Tfh-GC cells from tonsils (identified as $CXCR5^{hi}PD\text{-}1^{hi}$) (Locci et al., 2013). In a more recent study where the TCR Vβ repertoires of Tfh-GC cells (identified as $CXCR5^{hi}PD\text{-}1^{hi}ICOS^{hi}$) and cTfh cells (identified as $CXCR5^+PD\text{-}1^+ICOS^{-/+}$) from matched tonsil and blood respectively were compared, limited overlap was observed between the two populations (Heit et al., 2017). More extensive studies to directly compare human cTfh with follicular Tfh-GC are therefore required. It is of paramount importance to know that the cTfh populations routinely studied in vaccine trials for example, are truly reflective of the GC response.

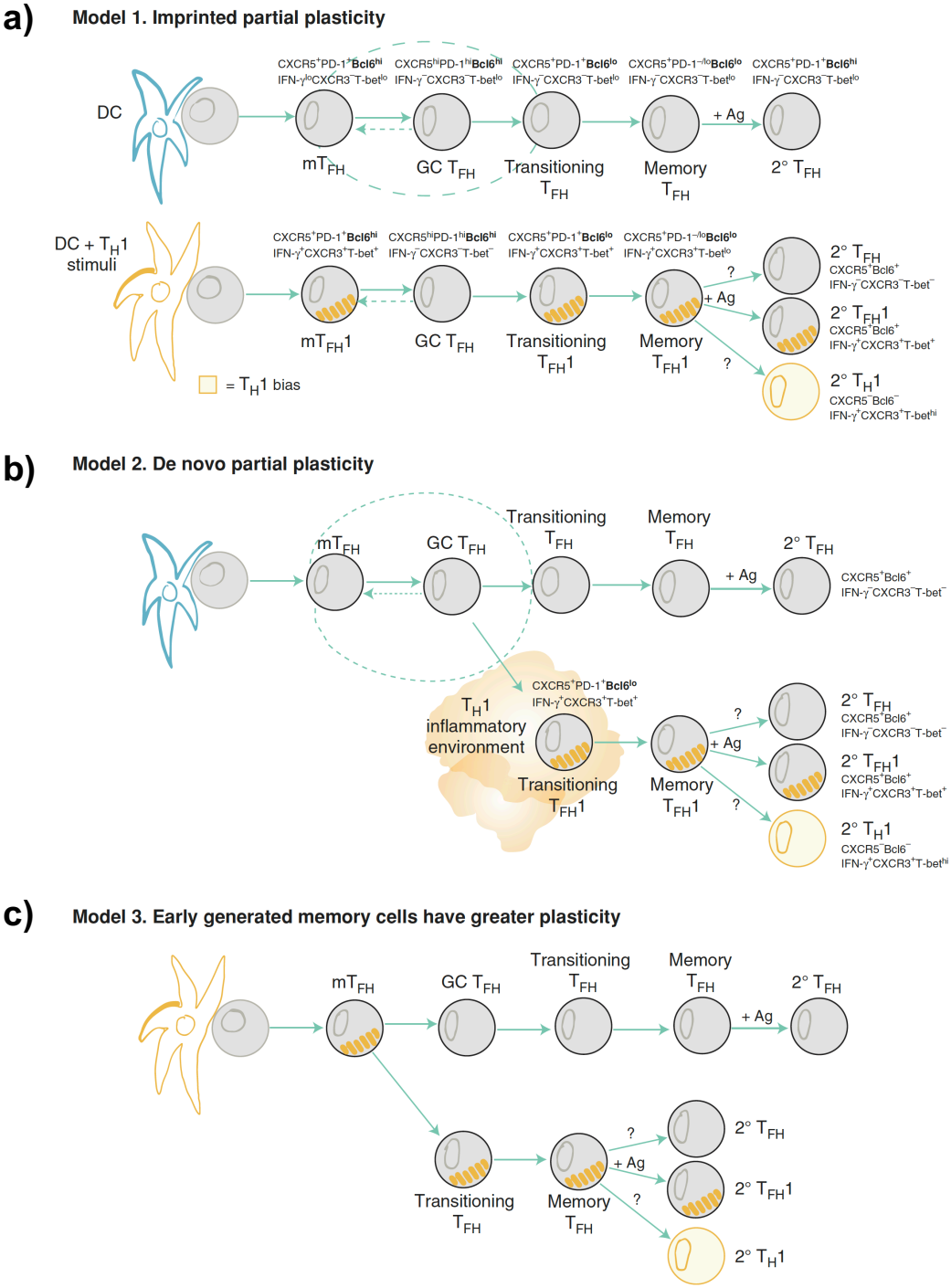

a)
Model 1. Imprinted partial plasticity
DC
CXCR5+PD-1+Bcl6hi IFN-γloCXCR3−T-betlo
CXCR5hiPD-1hiBcl6hi IFN-γ−CXCR3−T-betlo
CXCR5+PD-1+Bcl6lo IFN-γ−CXCR3−T-betlo
CXCR5+PD-1−/loBcl6lo IFN-γ−CXCR3−T-betlo
CXCR5+PD-1+Bcl6hi IFN-γ−CXCR3−T-betlo
mTFH
GC TFH
Transitioning TFH
Memory TFH
+ Ag
2° TFH
DC + TH1 stimuli
CXCR5+PD-1+Bcl6hi IFN-γ+CXCR3+T-bet+
CXCR5hiPD-1hiBcl6hi IFN-γ−CXCR3−T-bet−
CXCR5+PD-1+Bcl6lo IFN-γ+CXCR3+T-bet+
CXCR5+PD-1−/loBcl6lo IFN-γ+CXCR3+T-betlo
mTFH1
GC TFH
Transitioning TFH1
Memory TFH1
?
+ Ag
2° TFH CXCR5+Bcl6+ IFN-γ−CXCR3−T-bet−
2° TFH1 CXCR5+Bcl6+ IFN-γ+CXCR3+T-bet+
2° TH1 CXCR5−Bcl6− IFN-γ+CXCR3+T-bethi
= TH1 bias
b)
Model 2. De novo partial plasticity
mTFH
GC TFH
Transitioning TFH
Memory TFH
+ Ag
2° TFH CXCR5+Bcl6+ IFN-γ−CXCR3−T-bet−
TH1 inflammatory environment
CXCR5+PD-1+Bcl6lo IFN-γ+CXCR3+T-bet+
Transitioning TFH1
Memory TFH1
?
+ Ag
2° TFH CXCR5+Bcl6+ IFN-γ−CXCR3−T-bet−
2° TFH1 CXCR5+Bcl6+ IFN-γ+CXCR3+T-bet+
2° TH1 CXCR5−Bcl6− IFN-γ+CXCR3+T-bethi
c)
Model 3. Early generated memory cells have greater plasticity
mTFH
GC TFH
Transitioning TFH
Memory TFH
+ Ag
2° TFH
Transitioning TFH
Memory TFH
?
+ Ag
2° TFH
2° TFH1
2° TH1

Figure 1.6 Three model hypotheses about Tfh memory heterogeneity.
Model 1 (**a**): "imprinted partial plasticity" supports the idea that during priming the Tfh cell receives precise stimuli to acquire a specific phenotype. Model 2 (**b**): "de novo plasticity" hypothesizes that non-imprinted Tfh-GC cells are induced to differentiate into Th1, Th2 or Th17 during its transit to become memory cells. Model 3 (**c**): heterogeneous memory Tfh cells derive from mantle Tfh, so are produced during the early stage of the response just after being primed by a DC but before migrating into the follicle (Reprinted figure from Cold Spring Harbor Laboratory press: Perspectives in Biology. Complexities of Interpretation due to the Heterogeneity of Memory CD4 T Cells, Including T Follicular Helper Cells. Shane Crotty, Copyright 2018).

1.9 T cell response to Influenza virus

Influenza viruses cause infections of the respiratory tract and are responsible for an estimated 3 to 5 million clinical infections and half a million deaths every year worldwide (World Health Organization, 2011). The circulating influenza viruses that cause human disease are divided into two types, influenza A and B, which are further divided into subtypes on the basis of their haemagglutinin (HA) and neuroaminidase (NA) protein expression (eg the H1N1 and H3N2 subtypes of influenza A) (World Health Organization, 2011). The diversity of influenza subtypes, each of which also undergoes antigenic variation, facilitates virus persistence at the population level by enabling serial infection of individuals with antigenically diverse influenza viruses.

Neutralizing antibody responses to influenza usually target the two main surface glycoproteins, HA and NA (Grant et al., 2014). Analysis of the B cells responding to influenza virus have enabled isolation and characterization of panels of

monoclonal antibodies against HA and NA that directly bind the virus surface, preventing entry into host cells, and exhibit varying levels of protection activity against diverse influenza strains (Corti et al., 2011; Sui et al., 2009; Wrammert et al., 2011). T cells play an important role in the response to influenza virus (Kreijtz et al., 2011). Activated antigen-specific $CD8^+$ T cells migrate to the site of infection and clear infected cells by cytotoxic activities, such apoptosis induction via Fas/FasL, cytotoxic granule production (perforin and granzymes) and production of various cytokines (IFN-γ, IL-1β and TNF-α) that help the recruitment of other immune cells (Bender et al., 1992; Hamada et al., 2013; Topham et al., 1997). After the acute infection phase, memory influenza-specific $CD8^+$ T cells continue to circulate and can be rapidly recalled for a secondary infection (Grant et al., 2014; Murali-Krishna et al., 1998). $CD4^+$ T cells are also implicated in the immune response against influenza: they act by providing cytokines and costimulatory signals to promote B cell activation and $CD8^+$ T cell help during the effector phase (Boyden et al., 2012; Sun and Bevan, 2003). $CD4^+$ T cells can also directly kill infected cells in the site of infection similar to $CD8^+$ T cells, although obviously less efficiently, and assume a cytotoxic function (Soghoian and Streeck, 2010). Moreover, the importance of memory $CD4^+$ T cell in influenza is crucial for viral clearance of a secondary infection (Belz et al., 2002). Recent studies have focused on the importance of pre-existing T cell repertoire in disease protection on the re-infection with influenza virus and have shown a specific correlation between influenza-specific $CD4^+$ T cells and limitation of illness severity (Wilkinson et al., 2012). High precursor frequencies of influenza-specific $CD4^+$ T cells are predominantly found in T helper 1 cells, which are cells characterized to secrete IFN-γ and TNF-α (Zielinski et al., 2011). In

addition, generation of T follicular helper cells with a Th1 phenotype (Tfh-Th1) is also observed during influenza virus infection (Bentebibel et al., 2013; Boyden et al., 2012; Velu et al., 2016).

As adults have frequently been infected multiple times in their lifespan by different influenza strains, it is common to find memory influenza-specific $CD4^+$ and $CD8^+$ T cells in healthy individuals with reactivity against different influenza subtypes (Alam and Sant, 2011; Fazilleau et al., 2007; Sant et al., 2018). Because of the frequent mutation of this virus, influenza vaccines need to be updated annually, although the efficacy of the vaccine can be limited if the predicted strain does not match the one that subsequently circulates, so vaccines commonly provide sub-optimal protection (Grant et al., 2014). Research efforts have focused on strategies to optimise influenza vaccinations by developing an influenza vaccine that elicits universal protection against different influenza strains and could prevent pandemic and seasonal outbreaks in the future (Wang et al., 2018). Improved understanding of the specificity, phenotype and function of Tfh cells in the context of influenza would be of substantial benefit to this concerted vaccine development effort.

1.10 Research questions and objectives

The T follicular helper T cell subset was only described 18 years ago and so there are a large number of open questions in the field. The detailed description of different phenotypes and functions of Tfh cells at different stages of an immune response in the last 10 years have highlighted the heterogeneity of these cells and suggested that Tfh cells undergo different phases of differentiation from a naïve T cells to effector

and then memory Tfh, in parallel with a canonical immune response process. Although the differentiation of Tfh cells from naïve T cells is becoming clearer, several elements about Tfh cells heterogeneity remain unknown. There is for instance little understanding about the lineage relationships between primed Tfh-like cells, effector Tfh-GC and memory Tfh cells in the circulation. Since tracking a Tfh cell *in vivo* to explore its fate is an ambitious challenge, the major limitations regarding the lack of understanding in this field remain the techniques and the parameters used to compare and identify Tfh cells in different compartments as well as the availability of different tissues from the same donor in human studies.

Open research questions:

• The relationship between antigen-experienced Tfh-like or effector Tfh-GC cells in secondary lymphoid organs and peripheral Tfh memory cells is still poorly understood. This question is important for informing future immunological studies in human since it is still not clear how much focusing on peripheral Tfh cells (and which are the best markers to identify them) reflects the activity of effector follicular Tfh cells in the GC. Elucidation of this point might give insight into the origin and the role of circulating memory Tfh cells in the periphery.

• The ontogeny of memory Tfh populations and their relationship with the total $CD4^+$ memory compartment is an open question and it is still not clear whether, after a secondary antigen exposure, effector Tfh cells are generated from memory Tfh and/or from $CXCR5^-$ memory cells (non-Tfh memory cells). An in-depth examination of the relationship between $CD4^+$ memory Tfh and non-Tfh cells would

go to help answer this point. This issue is of great importance in the context of vaccination strategies: we need to know whether investigating the response of Tfh cells after an immune challenge requires focusing specifically on these populations rather than studying total memory $CD4^+$ T cells. This is a crucial question for clinical trials where T cell responses are being investigated and has significant implications in terms of the size of blood draw that is required to gain an accurate representation of the GC response.

• Although several studies have shown functional similarities between follicular and circulating Tfh cells, there is still little known about the precise and delimited signals in the immune synapse between Tfh and B cells. The impact that Tfh peptide-avidity has on B cell activation is also unclear and whether this may differ between antigen-specific effector or Tfh-like cells from secondary lymphoid organs and circulating Tfh cells. Improved understanding of immune synapses may delineate important elements, like the role of T cell peptide-avidity and its impact on molecules trafficking from the T to the B cell, that determine B cell effector function and antibody maturation. An understanding of how clonal avidity of the T cells affects antibody responses would be of importance to vaccine studies.

In the light of these questions, the objectives of this thesis were:

1) To develop methodologies required to define, isolate and phenotype different Tfh and non-Tfh cell subsets from tonsillar tissue and peripheral blood in addition to developing techniques to enable analysis of the repertoires of $CD4^+$ T cell subsets from both tissues. Defining phenotypically-distinct

subsets of antigen-experienced $CD4^+$ T cells in blood and tonsils was fundamental to enabling the direct comparison of different populations of circulating and follicular Tfh cells (section 3).

2) To directly compare the repertoire of circulating and follicular Tfh cells from peripheral blood and tonsils, as well as Tfh and non-Tfh cells, by considering a stable T cell parameter, such as the T cell receptor (TCR) (section 4).
3) To extend conclusions made in section 4 to antigen-specific cells (using haemagglutinin protein from influenza virus as a model antigen), by generating antigen-specific Tfh and non-Tfh cell clones and correlating peptide specificity with CDR3 sequence of the TCR. This study also enabled comparison of TCR usage by antigen-specific circulating Tfh with tonsillar Tfh and non-Tfh repertoires (section 5).
4) To establish techniques that could be used to investigate the role of T cell avidity in a cognate synapse. High-resolution technologies describing microvesicle trafficking in the immune synapses together with T-B cell co-culture assays were optimised to further distinguish precise and delimited signals between Tfh and B cells (section 6).

2 Materials and methods

2.1 Cohorts and ethics

In order to obtain tonsillar nodules and peripheral blood samples from adult donors we amended an existing cohort (LABFLU002), which was designed to collect tonsils and adenoids from children, in collaboration with Prof Sarah Gilbert from the Jenner Institute and Mr James Ramsden from the John Radcliffe Hospital in Oxford. Ethical approval for the study was given by REC Oxford B committee, reference is 13/SC/0152. The study amendment allowed tonsil and/or adenoid tissues to be collected from 30 volunteer adult donors (16-50 years old) who were admitted to the John Radcliffe Hospital in Oxford for elective tonsillectomy or adeno-tonsillectomy. In addition to tonsil and/or adenoid tissues the donors also consented to donate, the day of the surgery, peripheral blood (80-100 mL). Informed consent was taken the day of the operation and few demographic data were recorded by the clinical team, such as date of birth, gender and previous immunisation against influenza. Patients were excluded from the study if they were affected by immunodeficiency, serious infection (eg. Hepatitis B, Hepatitis C or HIV infection), lymphoid malignancy, cytogenetic disorders, history of cancer, patients with any pre-existing heart disease or blood clotting disorder. The participants were only enrolled for collection of samples at the day of their operation and were not followed-up by the study team.

PBMC from cone samples used for feeder cells, titration or optimisation were processed from healthy donors from the UK National Blood Service.

2.2 Media preparation

All media were sterile filtered (0.45 μm) before use. T cells in culture were expanded in complete media (**Figure 2.1**) supplemented with interleukin-2, IL-2 (500 U/mL). **Figure 2.1** lists the different media used for the cellular assays described herein: MACS buffer, HSA buffer, freezing media, FACS buffer and wash buffer. IL-2 was produced in house by harvesting the supernatant of cultured T-6 cell line which produces high concentrations of IL-2. The concentration of IL-2 was then calculated using a cytotoxic T cell lines (CTLL) cultured in different IL-2 concentration conditions and the proliferation measured using [3H]-thymidine incorporation (Gillis and Watson, 1980; Gillis et al., 1978).

Tonsil samples growth and viability was optimised using 3 different media conditions (**Figure 2.2**) containing IL-2 (500 U/mL).

Name of the medium	Reagents
Complete media (CM)	Roswell Park Memorial Institute medium RPMI Glut [-] (Invitrogen), Non-essential amino acids (1%, Invitrogen), Sodium pyruvate (1%, Invitrogen), Glutamine (1%, Invitrogen), Pooled AB Human Sera (5%, UK National Blood Service), β-mercaptoethanol (0,1%, Invitrogen), Penicillin Streptomycin (1%, Invitrogen)
Complete media IL-2 (CM IL-2)	Complete Media with 500 U/mL of IL-2
MACS buffer	Dulbecco's phosphate buffered saline (Sigma), Fetal Bovine Serum (3%, Sigma), EDTA (1mMol, Invitrogen)
HSA buffer	Human serum albumin (HSA)-supplemented HEPES-buffered saline (HBS)
Freezing media	Pooled AB Human Sera (50%, UK National Blood Service), Roswell Park Memorial Institute medium RPMI Glut [-] Hepes [+] (40%, Invitrogen), Dimethyl sulfoxide (10%, Sigma)
Wash buffer	Roswell Park Memorial Institute medium RPMI Glut [-] Hepes [+] (Invitrogen), Complete media (10%)

Figure 2.1 General media reagents.

The name and the reagents composition for each medium are listed in the table.

Reagent and concentration used	MEDIA 1 (Complete media, CM)	MEDIA 2	MEDIA 3
Roswell Park Memorial Institute medium RPMI Glut [-] (Invitrogen)	✓	✓	✓
Non-essential amino acids (1%) (Invitrogen)	✓	✓	✓
Sodium pyruvate (1%) (Invitrogen)	✓	✓	✓
Glutamine (1%) (Invitrogen)	✓	✓	✓
Pooled AB Human Sera (5%) (UK National Blood Service)	✓	✓	✓
Antibiotics (1%)	**Penicillin Streptomycin** (Invitrogen)	**Gentamicin** (Sanofi)	**Gentamicin** (Sanofi) **Timentin** (GlaxoSmithKline)
β –mercaptoethanol (0,1%, Invitrogen)	✓	✗	✗
Antifungal drugs (1%, Invitrogen)	✗	✓	✓
Inteleukin-7 (1µg/mL, Sigma)	✓ / ✗	✓ / ✗	✓ / ✗

Figure 2.2 List of reagents used for different media conditions.

The reagent compositions of Media 1, Media 2 and Media 3 used for tonsil optimisation are listed in the table. ✓= reagent was present, ✗= reagent was not present, ✓ / ✗ = the media was used with and without the reagent.

2.3 Peripheral blood and tonsil tissues processing

2.3.1 PBMC separation

Peripheral blood from patients who underwent tonsillectomy or cone samples from healthy donors from UK National Blood Service were processed using density centrifugation. Briefly whole blood was diluted 1:2 with HBSS (Hank's Balance Salt Solution, Sigma) and then layered over 20 mL Histopaque-1077 (Sigma-Alderich). Following centrifugation at 800 g for 30 minutes (no brakes) the peripheral blood mononuclear cell fraction (PBMC) was isolated and washed 3 times with 50 mL HBSS using 350 g x 10 minutes centrifugation cycles. Cells were counted using automated cell counter T20 (Bio-rad) and viability determined with Trypan Blue Stain exclusion (Invitrogen).

Plasma samples were collected from a non-diluted 5 mL of the whole blood from each patient who underwent tonsillectomy, after 30 minutes centrifugation at 800 g (no breaks) plasma samples were stored at -80°C.

2.3.2 Mononuclear cells from tonsil (MNC-T) separation

Tonsil nodules from adult donors who underwent tonsillectomy were collected and processed within 2 hours of surgery in CM and kept on ice during the transportation. Tonsillar tissues were cleared from fatty and necrotic sections, and weighed. Two examples of tonsil nodules from two different patients, are shown (**Figure 2.3 a**). Half of the nodule was then processed manually, while the other half was processed using gentleMACS (Miltenyi) and enzymes (Collagenase D type IV 1 mg/mL, Invitrogen; Deoxiribonuclease-I, DNase-I, 3000 U/mL, Invitrogen; Dispase-II, 0.04 mg/mL, Sigma).

The tissue for manual processing was first cut into 2-3 mm sections using scalpels and scissors. The sections were then passed through a 70 μm cell strainer and then filtered with a 40 μm strainer (Grivel and Margolis, 2009).

The gentleMACS (Miltenyi) protocol for processing MNC-T was adapted and optimised from the published, manufacturers protocol (Cupedo and Papazian, 2012). Briefly, the 2-3 mm sections of clean tonsil tissue were transferred into gentleMACS C tubes and re-suspended in CM with activated Collagenase DNase-I, and Dispase-II. After performing 2 runs of Program C for 1 minute in the gentleMACS Dissociator, cells in suspension were subsequently filtered on a 70 μm and 40 μm cell strainers.

Cells from tonsillar tissues, from both processing protocols, were then layered over 30 mL Histopaque-1077 (Sigma-Alderich). Following centrifugation at 800 g for 30 minutes (no brakes) the MNC-T were isolated and washed 3 times with 50 ml CM using 350 g x 10 minutes centrifugation cycles. The cells were counted using automated cell counter T20 (Bio-rad) and viability determined with Trypan Blue Stain exclusion (Invitrogen). Each tonsil sample was tested for Mycoplasma contamination using MycoAlert Mycoplasma Detection Kit (Lonza) and cells were kept in culture in antibiotic-free media for 2 days to check for fungi and bacteria contamination. **Figure 2.3 b** shows an example of a flow cytometry staining (panel C, see Figure 2.5) in MNC-T processed either manually or with gentleMACS. The biased expression of CXCR5 in the last dot plot, probably caused by the enzymes used and the mechanical stress during the gentleMACS processing, did not allow the proper distinction of the $CD4^+$ memory populations of interest. For this reason, tonsil data presented in this thesis are derived from MNC-T processed manually.

Tonsil samples used for optimisation studies, such as testing media conditions and viability during expansion from chapter 3, were tonsil samples from children from the same ethic study (LFU 002), manually dissociated, already cryopreserved and stored in liquid nitrogen.

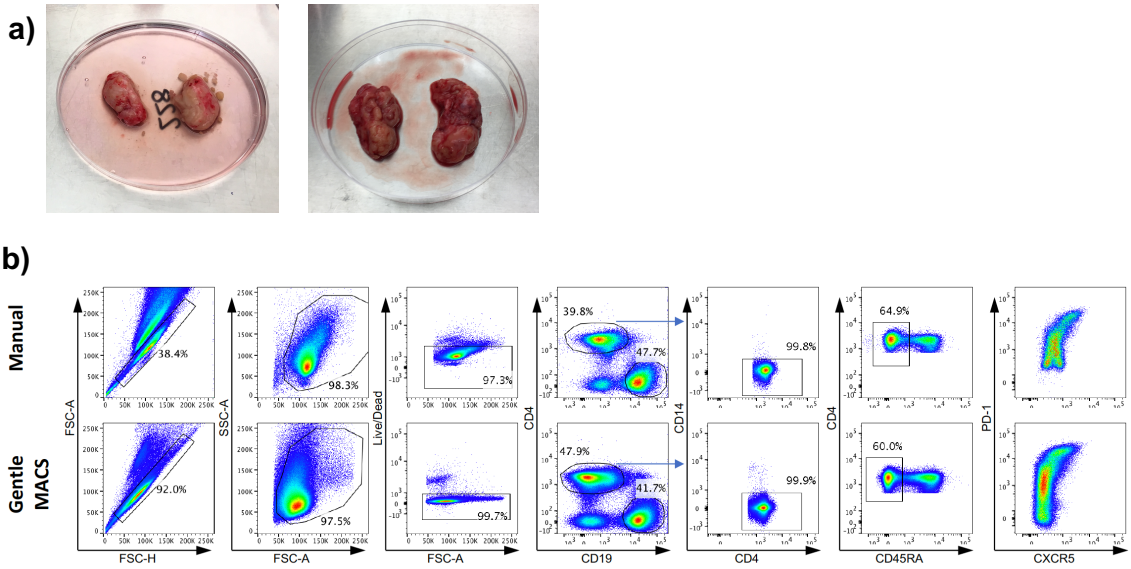


Figure 2.3 Tonsil processing and flow cytometry staining comparison.

Two tonsil nodules from two different patients, (**a**) cleared from fatty and necrotic sections, are shown. (**b**) Example of one tonsil donor processed manually or with gentleMACS is shown. From singlet cells, identified with FSC-A and FSC-H, lymphocytes were gated based on FSC-A and SSC-A. The cells were then negatively selected for dead/dying cells and the $CD4^+$ were gated. $CD14^+$ were gated out of the $CD4^+$ T cells and within memory $CD45RA^-CD4^+$ it is shown the expression of PD-1 and CXCR5.

2.3.3 Preparation of feeder cells

PBMC from cone samples were processed from healthy donors, UK National Blood Service, as described above (section 2.3.1). PBMC was then irradiated at 45 Gy (Cesium-137) at the John Radcliffe Hospital, washed, counted, and re-suspended in the same media of the cells that needed to be expanded, which was usually CM IL-2. If different donors were processed, cells were mixed after irradiation. Allogeneic feeder was always used at $0.5x10^6$ cell/mL.

2.4 Flow cytometry analysis and sorting strategy

For experiments that required sorted lymphocytes, the gating was performed on singlet population first (FSC-H versus FSC-A), then the size and the granularity of cells used to identify lymphocytes. Surface markers of natural killer cells (CD16 and CD56) and $CD8^+$ T cells in addition with dead/dying cells were used to exclude cells we did not wish to study. From this backbone gating strategy (**Figure 2.4**) $CD4^+$ and $CD19^+$ cell populations were sorted. The live lymphocyte fraction was stained using surface or intracellular markers antibodies to allow identification and isolation of the various populations of interest.

The table in Supplementary material (**Figure 8.1**) contains the complete list of anti-human antibodies used along different experiments and the respective fluorocrome, manufacture, clone and titration optimised (Brodie et al., 2013).

For each experiment, the flow cytometry panel was internally validated using single stain compensation beads (BD) for the generation of a compensation matrix. For internal validation compensation values for each panel were not permitted to exceed 90 %. The list of flow panels optimised, is shown in the table (**Figure 2.5**).

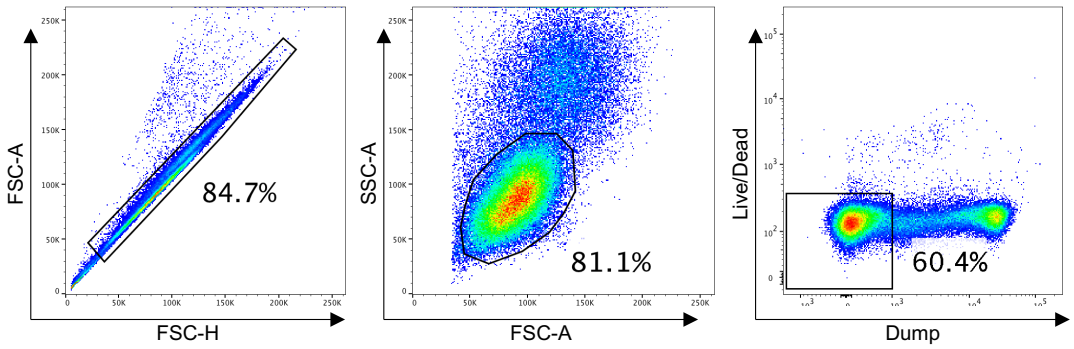


Figure 2.4 Gating strategy for T cell analysis.

Example from a PBMC healthy donor. From singlet cells, identified with Forward Scatter-Area (FSC-A) and Forward Scatter-Height (FSC-H), lymphocytes were gated based on FSC-A and Side Scatter-Area (SSC-A). The cells were then negatively selected for dead/dying cells and dump markers (CD16, CD56, CD8) in addition with other dump markers that vary in each different flow cytometry panel, depending on the cells that needed to be excluded.

Panel A: Tfh surface markers	
Antibody	**Fluorocrome**
Anti-CXCR5	A488
Anti-CXCR3	PE Cy5
Anti-PD-1	BV421
Anti-CD4	APC Cy7
Anti-CD3	BV605
Anti-CD45RA	PETR
Dump (CD8, CD14, CD25, CD16, CD56)	PE Cy7

Panel B: Tfh intracellular markers	
Antibody	**Fluorocrome**
Anti-CXCR5	A488
Anti-CXCR3	PE Cy5
Anti-PD-1	BV421
Anti-CD4	APC Cy7
Anti-CD45RA	PETR
Dump (CD8, CD14, CD25, CD16, CD56)	PE Cy7
Anti-IL-21	A467
Anti-IL-4	PE
Anti-IL-10	BV785
Anti-IFN-γ	A700

Panel C: T and B cells composition	
Antibody	**Fluorocrome**
Anti-CD14	PE
Anti-CD19	BV650
Anti-CD127	BV785
Anti-HLA-DR	PerCp
Anti-CD4	APC Cy7
Anti-CD45RA	PETR
Anti-PD-1	BV421
Anti-CXCR5	A488
Anti-CXCR3	PE Cy5
Anti-CD25	PE Cy7
Anti-CCR6	BV605
Anti-ICOS	BV711
Anti-CD8	A700
Anti-Foxp3	A647
Anti-Bcl-6	PE

Panel D: antigen-enriched panel	
Anti-CD4	APC Cy7
anti-CD3	PETR
Anti-ICOS	PE
Anti-CD25	PE Cy7
Dump (CD14)	FITC

Panel E: Vesicle transfer	
Antibody	**Fluorocrome**
Anti-BST2	PE
Anti-CD4	PerCP/Cy 5.5
Anti-CD40L (CD154)	A647
Anti-$\alpha\beta$TCR	A700
Silica beads	BV421
Anti-ICOS	BV785

Panel F: cTfh intracellular phenotyping	
Antibody	**Fluorocrome**
Anti-CXCR5	A488
Anti-CXCR3	PE Cy5
Anti-CD3	BV605
Anti-CD4	APC Cy7
Anti-CD45RA	PETR
Dump (CD8, CD14, CD25, CD16, CD56)	PE Cy7
Anti-IL-21	A467
Anti-IL-4	PE
Anti-IFN-γ	A700
Anti-IL-17A	BV421

Panel G: TCR Vβ staining	
Antibody	**Fluorocrome**
Anti-CXCR5	A647
Anti-CXCR3	PE Cy5
Anti-PD-1	BV421
Anti-CCR6	BV605
Anti-CD4	APC Cy7
Anti-CD45RA	PETR
Dump (CD8, CD14, CD25, CD16, CD56)	PE Cy7

Panel H: sorting T cell clones	
Antibody	**Fluorocrome**
Anti-CD4	APC Cy7
Anti-CD3	PerCp

Panel I: T-B cell co-culture	
Antibody	**Fluorocrome**
Anti-CD4	APC Cy7
Anti-CD3	PETR
Anti-CXCR5	PerCP/Cy 5.5
Anti-CD40	A700
Anti-CD40L (CD154)	PE
Anti-CD86	PE Cy5
Dump (CD8, CD14, CD25, CD16, CD56)	PE Cy7
Anti-CD19	BV605
Anti-CD27	APC Fire
Anti-ICOS	BV650
Anti-ICOSL	BV421
Anti-$\alpha\beta$TCR	BV711
Anti-CD38	BV785

Panel L: T cell clones and B cell co-culture	
Antibody	**Fluorocrome**
Anti-CD3	PETR
Anti-CD19	APC Cy7
Anti-CD40	A700
Anti-CD86	PE Cy5
Anti-CD38	BV785
Dump (CD8, CD14, CD25, CD16, CD56)	PE Cy7
Anti-ICOSL	BV421
Anti-$\alpha\beta$TCR	BV711
Anti-ICOS	PE

Figure 2.5 List of optimized flow cytometry panels used within this thesis.

Antibodies and fluorocromes of different flow cytometry panels are listed in the table.

2.5 Peptide pools, matrices and antigen screening

$CD4^+$ T cells were screened for antigen-specificity using either a proliferative approach (3H-thymidne incorporation), or IFN-γ production (ELISpot), with pools of peptides or whole proteins (**Figure 2.6**). Peptides were commercially synthetized from GenScript or provided by BEI Resources (Biodefence and Emerging Infection Research Resources Repository) and the purity defined using mass spectrometry. Sequences of overlapping peptides are listed (Supplementary **Figure 8.2** and **Figure 8.3**). Master stock of each peptide was made by reconstitution in 100 % DMSO (Sigma, UK) to a final concentration of 40 mg/mL and stored at –80°C. Peptides were used at a final concentration of 2 μg/mL and working stocks of 20 μg/mL were made in CM. In-house quality control was performed to ensure that pools of interest had not become contaminated by culturing in antibiotic-free media for one week.

Antigen-specific T cell clones were mapped at the peptide level. Peptide matrices from HA/California and HA/Wisconsin peptides were designed using "Deconvolute This!" (Precopio et al., 2008) with an ambiguity of 1 and a coverage of 3. After 4 hours of resting in CM, $1.5x10^5$ T cell/well were cultured with the matrix of peptides. At day 3 of stimulation after 16 hours of 1 uCi/ml [^{3}H]-thymidine incorporation (Perkin Elmer) the proliferation was measured using a β-counter reader (Perkin Elmer). Positive responses were defined as >1000 cpm (counts per minute), with a stimulation index >5 (**Figure 2.7 a)**. Cells clones were excluded from analysis if the background counts were >1000 cpm. Some clones were mapped using ELISpot assay rather than proliferation response. Positive responses were defined as >100 SFU/10^6 (Spot Forming Unit), with a stimulation index >5 (**Figure 2.7 b)**.

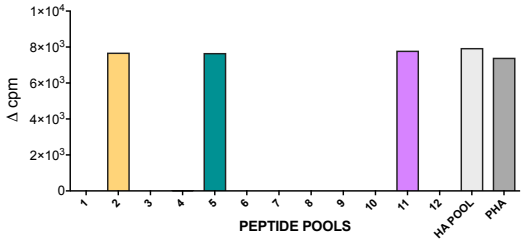
Cell clones were excluded from analysis if the background counts were >100 SFU/10^6. The specificity for the peptides resulted from the matrix stimulation was then confirmed again after 3 days stimulation.

Pool name	Description	Final concentration	N. of peptides in pool
HA/Wisconsin peptides array	Peptides are 13- to 17-amino acids long, with 7 to 12 amino acid overlap spanning the entire Haemmaglutinine protein (A/Wisconsin/67/2005, H3N2, from BEI)	2 μg/mL	93
HA/Wisconsin protein	Haemmaglutinine protein (A/Wisconsin/67/2005, H3N2, from BEI)	5 μg/mL	-
HA/California peptides array	Peptides are 15- to 18-amino acids long, with 12 amino acid overlap spanning the entire Haemmaglutinine protein (A/California/04/2009, H1N1, from GenScript)	2 μg/mL	70
SEB	Superantigen Staphylococcal Enterotoxin-B (Sigma, S4881)	1 μg/mL	-
Control antigens			
DMSO	Dimethyl sulfoxide (DMSO) in CM as negative control (Sigma)	0.45%	-
PHA	Phytohemagglutinin as positive control (Sigma)	5 μg/mL	-
IL-2	Interleukin-2 produced in house	500 U/mL	-

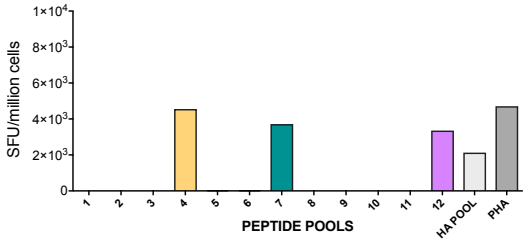
Figure 2.6 Antigens and controls.

Peptide pools, antigens and controls used for screening T cell libraries, confirming specificity of clones, stimulating T and B cells in co-culture. The columns showed the name of the pool/antigen, description, final concentration used and number of peptides in case of peptide pools.

a)



b)



c)

HA/California Matrix		PEPTIDE ID																	
DIMENSION 1	POOL 1	16	69	14	61	70	48	8	24	47	17	43	42	23	3	21	57	5	7
	POOL 2	51	18	**45**	**56**	59	4	35	10	32	38	68	27	33	31	46	15	62	11
	POOL 3	1	/	67	25	19	22	6	30	9	44	53	39	26	/	40	58	63	12
	POOL 4	34	13	37	28	20	52	60	55	36	49	41	2	29	64	54	66	50	65
DIMENSION 2	POOL 5	16	69	14	61	70	51	18	**45**	**56**	59	1	/	67	25	34	13	37	28
	POOL 6	48	8	24	47	17	4	35	10	32	19	22	6	30	20	52	60	55	36
	POOL 7	43	42	23	3	21	38	68	27	33	9	44	53	39	49	41	2	29	64
	POOL 8	57	5	7	31	46	15	62	11	26	/	40	58	63	12	54	66	50	65
DIMENSION 3	POOL 9	16	69	48	43	57	51	4	35	38	31	1	19	9	26	34	20	49	54
	POOL 10	14	61	8	42	5	18	10	68	46	/	22	44	/	13	52	41	66	50
	POOL 11	70	24	47	23	7	**45**	**56**	32	27	15	67	6	53	40	37	60	2	65
	POOL 12	17	3	21	59	33	62	11	25	30	39	58	63	12	28	55	36	29	64

Figure 2.7 Example of T cell clones mapping results.

Antigen-specific T cell clones were mapped using a 3-dimensional matrix: yellow=1st dimension, green=2nd dimension, purple= 3rd dimension. The responses were evaluated with either proliferation or by IFN-γ production. (**a**) An example of [3H]-Thymidine incorporation assay is shown. The values on the y-axis indicate the count per minute with background subtraction (Δcpm). (**b**) An example of ELISpot assay is shown. The values on the y-axis indicate the Spot Forming Unit per million cells (SFU/million cells). In both graphs the peptide pools are listed on the x-axis with the positive controls (HA pool=light-grey and PHA=dark grey). (**c**) In the HA/California matrix from the positive pools, the responding peptides recurring 3 times were highlighted and re-confirmed.

2.6 Repertoire analysis

2.6.1 T cell library technique

From PBMC, $CD14^+$ and $CD4^+$ cells were enriched using microbeads positive selection (Miltenyi Biotec). The $CD14^+$ fraction was cryopreserved in Freezing media (see Figure 2.1), to use later as antigen presenting cells. $CD4^+$ T cells were stained for flow cytometry panel A (see Figure 2.5) and sorted at the FACSAria (BD Bioscience). The sorting was performed at 4-Way purity to sort 3-5x10^5 cell per subset, although some donor variations were detected, purity was never lower than 90 %. Sorted T cells were counted using automated Z1 counter (Beckman coulter) and seeded in CM-IL-2 at limiting dilution of 1,000 cell/well and expanded polyclonally with 1 μg/mL of phytohemagglutinin (PHA, Rebel) and allogeneic feeder cells in 96-well Round-bottom plates. After 20-25 days of expansion, during which time cells supplemented with IL-2 were transferred to 24-well plates, each line was screened for the capacity to proliferate to different antigens. The day of screening, irradiated autologous $CD14^+$ monocytes, 2.5x10^4 cell/well, were stimulated for 5-6 hours in 96-well Flat-bottom plates with the antigen of interest (see Table 2.6). Dimethyl sulfoxide (DMSO, Sigma) and IL-2 were used as negative and positive controls respectively. T cell lines were washed from IL-2 and after 4-6 hours of resting in CM, 2.5x10^5 T cell/well were added to the monocytes. At day 3 of stimulation 1 μCi/mL [3H]-thymidine was added and 16 hours later the proliferation was read using a beta-counter reader (Perkin Elmer). The positive responses were defined as >3000 cpm, with a stimulation index>5, after background subtraction, which consisted on the cpm of the negative condition. Because the cells

were seeded at a limiting dilution, the precursor frequency of responding cells per million was calculated based on the number of negative wells according to the Poisson distribution (Campion et al., 2014; Geiger et al., 2009). The 95 % confidence intervals were determined for each data according to the modified Wald method (Harrell, 2013).

2.6.2 T cell receptor Vβ repertoire staining

Total PBMC from peripheral blood or matched MNC-T from tonsil were stained for the flow cytometry panel G (see Figure 2.5) and divided into 10 FACS tubes (tube A, B, C, D, E, F, G, H, control 1, control 2) at $1x10^6$ cells/tube, according to the manufactures data sheet of IOTest Beta Mark (TCR Vβ Repertoire Kit, PMIM3497). This TCR Vβ Repertoire Kit covers 70 % of the Vβ human T cell repertoire. Each vial from the kit contains three TCRVβ antibodies, stained using PE, FITC and PE+FITC flow cytometry fluorocromes. Into each FACS tube, 20 μL of the correspondent vial of the Repertoire kit was added (ex. 20 μL of the vial A from the kit was added into FACS tube A, etc.) as a total volume of 100 μL of PBS and incubated for 20 minutes at room temperature in the dark. FACS tube "Control 1" unstained cells were incubated with 20 μL of vial A and FACS tube "Control 2" were stained only with flow cytometry panel G. After having been washed twice with PBS, each FACS tube was acquired at the flow cytometer LSR-Fortessa (BD Biosciences) and the same number of events was recorded and set at $CD4^+$ gate.

To monitor the TCR repertoire before and after expansion the PBMC of 3 cone samples from UK National Blood Service were processed and the $CD4^+$ cells were enriched using microbeads positive selection (Miltenyi Biotec). An aliquot of $CD4^+$

cells was divided into 10 FACS tubes and the TCR Vβ Repertoire staining (TCR Vβ Repertoire Kit, PMIM3497) was performed. The rest of $CD4^+$ cells were stained with Flow Cytometry panel G and sorted at the FACSAria (BD Bioscience) into Tfh-Th1 ($CD4^+CD45RA^-CXCR5^+PD\text{-}1^+CXCR3^+$), Tfh-Th2 ($CD4^+CD45RA^-CXCR5^+PD\text{-}1^+CXCR3^-$), ROM ($CD4^+CD45RA^-CXCR5^-$) and Naïve ($CD4^+CD45RA^+$) to be seeded and expanded according to the T cell library technique (see section 2.6.1). Two cone samples from UK National Blood Service were tested to be HLA-A2 and the PBMC processed to use as allogeneic irradiated feeder cells. After 26 days of expansion each subset was stained for flow cytometry panel G and for HLA-A2 biotin (BioLegend). After have been washed with PBS each tube was then stained for Streptavidin BV711 for 20 minutes at room temperature in the dark and then split into 10 FACS tubes to perform the TCR Vβ Repertoire staining (TCR Vβ Repertoire Kit, PMIM3497). Each FACS tube was acquired at the Flow Cytometer LSR-Fortessa (BD Biosciences) and the same number of events was recorded and set at $CD4^+$ gate. The HLA-$A2^+$ cells were gated out of the analysis.

2.7 Cytokine detection and phenotype analysis

Cytokine production from different $CD4^+$ T cell subsets was detected using surface and intracellular cytokine staining (ICS). $2x10^5$ cell/well in 96-well Round-bottom plates were stained in PBS for surface markers, flow cytometry panel B or F (see Figure 2.5). Cells were then stimulated with $2x10^{-7}$ Mol phorbol 12-myristate 13-acetate (PMA, Sigma-Aldrich) and 1 μg/mL Ionomycin (Sigma-Aldrich). After 2 hours of incubation at 37°C and 5 % CO_2, Brefeldin A (BFA, Sigma-Aldrich) was

added at 10 μg/mL for additional 3 hours of stimulation. The cells were fixed with Cytofix/Cytoperm 1X solution (BD Pharmingen) for 20 minutes on ice and stained in Permwash 1X solution (BD Pharmingen) with anti-CD4 and cytokine antibodies, panel B or F (see Figure 2.5). Stained cells were analysed at the flow cytometer LSR-Fortessa (BD Biosciences).

Surface markers phenotype was characterized *ex-vivo* from tonsil and blood by staining $2x10^5$ cell/well in 96-well Round-bottom plates for flow cytometry panel C, (see Figure 2.5). For transcription factor profile, the cells were fixed with Fixation buffer 1X (eBiosceince, Transcription Factor Staining buffer set, 00-5523-00) and stained in Permwash buffer 1X for anti-Foxp3 A647 and anti-Bcl-6 PE for 45 minutes at room temperature in the dark. Stained cells were washed in PBS and analysed at flow cytometer LSR-Fortessa (BD Biosciences) the same day of the staining. An example of ICS for each marker analysed in this thesis is shown (**Figure 2.8**).

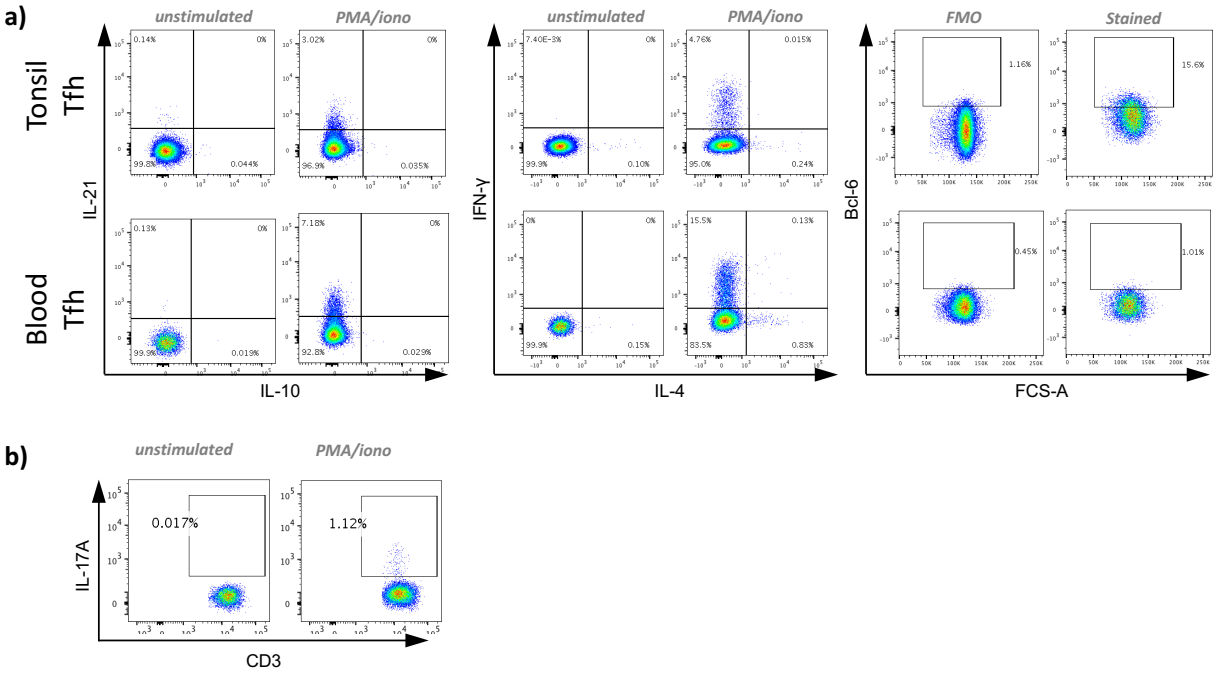


Figure 2.8 Intracellular cytokine staining and transcription factor gating.

(**a**) Examples of IL-21, IL-10, IFN-γ, IL-4, IL-17A and Bcl-6 flow cytometry staining in tonsil and blood samples. The cytokine production were gated based on an unstimulated condition, while the transcription factor Bcl-6 based on a Fluorocrome Minus One (FMO). The first row shows an example of $CD4^+$ memory Tfh cells ($CXCR5^+PD\text{-}1^+$) staining of tonsil and the second row an example of $CD4^+$ memory Tfh cells ($CXCR5^+PD\text{-}1^+$) staining of blood. (**b**) An example of IL-17A flow cytometry staining is also shown from ROM population of peripheral blood.

2.8 Antigen-specific T cell clone technique

Antigen-specific T cell clones were made from either frozen antigen-reactive T cell lines identified from the T cell library stimulation (section 2.6.1) or *ex-vivo* $CD4^+$ sorted subsets.

Antigen-enriched lines or $CD4^+$ sorted subsets ($3x10^5$ cells/well in 96-well Flat-bottom plates) were stimulated for 7 days with irradiated, autologous monocytes

$CD14^+$ ($1x10^5$ cells/well), pulsed with the antigen of interest for 4-6 hours at 37°C and 5 % CO_2. For each stimulation, a negative condition of irradiated, autologous monocytes without antigen or with DMSO only, was performed. Antigen-specific T cell clones from positive lines were generated by pulsing monocytes with HA/Wisconsin protein at 5 μg/mL. Antigen-specific T cell clones from *ex-vivo* frozen PBMC were generated by pulsing monocytes with HA/California peptides at 2 μg/mL. After stimulation T cells were stained for flow cytometry panel D (see Figure 2.5) for 15 minutes at 37°C and 5 % CO_2 and activated cells ($CD4^+CD14^-$ $ICOS^+CD25^+$) were sorted at the FACSAria (BD Bioscience) (**Figure 2.9**). Activated-cells were seeded at 0.4 cell/well in 384-well plates and expanded with irradiated allogeneic feeder, 1 μg/mlL of PHA (Rebel) and CM IL-2. After 14 days, the clones were identified by visual inspection of the discolouration of media and transferred into 96-well Round-bottom plates and kept in culture. To confirm the specificity, an aliquot of each clone ($1x10^5$ T cell/well, in 96-well Round bottom plates) was washed from IL-2 and, after 4-6 hours of resting in CM, 2 μg/mL of peptide pool was added to the cells. At day 3 of stimulation 1 μCi/mL [3H]-thymidine was added and 16 hours later the proliferation was read using a beta-counter reader (Perkin Elmer). The positive responses were defined as >1000 cpm, with a stimulation index>5. Cell clones were excluded from analysis if the background counts were >1000 cpm.

To calculate the EC50 (effective concentration) and so evaluate the avidity, each clone was stimulated with different concentrations of peptide (10, 3, 1, 0.6, 0.3, 0.1, 0.06, 0.03, 0.01, 0.006, 0.003, 0.001, 0.0006, 0.0003, 0.0001 μg/mL) and

proliferative response evaluated by 1 μCi/mL [3H]-thymidine incorporation, as described above. Each concentration was referred to the molarity value (μMol) of each single peptide. The EC50 was calculated as the concentration related to the 50% of the maximum response, per each clone.

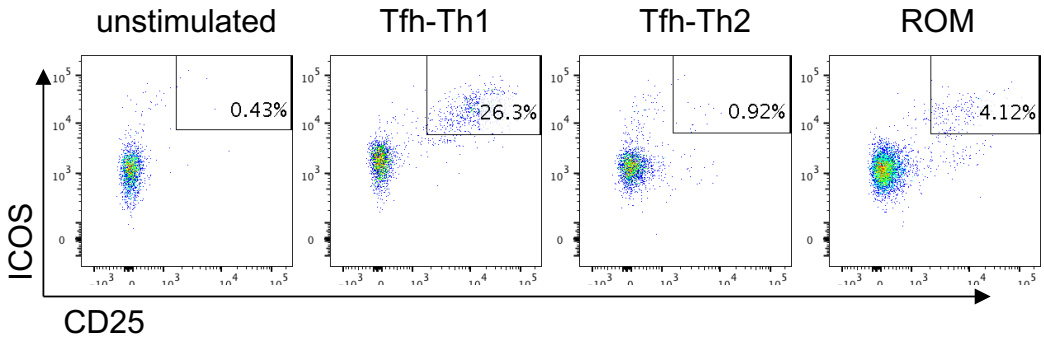


Figure 2.9 Gating strategy for antigen-enrichment.

From $CD4^+CD3^+CD14^-$ gate, the $ICOS^+CD25^+$ cells were gated after 7 days of stimulation with antigen and irradiated autologous monocytes, for each $CD4^+$ memory subsets considered. In this example, the unstimulated condition refers to unstimulated Tfh-Th1 cells. An example of staining from donor 234 is shown.

2.9 Human Leukocyte Antigen (HLA) type and restriction

2.9.1 HLA type on DNA extraction

HLA class I and class II typing from 5 donors was performed on DNA extraction from 2-3x10^6 PBMC or T cells. Cells were resupsended in 0.6 mL of Lysis Buffer (eBioscience) and rest overnight at 4°C. With filter tips 200 μL of Puregene Protein Precipitation Solution (Qiagen) was added in each sample, which was vortex immediately after that and span down (2000 rpm, 5 minutes). Supernatant was

conserved, 0.6 mL of Isopropanol (Sigma) was added and the tubes were inverted 50 times until seeing the floating DNA. Samples were span down (2000 rpm, 1 minute) and 0.6 mL of 70 % Ethanol (Sigma) was added to each tube to disrupt the pellet. After the last spin (2000 rpm, 1 minute), all the supernatant was removed and samples were left drying for 5 minutes. Finally, 0.1 mL of DNA Hydration Solution (Qiagen) was added. Samples were stable at 4ºC for a week. Before send the samples for sequencing (Sequencing Facility, Weatherall Institute of Molecular Medicine, Oxford), DNA amount and purity was checked at the absorbance ratio of 260/280 nm using Nano Drop Spectrophotometer (ThermoFisher).

2.9.2 Determination of HLA restriction of T cell clones

To determine the HLA class II restriction of $CD4^+$ T cell clones, DAP.3 fibroblast cell line transfected with a single HLA-DR molecule (kindly given and generated in Alessandro Sette's laboratory, La Jolla, CA, USA) were used (McKinney et al., 2013). L466.1 (DAP.3 transfected with HLA-DR 15:01) and L605.2 (DAP.3 transfected with HLA-DR 07:01) were expanded in culture at $3x10^6$ cell/T75 flask (Corning) in RPMI supplemented with 10% of FBS (foetal bovine serum), at a concentration of $1x10^7$ cell/mL. The day before the assay 100 μg/mL of Butyric acid (Sigma-Aldrich) was added to the cells in culture. The cells were incubated at 37°C and 5 % CO_2 overnight. The day of the assay the fibroblast cell lines were washed 3 times with PBS and harvested from the flask using 3 mL of Trypsin/EDTA (Lonza) for 3 minutes at 37°C and 5 % CO_2. Detached cells were removed from the flask, washed in PBS, seeded at $4x10^4$ cell/well in V-bottom 96-well plates and pulsed with

the peptide of interest (2 μg/mL) for 3 hours. Fibroblasts were then washed from the peptides with PBS and T cell clones rested in CM were added at $2x10^5$ cell/well on top of the fibroblasts. IFN-γ-producing cells were detected by ELISpot (Mabtech AB). For each experiment, a positive control with PHA and a negative control with DMSO was performed. Positive responses were defined as >100 SFU/10^6 (Spot Forming Unit), with a stimulation index >5. Cell lines were excluded from analysis if the background counts were >100 SFU/10^6.

2.10 T cell receptor sequencing

2.10.1 Clonotyping of antigen-specific $CD4^+$ T cell clones

T cell clones were washed in PBS and stained for flow cytometry panel H (see Figure 2.5). A maximum of $5x10^3$ $CD4^+CD3^+$ T cells were sorted into 100 μL of RNAlater (Ambion) in 1.5 mL tubes (Starstedt) at FACSAria (BD Bioscience) and stored at –80°C. T cell receptor (TCR) sequencing on mRNA of T cell clones was performed in the laboratory of Prof David Price at Cardiff University, UK (Quigley et al., 2011). Messenger RNA (mRNA) was isolated using Milteniy's μMACS mRNA isolation kit and cDNA from each mRNA tube was made (SMARTER™ RACE cDNA Amplification kit, Clonotech). TCR α- and β-chains were unbiased amplified using MAC2 and MBC2 primers respectively at 25 μMol (IDT) with Polymerase Chain Reaction (PCR) (**Figure 2.10**). PCR products were run on a 1 % agarose gel (Invitrogen) and stained with SYBR Gold (Invitrogen) (**Figure 2.11**). TCR α- and

β-chain bands were cut at 750bp and 500bp respectively and the gels were extracted with Macherey Nagel NucleoSpin Extract II kit (Fisher Scientific). Each amplicon was sub-cloned to be sequenced individually, ligated into a plasmid and transformed in DH5s-T1 competent cells (TOPO® TA cloning kit, One Shot Max Efficiency DH5a-T1^{R}, Invitrogen). Colonies with the insert were selected through the white/blue selection technique as an X-GAL-dependent growth (Ambion X-GAL, 5-Bromo-4-Chloro-3 Indolyl-Beta-D-thiogalactopyranoside, Invitrogen). After 18 hours of incubation at 37°C, white colonies are picked and moved to a 96-well plate; each amplicon is picked 12 times to cover the entire row (12 wells). The CDR3 amplicon is amplified by a PCR using 2 primer binding sites (M13 Forward primer and M13 Reverse primer, 5 μMol, Invitrogen) to amplify the inserted DNA (**Figure 2.10**). To confirm that the colony PCR has efficiently worked, 13 of the 96 PCR products were run on a 1 % agarose gel (Invitrogen) (**Figure 2.12**) and the plate, after have been diluted 1:1 with water (Sigma) in a Fast 96 Well Skirted plate (Fisher), is sent to be sequenced (Genewiz, Essex). Gene usage was determined according to the ImMunoGeneTics (IMGT) nomenclature (Lefranc et al., 2003).

Primer name	Primer sequence
MAC2	5'-ggaactttctgggctggggaagaaggtgtcttctgg-3'
MBC2	5'-tgcttctgatggctcaaacacagcgacct-3'
M13F	5'-ttttcccagtcacgac-3'
M13R	3'-caggaaacagctatgac-5'

Figure 2.10 Primer sequences.

Primer sequences to amplify the T cell receptor CDR3 region of α (MAC2) and β (MBC2) chains are listed. Sequences of primers M13 Forward (M13F) and M13 Reverse (M13R) are used to broader amplify the CDR3 region of both α and β chains.

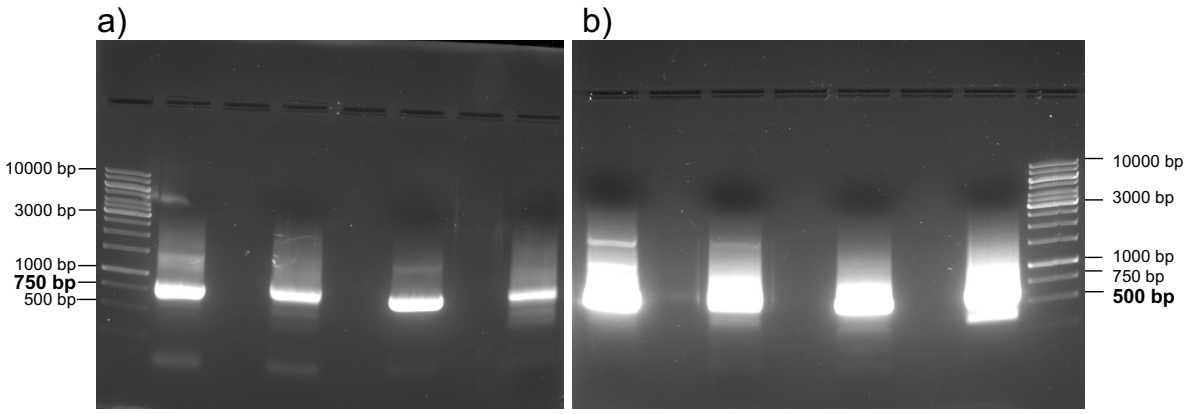


Figure 2.11 TCR alpha (α) and beta (β) chains amplification.

Example of PCR (**a**) α- and (**b**) β- chain products of the same 4 clones run on 1% agarose gel respectively at 750 bp and 500 bp.

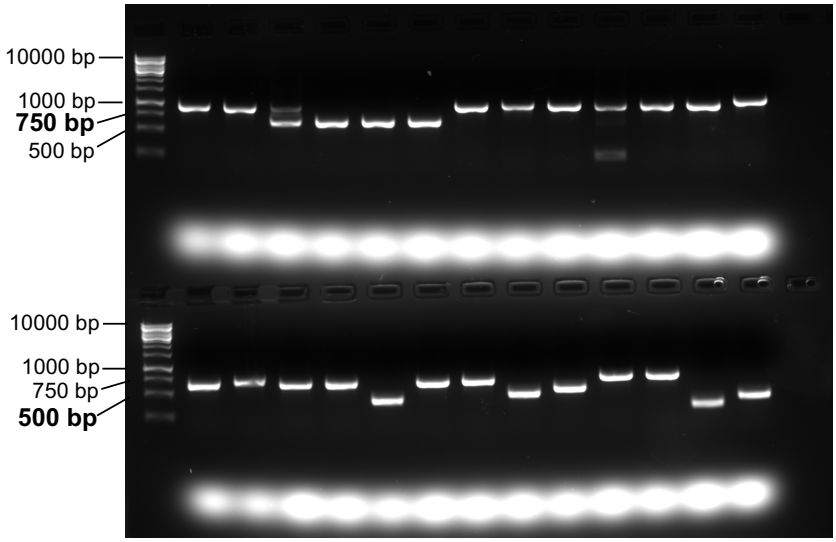


Figure 2.12 Plate of confirmation gel.

Example of confirmation colony PCR products run on 1% agarose gel. On the top part confirmation of α-chains (750bp) and on the bottom part β-chains (500bp) of the same clones.

2.10.2 Deep T cell receptor sequencing of bulk $CD4^+$ T cell populations

Defrosted PBMC and MNC-T were rested overnight in CM at 37°C, 5 % CO_2. $CD4^+$ T cells were enriched using microbeads positive selection (Miltenyi Biotec) and stained for flow cytometry panel A (see Figure 2.5). Subsets of $CD4^+$ T cells from tonsils were sorted at the FACSAria (BD Bioscience) into Tfh-Th1 ($CD4^+CD45RA^-CXCR5^{lo}PD\text{-}1^{lo}CXCR3^+$), Tfh-Th2 ($CD4^+CD45RA^-CXCR5^{lo}PD\text{-}1^{lo}CXCR3^-$), Tfh-GC ($CD4^+CD45RA^-CXCR5^{hi}PD\text{-}1^{hi}$) and ROM ($CD4^+CD45RA^-CXCR5^-$). $CD4^+$ T cells from blood were sorted into Tfh-Th1 ($CD4^+CD45RA^-CXCR5^+PD\text{-}1^+CXCR3^+$), Tfh-Th2 ($CD4^+CD45RA^-CXCR5^+PD\text{-}1^+CXCR3^-$) and ROM ($CD4^+CD45RA^-CXCR5^-$) (**Figure 2.13**). A maximum of $1.3x10^5$ T cells, with variability between subsets and donors, were sorted into 0.5 mL of RLT buffer (Qiagen), with an addition of 10 % of β-mercaptoethanol (Sigma), in 5 mL tubes (Eppendorf) at FACSAria (BD Bioscience) and stored at –80°C.

T cell receptor (TCR) sequencing on mRNA was performed in the laboratory of Prof Dmitriy Chudakov at the Central European Institute of Technology in Brno (Czech Republic). Total RNA was isolated using RNaesy Mini kit (Qiagen) and cDNA from each mRNA tube was made. Deep sequencing on RNA of the entire αβ T cell receptor (TCR) was performed using the NextSeq 500/550 High Output Kit v2 (300 cycles, Illumina). Data generated was the result of the nucleotide sequences of the CDR3 region analysed with MiXCR software by Prof Dmitriy Chudakov and his group (Bolotin et al., 2015). I performed the visualization analysis on the CDR3 β-chain with the open sources platforms VDJtools (vdjtools-doc.readthedocs.io) and Cytoscape (cytoscape.org) with the support of Prof Dmitriy Chudakov. F2 and D

metrics as well as Shannon-Wiener diversity analysis were performed using the first Vβ 1000 clonotype nucleotide sequences with the highest frequency (top1000) for each subset and the frequency normalized based on the total counts detected per subset. Clonotype sharing, networks and frequency comparisons are performed using the first Vβ 2000 clonotype nucleotide sequences with the highest frequency (top2000) for each subset and the frequency normalized. The clonotypes with the lowest frequency were randomized in order to have an unbiased approach on the selection.

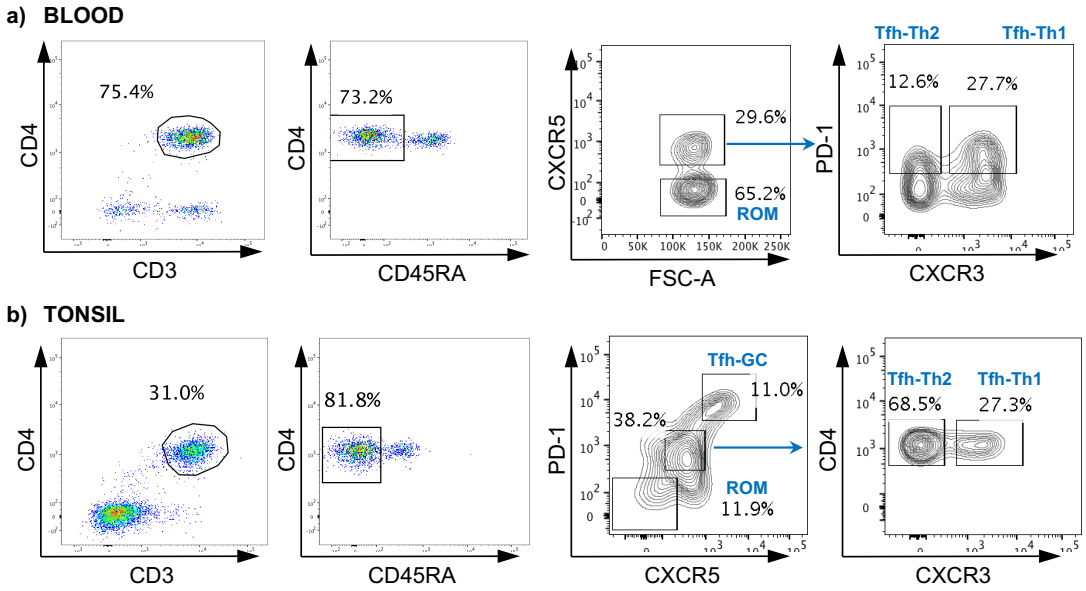


Figure 2.13 Sorting strategy of CD4⁺ populations for TCR deep-sequencing. Enriched $CD4^+$ T cells were stained and sorted into different subsets of $CD3^+CD4^+CD45RA^-$. The gating strategy to sort Tfh-Th1, Tfh-Th2 and ROM from blood is shown in **(a)**, while **(b)** shows Tfh-GC Tfh-Th1, Tfh-Th2 and ROM from tonsils. An example of staining from donor 239 is shown.

2.11 T and B cell co-culture

Co-culture experiments were performed either using total Tfh from peripheral blood or Tfh-Th1 clones. In the first case PBMC from 2 cone samples were processed and the $CD19^+$ B cells were isolated using Dynabeads/DetachBead (Invitrogen). From the negative fraction $CD4^+$ T cells were enriched using microbeads positive selection (Miltenyi Biotec). $CD4^+$ and $CD19^+$ cells were stained for flow cytometry panel I (see Figure 2.5) and sorted at the FACSAria (BD Bioscience) into $CD4^+$ Tfh ($CD4^+CD3^+CXCR5^+$), $CD4^+$ non-Tfh ($CD4^+CD3^+CXCR5^-$), $CD19^+$ naïve B cells ($CD19^+CD27^-$), $CD19^+$ memory B cells ($CD19^+CD27^+$). The sorting was performed at 4-Way purity and the purity was never lower than 90 %. Sorted Tfh and non-Tfh were co-cultured with either naïve or memory B cells at 1:1 ratio, 120,000 T+B cell/well at 10^6 cell/mL and stimulated with 1 μg/mL of Superantigen Staphylococcal Enterotoxin-B (SEB, Sigma). From each condition was also performed negative controls either with B cells only or without SEB. Cells from one donor were stained at day 2 of the co-culture (panel I, Figure 2.5) in duplicates and at day 5 intracellular staining was performed for the same panel I (see Figure 2.5), while supernatant from the other was collected at day 7 and day 10 to check IgG, IgM and IgA production by ELISA.

Co-culture with high and low avidity Tfh-Th1 clones was performed using 2 defrosted Tfh-Th1 clones specific for the same peptide 55. PBMC from the same donor were stained for panel L (see Figure 2.5) and autologous total B cells ($CD19^+$) were sorted at the FACSAria (BD Bioscience) 4-Way purity. Tfh-Th1 clones were co-culture with B cells, pulsed with either 0.5 μg/mL or 10 μg/mL of HA/Wisconsin whole protein. A condition without antigen was used as negative control. At day 4

cells were stained in duplicates for panel L (see Figure 2.5) and at day 6 intracellular staining was performed for the same panel L (see Figure 2.5). The supernatant from each condition was collected at day 7 and day 12 to check IgG, IgM and IgA production by ELISA.

2.12 Synaptic transfer on silica bead lipid bilayer

PBMC of 6 cone samples from UK National Blood Service were processed and the $CD4^+$ cells were enriched using microbeads positive selection (Miltenyi Biotec). $CD4^+$ T cells were stained for flow cytometry panel A, except for anti-PD-1 BV421 (see Figure 2.5) and sorted at the FACSAria (BD Bioscience) into Tfh-Th1 ($CD4^+CD45RA^-CXCR5^+CXCR3^+$), Tfh-Th2 ($CD4^+CD45RA^-CXCR5^+CXCR3^-$), Th1 ($CD4^+CD45RA^-CXCR5^-CXCR3^+$) and Th2 ($CD4^+CD45RA^-CXCR5^-CXCR3^-$). The sorting was performed at 4-Way purity to sort 1-8x10^6 cell per subset, purity was never lower than 90 %. In case of polyclonal expansion, sorted cells were then stimulated with anti-CD3/anti-CD28 Dynabeads (Life Technology) following the manufacturer guidelines and re-suspended in CM with 100 U/mL of IL-2. After 3 days Dynabeads were removed from the culture using a designated magnet and the cells suspended in CM with 100 U/mL of IL-2.

In case of co-culture expansion, sorted T cells were co-culture with isolated autologous $CD19^+$ B cells (EasySep, StemCell) and irradiated at 45GY. During the 10 days of co-culture T and B cells were stimulated with 1 μg/mL of SEB.

Cells in culture have been left expanding till day 10-12, when they were washed and rested in CM for 4 hours without IL-2. Before the co-culture with silica beads, cells

were washed, re-suspended in HSA buffer and kept at 4°C. Silica beads (as a 1:1 cell to bead ratio, 5μm diameter, Bangs Laboratories, Inc.) were prepared in Eppendorf tubes and coated with 0.4 mMol lipid solution: 0.2 Mol% ATTO 488 1,2-Dioleoyl-sn-glycero-3-phosphoethanolamine, 12.5 Mol% 1,2-dioleoyl-sn-glycero-3-[(N-(5-amino-1-carboxypentyl) iminodiacetic acid) succinyl] (nickel salt) and 0.05 Mol% 1,2-dioleoyl-sn-glycero-3-phosphoethanolamine-N-(cap biotinyl) (sodium salt) in 1,2-dioleoyl-sn-glycero-3-phosphocholine. All lipids were purchased from Avanti Polar Lipids, Inc. The lipid mono-layer was washed HAS buffer, blocked with 5% of Casein in PBS containing 100 μMol $NiSO_4$, to saturate NTA sites and then coated with Streptavidin at 50 μg/mL (Sigma Aldrich). Silica beads were incubated with ICAM-1 (200 Mol/μm^2, His-tagged) and either UCHT1-Fab (0, 50, 500 Mol/μm^2), monomer HLA-DRB1-15-pep74 (50, 500 Mol /μm^2) or HLA-DRB1-15-CLIP (50, 500 Mol /μm^2) (from NIH Tetramer Core Facility). In addition, CD40 (500 Mol /μm^2, BioLegend), and ICOSL (100 Mol /μm^2, BioLegend) were added to the mono-layer. The negative control (Signal 1, S1) was coated with ICAM-1 and UCHT1-Fab only. T cells and beads were co-culture in V-Bottom plates (Corning) at 1:1 ratio, $2.5x10^5$ cell/well. The co-culture was also re-suspended in EDTA (50 μMol, Invitrogen) to release the beads from the T cells. Beads were stained with the flow cytometry panel E (see Table 2.5) and then acquired at the flow cytometer LSR-Fortessa (BD Bioscience). To identify the molecule transferred into the immune synapses, the silica beads were gated and the percentage (%) or mean fluorescence intensity (MFI) was calculated using analysis software FlowJo (FlowJo version 10.3) (**Figure 2.14**).

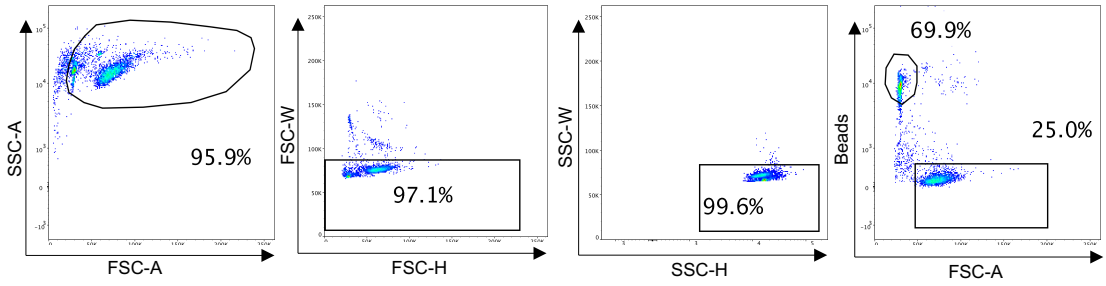


Figure 2.14 Example of the gating strategy for synaptic transfer analysis.
From the lymphocytes, gated based on FSC-A and SSC-A, singlet cells were identified with FSC-W vs FSC-H and SSC-W vs SSC-H. The silica beads were then selected for their flourocrome and the T cells were excluded using FSC-A.

2.13 Enzyme-Linked Immunosorbent Assay

Influenza-specific IgG titre in the plasma of 5 donors and total IgG, IgA and IgM from supernatant of T and B cell co-culture, were evaluated by Enzyme-Linked Immunosorbent Assay (ELISA).

To detect Influenza-specific IgG titre, Nunc Maxisorp plates were coated with commercial Trivalent Influenza Vaccine (TIV) from Sanofi-Pasteur 2011-2012 (containing HA California, Perth and Brisbane) and Haemagglutinin protein from Influenza A/California/2009 (NR 13691, BEI resources) at 0.75 µg/mL and 2 µg/mL respectively with Phosphate Buffered Saline (PBS, LifeTechnology) and incubated overnight at 4°C. After have been washed 6 times in PBS with 0.05 % of Tween (Sigma), plates were blocked with Casein blocker (Pierce), 100 µL/well for 2 hours at room temperature. The block was discarded and the diluted plasma samples (1:500, 1:1000, 1:2000, 1:4000) were added on both plates at 50 µL/well. Each

sample was run in duplicate and positive (plasma pool of all 5 donors) and negative (PBS only) controls were made for each plate. A reference plasma with the pool of the 5 donors, was used to generate a standard curve. After 2 hours incubation at room temperature, plates were washed 6 times with PBS+0.05 % Tween and incubate with alkaline phosphatase conjugated goat anti-human IgG (Sigma, 1:5000) in PBS+0.05 % Tween for 1 hour at room temperature. Plates were then washed 6 times with PBS+0.05 % Tween and substrate pNPP (20mg tablet from Sigma, dissolved at 1mg/mL in Diethanolamine Buffer, Pierce) was added, at 100 µL/well for 10 minutes in the dark at room temperature. Absorbance was red at 405 nm on Microplate Reader (BioTech) using Open Gen5 software.

The level of total IgG, IgA and IgM was determined from supernatant of T and B cell co-culture at different time points using Mabtech ELISA kit and following manufacture guidelines. Samples were diluted at 1:5 and 1:10 in duplicates.

Primary antibodies used:

- IgG: MT145
- IgA: MT57
- IgM: MT11/12

Secondary antibodies used:

- IgG: MT78-ALP
- IgA: MT20-ALP
- IgM: MT22-ALP

2.14 Statistical analysis

Statistical analysis from flow cytometry data are based on percentages from the same number of events acquired for each sample compared.

In chapter n. 3 the population Tfh-GC from blood, which includes very few cells, was excluded from the statistical analysis.

The statistical tests used to compare different parameters in all the chapters are listed:

- To compare analogous populations from different compartments (ex. Blood_Tfh-Th1 with Tonsil_Tfh-Th1) and TCR repertoire analysis comparison: paired t test for parametric data and Wilcoxon-matched pairs for non-parametric data;
- To compare different populations from the same compartment (ex. Tonsil Tfh-Th1 with Tons_Tfh-Th2) or general parameters comparison: one-way ANOVA test for parametric data and Kruskal-Wallis test for non-parametric data;
- Linear regression correlations are calculated using the coefficient of determination, square of Pearson correlation coefficient, (R^2), where $R^2=0$ is no correlation and $R^2=1$ is maximum correlation. The slope and the P value of the slope significantly different from zero are also indicated.

In the graphs from chapter 3 only statistic differences for each population of the same compartment are shown (ex. Blood_Tfh-Th1 vs Blood_Tfh-Th2) and between analogous populations from different compartments (ex. Blood_Tfh-Th1 vs Tonsil_Tfh-Th1).

Boxes show the mean and quartiles and whiskers minimum and maximum. The probability value, or P value, was calculated for each statistical test applied as the

probability that no difference is observed. For example a P value=0.05 it referes to the 0.05 probability (or 1 in 20) that a comparison observed is not true, given a specific statistical test. *P<0.05, **P<0.01, ***P<0.001, ****P<0.0001. Bar graphs show the mean and standard deviation (SD) or the standard error of the mean (SEM).

3 Results I: phenotypic profile of T follicular helper cell populations in peripheral blood and tonsils

3.1 Background and rationale

Effector T follicular helper (Tfh) cells are mainly localized in germinal centres (GC) of secondary lymphoid organs. In lymph nodes (LN) Tfh cells express high level of the chemokine receptor CXCR5, which binds to the B lymphocyte chemoattractant CXCL13 (Breitfeld et al., 2000; Havenith et al., 2014; Schaerli et al., 2000). These cells also express high level of PD-1, Bcl-6 and IL-21 and provide superior help to B cells (Kim et al., 2017; Vogelzang et al., 2008; Yu et al., 2009). In lymphoid organs $CD4^+$ memory T cells can express intermediate levels of CXCR5 and PD-1, but only cells expressing high level of CXCR5 and PD-1 ($CXCR5^{hi}PD\text{-}1^{hi}$) are localized in the germinal centre and therefore called germinal centre Tfh (Tfh-GC) (Shi et al., 2018). Differences in expression of surface markers could be related not only to the location of the T cells but also to their stage of differentiation or to the function (Crotty, 2018). Populations of $CD4^+$ memory T cells in the peripheral blood have been described that have similar characteristics to Tfh cells situated in the follicles, and are thought to represent circulating memory Tfh cells (cTfh) (Crotty, 2018; Hale and Ahmed, 2015). Many studies have focused on phenotyping circulating Tfh cells in human samples, identifying $CD4^+$ memory T cells in the periphery that express $CXCR5^+$ and distinguishing different subsets of Th1-like ($CXCR3^+CCR6^-$), Th2-like

(CXCR3$^-$CCR6$^-$) and Th17-like (CXCR3$^-$CCR6$^+$) Tfh, because of the similarities with canonical Th1 (CXCR3$^+$), Th2 (CXCR3$^-$) and Th17 (CCR6$^+$) (Bentebibel et al., 2013; Morita et al., 2011). Circulating memory Tfh cells express lower levels of PD-1, ICOS and the transcription factor Bcl-6, compared to Tfh-GC (He et al., 2013). The ontogeny of memory circulating Tfh cells and their relationship with effector Tfh-GC are still poorly understood. Few studies have compared circulating and follicular Tfh, with the caveat of comparing tonsils from children with adult's peripheral blood, adopting either phenotypical (Chevalier et al., 2011; He et al., 2013) or gene expression profile approaches (Locci et al., 2013). However, the relationship and how to define Tfh cells within circulating memory CXCR5$^+$CD4$^+$ T cells is still not clear. Poor availability of secondary lymphoid organs in humans hampers the comparison between the various CXCR5$^+$ and CXCR5$^-$ memory populations in blood and in lymph nodes.

To directly compare cTfh and lymph node Tfh populations, including germinal centre Tfh (Tfh-GC), we studied peripheral blood and tonsil samples from matched adult donors. We opted to study Tfh cells from tonsillar tissue since tonsil nodules are the most readily obtainable human secondary lymphoid organs. Ethical approval was granted to collect peripheral blood samples and tonsillar tissue from adult donors who were undergoing routine tonsillectomy.

The aim of the work presented in this chapter was to develop the methodologies required to define, isolate and phenotype different Tfh cell subsets from tonsillar tissue and peripheral blood in addition to develop techniques that would enable the repertoires specificity to be determined from both tissues. Although predominately technical challenges, the methodologies developed and presented herein were

fundamental to enabling the direct comparison of different populations of Tfh cells from blood and tonsils.

To achieve this aim, the goals of the work in this chapter were therefore:

- To define phenotypically-distinct subsets of memory $CD4^+$ T cells in blood and tonsils for analysis, characterising the surface markers, transcription factor expression and cytokine production profile of each population (section 3.2).
- To optimise the T cell library technique for the study the specificity of Tfh cells and to determine its utility for analysis of the repertoire of circulating (section 3.3) and tonsillar (section 3.4) Tfh cells subsets. The T cell library is a method established in Prof Sallusto's laboratory to characterize the specificity and to calculate the precursor frequency of a certain T cell population (Campion et al., 2014; Geiger et al., 2009).

3.2 Surface marker, transcription factor and cytokine production profile of Tfh cells from blood and tonsils

In order to compare the different Tfh populations present in the germinal centre and in the circulation, we first needed a means by which to identify and characterise Tfh cells in each tissue. To characterise $CD4^+$ memory T cell populations in tonsils and blood of the same donor, multi-parameter flow cytometry analysis of peripheral blood mononuclear cells (PBMC) and mononuclear cells from tonsil (MNC-T) (panel C, see Figure 2.5) was performed within 4 hours from the sample collection.

After a lymphocyte gating strategy, cells were negatively selected for dead/dying cells and for cell markers not of interest in this study, such as CD8 and CD14 (**Figure 3.1 a**). An example of data from a representative matched blood and tonsil sample pair is shown to illustrate the lymphocyte cell composition in each. As expected, based on published data (Havenith et al., 2014; VanKempen M.J.P. et al., 2007), the percentage of $CD19^+$ B cells within lymphocytes was statistically higher in tonsils compared to blood, while no differences were observed in the proportion of $CD4^+$ T cells within lymphocytes (**Figure 3.1 b**). The composition of $CD4^+CD45RA^-$ T cell subsets was notably diverse, especially the expression of chemokine receptors such as CXCR5 and CXCR3 and the surface marker PD-1. In particular, a population with high expression of PD-1 and CXCR5 was observed in each tonsil sample analysed, that was not present in the corresponding peripheral blood sample (**Figure 3.1 d, e**). This population has been described before in human tonsils and named germinal centre Tfh (Tfh-GC) and it has also been shown to have an effector function inside the dynamic GC reaction (Crotty, 2011). Interestingly Tfh-GC cells in tonsils are enriched in $CXCR3^-$ cells (**Figure 3.1 e**). CXCR3 was also differently expressed in blood and tonsil $CD4^+$ memory: in tonsil, populations with lower expression of CXCR5 and PD-1 had the highest proportion of $CXCR3^+$ cells, while in blood no significant difference was observed between $CXCR5^{+/-}$ and $PD\text{-}1^{+/-}$ subsets (**Figure 3.1 c, e**). The chemokine receptor CXCR3 expression is induced after activation in naïve $CD4^+$ and $CD8^+$ T cells, as well as in Natural Killer (NK) cells after a intracellular-type inflammation (Groom and Luster, 2011a). CXCR3 directs effector cells to inflamed tissues, in which CXCR3 ligands (CXCL9, CXCL10 and CXCL11)

are highly expressed (Djuretic et al., 2007). The lack of this marker in Tfh-GC cells would suggest a specific effector function of these cells inside the GC, where they do not need to directly face the inflammation in peripheral tissues but actively participate to the formation of neutralizing antibodies against the specific infection. To support this observation, recent studies showed how Tfh-GC cells from tonsils correlate best with the blood circulating Tfh CXCR3$^-$ subset in terms of phenotype, function and gene expression profile (He et al., 2013; Locci et al., 2013).

Due to the wide differences in blood and tonsil T cell phenotype, different Tfh subsets were identified from each compartment. Populations of CD4$^+$CD45RA$^-$ T cells were chosen for comparison in this thesis, because correlated to populations already identified in the literature (**Figure 3.2**). From the peripheral blood were identified: CXCR3$^+$ (termed Tfh-Th1) and CXCR3$^-$ (termed Tfh-Th2) within CXCR5$^+$PD-1$^+$ cells, CXCR5$^-$ memory CD4$^+$ T cells were called "rest of memory" (ROM) (**Figure 3.2 a**). In tonsil, high expression of PD-1 and CXCR5 identified Tfh-GC (PD-1^{hi}CXCR5^{hi}), in contrast to Tfh-Low (PD-1^{lo}CXCR5^{lo}) populations, and ROM (PD-1$^-$CXCR5$^-$). Within Tfh-Low two subsets of Tfh cells were determined based on the expression of CXCR3: Tfh-Th1 (CXCR3$^+$) and Tfh-Th2 (CXCR3$^-$) (**Figure 3.2 b**). Gating strategy of Tfh-Th1 and Tfh-Th2 was very similar to previous circulating Tfh studies (Morita et al., 2011), reason why herein they were called Tfh-Th1 and Tfh-Th2. The percentage of each population within the CD4$^+$CD45RA$^-$ T cells, was evaluated in each tonsil and blood sample collected. The Tfh-GC subset was not found in the circulation, and Tfh subsets from peripheral blood were rarer, whilst CXCR5$^-$ cells were more abundant (**Figure 3.2 c**). In this thesis the CXCR5$^+$CXCR3$^-$ subset from blood and tonsils, that I will term herein for simplicity

"Tfh-Th2", includes both Tfh Th2-like ($CXCR5^+CXCR3^-CCR6^-$) and Tfh Th17-like ($CXCR5^+CXCR3^-CCR6^+$) populations previously identified (Boswell et al., 2014; Morita et al., 2011).

Expression of the transcription factor Bcl-6 and the surface marker ICOS, which are two well-defined Tfh markers (Kitano et al., 2011; Nurieva et al., 2008; Yu et al., 2009), were maximal in Tfh-GC cells from tonsil but considerably lower in every Tfh or non-Tfh subset from peripheral blood. There was variability between donors in Bcl-6 expression but a few donors also expressed this transcription factor in the Tfh-Th1 compartment from tonsil (**Figure 3.3 a**). ICOS was expressed at significantly greater levels in all the Tfh subsets from tonsil compared to the blood Tfh. Moreover, there was a trend towards higher expression of ICOS in Tfh-Th1 and Tfh-Th2 in the blood compared with ROM (**Figure 3.3 b**). The importance of the chemokine receptor CCR6 to localize B cells in the light zone (LZ) of the GC (Suan et al., 2017; Wiede et al., 2013) and its relevance on circulating Tfh-Th17 phenotype shown in few studies (Boswell et al., 2014; Li et al., 2012), led us to evaluate its expression in our blood and tonsil cohort. Despite high variability between different donors, Tfh-GC subset was the population where CCR6 was expressed at the highest level, while in the blood, CCR6 was mainly expressed in Tfh-Th2 and ROM (**Figure 3.3 c**). CCR6 is known to bind CCL20, which is a common factor expressed in lymphoid tissues after immune challenge (Reimer et al., 2017). CCR6 expression in Tfh-GC cells is interesting and might influence the localization of Tfh-GC cells in the light zone (LZ) of the germinal centre, as in line with what it was already described for GC B cells (Suan et al., 2017; Wiede et al., 2013).

To complete the phenotypic profile of Tfh and non-Tfh cells from blood and tonsils, cytokine production by each subset was evaluated *ex vivo* after PMA/ionomycin stimulation, using flow cytometric analysis (panel B, see Figure 2.5) (**Figure 3.4**). PMA (Phorbol 12-myristate 13-acetate) is a protein kinase-C and NF-kB activator, while Ionomycin is a calcium ionophore. Together PMA/Ionomycin is a general stimulus that does not depend on TCR-signalling but activate intercellular T cell pathways, such as cytokine release. This type of stimulation is often used to observe the unbiased ability of specific subsets of T cells to produce certain cytokines, independently of the antigen (Ai et al., 2013). The cytokine profiles supported the observation that Tfh-GC cells were indeed the subset with the highest follicular characteristics, because these cells proved to be the major producers of IL-21 and IL-4 (**Figure 3.4 a, b**), crucial cytokines for Tfh cells differentiation and B cell survival (Nurieva et al., 2008; Reinhardt et al., 2009; Yusuf et al., 2010). The production of IL-21 was less in the Tfh-Th1 and Th2 subsets from tonsil, reaching and showed minimal levels in the ROM population. No significant differences were instead described between Tfh and non-Tfh cells from blood for both IL-21 and IL-4 production, as expected. The Tfh-GC cell phenotype was also associated with a low production of IFN-γ (**Figure 3.4 c**), consistent with published data (Ma et al., 2009; Ploquin et al., 2011). The lack of IFN-γ production by Tfh-GC cells is in line with the poor expression of CXCR3 previously observed and suggests a specific effector role of these cells into the GC rather than an anti-viral function in the periphery. In contrast, the major producers of IFN-γ were the Tfh-Th1 subsets and the ROM from blood, which includes the canonical $CD4^+$ Th1 phenotype, known to be the highest producer of anti-viral cytokines (Djuretic et al., 2007; Morita et al., 2011). There was

high variability, with no statistical differences, for the low production of IL-10 (**Figure 3.4 d**). Although IL-10 is known to enhance plasma cell differentiation (Arpin et al., 1995) our data confirmed the low production of this cytokine by Tfh cells (Chtanova et al., 2004; Ma et al., 2009).

The identification of Tfh and non-Tfh cells described in this section was fundamental for this study to define different Tfh cell subsets from donor-matched tonsillar tissue and peripheral blood and therefore determine the populations from blood and tonsils that we wish to compare.

T cell phenotype and function are possibly shaped by environmental influences of the tissue where they are localized, therefore the heterogeneity observed between Tfh cells from blood and tonsils in this section does not deny a relationship between the two compartments. In order to evaluate the correlation of circulating and tonsillar Tfh cells, we sought to study a parameter that does not change with the location and the approach we took was to examine the T cell repertoire.

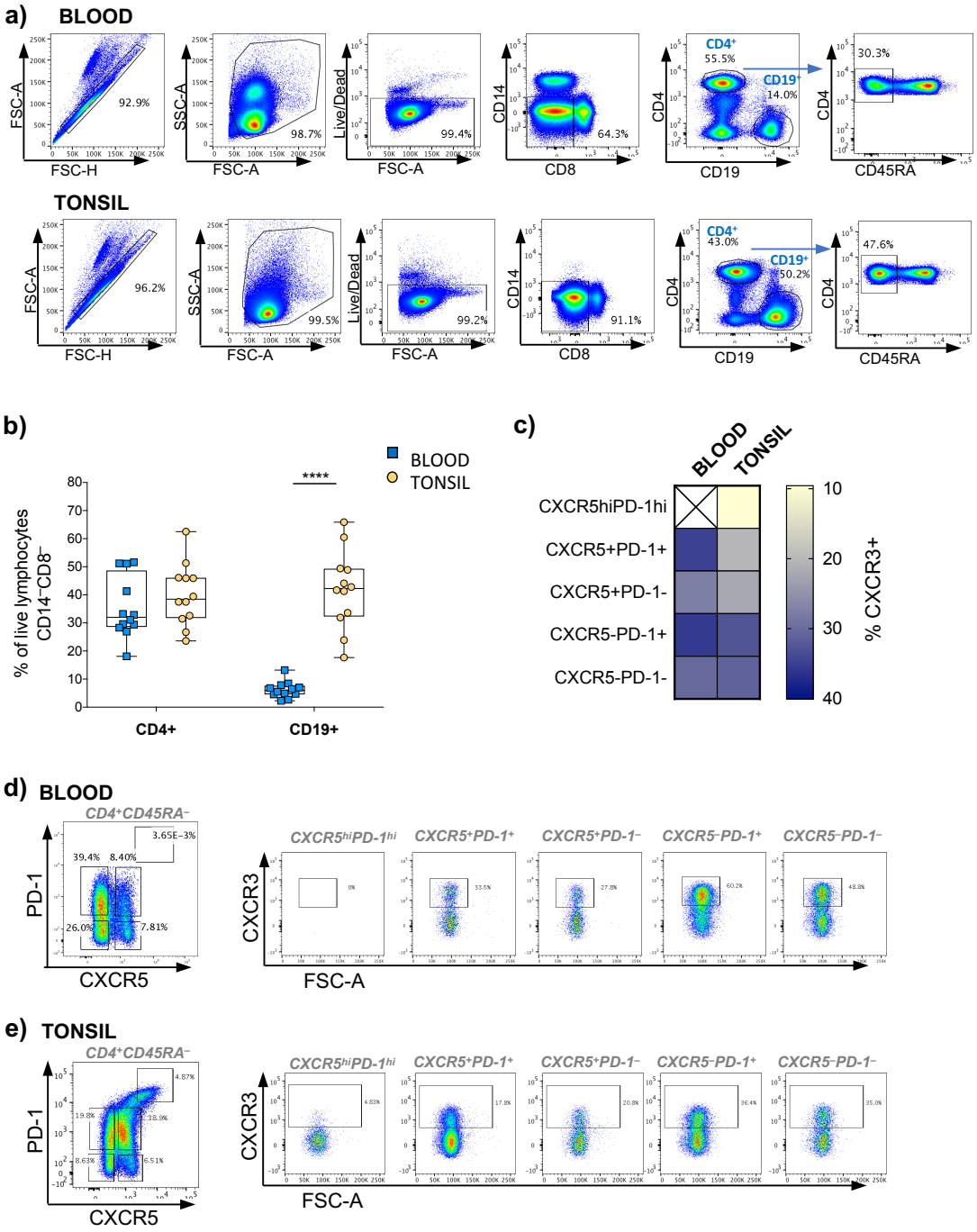


Figure 3.1 Blood and tonsil lymphocyte composition.

Matched peripheral blood mononuclear cells (PBMC) and mononuclear cells from tonsils (MNC-T) from 12 adult donors were stained *ex vivo*. (**a**) An example of gating strategy of matched blood and tonsil cell suspensions from one representative donor is shown, illustrating how $CD4^+$ and $CD19^+$ cells were gated. (**b**) Percentage of $CD4^+$ and $CD19^+$ cells within lymphocytes in the donors analysed is shown. Boxes show

the mean and quartiles and whiskers minimum and maximum. *P<0.05, **P<0.01, ***P<0.001, ****P<0.0001. Expression of PD-1, CXCR5 and CXCR3 in $CD4^+CD45RA^-$ T cells *ex vivo* from (**d**) blood and (**e**) tonsils are shown from one representative donor. The heat map (**c**) represents the mean percentage of $CXCR3^+$ cells in the indicated subsets of memory $CD4^+$ T cells.

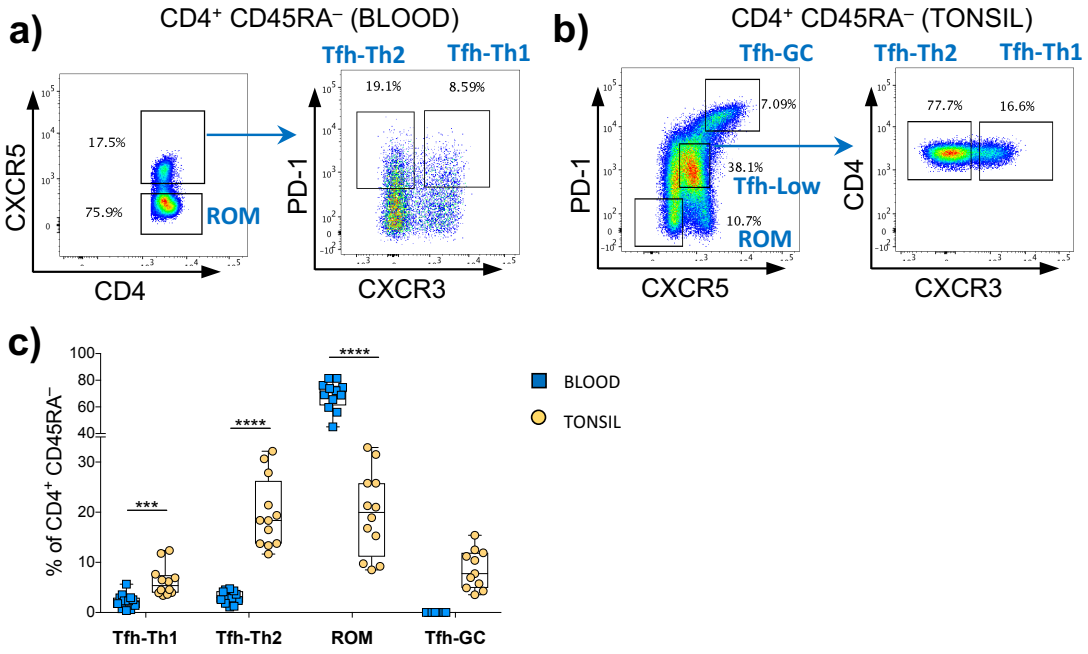


Figure 3.2 $CD4^+$ T cell subsets compared from blood and tonsil.

An example of gating within $CD4^+CD45RA^-$ cells (identified as in Figure 3.1) from blood and tonsil showing the identification of ROM, Tfh-Th1 and Tfh-Th2 populations from (**a**) blood and ROM, Tfh-GC, Tfh-Low, Tfh-Th1 and Tfh-Th2 populations from (**b**) tonsils. The statistic from all the donors is shown (**c**): the graph only shows paired t test statistics between similar populations from different compartments (ex. Blood_Tfh-Th1 vs Tonsil_Tfh-Th1). Boxes show the mean and quartiles and whiskers minimum and maximum. *P<0.05, **P<0.01, ***P<0.001, ****P<0.0001.

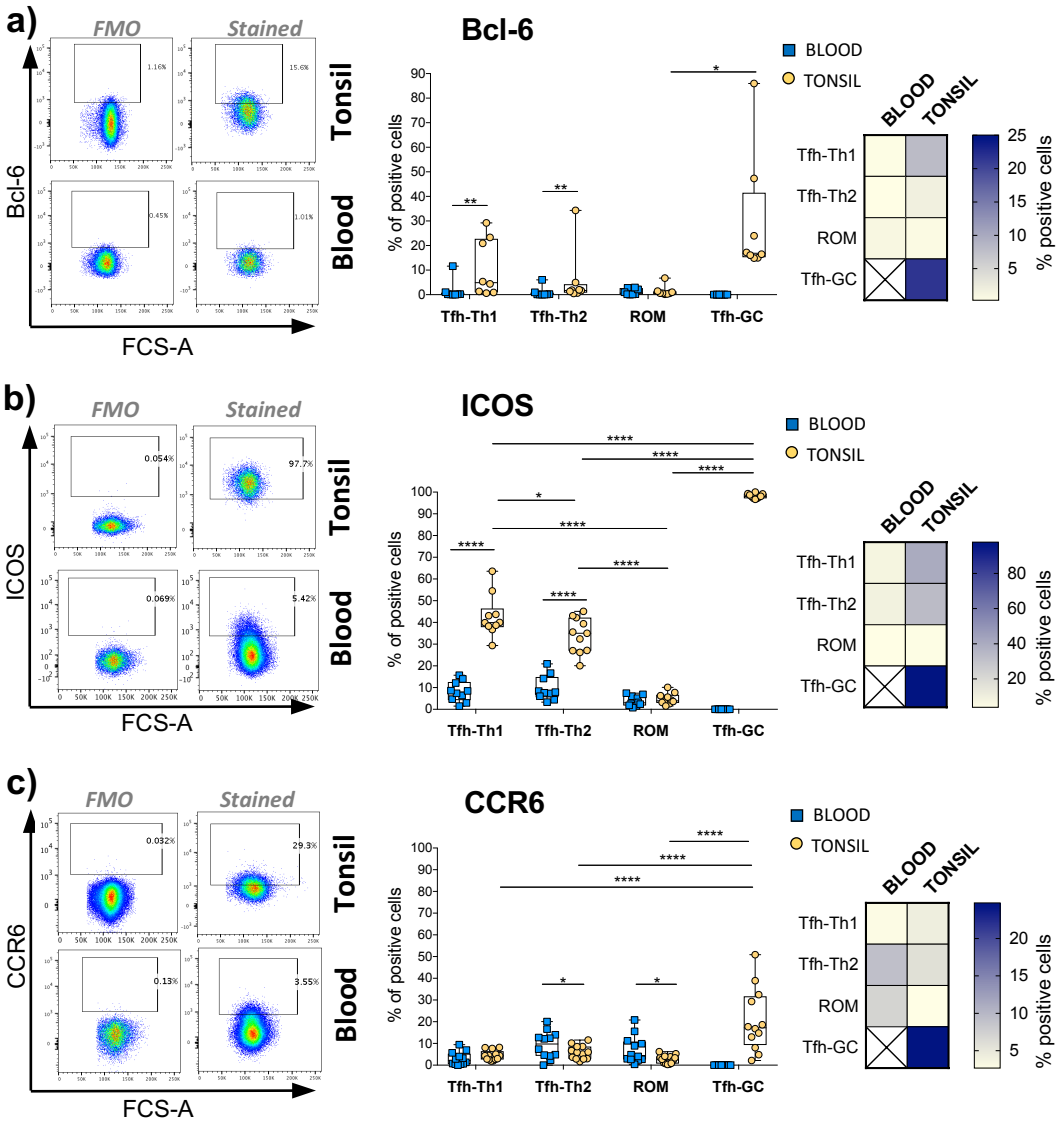


Figure 3.3 Tfh markers comparison between blood and tonsil CD4⁺ T cell subsets. (**a**) Bcl-6, (**b**) ICOS and (**c**) CCR6 flow cytometry staining was performed *ex vivo* on different populations of blood and tonsil $CD4^+CD45RA^-$ T cells (Tfh-Th1, Tfh-Th2, ROM and Tfh-GC), from each donor. The dot plots on the left are example of gating based on a Fluorocrome Minus One (FMO). The first row shows an example of $CD4^+$ memory Tfh cells ($CXCR5^+PD\text{-}1^+$) staining of tonsil and the second row an example of $CD4^+$ memory Tfh cells ($CXCR5^+PD\text{-}1^+$) staining of blood. The statistics is shown from each donor: boxes show the mean and quartiles and whiskers minimum and maximum. *P<0.05, **P<0.01, ***P<0.001, ****P<0.0001. The heat maps on the side represent the mean percentage of each marker cells in the indicated subsets of memory $CD4^+$ T cells.

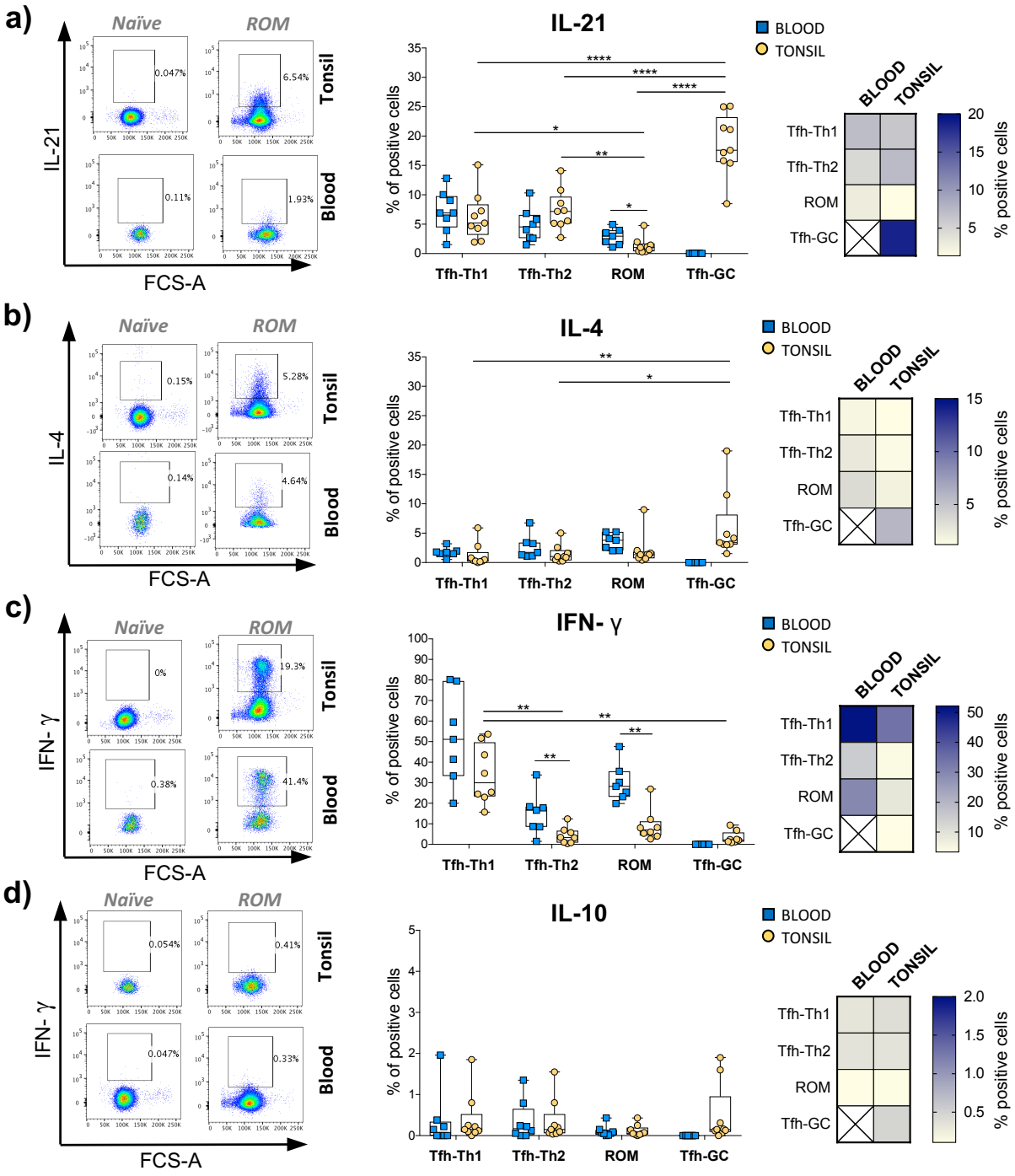

a)
Naïve
ROM
Tonsil
Blood
IL-21
FCS-A
0.047%
6.54%
0.11%
1.93%
IL-21
% of positive cells
Tfh-Th1
Tfh-Th2
ROM
Tfh-GC
BLOOD
TONSIL
% positive cells
b)
IL-4
0.15%
5.28%
0.14%
4.64%
c)
IFN- γ
0%
19.3%
0.38%
41.4%
d)
IL-10
0.054%
0.41%
0.047%
0.33%

Figure 3.4 Cytokine production profiles of blood and tonsil $CD4^+$ T cell populations.

(**a**) IL-21, (**b**) IL-4, (**c**) IFN-γ and (**d**) IL-10 cytokine production was measured intracellularly by flow cytometry after PMA/ionomycin stimulation in different populations of blood and tonsil $CD4^+CD45RA^-$ T cells (Tfh-Th1, Tfh-Th2, ROM and Tfh-GC) from each donor. The dot plots on the left are example of ROM gating based on naïve population ($CD4^+CD45RA^+$). The statistics is shown from each donor: boxes show the mean and quartiles and whiskers minimum and maximum. *P<0.05, **P<0.01, ***P<0.001, ****P<0.0001. The heat maps on the side represent the mean percentage of each marker cells in the indicated subsets of memory $CD4^+$ T cells.

3.3 Evaluation of the utility of the library method for repertoire analysis of circulating Tfh cell populations

Having shown that the cytokine production and the expression of transcription factors differed between cTfh and tonsillar Tfh, we next wished to assess whether the specificity of each subset differed. If two populations of T cells share the same antigen specificity repertoire and have similar precursor frequencies, they are most likely to have a common clonal origin, despite expressing a different phenotypic profile, imposed by the particular environment in which the cells are temporarily situated. The T cell library technique, developed by Professor Federica Sallusto and her colleagues (Geiger et al., 2009), was the first method we chose to directly compare the antigen specific repertoires of tonsil and blood Tfh cells and to characterise the specificity of different subsets of $CD4^+$ T cells in blood and tonsils from the same donors. T cell library method consists on expanding sorted T cells polyclonally in culture and to screen them after expansion for the specificity to

certain antigens using autologous monocytes as antigen presenting cells (APC). Because the T cells are seeded at a limiting dilution, it is possible to calculate the precursor frequency of antigen-specific T cells specific, based on the Poisson distribution (see section 2.6.1).

In order to ensure that the non-specific T cell expansion required for the T cell library method would not modify the TCR profile, but rather expands each clonotype evenly, the repertoire of $CD4^+$ T cell memory populations from the blood of 3 donors was monitored by flow cytometry before (day 0) and after expansion (day 27) using a set of TCR Vβ specific monoclonal antibodies that covers 70% of the human Vβ T cell repertoire (panel G, see Figure 2.5). Data in **Figure 3.5** show the percentage of cells expressing the different Vβ receptor families in each $CD4^+$ T cell subset considered (Naïve, ROM, Tfh-Th1 and Tfh-Th2) from peripheral blood of one out of 3 donors studied (**Figure 3.5 a**). The Vβ repertoire at day 0 was notably similar to the one at day 27 after a polyclonal expansion in each of the subsets analysed (R^2>0.65, slope>0.75, P<0.0001). Linear regression correlation between all the subsets of interested was calculated from each donor (**Figure 3.5 b**). Each dot is a Vβ and the coordinates (x,y) indicate the expression of the same receptor at either day 0 or day 27. The strong positive correlation between the day 0 and day 27 repertoires observed in each of the 3 donors demonstrates that cells expressing each Vβ underwent unbiased polyclonal expansion and supports the utility of this method for comparison T cell repertoire after an *in vitro* expansion. A similar approach was used to validate the utility of the library method for analysis of the $CD4^+$ T cell naïve repertoire in the study from 2009 by Geiger et al., where the Vβ usage of $CD4^+$ naïve

T cells from different time points of polyclonal expansion resulted comparable (Geiger et al., 2009).

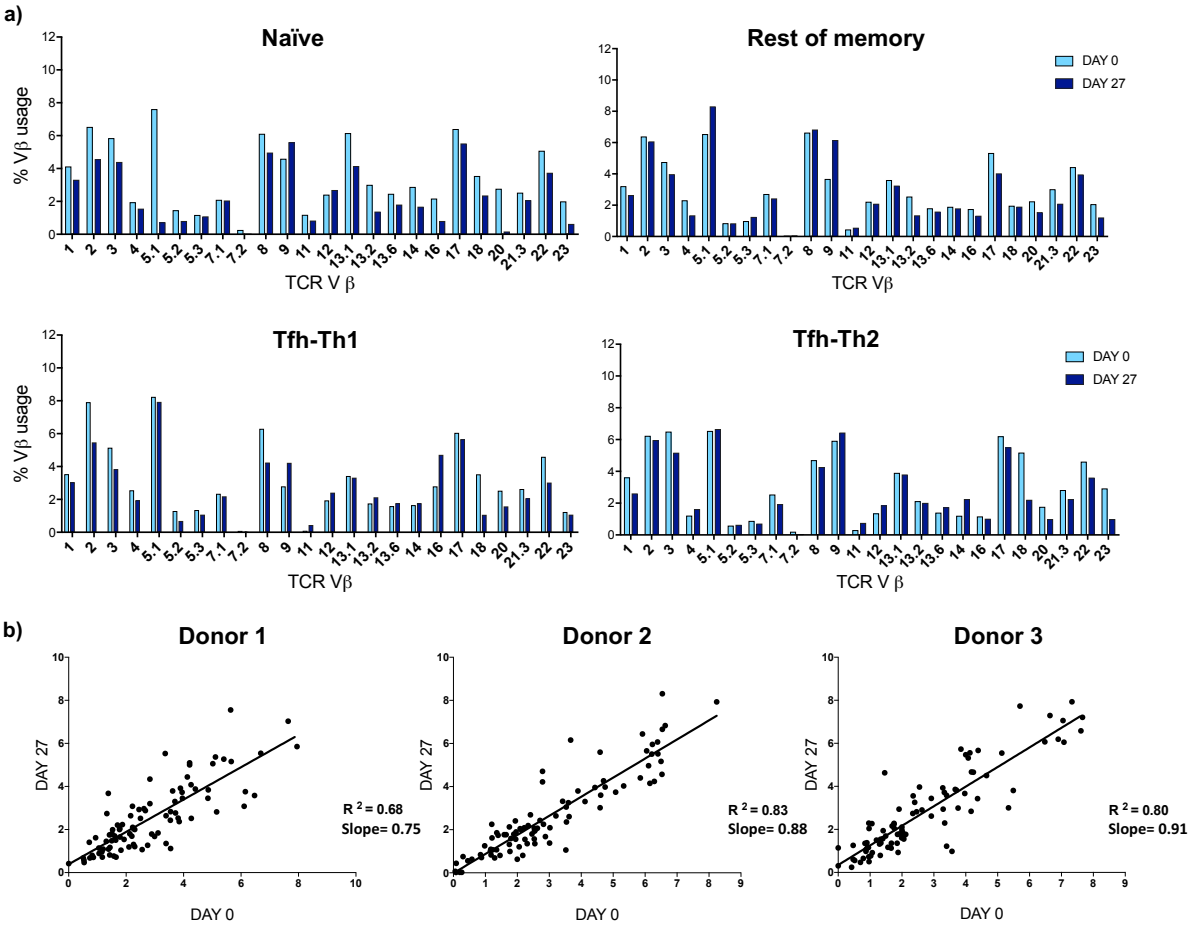


Figure 3.5 TCR Vβ repertoire maintenance in blood CD4$^+$ T cell subsets after culture.

Different subsets of CD4$^+$ T cells (naïve, ROM, Tfh-Th1, Tfh-Th2) were analysed for the TCR Vβ percentage expression using flow cytometry before (day 0) and after (27 days) a polyclonal expansion. (**a**) Data from one representative donor is shown and TCR Vβ families are listed on the x-axis. (**b**) The coefficient of determination (R^2) and the slope of the linear regression were calculated for each donor. The P value was constantly <0.0001 for each correlation. Linear regression graphs plot together the values of all four populations considered.

3.4 Media optimisation for tonsil cell culture and cytokine receptors profiling of tonsil and blood cells during expansion

In order to adapt the T cell library method and use it with tonsil samples, media optimisation was required to best maintain tonsil cells viability during expansion. Tonsils are solid tissues not sterile and often contaminated, particularly with mycoplasma and therefore, as used by many research groups working with tonsillar cells, we supplemented our media with different antibiotics (Penicillin, Streptomycin, Gentamicin and Timentin) and antifungal drugs (Fungizone) (Grivel and Margolis, 2009). Three different media conditions were tested: media 1 contained Penicillin and Streptomycin (also called Complete Media, CM), media 2 was supplemented with Gentamicin and Fungizone and media 3 with Gentamicin, Timentin and Fungizone. In addition to the antibiotics and anti-fungal drugs, all the three media contained the canonical reagents often used for PBMC culture cells, such as sodium pyruvate, non-essential amino acids, glutamine and pool of human sera (see Figure 2.2). Since the precursor frequency is calculated based on the initial limiting dilution, it was also necessary to confirm, that cells in each subset of $CD4^+$ T cells from tonsil expand equally in culture. This aspect acquired a particular importance in T cells from tonsil tissues since those cells are more fragile *in vitro*, especially if treated in liquid suspension, compared to PBMC, probably because they are usually localized in solid tissue.

The toxicity of the 3 media conditions with or without IL-7, commonly used to augment the T cell viability in previous studies (Murray et al., 1989; Okazaki et al., 1989), was initially tested on $CD4^+$ naïve ($CD45RA^+$) and memory ($CD45RA^-$) T

cells from the blood of 2 donors (panel A, see Figure 2.5 without anti-CXCR5, anti-CXCR3 and anti-PD-1) (**Figure 3.6**). A T cell library of 24 wells per condition, seeded at 1,000 cell/well for the memory and 2,000 cell/well for the naïve compartment, were expanded polyclonally using irradiated allogeneic feeder cells, PHA and IL-2 for 20 days in culture. Growth (**Figure 3.6 a**, **b**) and viability (**Figure 3.6 c**, **d**) were monitored, at serial time points from 5 to 20 days of expansion, by counting 4 wells per condition, using automated cell counter T20 (Bio-rad) and Trypan Blue Stain exclusion. Cells cultured in media 2 and 3 had a high percentage of dead cells (30 %) during the initial culture period. Cells expanded in Media 1 instead had a good expansion and high viability throughout the culture period. After 20 days of expansion each subset was washed from the IL-2, rested for 4 hours and screened for the capacity to proliferate in response to a polyclonal stimulus, PHA. Since PHA is often used as a positive control, T cells stimulated with this agent are all expected to proliferate (as assessed by [3H]-thymidine incorporation). **Figure 3.6** shows the stimulation results of both donors from naïve (**Figure 3.6 e)** and memory $CD4^+$ T cells (**Figure 3.6 f**). The stimulation confirmed the greatest response of cells cultured with Media 1, since many of the wells cultured in Media 2 and 3 did not have a proliferation higher than 3000 cpm, a cut-off defined using a stimulation index >5.

Media 1 was then tested in culture for mononuclear cells from tonsils (MNC-T) expansion. The growth of total $CD4^+$ T cells isolated with magnetic beads from one tonsil sample was monitored during 25 days of polyclonal expansion, using total $CD4^+$ T cells from peripheral blood of a non-matched donor as a control (**Figure 3.7**). T cells were seeded at 1,000 cell/well for a total of 24 wells per condition. The

expansion was exponential (**Figure 3.7 a**) and the viability was >94% in both tonsil and blood samples (**Figure 3.7 b**). Each well was then stimulated for the capacity to proliferate in response to two different stimuli: PHA (**Figure 3.7 d**) and IL-2 (**Figure 3.7 e**). $CD4^+$ T cells from tonsils showed a comparable proliferation to the $CD4^+$ T cells from blood.

Even though the total $CD4^+$ T cell expansion and proliferation from tonsils was optimal using Media 1, when $CD4^+$ T cells were split into different subsets of Tfh (Tfh-GC and Tfh-Low) and non-Tfh (naïve and ROM), the expansion and the viability during culture was rather poor, especially for the Tfh-GC population (data not shown). For this reason, a supplement optimisation of the Media 1 was performed, and the viability of cells of each subpopulation was checked at serial time points from as early as 24 hours of expansion. Four different subsets of $CD4^+$ T cells from 2 tonsil samples, naïve, ROM, Tfh-GC and Tfh-Low (**Figure 3.8 a**), and four subsets of $CD4^+$ T cells from two healthy blood donors, naïve, ROM, Tfh-Th1 and Tfh-Th2, run in parallel as a control (**Figure 3.8 b**). T cells were sorted and seeded at 1,000 cell/well and 48 wells per condition (panel A, see Figure 2.5). Each T cell subset was split in 3 and expanded in the presence of 3 different CM with either 5, 10 or 20 % of human serum (HS) for 30 days. Growth and viability were checked during the expansion (**Figure 3.8 c, d**). Cell viability in the first few days of culture was unfortunately difficult to assess, as T cells were cultured with allogeneic irradiated feeder cells, which died in the first 72 hours of culture, causing difficulties in distinguishing the viability of sorted T cells. But as the presence of feeder cells was a common variable in all conditions, the number of viable cells was compared. Compared with $CD4^+$ T cells from the blood, Tfh cells from tonsils were notably

slower to expand, reaching a plateau earlier than the other subsets, mainly due to their poor viability at the beginning of the culture. However, a higher growth in the first 24 hours was registered in Tfh-GC and ROM cells cultured with 20% HS, although after 10 days this was the condition that correlated most weakly with T cell growth. No difference was observed between 5 and 10 % HS conditions. After 20 days of culture, each condition was washed and rested for few hours in CM and screened for the capacity to proliferate to IL-2. **Figure 3.9** shows data from both donors combined and no difference was observed between the 2 donors for both blood and tonsil samples. Overall the proliferation in tonsil was <50 % and particularly low in Tfh-GC cells with not much difference between the different media conditions (**Figure 3.9 a**). Tonsil proliferation was compared to $CD4^+$ T cell proliferation from blood, which was >75-95 %, as expected (**Figure 3.9 b**). The background from both compartments was always below the threshold, even though it was quite high in the 20% HS condition (**Figure 3.9 c, d**).

Together with the growth and the viability, it was also important to know how the phenotype of T cell subsets changed during the long period of culture that the T cell library method requires. For this purpose, the stability of surface marker expression in Tfh and non-Tfh populations was monitored by flow cytometry throughout the 34 days of expansion in CM IL-2 with 5% HS (**Figure 3.10**). The GC homing receptor CXCR5 was downregulated in both tonsil and blood Tfh cells before day 10, possibly due to the lack of cytokines and stimuli from B cells in the culture environment compared with the lymph nodes and peripheral blood. The PD-1 marker in Tfh subsets was steady even after 30 days of culture, except for Tfh-GC where the same marker was unstable and downregulated to < 45% at day 34. Both

CXCR5 and PD-1 expression, which can be upregulated in $CD4^+$ T cells following activation, were consistently increased at day 5-8 and then immediately decreased in naïve and ROM populations. Although CXCR3 was not evaluated in the tonsil panel, a notable increase in the percentage of T cells expressing this Th1-related receptor was detected in all subsets of $CD4^+$ T cells from blood, probably due to the polyclonal stimulus given and the supplementation with exogenous IL-2 in culture. The stability of Tfh markers until day 10, had previously only been demonstrated for PD-1 in peripheral blood $CD4^+$ Tfh cells (Locci et al., 2013). The loss of the main Tfh markers during the following 20 days of culture, was probably due by the lack of IL-21 and IL-6 cytokines in the environment (Choi et al., 2013; Nurieva et al., 2008; Vogelzang et al., 2008).

Overall T cells from tonsils showed technical challenges for an equal polyclonal expansion *in vitro* required for the T cell library technique and these difficulties did not allow to use this method to address the T cell repertoire comparison between blood and tonsil.

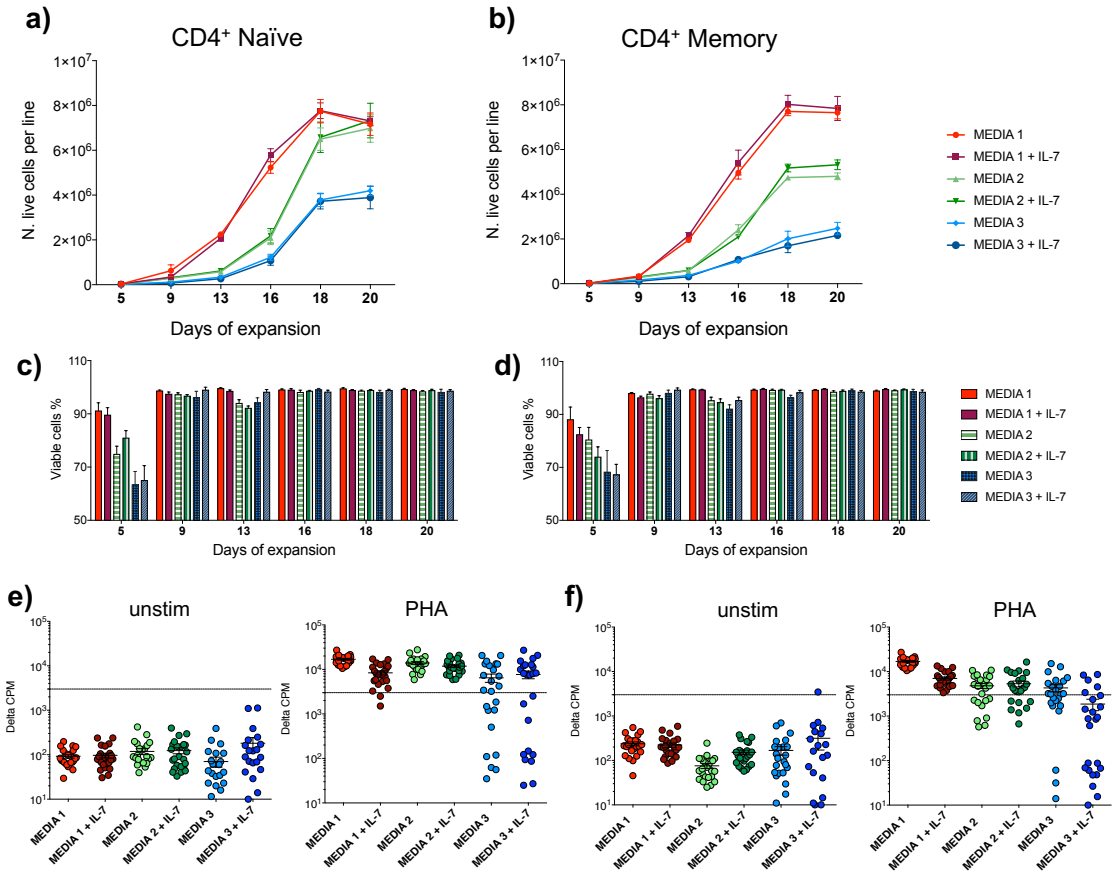


Figure 3.6 Media optimisation using naïve and memory CD4⁺ T cells from peripheral blood.

Growth and viability of CD4⁺ (**a**, **c**) naïve and (**b**, **d**) memory T cells from 2 blood donors were tested and monitored throughout the culture of 20 days in 3 different media conditions with or without IL-7. Media 1= Penicillin and Streptomycin; Media 2= Gentamicin and Fungizone; Media 3= Gentamicin, Timentin and Fungizone. All three media contained sodium pyruvate, non-essential amino acids, glutamine and pool of human sera. Each data point represents the mean and the bars the SEM of 4 wells. After expansion, (**e**) naive and (**f**) memory T cells were stimulated with PHA and the proliferation was measured using [3H]-thymidine incorporation. Each dot represents the counts per minute (cpm) proliferation in a single well and each value was background subtracted.

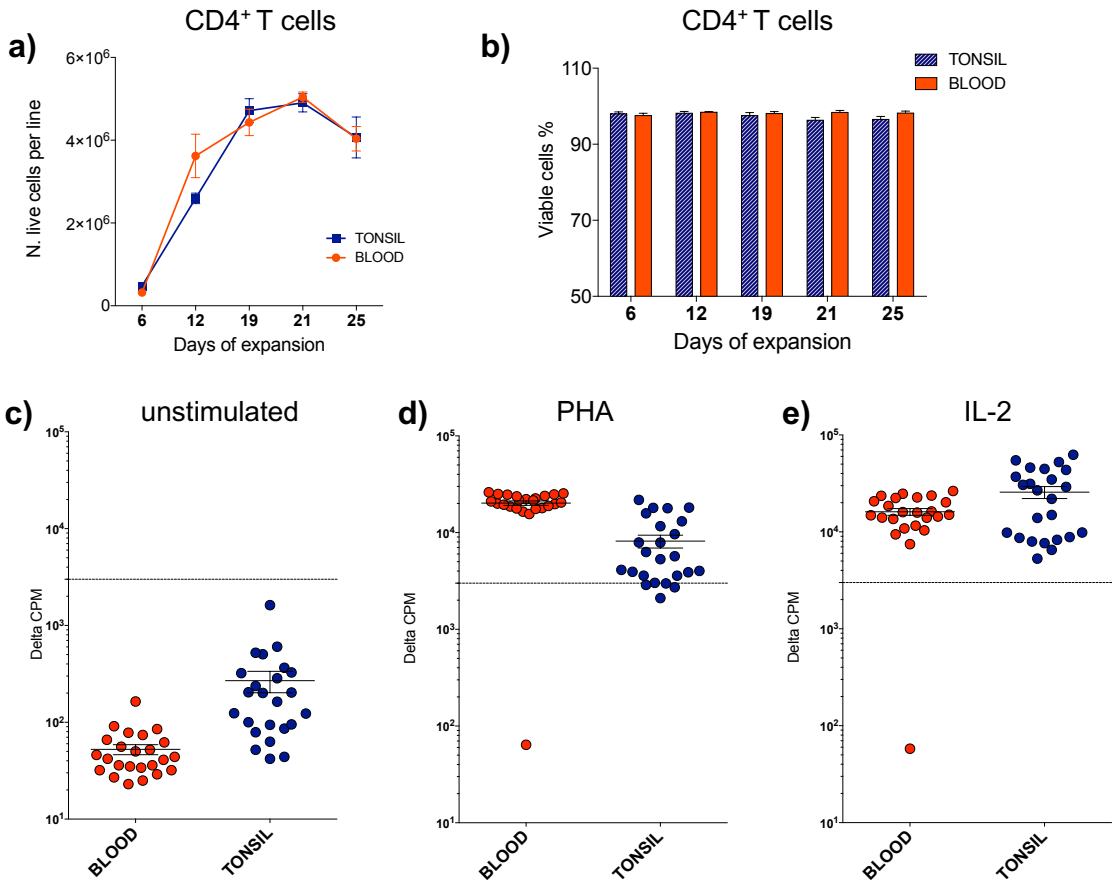


Figure 3.7 Media check on CD4⁺ T cells from tonsils.

CD4⁺ T cells from one tonsil sample were cultured in Media 1 and CD4⁺ T cells from peripheral blood of an unmatched donor were run in parallel. (**a**) Growth and (**b**) viability was monitored throughout 25 days of culture, each data point represents the mean and the bars the SEM of 4 wells. The capacity for proliferation was measured after stimulation with (**d**) PHA and (**e**) IL-2. Each dot represents the counts per minute (cpm) proliferation in a single well and each value was (**c**) background subtracted. The cut-off was defined at 3000 cpm, using a stimulation index >5.

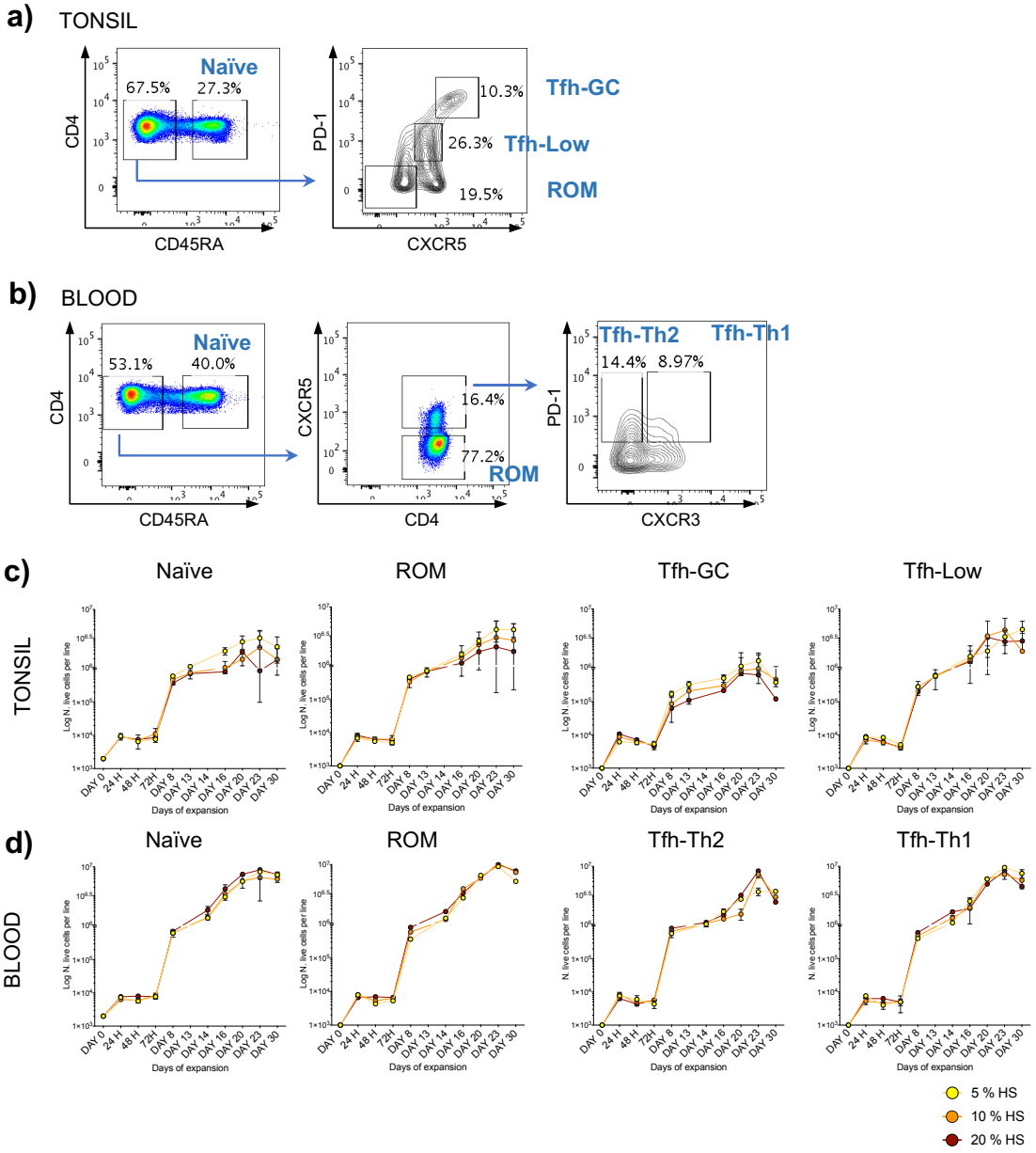


Figure 3.8 Serum media optimisation in tonsils: gating and culture growth.

Different populations of $CD4^+$ T cells from two (**a**) tonsil samples and two (**b**) blood non-donor-matched blood samples were sorted and cultured in 3 Media conditions, differing in the percentage of human sera (yellow=5%, orange=10% or red=20%). The growth of each cell population from (**c**) tonsil and (**d**) blood was monitored during 30 days expansion. Each data point represents the mean and the bars the SEM of 4 wells.

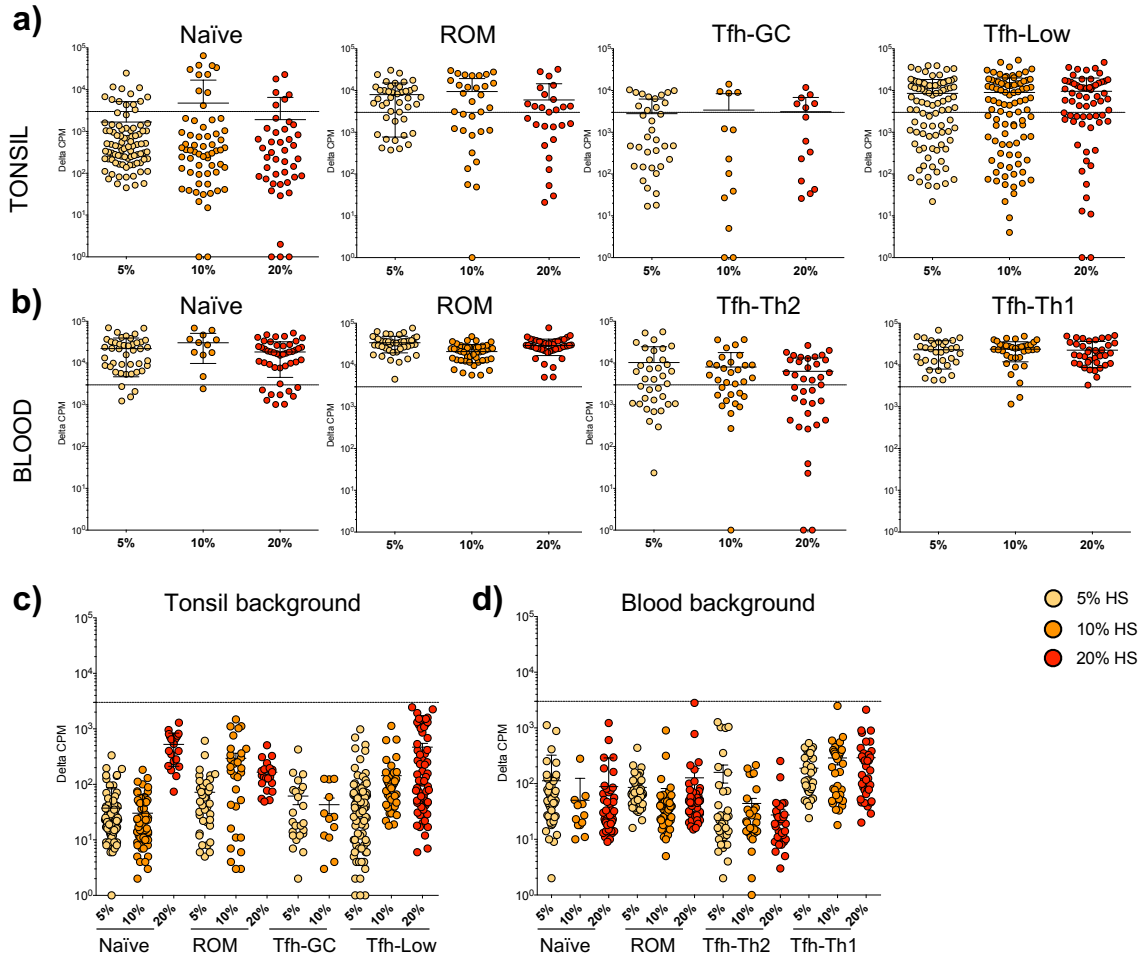


Figure 3.9 Serum media optimisation in tonsils: proliferation capacity.

The capacity to proliferate in response to IL-2 was assessed in each $CD4^+$ T cell population and from each media condition at day 20 of expansion from both (**a**) tonsil and (**b**) blood. Each dot represents the counts per minute (cpm) proliferation in a single well and each value was (**c**, **d**) background subtracted. A usual cut off of 3000 cpm was considered, with a stimulation index >5

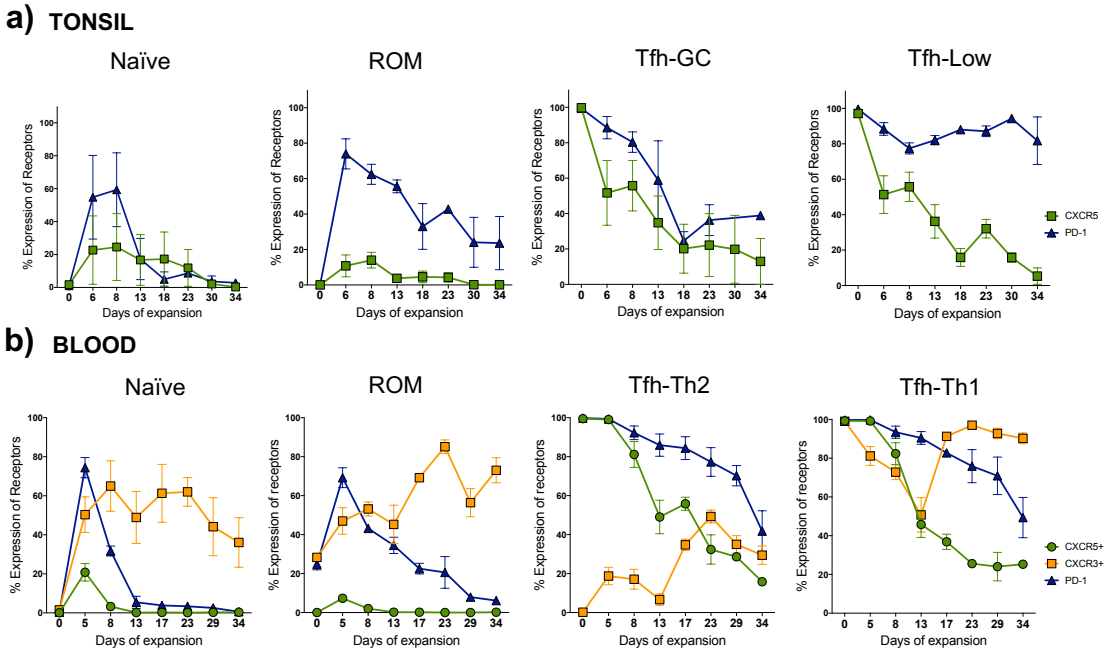


Figure 3.10 Surface marker expression profile of T cell subsets during culture. $CD4^+$ T cells from (**a**) two tonsil samples were sorted into naïve, ROM, Tfh-GC and Tfh-Low cells and the surface markers PD-1 and CXCR5 were monitored by flow cytometry during 34 days of culture. $CD4^+$ T cells from (**b**) two blood donors were sorted into naïve, ROM, Tfh-Th1 and Tfh-Th2 and the surface markers PD-1, CXCR5 and CXCR3 were monitored by flow cytometry during 34 days of culture. Each data point represents the mean of the expression and the bars the SEM of 4 wells.

3.5 Conclusions

Throughout this section I identified different $CD4^+$ T cell populations based on surface markers and chemokine receptors, especially focusing on Tfh cells. The *ex vivo* data identified a PD-1^{hi}CXCR5^{hi}ICOS^{hi} population with features characteristic of Tfh-GC cells from tonsils previously described, which was absent in peripheral blood (He et al., 2013; Locci et al., 2013). Tfh-GC cells were the best producers of IL-21 and IL-4 and had the highest expression of transcription factor Bcl-6, well-

defined factors that characterized a follicular helper phenotype and known to be involved in Tfh cell differentiation and development (Nurieva et al., 2008; Yu et al., 2009). The high expression of CCR6 in Tfh-GC cells might influence the localization of Tfh-GC in the LZ of the GC, as it does for B cells (Suan et al., 2017; Wiede et al., 2013). Tfh-GC cells also showed a remarkable non-Th1 phenotype with lacking of IFN-γ production and CXCR3 expression, as partially previously described (Ma et al., 2009; Ploquin et al., 2011) and suggested a specific effector role of these cells into the GC rather than an anti-viral function in the periphery. The combination of CXCR5, PD-1 and CXCR3 differently expressed, also identified populations with an intermediate Tfh phenotype (PD-1^{lo}CXCR5^{lo}) in both blood and tonsils, such as Tfh-Th1 and Tfh-Th2 cells. Cells with this intermediate Tfh phenotype, called "memory" Tfh cells for simplicity even though the nature of those is still not clear, showed a similar cytokine profile, but a more pronounced expression of ICOS in tonsils compared with blood. In particular Tfh-Th1 subset in both blood and tonsils showed a clear skew to a canonical Th1 phenotype (IFN-γ production and CXCR3 expression) and the comparison between the two tissues underlines few similarities between Tfh-Th1 from tonsil and blood (section 3.2).

Although not having donors with an ongoing infection is clearly a limitation to study Tfh cells, the phenotype analysis was fundamental to identify the populations of interest and to describe that Tfh cells from different compartments of the same donor showed a variety of the phenotype, which is probably related and influenced by the specific function they have in the tissue. This observation does not deny a relationship between the two tissues, but it suggested that a different approach was required to consider a parameter of T cells that does not change with the location

and namely the T cell antigen specificity repertoire, which is based on the unalterable expression of the T cell receptor (TCR). The T cell library method (Campion et al., 2014; Geiger et al., 2009) was chosen to analyse the T cell repertoire and the utility of this method was supported by the polyclonal expression of Vβ repertoire on $CD4^+$ memory T cells after an *in vitro* expansion (section 3.3). This method has previously only been used for analysis of circulating $CD4^+$ T cell subsets (Campion et al., 2014), and total cTfh cells (Bruno et al., 2016).

It was then necessary to optimise this method to different $CD4^+$ T cell memory populations from tonsils. Overall tonsil cells, especially the effector cell subset Tfh-GC with the highest expression of PD-1, well known to be an exhaustion marker in $CD4^+$ and $CD8^+$ T cells (Cho et al., 2017; D'Souza et al., 2007; Day et al., 2006), did not perform well in long-term culture *in vitro* and this difficulty in expanding them polyclonally was a serious issue for the repertoire analysis. Several experiments have focused on optimising culture medium with different antibiotics and different concentration of human sera to maintain T cells from tonsils viable from the beginning of the culture and to expand them polyclonally (section 3.4), as the T cell library required. The method in fact requires a precise number of starting cells to calculate the precursor frequency, but having an early low viability in the culture would likely bias the estimation of antigen-specific cells/million. Although the culture media was optimised and was suitable to grow surviving tonsil cells in culture for at least 10 days, the poor recovery of tonsil cells in the first few days of expansion, did not allow application of this technique to examine the tonsil repertoire. Further analyses could have been conducted, for example by labelling sorted T cells to enable better tracking of their early viability, performing a Vβ TCR staining before and after

cell culture to validate the expansion of each cell clonotype from tonsils or co-culturing cells with different cytokines in the medium. However, it was decided not to pursue further experiments, as the results obtained from the initial analyses indicated that the T cell library method, which works very well for PBMC (Bruno et al., 2016; Campion et al., 2014), was not an appropriate technique for tonsil $CD4^+$ T cells and therefore was inappropriate for comparisons between tonsil and blood $CD4^+$ T cell subsets.

4 Results II: comparison of T cell receptor repertoire in circulating and tonsillar Tfh and non-Tfh cells

4.1 Background and rational

In the previous chapter (section 3) different populations of circulating and tonsillar Tfh cells were described based on the expression of surface markers and cytokine production. From the phenotype profile described and the comparison of multiple studies in the literature, we decided to consider the following populations to compare blood and tonsil Tfh and non-Tfh cells for the purpose of this study. In the peripheral blood three populations of $CD4^+$ memory T cells are identified: Tfh-Th1 ($CXCR5^+PD\text{-}1^+CXCR3^+$), Tfh-Th2 ($CXCR5^+PD\text{-}1^+CXCR3^-$) and ROM as rest of memory ($CXCR5^-$). In parallel from the matched tonsillar tissue, four populations of $CD4^+$ memory T cells are considered: Tfh-GC ($CXCR5^{hi}PD\text{-}1^{hi}$), Tfh-Th1 ($CXCR5^{lo}PD\text{-}1^{lo}CXCR3^+$), Tfh-Th2 ($CXCR5^{lo}PD\text{-}1^{lo}CXCR3^-$) and ROM ($CXCR5^-PD\text{-}1^-$). Having described the heterogeneity of the phenotype profile of these subsets, mainly due by the environment and stimuli they received in the different compartments, to directly compare cTfh with tonsillar Tfh as well as Tfh versus non-Tfh, it was necessary to consider a stable T cell parameter, such as the T cell receptor (TCR). The T cell receptor (TCR) expression is an invariable characteristic which does not change with the location and can be used to study the same clonal populations of T cells in different tissues, such as peripheral blood and tonsils.

Two different α and β chains compose the TCR. After undergo rearrangement in the thymus, both α and β chains consist of a constant region (C), a VJ segment for the

α and VDJ for the β. Additionally, random nucleotides are added or deleted between the junctions (Davis and Bjorkman, 1988). VJ and VDJ segments encode the hypervariable of complementarity-determining regions (CDRs): CDR1, CDR2 and CDR3 loops. CDR3 region is the most variable loop of the TCR and it derived from the thymic recombination of the VJ junction region from the α chain and from the VDJ junction region of the β chain (Nikolich-Žugich et al., 2004). The extreme variability of the CDR3 region for each different T cell (clonotype) is the key element for the nature of the extraordinary T cell repertoire diversity, which allows a wide antigen recognition property.

The rearrangement and the selection processes occurring in the thymus (see section 1.3) produce a single functional β-chain and one or more α-chains per T cell, however it is unlikely that different α-chains produce more than one functional paired αβTCRs with same β-chain (Padovan et al., 1993; Petrie et al., 1993). Therefore, the RNA transcript of a single T cell can present more than one α-chain and this is the main reason why TCR-based analysis often rely on the β- rather than on the α-chain sequence to identify single T cell clonotypes.

The diversity of the TCR repertoire makes it difficult to create a comprehensive view of it. Spectratyping techniques based on quantitative polymerase chain reaction (PCR) strategies or monoclonal antibodies provided a limited overview of the repertoire in the past (Six et al., 2013). Since the next generation sequencing (NGS) methods developed, high-throughput techniques to perform deep analysis of TCR sequences became available (Rosati et al., 2017).

The difficulties encountered in the previous chapter to apply the T cell library method (Geiger et al., 2009) to tonsil samples in order to characterize the specificity of the T cell repertoire, led me to adopt different approaches, either based on flow cytometry monoclonal antibodies or to a high-throughput targeted sequence-based analysis of the TCR.

For the targeted sequence-based analysis, we decided to detect the TCR expression based on the mRNA level of bulk T cell populations, rather than DNA. Although DNA is more stable than RNA and it allows the calculation of the absolute frequency of a certain clonotype since there are always two copies of DNA in a cell, it does not provide information on the expression level of the TCR and often carries VDJ rearrangement residuals. Moreover DNA-based analysis requires a higher level of multiplex amplification that might bias the quantitative information during the analysis (Mamedov et al., 2013). mRNA-based sequence instead, contains the final product of the TCR expressed and the repertoire coverage is higher (Rosati et al., 2017).

Thus, the aims of this chapter were:

- To evaluate the feasibility of a low-resolution method based on flow cytometry monoclonal antibodies to study the TCR Vβ repertoire between blood and tonsil (section 4.2).
- To compare the TCR repertoire between circulating and tonsillar Tfh cells by high-throughput RNA-based deep-sequencing analysis (section 4.3).
- To compare the TCR repertoire between Tfh and non-Tfh cells in blood and tonsil by high-throughput RNA-based deep-sequencing analysis (section 4.4).

- To analyse the TCR repertoire diversity in different populations of Tfh and non-Tfh cells in blood and tonsil by high-throughput RNA-based deep-sequencing analysis (section 4.4).

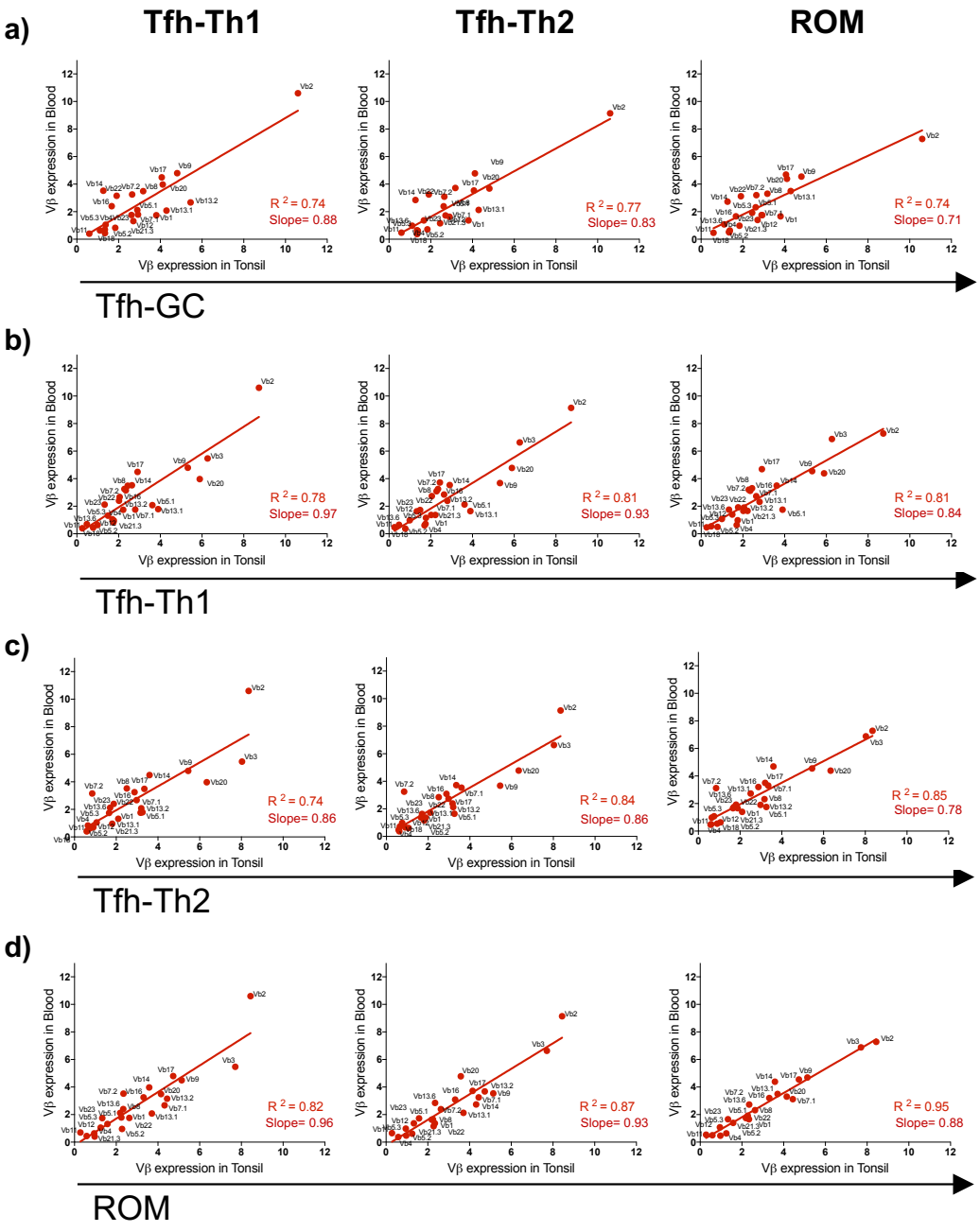
4.2 T cell receptor Vβ profile by flow cytometry

Because of the difficulties of applying the T cell library method in T follicular helper (Tfh) cells from tonsils, I decided to use the flow cytometry-based technique used in section 3.3, which consists of TCR Vβ specific monoclonal antibodies that cover 70% of the Vβ T cell repertoire to look at the general TCR Vβ repertoire composition. Even when samples of blood and tonsil were derived from the same donors, I hypothesized that there would be a determinant distinctiveness between the different $CD4^+$ memory T cell subsets. Examination of T cell receptors would be informative to highlight either similarities or differences between Tfh subsets between blood and tonsil but also between Tfh and non-Tfh populations.

Matched mononuclear cells from blood (PBMC) and tonsil (MNC-T) from 2 donors (230 and 231) were stained by flow cytometry panel G (see Figure 2.5) identifying a plethora of different memory $CD4^+$ T cell subsets based on expression of the surface marker PD-1 and the chemokine receptors CCR6, CXCR5 and CXCR3. From each subset of $CD4^+$ T cells the expression of each of the 24 Vβ families, was measured by either percentage or Median Fluorescent Intensity (MFI). In **Figure 4.1** TCR usage is expressed with percentage, since no difference was registered using either MFI (data not shown) or percentage analysis. In order to correlate in a linear regression the expression of each Vβ family, the coefficient of determination (R^2),

the slope and the P value for each combination of $CD4^+$ T cell subsets identified were calculated. Overall the R^2 calculated from both donors varied in a range of $0.6 < R^2 < 1$ and showed consistent results for any combinations considered. The slope was > 0.7 and the P values were always <0.0001. In particular **Figure 4.1** shows the linear regressions from donor 230 of the tonsillar populations of interest on the x-axis, including Tfh-GC (**Figure 4.1 a**), Tfh-Th1 (**Figure 4.1 b**), Tfh-Th2 (**Figure 4.1 c**) and ROM (**Figure 4.1 d**) compared with specific populations of blood on the y-axis (Tfh-Th1, Tfh-Th2, ROM). The tables (**Figure 4.1 e**) summarize the R^2 from both donors 230 and 231. From this experiment, all the combinations analysed showed a significant correlation even the ones less expected, such as naïve and memory $CD4^+$ T cells. Comparison between Tfh versus non-Tfh cells (ROM) from the same compartment also showed a good correlation (data not shown).

It is highly unlikely that each subset of $CD4^+$ T cells in the circulation and in the tonsil tissues is very similar to each other, therefore it would seem this method lacks sensitivity and so it is not entirely suitable to address our initial question. In particular, measurement of just the Vβ chain usage could miss important differences in TCR sequence in the CDR3 region that profoundly influence the specificity of the T cells. Therefore, a targeted sequence-based high-resolution analysis of the T cell receptor was undertaken to give a far more comprehensive and precise analysis.



e)

DONOR 230		BLOOD		
	R^2	**Tfh-Th1**	**Tfh-Th2**	**ROM**
TONSIL	**Tfh-GC**	0.74	0.77	0.74
	Tfh-Th1	0.78	0.81	0.81
	Tfh-Th2	0.74	0.84	0.85
	ROM	0.82	0.87	0.95

DONOR 231		BLOOD		
	R^2	**Tfh-Th1**	**Tfh-Th2**	**ROM**
TONSIL	**Tfh-GC**	0.77	0.64	0.86
	Tfh-Th1	0.73	0.72	0.80
	Tfh-Th2	0.84	0.70	0.77
	ROM	0.90	0.68	0.75

Figure 4.1 TCR Vβ profile between tonsil and blood by flow cytometry.

The graphs show the linear regression of the % of TCR V**β** families expression between a reference population of tonsil on the x-axis, (**a**) Tfh-GC, (**b**) Tfh-Th1, (**c**) Tfh-Th2, (**d**) ROM, with a variable population of blood on the y-axis. The flow cytometry staining was performed on frozen PBMC and MNC-T samples and linear regression graphs represent data from donor 230. (**e**) Tables of donor 230 and 231 summarise the coefficient of determination (R^2) calculated for each combination.

4.3 Comparison of T cell receptor sequences repertoire between circulating and tonsillar Tfh cells

The definitive way to compare T cell repertoire is by high-throughput TCR sequencing. A few studies in the literature have compared T cell subsets by sequencing the TCR (Becattini et al., 2014; Heit et al., 2017; Herati et al., 2017; Maceiras et al., 2017). T cell receptor is a constant for each T cell clone and is independent of the environment or the antigenic or other stimuli received.

We decided to pursue this approach to compare the TCR repertoire of different $CD4^+$ T cell memory populations, included Tfh and non-Tfh cells. Frozen PBMC and MNC-T of 5 matched-donors (234, 239, 242, 243, 244) were stained for panel A (see Figure 2.5) and $CD4^+$ T cell memory subsets from tonsil samples were FACS sorted using FACS-Aria into: Tfh-GC ($CXCR5^{hi}PD\text{-}1^{hi}$), Tfh-Th1 ($CXCR5^{lo}PD\text{-}1^{lo}CXCR3^+$), Tfh-Th2 ($CXCR5^{lo}PD\text{-}1^{lo}CXCR3^-$) and ROM ($CXCR5^-$). $CD4^+$ T cell memory populations from the blood of the same donors were sorted into: Tfh-Th1 ($CXCR5^+PD\text{-}1^+CXCR3^+$), Tfh-Th2 ($CXCR5^+PD\text{-}1^+CXCR3^-$) and ROM ($CXCR5^-$). A maximum of $1.3x10^5$ $CD4^+$ T cells per subset were sorted into RLT buffer and

both α- and β-chains of the TCR were sequenced, based on mRNA expression. The number of cells sorted was a caveat for the whole TCR repertoire analysis, but considering the usual low frequency of circulating Tfh populations in the peripheral blood and the scarcity of human samples, the number of cells sorted from each donor was confidently acceptable.

We decided to sequence only the Complementarity-Determining Region 3 (CDR3) of each chain of the TCR since this is the most variable segment of the receptor and the region that determines the specificity and identity of each T cell clonotype (Mahe et al., 2018; Nikolich-Zugich et al., 2004). Sequencing and analysis were performed in collaboration with Professor Dmitriy Chudakov and his team at the Central European Institute of Technology in Brno, Czech Republic (see section 2.10.2). Data in the tables (**Figure 4.2**) show the number of cells sorted for each subset in donors 234, 239, 242, 243, 244 (**Figure 4.2 a**). The number of sorted circulating Tfh cells was consistently lower compared to tonsillar Tfh cells, as well as the number of reads from the sequencing (counts) of the β-chain, which is consistent with our previous description about the lower frequencies of Tfh in the peripheral blood compare to tonsil nodules (**Figure 4.2 b**). Although the number of cells was variable between populations sorted within different donors, the frequency of each count was normalized before the analysis. Given that each T cell has a constant expression of TCR mRNA transcript (Egorov et al., 2015; Marinov et al., 2014), the efficiency was calculated based on the number of sorted cells and the number of counts detected. The sequencing efficiency was in a range of 40 to 90 %, except for donor 239 where in each subset the efficiency was lower than 11 % (**Figure 4.2 c**). Because of the low

efficiency in the TCR sequencing and therefore a low confidence on the results, donor 239 was excluded from the analysis of this thesis.

As explained above a T cell clone expresses one single β-chain of the TCR (T cell clonotype), but can often express two α-chains (Padovan et al., 1993; Petrie et al., 1993) and it was not possible from the bulk-sequencing data to determine the pairing of α and β chains. Therefore, only the CDR3 of the β-chain was considered for the repertoire comparison analysis that will follow in this section. To compare circulating and tonsillar $CD4^+$ T cell memory populations, the Vβ CDR3 region of shared clonotypes between subsets Tfh-Th1, Tfh-Th2 and ROM from peripheral blood were compared with each tonsil populations of interest. Because of the variable counts detected for the different subsets, the most frequent 2000 clonotypes (top 2000) from each sample were selected and the frequency normalized based on the total counts detected per subset. I have initially visualised the clonotype sharing between blood and tonsil using Cytoscape software. The network analysis (**Figure 4.3**) illustrates the shared clonotypes between different populations of tonsil (Tfh-GC, Tfh-Th1, Tfh-Th2, ROM) and each population of blood in an exemplifying donor (donor 234) without showing the connections between each tonsil populations. Tfh-Th1 from tonsil was found to be the subset that best correlates with Tfh-Th1 from blood (12.8 %) (**Figure 4.3 a**), as well as ROM from blood shares most of the clonotypes with ROM from tonsil (19.2 %) (**Figure 4.3 c**). Tfh-Th2 population connections were less restricted to a single subset, but rather shared mainly between Tfh-GC (3.25 %) and Tfh-Th2 (2.15 %) with clonotypes shared between all 3 compartments (2.05 %) (**Figure 4.3 b**).

Percentage of clonotype sharing between blood and tonsil populations was then calculated for each donor (**Figure 4.4 a**). Circulating Tfh-Th1 cells confirmed the greatest sharing with tonsillar Tfh-Th1 in each of the 5 donors analysed (5-13 %), as well as peripheral ROM with ROM from tonsil (6-20 %). Interestingly, and consistent with previous gene expression profile studies (Locci et al., 2013), Tfh-GC (5-7 %) and Tfh-Th2 (3-5 %) were the subsets of tonsil that best correlated with circulating Tfh-Th2 from blood in each of the donor analysed. Tfh-GC have been described to be the effector follicular Tfh during an immune response (Crotty, 2011) and considering the non-immune challenge condition of these samples, finding a correlation between the effector subset Tfh-GC with Tfh in the circulation it was encouraging. The normalised number of shared clonotypes between blood Tfh-Th1 (**Figure 4.4 b**), Tfh-Th2 (**Figure 4.4 c**) and ROM (**Figure 4.4 d**) with each of the tonsil population, is resembled on the D metric, which is the frequency of the overlapped clonotypes between two populations and it is normalized for each donor based on the total counts detected per subset. This value however does not consider the size of each clonotype but only the relative overlap. Therefore, if a clonotype is highly abundant in one population and little frequent in the other population, the D metric analysis of the two populations overlap does not differentiate this diversity, but it would only recognize that there is a clonotype shared. Hence, although the D metric is an important parameter to consider, it is not sufficient to describe a repertoire overlap. For a deeper TCR repertoire comparison, it was necessary to consider not only the number of shared sequences, but also the size of each clonotype and so the frequency correlation between those overlaps.

For each tonsil and blood comparison the F2 metric was then calculated, which is the sum of the geometric means between the frequencies of shared clonotypes. The greater the F2 value, the higher the number of shared clonotypes and the homogeneity of their size (Izraelson et al., 2017). This value therefore better resembles the proximity of the repertoire between two populations of T cells, by considering a weighted composition. The F2 metric of the overlap between subsets from blood with all the different tonsillar populations on the x-axis, confirmed the striking repertoire similarity between circulating Tfh-Th1 with tonsillar Tfh-Th1 cells and blood ROM with tonsillar ROM (**Figure 4.5 a, c**). This type of analysis, also called "weighted" since it considers the "weight" of each clonotype, validated also the correlation between blood Tfh-Th2 with Tfh-GC and Tfh-Th2 from tonsil, and furthermore identified a similar connection with tonsillar Tfh-Th1 (**Figure 4.5 b**), which was not detected by using the D metric parameter. To better visualize the similarity between the two compartments, the frequencies from blood and tonsil of each shared clonotype were analysed in a linear regression correlation and the coefficient of determination (R^2), the slope and the P value (of the slope different from zero) were measured. The linear regressions highlighted interesting perspectives of the repertoire overlap. Firstly, the correlation between Tfh-Th1 from tonsil and blood remained the strongest overlap since not only presented a high F2 metrics, but also the sizes of the shared clonotypes were very similar, resulted significant in 3 out of 4 donors. However, the number of clonotypes shared does not always positively correlate with a significant frequency correlation (R^2): for example, in case of blood-ROM vs tonsil-ROM correlation despite the high number of shared clonotypes (124-386) in all the 4 donors, the size of these clones is actually very

different in the two compartments of tonsil and blood and in 3 out of 4 donors the correlation is not significant (**Figure 4.5 c**). A similar observation could be done for tonsil Tfh-GC versus blood Tfh-Th2 overlap: although the F2 metric and the reasonably high number of clonotypes shared (84-129), the comparison between the size of the same clone in the two different compartments was poor, resulted significant in 2 out 4 donors analysed with a low R^2 (0.08 and 0.14) (**Figure 4.5 b**). In all the cases, the slope of shared clonotypes in correlation was <1, indicating that in tonsils most of the clones are more expanded than in the blood. This result could mean that some of the T cell clones that circulate between the two tissues were retained in tonsils rather than in the blood, probably due by a possible ongoing chronic infection. It is also possible a technical limitation: the frequency of clonotypes detected from tonsil may be more accurate and representative considering the ratio between the total volume of two tissues and the volume of sample analysed from each.

In conclusion, both F2 metrics and the number of clonotypes shared are very important in this context since they do confirm a direct relationship between tonsil and blood populations.

a)

N. cells	BLOOD			TONSIL			
DONOR ID	**Tfh-Th1**	**Tfh-Th2**	**ROM**	**Tfh-GC**	**Tfh-Th1**	**Tfh-Th2**	**ROM**
234	23,000	50,000	50,000	100,000	100,000	100,000	100,000
239	120,000	90,000	120,000	130,000	116,000	100,000	123,000
242	13,000	20,000	50,000	130,000	100,000	100,000	100,000
243	8,000	17,000	80,000	123,000	119,000	120,000	120,000
244	12,000	30,000	50,000	120,000	100,000	100,000	100,000

b)

Counts	BLOOD			TONSIL			
DONOR ID	**Tfh-Th1**	**Tfh-Th2**	**ROM**	**Tfh-GC**	**Tfh-Th1**	**Tfh-Th2**	**ROM**
234	16,782	36,333	31,742	94,745	97,883	65,386	60,354
239	3,827	7,263	4,690	14,071	11,314	10,934	536
242	9,345	17,143	27,817	125,249	76,651	63,444	44,380
243	5,354	13,179	38,453	94,155	78,065	60,526	48,934
244	6,466	19,239	27,921	114,448	95,522	51,691	39,164

c)

Sequencing Efficiency %	BLOOD			TONSIL				
DONOR ID	**Tfh-Th1**	**Tfh-Th2**	**ROM**	**Tfh-GC**	**Tfh-Th1**	**Tfh-Th2**	**ROM**	Mean
234	72.97	72.67	63.48	94.75	97.88	65.39	60.35	*75.35*
239	3.19	8.07	3.91	10.82	9.75	10.93	0.44	*6.73*
242	71.88	85.72	55.63	96.35	76.65	63.44	44.38	*70.58*
243	66.93	77.52	48.07	76.55	65.60	50.44	40.78	*60.84*
244	53.88	64.13	55.84	95.37	95.52	51.69	39.16	*65.09*
Mean	*53.77*	*61.62*	*45.39*	*74.77*	*69.08*	*48.38*	*37.02*	

Figure 4.2 Number, count and efficiency of the TCR Vβ CDR3 sequenced from CD4$^+$ T cells.

The tables (**a**) show the total number of CD4$^+$ memory T cells from different subsets of 5 donors (234, 239, 242, 243, 244) sorted into RLT buffer for RNA-based TCR deep-sequencing analysis. From each donor is shown (**b**) the total number of β-chain CDR3 reads (count) and (**c**) the sequencing efficiency calculated in percentage. Mean of each row and column are also indicated.

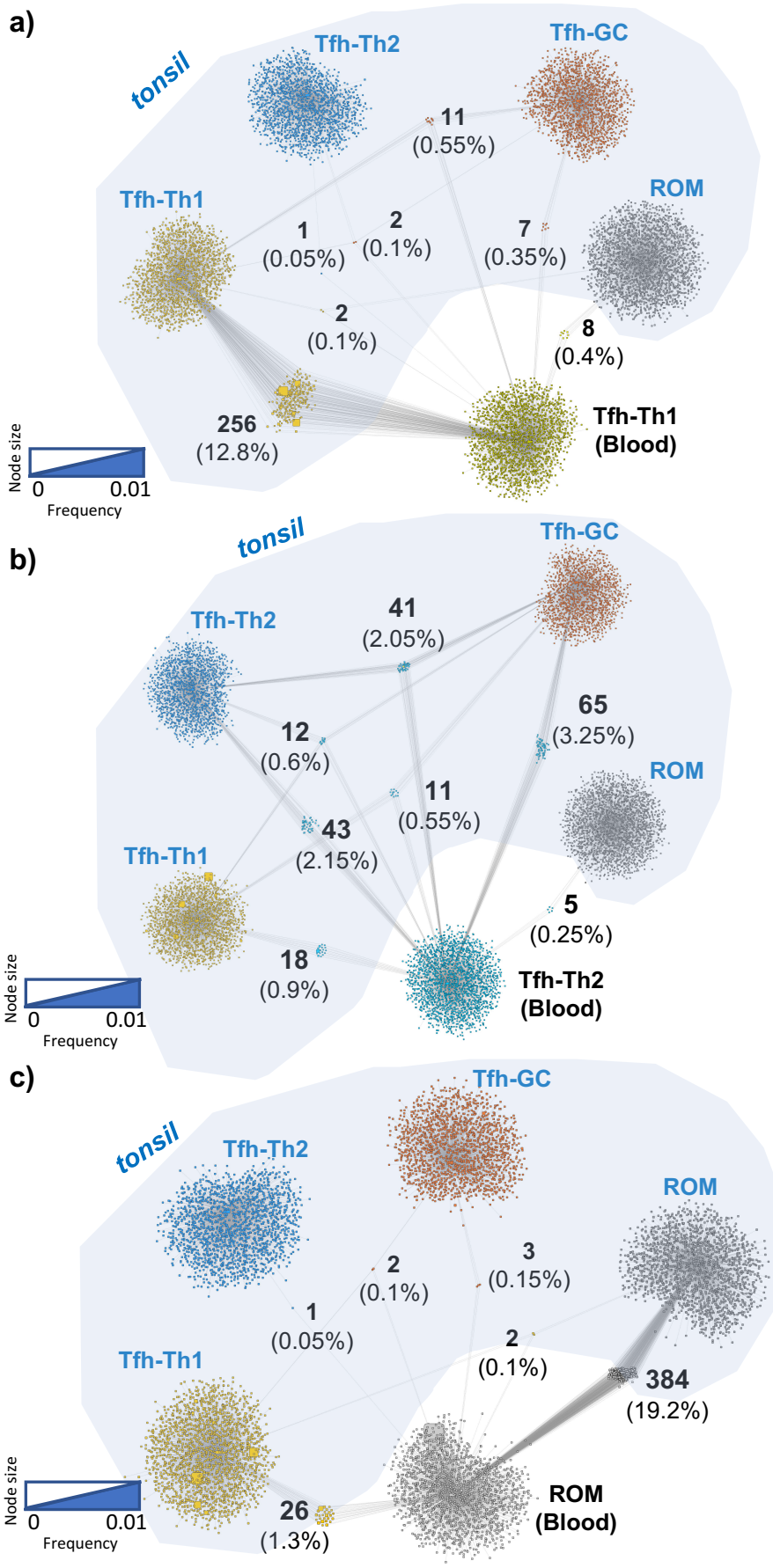

a)
tonsil
Tfh-Th2
Tfh-GC
11
(0.55%)
Tfh-Th1
1
(0.05%)
2
(0.1%)
7
(0.35%)
ROM
2
(0.1%)
8
(0.4%)
256
(12.8%)
Tfh-Th1
(Blood)
Node size
0
0.01
Frequency
b)
tonsil
Tfh-GC
Tfh-Th2
41
(2.05%)
65
(3.25%)
12
(0.6%)
ROM
11
(0.55%)
43
(2.15%)
Tfh-Th1
5
(0.25%)
18
(0.9%)
Tfh-Th2
(Blood)
Node size
0
0.01
Frequency
c)
tonsil
Tfh-GC
Tfh-Th2
ROM
2
(0.1%)
3
(0.15%)
1
(0.05%)
2
(0.1%)
Tfh-Th1
384
(19.2%)
26
(1.3%)
ROM
(Blood)
Node size
0
0.01
Frequency

Figure 4.3 Network visualisation of shared clonotypes between tonsil and blood $CD4^+$ T cell memory populations.

Top 2000 of the Vβ CDR3 nucleotide sequences were analysed using Cytoscape networking analysis. The figure shows an example for donor 234. Each population of blood, (**a**) Tfh-Th1, (**b**) Tfh-Th2 and (**c**) ROM, was compared with 4 populations of tonsil: Tfh-Th1=yellow, Tfh-Th2=blue, Tfh-GC=red and ROM=grey. Only connections between the 2 tissues are shown. Each square is a different clonotype and the size is proportional to the frequency (for shared clonotypes is visualised the blood frequency). Each connection shows the number of shared clonotypes in bold and the respective percentage within the 2000 sequences considered.

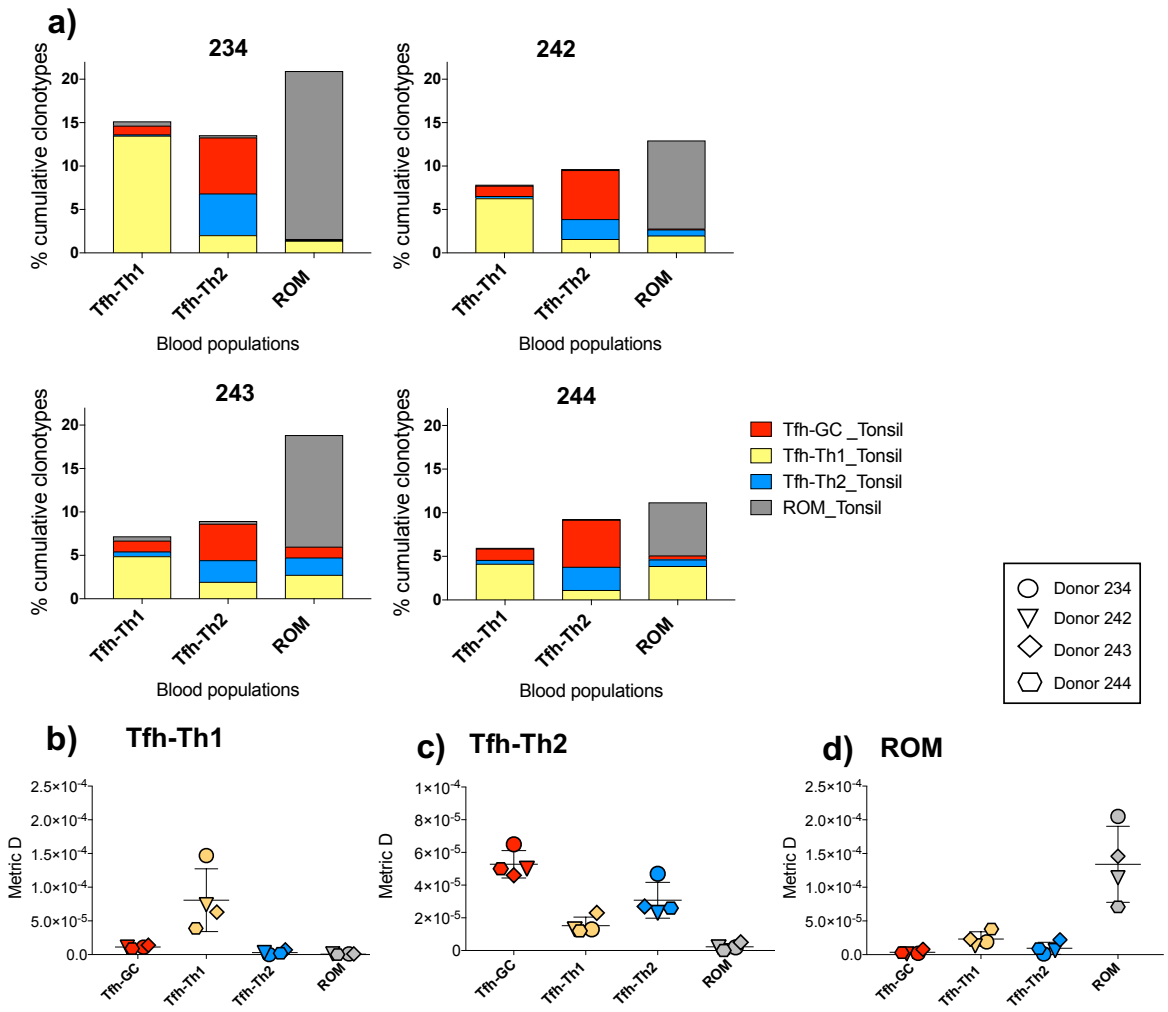
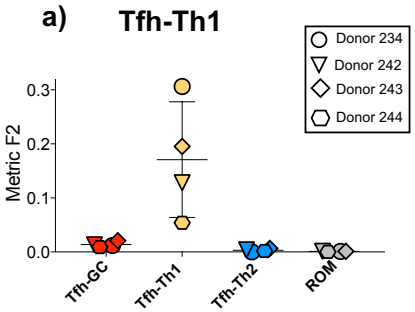
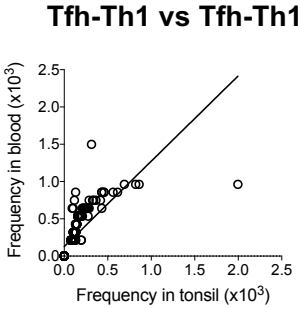


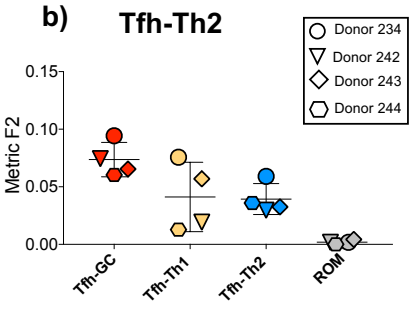
Figure 4.4 Cumulative clonotype sharing between tonsil and blood CD4⁺ memory T cells.

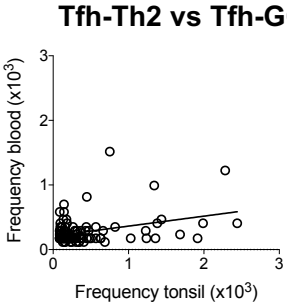
The percentage (**a**) of the most 2000 frequent clonotypes (top2000) shared between tonsil and blood in donors 234, 242, 243 and 244 was calculated and visualised in the stacked bar graphs. For each population of blood on the x-axis was analysed the shared clononype percentage with each population of tonsil (Tfh-GC=red, Tfh-Th1=yellow, Tfh-Th2=blue, ROM=grey). Normalized Metric D is shown for each comparison of blood (**b**) Tfh-Th1, (**c**) Tfh-Th2 and (**d**) ROM against each population of tonsil on the x-axis with mean and SEM.



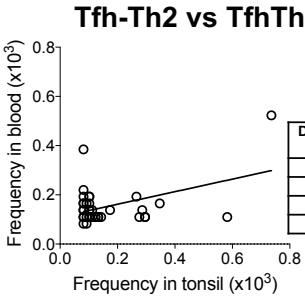


Donor ID	Shared clonotypes	R^2	P value	Slope
1	271	0.46	<0.0001	0.27 ± 0.02
2	109	0.91	<0.0001	0.93 ± 0.03
3	99	0.38	<0.0001	0.34 ± 0.04
4	83	0.01	ns	0.13 ± 0.37

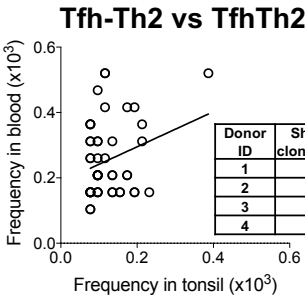




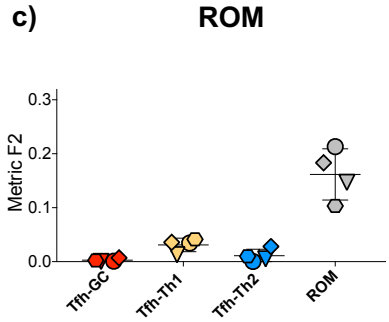
Donor ID	Shared clonotypes	R^2	P value	Slope
1	129	0.14	<0.0001	0.05 ± 0.01
2	113	0.08	0.0026	0.09 ± 0.03
3	84	0.01	ns	-0.01 ± 0.04
4	108	0.02	ns	0.09 ± 0.06

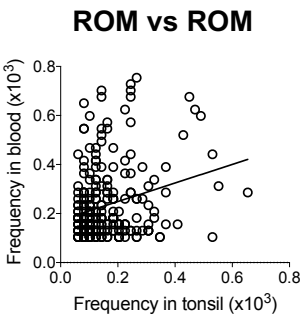


Donor ID	Shared clonotypes	R^2	P value	Slope
1	41	0.41	<0.0001	0.05 ± 0.01
2	32	0.04	0.2991	0.15 ± 0.14
3	82	0.18	0.0055	0.04 ± 0.01
4	23	0.01	ns	0.02 ± 0.59



Donor ID	Shared clonotypes	R^2	P value	Slope
1	96	0.09	0.0029	0.17 ± 0.06
2	59	0.18	0.0010	1.16 ± 0.33
3	50	0.04	ns	0.35 ± 0.26
4	53	0.24	0.0002	2.20 ± 0.55





Donor ID	Shared clonotypes	R^2	P value	Slope
1	386	0.003	ns	-0.25 ± 2.06
2	200	0.002	ns	0.21 ± 0.32
3	257	0.04	0.0007	0.39 ± 0.11
4	124	0.01	ns	0.31 ± 0.27

Figure 4.5 Weighted analysis of the repertoire overlap between blood and tonsil populations.

The most 2000 frequent TCR sequences (top 2000) of circulating (**a**) Tfh-Th1, (**b**) Tfh-Th2 and (**c**) ROM population repertoires from blood were compared to tonsillar Tfh-Th1 (yellow), Tfh-Th2 (blue), Tfh-GC (red) and ROM (grey) on the x-axis in a normalized F2 metric analysis. Each dot represents a different donor and the lines show the mean with SEM. The frequencies comparison of each shared clonotype from blood and tonsil, were analysed in a linear regression correlation, where each dot represents a shared clonotype. The tables summarise the number of shared clonotypes, coefficient of determination (R^2), the slope and the P values for each combination. ns= not significant.

4.4 Comparison of T cell receptor sequences repertoire between Tfh and non-Tfh cells

One of the biggest questions in the field of T follicular helper cells regards the identity of these subsets and whether Tfh cells are actually a unique and distinct compartment in the $CD4^+$ memory T cells, or whether they belong to a plastic population of memory cells formed after an immune response that can interchange. This question assumes even more importance in the context of vaccination strategies: we need to know whether investigating the response and the specificity of Tfh cells after an immune challenge requires purification of these populations rather than focusing on total memory $CD4^+$ T cells. This is still a crucial question for clinical trials, where T cell responses are being investigated.

If Tfh cells are not a separate lineage of the $CD4^+$ memory T cell compartment, in steady state conditions this subset should not be distinct from the rest $CD4^+$ memory T cells and CXCR5 might be expressed temporarily by few activated $CD4^+$ memory

cells. In contrast if CXCR5 is a marker that, together with other surface markers, identifies a precise population of $CD4^+$ Tfh cells, then $CXCR5^+$ and $CXCR5^-$ T cells should not share the TCR repertoires. The Cytoscape network analysis of the top 2000 Vβ CDR3 region of the TCR sequences was a useful way of visualising shared clonotypes between Tfh-Th1, Tfh-Th2 and ROM subsets from the blood compartment in each of the 4 donors analysed (**Figure 4.6 a**). The network interactions showed little repertoire overlap between Tfh-Th1, Tfh-Th2 and ROM populations in the blood compartment, consistently in all the 4 donors. This was true for both Tfh-Th1 versus Tfh-Th2 (0.8 -1.3 %) and Tfh (either Th1 or Th2) versus ROM (0.1 - 1.6 %). There were also very few clonotypes shared within all the 3 populations (0.1 - 0.2 %). The Venn diagram reveals the mean of the percentages in the 4 donor interactions between the 3 populations and validates the hypothesis that circulating Tfh-Th1 and Tfh-Th2 are distinct lineages from the $CD4^+$ rest of memory T cells (**Figure 4.6 b**).

The same analysis was performed for Tfh (Tfh-Th1, Tfh-Th2 and Tfh-GC) and non-Tfh (ROM) subsets from tonsil samples in the same 4 donors (**Figure 4.7 a**). Similar to the peripheral blood, also in the tonsil compartment Tfh cells (either Tfh-Th1, Tfh-Th2 or Tfh-GC) were notably distinct from the ROM population with very little repertoire overlap (0.1 – 0.9 %). Surprisingly however, the 3 Tfh populations showed a consistent overlap within each other:

- Tfh-Th1, Tfh-Th2, Tfh-GC: 0.7 – 3.1 %
- Tfh-Th1, Tfh-Th2: 2.6 – 6.2 %
- Tfh-Th1, Tfh-GC: 3.5 – 8.3 %
- Tfh-Th2, Tfh-GC: 4 – 14.9 %

The average of the percentages in the 4 donors is illustrated in the Venn diagram (**Figure 4.7 b**). Although the repertoire overlap of the Tfh populations is variable within the donors, the proximity of all the 3 Tfh cell populations was persistent, especially within Tfh-Th2 and Tfh-GC (8.5 %).

This similarity was investigated more in detail by the F2 metric of the overlap between tonsillar Tfh-Th1, Tfh-Th2 and Tfh-GC (**Figure 4.8 a**) with all the other subsets from tonsil respectively. Weighted analysis confirmed the overlap between Tfh-Th2 and Tfh-GC as well as between Tfh-Th1 and Tfh-GC and the repertoire distance between all Tfh populations with ROM. Yet the repertoire of tonsillar Tfh subsets did not present a similar composition of the different clonotypes, as shown from the R^2, slope and P value in the table (**Figure 4.8 b**). The R^2 represents the coefficient of determination of the linear regression correlation between frequencies from blood and tonsil of each shared clonotype. Despite the numerous clonotypes shared between Tfh-Th1 and Tfh-Th2 (70-172), Tfh-Th1 and Tfh-GC (89-214), Tfh-Th2 and Tfh-GC (96-360), the correlations were all $R^2 < 0.36$ and in the majority of the cases not significant. It is difficult to explain such a discrepancy on the linear regression results, but it is possible that if Th-Th1 and Tfh-Th2 represent a different maturation stage of Tfh-GC cells (see graphical abstract, section 7), then the size of the clones in each subset will be different. Future TCR sequencing experiments of duplicate samples might help to understand how representative are the number of cells that were sequenced in this experiment and to better define a threshold of comparison.

Together with the overlap, the repertoire diversity of a T cell population is an important aspect to consider for comparing two populations. The Shannon-Wiener

index was calculated for each blood (**Figure 4.8 c**) and tonsil (**Figure 4.8 d**) population in the 4 donors. The index measures the entropy of a set of TCR sequences and it is based on the uncertainty of predicting the next sequence in a string. In the context of normalised data, if a set of sequences consists of the same sequence, the Shannon-Wiener index is equal to 1 and so the diversity is null, if instead the set is composed by all diverse sequences, the Shannon-Wiener index is equal to 0 and the diversity is maximal. In line with the hypothesis that Tfh subsets are specialized and a distinct $CD4^+$ T cell compartment, circulating Tfh-Th1 and Tfh-Th2 sets showed a uniform composition, compared to the ROM population in the blood (**Figure 4.8 c**). The diversity index also reflexes the structural complexity of $CXCR5^-$ cells within the $CD4^+$ memory T cell population (ROM) considering that this subset includes several diverse groups of T cells with different functions, such as for instance the canonical Th1, Th2 and Th17 subsets. Even though the correlation between ROM from tonsil and ROM from blood was consistently high in all the donors analysed (see paragraph 4.3), tonsillar ROM cells more homogenous than peripheral ROM cells, as well as Tfh-Th2 from tonsil. Tfh-GC and Tfh-Th1 from tonsil showed instead a slightly more diverse repertoire (**Figure 4.8 d**).

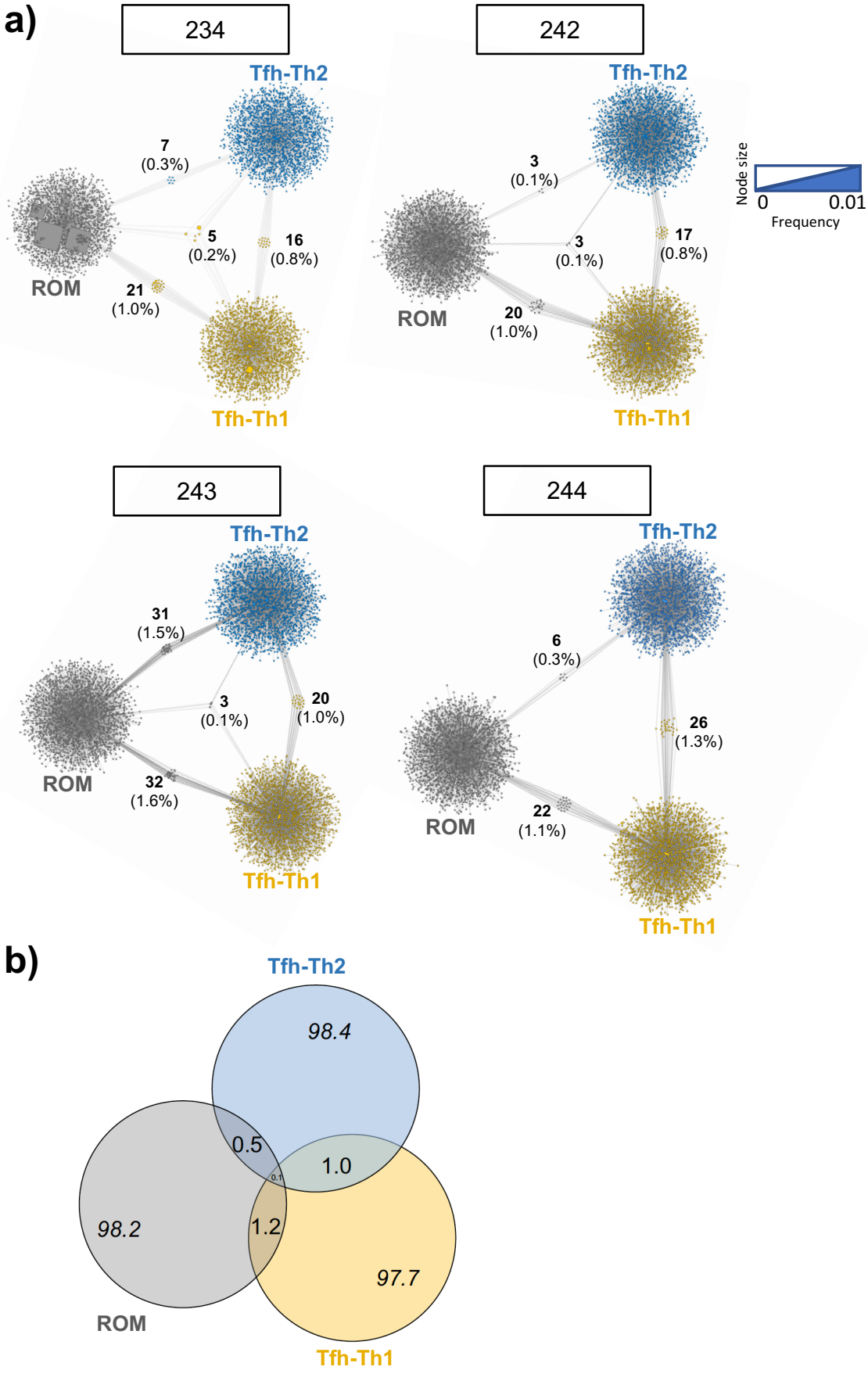

a)
234
Tfh-Th2
7
(0.3%)
5
(0.2%)
16
(0.8%)
ROM
21
(1.0%)
Tfh-Th1
242
Tfh-Th2
3
(0.1%)
3
(0.1%)
17
(0.8%)
ROM
20
(1.0%)
Tfh-Th1
Node size
0
0.01
Frequency
243
Tfh-Th2
31
(1.5%)
3
(0.1%)
20
(1.0%)
ROM
32
(1.6%)
Tfh-Th1
244
Tfh-Th2
6
(0.3%)
26
(1.3%)
ROM
22
(1.1%)
Tfh-Th1
b)
Tfh-Th2
98.4
0.5
1.0
0.1
98.2
1.2
97.7
ROM
Tfh-Th1

Figure 4.6 Repertoire comparison of circulating Tfh versus non-Tfh cells in peripheral blood.

Top 2000 of the TCR Vβ CDR3 nucleotide sequences were analysed using Cytoscape networking analysis. The figure shows (**a**) the interaction between Tfh-Th1 (yellow), Tfh-Th2 (blue) and ROM (grey) populations from blood compartment in donors 234, 242, 243, 244. Each square is a different clonotype and the size is proportional to the frequency (for shared clonotypes with different frequency in the two populations is visualised the biggest frequency). Each connection shows the number of shared clonotypes in bold and the respective percentage within the 2000 sequences considered. The Venn diagram (**b**) surmises the repertoire overlap between Tfh-Th1, Tfh-Th2 and ROM illustrating the average of percentages interaction between the 3 populations.

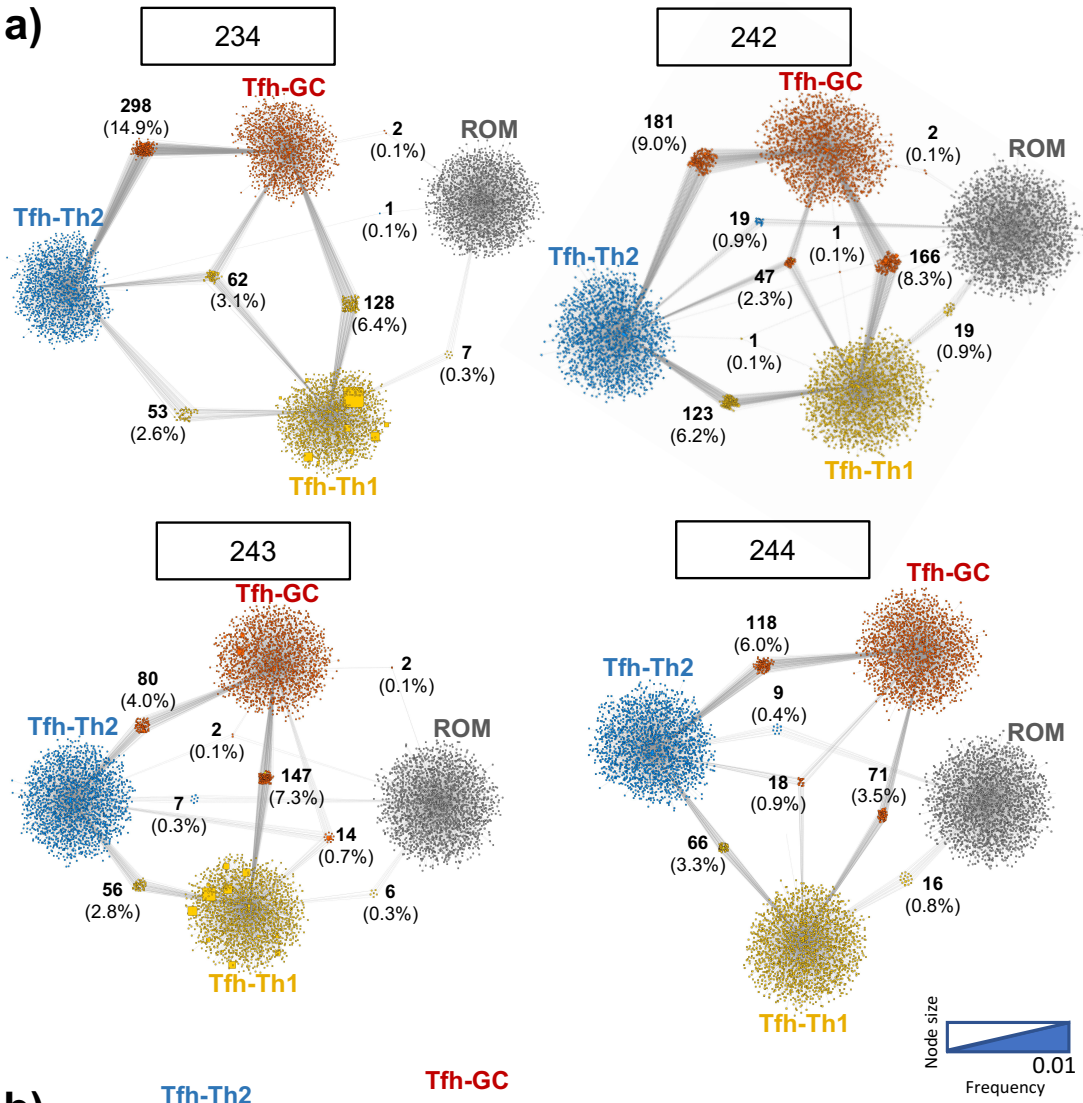
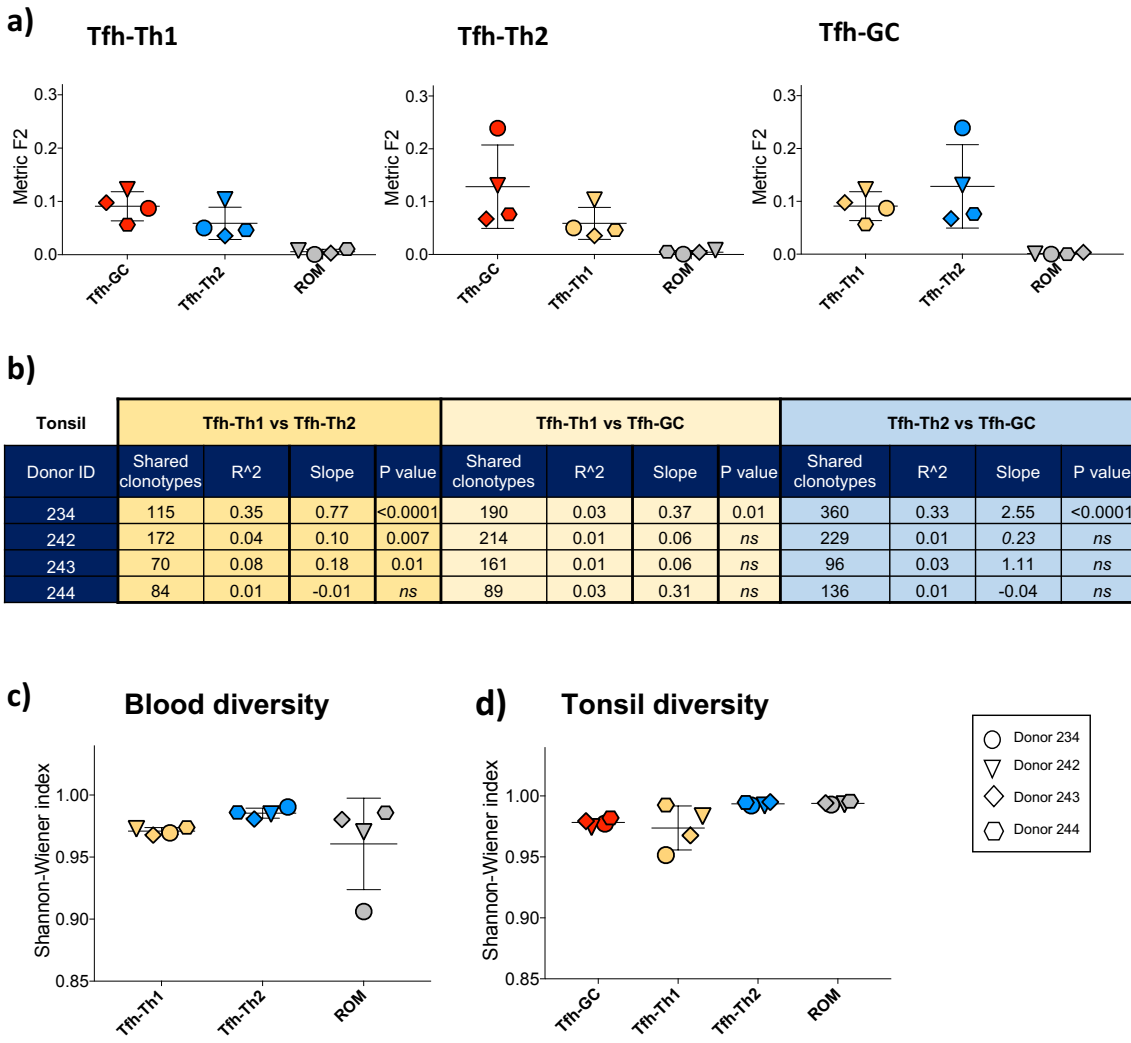

a)
234
Tfh-GC
298
(14.9%)
2
(0.1%)
ROM
1
(0.1%)
Tfh-Th2
62
(3.1%)
128
(6.4%)
7
(0.3%)
53
(2.6%)
Tfh-Th1
242
Tfh-GC
181
(9.0%)
2
(0.1%)
ROM
19
(0.9%)
1
(0.1%)
Tfh-Th2
166
(8.3%)
47
(2.3%)
19
(0.9%)
1
(0.1%)
123
(6.2%)
Tfh-Th1
243
Tfh-GC
80
(4.0%)
2
(0.1%)
Tfh-Th2
2
(0.1%)
ROM
147
(7.3%)
7
(0.3%)
14
(0.7%)
56
(2.8%)
6
(0.3%)
Tfh-Th1
244
Tfh-GC
118
(6.0%)
Tfh-Th2
9
(0.4%)
ROM
18
(0.9%)
71
(3.5%)
66
(3.3%)
16
(0.8%)
Tfh-Th1
Node size
0.01
Frequency
b)
Tfh-Th2
Tfh-GC
85.5
80.1
Tfh-Th1
3.7
8.5
88.6
ROM
1.8
0.1
0.0
5.8
0.0
99.4
0.0
0.1
0.4
0.0

Figure 4.7 Repertoire comparison of tonsillar Tfh versus non-Tfh cells.

Top 2000 of the TCR Vβ CDR3 nucleotide sequences were analysed using Cytoscape networking analysis. The figure (**a**) shows the interaction between Tfh-Th1 (yellow), Tfh-Th2 (blue), Tfh-GC (red) and ROM (grey) populations from tonsil compartment in donors 234, 242, 243, 244. Each square is a different clonotype and the size is proportional to the frequency (for shared clonotypes with different frequency in the two populations is visualised the biggest frequency). Each connection shows the number of shared clonotypes in bold and the respective percentage within the 2000 sequences considered. The Venn diagram (**b**) summarizes the repertoire overlap between Tfh-Th1, Tfh-Th2, Tfh-GC and ROM illustrating the average of percentages interaction between the 4 populations.



Tonsil	Tfh-Th1 vs Tfh-Th2				Tfh-Th1 vs Tfh-GC				Tfh-Th2 vs Tfh-GC			
Donor ID	Shared clonotypes	R^2	Slope	P value	Shared clonotypes	R^2	Slope	P value	Shared clonotypes	R^2	Slope	P value
234	115	0.35	0.77	<0.0001	190	0.03	0.37	0.01	360	0.33	2.55	<0.0001
242	172	0.04	0.10	0.007	214	0.01	0.06	*ns*	229	0.01	*0.23*	*ns*
243	70	0.08	0.18	0.01	161	0.01	0.06	*ns*	96	0.03	1.11	*ns*
244	84	0.01	-0.01	*ns*	89	0.03	0.31	*ns*	136	0.01	-0.04	*ns*

Figure 4.8 Weighted analysis of the repertoire overlap of tonsillar Tfh populations and repertoire diversity in blood and tonsils.

(**a**) Top 1000 TCR sequences of Tfh-Th1, Tfh-Th2 and Tfh-GC population repertoires from tonsil were compared to each other and to tonsillar ROM population in a normalized F2 metric analysis. Each dot represents a different donor and the bars show the mean with standard deviation. The frequencies comparison of each shared clonotype from tonsil, were analysed in (**b**) a linear regression correlation. The table summarises the number of shared clonotypes, coefficient of determination (R^2), the slope and the P value for each combination. ns= not significant. For each population of (**c**) blood and (**d**) tonsil was calculated the normalised Shannon-Wiener diversity index. Each dot represents a different donor and the bars show the mean with SEM.

4.5 Conclusions

This chapter highlights the relationship between $CD4^+$ memory T cell populations from the peripheral blood and tonsil compartments. In particular Tfh-Th1 from tonsil correlated best with Tfh-Th1 from blood and ROM from tonsil with ROM from blood (section 4.3). Tonsil Tfh-Th2 together with the effector subset Tfh-GC, which presented the most follicular phenotype described in details in section 3, showed a weaker but consistent correlation with circulating Tfh-Th2 from blood. The closeness of tonsillar Tfh-Th2 and Tfh-GC to each other, shown in section 4.4, supports the tight correlation between Tfh-Th2 from blood to both these follicular subsets in tonsil. An overview of the overlaps for each donor is shown in the heat maps (**Figure 4.9**).

The evidence that Tfh cells are a distinct population to the $CD4^+CXCR5^-$ rest of memory compartment (ROM) was a striking and relevant find (section 4.4). As it was shown in section 3.2, ROM is the major $CD4^+$ T cell population in the blood and predominates in clinical trial assays on unseparated blood $CD4^+$ T cells. It is therefore crucial to know that it is necessary to purify circulating $CXCR5^+$ T cells to investigate Tfh responses after immune challenge, since considering total $CD4^+$ T cell is limiting.

A limitation of the whole sequencing analysis however is the size of the sample and so the number of T cells sequenced. This is always a constraint for TCR repertoire analysis in humans, considering the number of T cells available, particularly for the rare subsets, in the context of the total repertoire of $CD4^+$ T cells in the immune system. The sampling size is also a caveat to determine technical replicates and to interpret correctly whether a correlation is relevant or rather weak. Unfortunately,

due to the novelty of the analysis and the diversity of the samples that can be analysed, there is no good positive criteria or threshold for the F2 metric. Theoretically a replicate of a $CD4^+$ T cell population sequenced twice has an F2 metric of 1, but experimentally the same 10 ng of RNA from human samples have an F2 metric equal to 0.3 - 0.5 (Egorov et al., 2015; Izraelson et al., 2017). A useful and essential experiment will focus on the comparison of the TCR repertoire between the same sample sequenced multiple times. The results will be important to set the reproducibility of the deep-sequencing method but also the diversity of the TCR repertoire in question. Nevertheless, these results are encouraging especially considering the evidence that the deeper a sample is sequenced, the larger is the clonotype overlap (Shugay et al., 2013).

Because the subsets of Tfh cells examined here have big differences in frequency within the $CD4^+$ memory compartment, the normalisation of a set number of clonotypes considered was necessary, and we considered only the most frequent 1000 or 2000 clonotypes sequenced.

An important observation throughout the chapter was the alignment of results between weighted and unweighted analysis of the repertoire overlap, with or without consideration of the size of the shared clonotypes and this aspect is particularly relevant in a RNA-based TCR sequencing analysis. Although RNA-based TCR sequencing techniques give good repertoire coverage, which was why we chose this approach, variation in TCR expression between each T cell does not allow to refer each count to a single cell and so to calculate the absolute frequency of each clonotype, as it would for a DNA-based sequencing analysis. Therefore, in case of TCR sequences based on RNA expression it is extremely important to combine both

weighted and unweighted analysis and to detect similar trends between both. However, previous studies have compared clonal frequency based on RNA expression and indicated that a single T cell always expresses a similar amount of TCR on the mRNA level, either one or two copies (Douek et al., 2002; Egorov et al., 2015; Marinov et al., 2014). We can then conclude that when we observed a similarity between the repertoire of 2 populations using a weighted RNA-based analysis, these results are reliable and do reflect the repertoire proximity rather than different expressions of the same T cell receptor in multiple compartments.

In conclusion, such evident relationship between circulating and follicular $CD4^+$ T cells is important, considering that less than 130,000 T cells per subset were sequenced and that the experiments were performed under "steady-state" conditions, without examining antigen specificity in the absence of any known acute immune response. The peptide specificity of the TCR clonotypes will be investigated in more detail in the next section, as a different but strongly related aspect that together with the TCR sequences repertoire improves the understanding of T cell populations similarity.

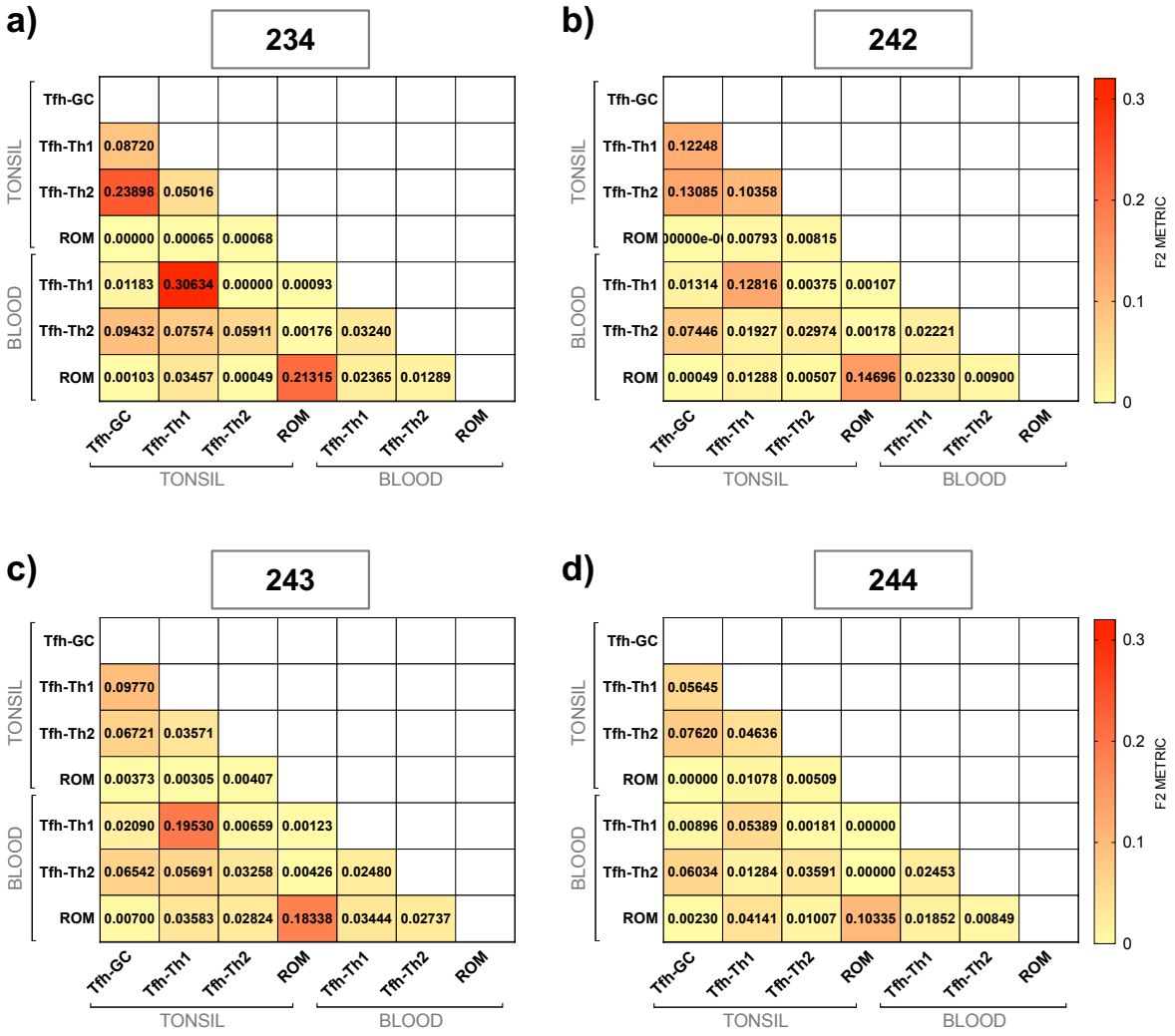


Figure 4.9 Repertoire overlap in 4 matched-tonsil and blood donors.

F2 metric values of different TCR Vβ overlap (top1000) combinations between blood and tonsil of donors (**a**) 234, (**b**) 242, (**c**) 243 and (**d**) 244 are shown in the heat maps.

5 Results III: characterising the specificity of circulating Tfh and non-Tfh cells using Haemagglutinin protein

5.1 Background and rational

The $CD4^+$ T cell repertoire comparison between peripheral blood and tonsil in the previous chapter (section 4) showed a notable correlation between the 2 tissues: Tfh-Th1 from tonsil correlated with Tfh-Th1 cells from blood; Tfh-GC and Tfh-Th2 cells from tonsil correlated best with Tfh-Th2 cells from blood; ROM cells from tonsil have a remarkable overlap with ROM cells from blood. In addition, the evidence that Tfh cell populations in both peripheral blood and tonsils were distinct from ROM, was an important evidence that needs to be considered for future clinical trials where purification of $CXCR5^+$ cells from total $CD4^+$ memory T cells will be necessary to investigate the Tfh cell response after an immune challenge.

However, one of the limitations of the work presented herein to date is that the experiments did not consider antigen specificity or an acute immune response. The T cell receptor (TCR) sequence, especially the CDR3 variable region of the TCR, not only establishes the identity of a certain T cell clonotype but most importantly it determines the specificity, a unique characteristic of each clonotype (Mahe et al., 2018; Nikolich-Zugich et al., 2004). During an immune response, only the T cell clonotypes specific for the antigen will expand and the T cell repertoire is skewed and shaped to the specificity in question (McHeyzer-Williams and Davis, 1995;

McHeyzer-Williams et al., 1999). This process facilitates the clearance of the pathogen during an acute immune response and it leads to the formation of an immediate effector and a later memory response. Consequently, comparing the TCR repertoire after an immune response is technically easier and the clonotypes identified are usually fewer, due to the clonal expansion (McHeyzer-Williams and Davis, 1995; Vogel et al., 2002; Weidmann et al., 1993). The investigation of antigen specificity is an important element to consider because, peptide specificity in combination with the TCR sequences are remarkable tools to identify whether two T cell populations are related to each other or whether they belong to different lineages. Therefore, studying the T cell specificity becomes a particularly relevant aspect in this context for the comparison of T cells from two different compartments, such as circulating and tonsillar Tfh cells. Thus, the aims of this chapter were:

- To detect and expand antigen-specific $CD4^+$ T cell clones *in vitro* at the peptide level, using Influenza haemaggluninin protein as a model antigen and compare Tfh and non-Tfh cells specificity: have Tfh cells a unique pattern of peptide specificity, which is different from non-Tfh cells? (sections 5.3 and 5.4)
- To study in detail the correlation between the peptide specificity and the CDR3 sequence of the TCR: are the clones specific for the same peptide but derived from different T cell populations have the same TCR sequence? (section 5.5)
- To search the TCR sequences of antigen-specific Tfh and non-Tfh cells from peripheral blood into the deep-sequencing analysis of tonsil populations and analyse the comparisons (section 5.5).

5.2 Influenza strains comparison

From the cohort of matched tonsil and blood samples, we were unable to obtain secondary lymphoid organs and peripheral blood from vaccinated or infected donors. Although not having donors with an ongoing infection or recent vaccination is clearly a limitation of the study, we opted to use Haemagglutinin protein (HA) from Influenza virus, which is one of the most frequent seasonal infections and something to which undoubtedly all donors would have been exposed and vaccinated against (43 % of patients in this cohort were vaccinated for the annual influenza). Therefore, HA-specific effector and memory T cells should be in secondary lymphoid organs and peripheral blood (Alam and Sant, 2011; Fazilleau et al., 2007; Sant et al., 2018) and using HA we were able to describe and compare the antigen-specific repertoire between tonsil and blood. In the following sections two different strains of HA protein have been used:

- Haemagglutinin from Influenza A/Wisconsin/67/2005, H3N2
- Haemagglutinin from Influenza A/California/04/2009, H1N1

Influenza A/Wisconsin strain was recommended in the vaccines from 2006 to 2008 in the Northern Hemisphere and commonly used as antigen for B and T cell *in vitro* assays (Influenza Research Database, 2018; Su et al., 2016). HA/Wisconsin was used to broadly identify HA-specific $CD4^+$ T cells in Tfh and non-Tfh compartments and to calculate the precursor frequency using the T cell library method from 4 healthy donors. HA/California instead was used to compare the HA specificity between T cell clones from blood and tonsil TCR repertoire. The latter was particularly chosen since it is one of the most conserved component of trivalent Influenza vaccines in the last 7 years in the Northern Hemisphere (Influenza

Research Database, 2018; World Health Organization, 2018). HA protein is one of the most variable region of Influenza virus and widely described to show substantial variations throughout different strains (Burke and Smith, 2014; Gong et al., 2012; Influenza Research Database, 2018). Although the alignment of Wisconsin and California HA proteins showed only 42 % of identity match and 59 % of residues between the two strains shared similar chemical properties (positives) (**Figure 5.1**), the frequency of antigen-specific cells within $CD4^+$ memory subsets was very similar amongst the 9 donors tested in the following chapter and underlined the importance of role of Tfh-Th1 subset in Influenza response.

a)

```
A/California/04/2009(H1N1)      MKAILV---VLLYTF------ATANADTLCIGYHANNSTDTVDTVLEKNVTVTHSVNLLE    51
                                ||:|:.   :|  .|         .: |||:|:||  .   |.|: :.:: ||::.:|::
A/Wisconsin/67/2005(H3N2)       MKTIIALSYILCLVFAQKLPGNDNSTATLCLGHHAVPNGTIVKTITNDQIEVTNATELVQ    60

A/California/04/2009(H1N1)      DKHNGKLCKLRGVAPLHLGKCNIAGWILGNPECESLSTASSWSYIVETPSSDNGTCYPGD    111
                                .. .| :|.      |.  :|.: . :||:|:|:.:.. ..|. :||  |.  ..||| |
A/Wisconsin/67/2005(H3N2)       SSSTGGICDSPH-QILDGENCTLIDALLGDPQCDGFQN-KKWDLFVER-SKAYSNCYPYD    117

A/California/04/2009(H1N1)      FIDYEELREQLSSVSSFERFEIFPKTSSWPNHDSNKGVTAACPHAGAKSFYKNLIWLVKK    171
                                . || .||. ::| .::   |:  :: .| .  :::|.:::| : . :||:..| ||.:
A/Wisconsin/67/2005(H3N2)       VPDYASLRSLVASSGTL---EFNDESFNWTGV-TQNGTSSSCKRRSNNSFFSRLNWLTHL    173

A/California/04/2009(H1N1)      GNSYPKLSKSYINDKGKEVLVLWGIHHPSTSADQQSLYQNADTYVFVGSSRYSKKFKPEI    231
                                  .|| |. :  |::  : | :||:|:|| |. ||  || :|.  : |.:.| .:.. |:|
A/Wisconsin/67/2005(H3N2)       KFKYPALNVTMPNNEKFDKLYIWGVHHPVTDNDQIFLYAQASGRITVSTKRSQQTVIPNI    233

A/California/04/2009(H1N1)      AIRPKVRDQEGRMNYYWTLVEPGDKITFEATGNLVVPRYAFAMERNAGSGIIISDTPVHD    291
                                . ||::|:  .|:. |||:|:||| : :::||||:.||  | :. .. |.|: ||:|: .
A/Wisconsin/67/2005(H3N2)       GSRPRIRNIPSRISIYWTIVKPGDILLINSTGNLIAPRGYFKIR-SGKSSIMRSDAPIGK    292

A/California/04/2009(H1N1)      CNTTCQTPKGAINTSLPFQNIHPITIGKCPKYVKSTKLRLATGLRNIPSIQSRGLFGAIA    351
                                ||: | ||:|:| .. ||||:: || | ||:|||...|:||||:||:|. |:||:|||||
A/Wisconsin/67/2005(H3N2)       CNSECITPNGSIPNDKPFQNVNRITYGACPRYVKQNTLKLATGMRNVPEKQTRGIFGAIA    352

A/California/04/2009(H1N1)      GFIEGGWTGMVDGWYGYHHQNEQGSGYAADLKSTQNAIDEITNKVNSVIEKMNTQFTAVG    411
                                ||||.|| |||||||::|||.:| | |||||||| ||::|..|:| :| | | :|  :
A/Wisconsin/67/2005(H3N2)       GFIENGWEGMVDGWYGFRHQNSEGIGQAADLKSTQAAINQINGKLNRLIGKTNEKFHQIE    412

A/California/04/2009(H1N1)      KEFNHLEKRIENLNKKVDDGFLDIWTYNAELLVLLENERTLDYHDSNVKNLYEKVRSQLK    471
                                |||..:| ||::|:| |:|  :|:|:|||||| |||::|:|  ||::::|:|:.:.||:
A/Wisconsin/67/2005(H3N2)       KEFSEVEGRIQDLEKYVEDTKIDLWSYNAELLVALENQHTIDLTDSEMNKLFERTKKQLR    472

A/California/04/2009(H1N1)      NNAKEIGNGCFEFYHKCDNTCMESVKNGTYDYPKYSEEAKLNREEIDGVKLESTRIYQIL    531
                                :||:::|||||::|||||:|: |::|||||:  | :||  || :|.||:|:|     ||
A/Wisconsin/67/2005(H3N2)       ENAEDMGNGCFKIYHKCDNACIGSIRNGTYDHDVYRDEALNNRFQIKGVELKSGYKDWIL    532

A/California/04/2009(H1N1)      AIYSTVASSLVLVVSLGAISFWMCSNGSLQCRICI     566
                                 |   . |.::| |:| .: :| |.:|.::|.|||
A/Wisconsin/67/2005(H3N2)       WIS-FAISCFLLCVALLGFIMWACQKGNIRCNICI     566
```

b)

Identities	Positives	Gaps
243/578 (42%)	344/578 (59%)	24/578 (4%)

Figure 5.1 Alignment of Haemagglutinin (HA) protein from Wisconsin and California Influenza A strains.

Amino acids (AA) sequence of HA from Influenza A/California/04/2009 was aligned (**a**) to HA from Influenza Wisconsin/67/2005, using the Clustal Omega alignment, from EMBL-EBI website (European Molecular Biology Laboratory-European Bioinformatics Institute). The numbers showed the AA position, vertical lines (|) denote identity, colons (:) and periods (.) denote strongly and weakly similar residues respectively. The table (**b**) shows the percentage of identity, number of residue with similar chemical properties (positives) and insertions (gaps) between the 2 proteins aligned.

5.3 Precursor frequency and specificity for Haemagglutining in circulating Tfh and non-Tfh cells

Virus-specific $CD4^+$ T cells are mainly found in memory Th1 subset (usually defined as IFN-γ^+ and enriched in $CCR5^+CXCR3^+$) (Palladino et al., 1991; Sallusto and Lanzavecchia, 2009; Yang et al., 2013; Zielinski et al., 2011). Also circulating Tfh-Th1 cells were found to be important for Influenza response and to help B cells to produce influenza-specific antibody response (Bentebibel et al., 2013; Velu et al., 2016), although increasing of Tfh-Th1 effector cells was often not in line with an efficient antibody production and productive germinal centre response (Cubas et al., 2015; Obeng-Adjei et al., 2015; Ryg-Cornejo et al., 2016).

To better asses the specificity of Tfh-Th1 and Tfh-Th2 subsets of the HA of interest, the T cell library method was used to calculate the precursor frequency and to characterize the Tfh and non-Tfh $CD4^+$ memory repertoire. Circulating $CD4^+$ memory Tfh-Th1 ($CXCR5^+PD\text{-}1^+CXCR3^+$), Tfh-Th2 ($CXCR5^+PD\text{-}1^+CXCR3^-$) and ROM ($CXCR5^-$) cells from the peripheral blood of 4 healthy volunteers were FACS sorted, with a purity >90% (panel A, see Figure 2.5) and seeded at 1,000 cell/well, 90-190 wells per subset. $CD4^+$ T cells were expanded polyclonally in culture with exogenous IL-2, irradiated allogeneic feeder and PHA (see section 2.6.1) and after 20 days of culture were screened for the capacity to respond to HA protein, from Influenza Virus A/Wisconsin/67/2005, H3N2 at 5µg/mL (**Figure 5.2**). IL-2 (500 U/mL) and DMSO (0.045 %) were used as positive and negative controls respectively and the results presented herein are background subtracted. Positive

lines were defined as >3000 cpm, with a stimulation index > 5. Three out of four donors showed enrichment of HA-specific T cells in the Tfh-Th1 and ROM populations, while few HA-specific Tfh-Th2 cells were found and could only be isolated from donor 2 (**Figure 5.2 a**). This dominance of a Th1 response is in agreement with previously published literature (Bentebibel et al., 2013; Palladino et al., 1991; Yang et al., 2013). It was not surprise to detect a low number of Influenza-specific Tfh-Th2 cells, even if only in donor 2, in line with several studies that showed low efficiency of Th2 profile in response to influenza (Pedersen et al., 2014; Yoon et al., 2017). Tfh-Th2 cells was also the slowest subset in culture with limited response to IL-2 as positive proliferative control, as shown previously (see section 3.4). Both the low Influenza-frequency and the limited expansion in culture might have contributed to the little detection of HA-specific Tfh-Th2 in this assay. The ROM population contains the canonical Th1 subset ($CD4^+$ memory $CCR5^+CXCR3^+$), which are known to be specific for viral proteins (Zielinski et al., 2011); therefore, we expected to see consistent HA enrichment in the ROM compartment. The lines which had a high background proliferation, > 3000 cpm, with DMSO only, were not considered in the analysis (**Figure 5.2 b**). Because $CD4^+$ T cells were seeded at a limiting dilution it was possible to calculate the precursor frequency based on the number of negative wells according to the Poisson distribution (Campion et al., 2014; Geiger et al., 2009; Mele et al., 2017) (**Figure 5.2 c**). Since the percentage for each of the circulating subsets Tfh-Th1, Tfh-Th2 and ROM cells in the $CD4^+$ memory compartment is different, as observed and described in the section 3.2, the number of antigen-specific cells per million was calculated within each subset and not within the total $CD4^+$ memory T cell population. Donor

2 and 3 showed the highest precursor frequency in both Tfh-Th1 and ROM populations (530-550 and 280-150 antigen-specific cells/million). Overall the frequencies were different throughout the 4 donors analysed, since the memory response may reflect the diverse antigen experiences of each individual. However, it was interesting to register and to report the trend of a high viral-specificity in the Tfh-Th1 subset, which well resembles the specificity of the canonical $CD4^+$ Th1 subset.

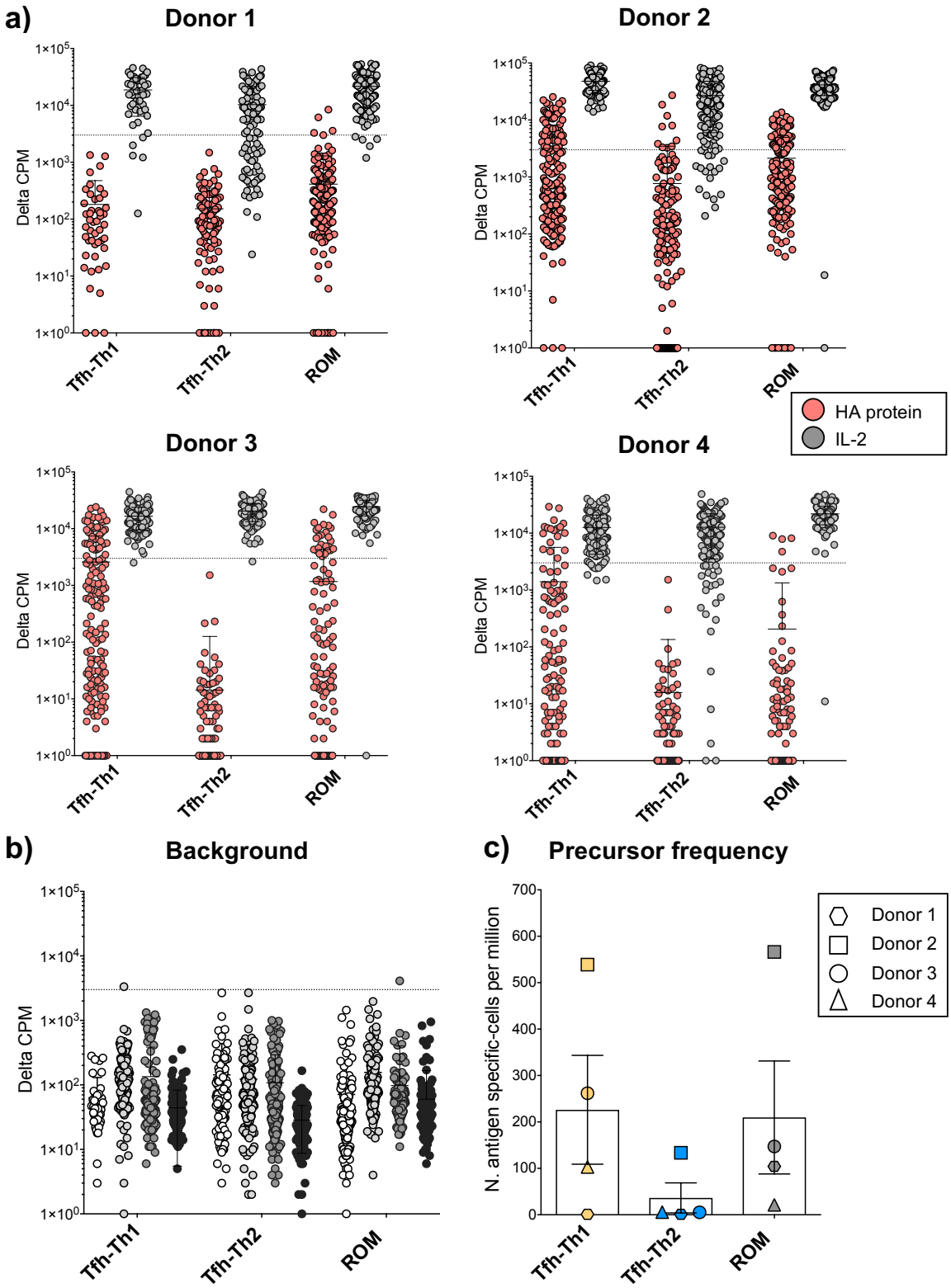

a)
Donor 1
Donor 2
Donor 3
Donor 4
Delta CPM
1×10^5
1×10^4
1×10^3
1×10^2
1×10^1
1×10^0
Tfh-Th1
Tfh-Th2
ROM
HA protein
IL-2
b)
Background
c)
Precursor frequency
N. antigen specific-cells per million
700
600
500
400
300
200
100
0
Donor 1
Donor 2
Donor 3
Donor 4

Figure 5.2 Haemagglutinin-specificity in CD4$^+$ memory circulating Tfh and non-Tfh cells.

CD4$^+$ memory Tfh-Th1, Tfh-Th2 and ROM subsets were screened for the specificity of HA/Wisconsin/2005 protein (5μg/mL), in red, using the T cell library method (**a**) in PBMC of 4 donors. IL-2 in grey was used as a positive control (500 U/mL). Each dot represents an individual cell line and the proliferative response was measured by delta counts per minute (Delta CPM), background subtracted. The positive lines are defined as >3000 cpm, with a stimulation index > 5. The background (**b**) for each subset is shown: white=donor 1, light-grey=donor 2, dark-grey=donor 3, black=donor 4. The precursor frequency (**c**) for each donor calculated within each subset is shown. SD and mean are indicated.

5.4 Haemagglutinin-specific Tfh cell clones generation and peptide specificity

Having shown that Haemagglutinin-specific Tfh cells are present in the peripheral blood, antigen-specific circulating Tfh (cTfh) repertoire were next compared with tonsil tissue from the same donor. To achieve this, Tfh cell clones specific for HA protein were generated from peripheral blood. The epitope response of T cell clones was mapped to the peptide level and the αβTCR was sequenced and compared to each TCR from the tonsillar Tfh repertoire data, generated by a deep-sequencing approach. In order to use HA as a model antigen, it was important to check first for the presence of IgG anti-Influenza antibodies in the plasma of the donors considered, as a confirmation of a recent exposure (Bone et al., 2012; Mcvernon et al., 2014). Although IgG antibodies can be detected in the circulation even weeks after the infection when the acute immune response is already resolved, the presence of influenza-specific IgG screening was an important proof of a recent exposure and of

a possible presence of effector memory response. For this reason, the plasma of 5 adult donors (234, 239, 242, 243, 244) were screened for the presence of IgG anti-HA protein, from Influenza virus strain A/California/07/2009, H1N1 (**Figure 5.3 a**) and IgG anti-Trivalent Influenza Vaccine 2017 (TIV) (**Figure 5.3 b**). The antibody titre was evaluated using Enzyme-Linked Immunosorbent Assay (ELISA) and since there is no uniform standard for experimental vaccine antigens, the results were plotted as "ELISA arbitrary units" and standardised using a pool of all the 5 plasma samples across the experiment (see section 2.13) (Miura et al., 2008). Considering the caveat that the antibody titre was evaluated by the ELISA method without using an inhibition assay which would have been more specific for the antigens considered, all 5 donors screened showed a notable Influenza antibody titre for both HA protein (1.45 - 2.1 x 10^6 arbitrary units) and TIV (2.4 – 3.2 x10^6 arbitrary units), however donor 243 showed the lowest level in both conditions.

The detection of Influenza-specific IgG antibodies, indicated the presence of memory immune response against influenza in all the 5 donors considered. Therefore, 15-18-mer long peptides overlapping by 12 amino acids were designed to cover the entire HA/California, and used to generate antigen-specific $CD4^+$ T cell clones from the PBMC of these 5 donors. Sequences of overlapping peptides and peptide identification are listed (Supplementary **Figure 8.3**). From frozen PBMC, $CD4^+$ memory T cells were isolated and FACS sorted into Tfh-Th1 ($CXCR5^+PD\text{-}1^+CXCR3^+$), Tfh-Th2 ($CXCR5^+PD\text{-}1^+CXCR3^-$) and ROM ($CXCR5^-$) (panel A, see Figure 2.5). Each $CD4^+$ T cell subset was stimulated *ex vivo* with irradiated autologous monocytes, pulsed with HA/California peptides. After 7 days, activated $CD4^+$ T cells were identified as $ICOS^+CD25^+$, FACS sorted (panel D, Figure 2.5)

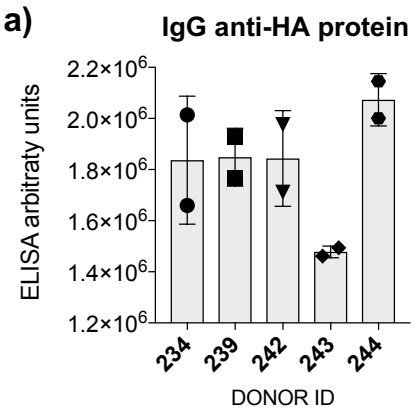
and seeded at 0.4 cell/well. T cell clones were expanded in culture with irradiated allogeneic feeder cells, in addition with IL-2 and PHA. After 10 days T cell clones were re-screened for their specificity to the same pool of peptides in order to exclude clones selected for the initial bio-standard activation. The Table (**Figure 5.3 c**) shows the number of HA-specific $CD4^+$ T cell clones generated from each donor derived from either Tfh-Th1, Tfh-Th2 or ROM subsets, while the graph (**Figure 5.3 d**) illustrates the cloning efficiency, so the percentage of T cell clones that confirmed the specificity after cloning expansion. The highest number of HA-specific clones generated derived from either Tfh-Th1 or ROM populations, which were also the subsets with the greatest percentage of cloning efficiency. Based on the percentage of activated $ICOS^+CD25^+$ and the adjustment based on the cloning efficiency, it was possible to calculate the number of HA-specific clones within each subset (**Figure 5.3 e**), or within the $CD4^+$ memory compartment (**Figure 5.3 f**). This estimate was however not a precursor frequency calculation, since it was biased by the proliferation of antigen-specific T cells during the 7 days of stimulation. Albeit a variability between the donors, the data confirmed that HA-specific T cells are enriched in the Tfh-Th1 and ROM populations, while only few HA-specific were found in the Tfh-Th2 compartment, as expected (Bentebibel et al., 2013; Palladino et al., 1991; Pedersen et al., 2014; Yang et al., 2013; Yoon et al., 2017).

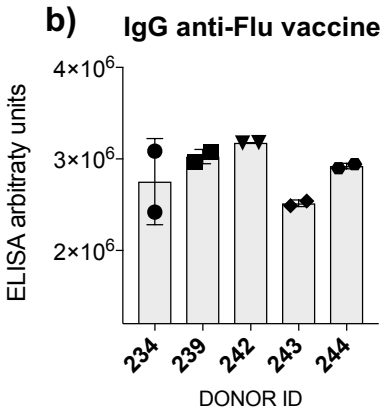
HA-specific T cell clones were then mapped at the peptide level using a 3-dimensional matrix from HA/California overlapping peptides and either the proliferative ([3H]-thymidine incorporation) or a IFN-γ response (ELISpot) was measured to determine the peptide specificity (see section 2.5). The frequency of each peptide specificity was normalized throughout the 5 donors (**Figure 5.4 a**). The

data of Tfh-Th1, Tfh-Th2 and ROM clones highlight the breath of HA epitopes recognized in each donor and already suggest a difference in the pattern of epitope repertoire by Tfh and non-Tfh subsets, since only few peptides per donor were recognized by all the three types of cells. Data of HLA type for each donor presented in the table (**Figure 5.4 b**) shows a similar pattern between donors 243 and 244. Despite a close similarity on the HLA-class II profile, these donors presented a different peptide recognition profile since only one peptide (433-450) is recognized by both donors and in both cases concerned Tfh-Th1 clones. The same peptide could be presented by different HLA class II molecules, which are indeed highly promiscuous (Kim et al., 2012; Paul et al., 2015; Sinigaglia and Hammer, 1994).

Given the diversity of the peptide recognition, even in donors with similar HLA-classes II genes, the focus of the analysis shifted onto the subset repertoire to see whether a distinct subset of T cell recognized a specific pattern of peptides. The peptide specificity data were then plotted by grouping the peptides recognized by either Tfh-Th1, Tfh-Th2 or ROM clones in the 5 donors, identified with different symbols (**Figure 5.5**). Tfh-Th1 clones (**Figure 5.5 a**) showed a wide diversity on the repertoire specificity and just 4 peptides (265-282, 393-410, 433-450, 441-458) were recognized by more than 2 donors, 9.5 % of the peptides identified. Although the number of Tfh-Th2 clones (**Figure 5.5 b**) was low, as shown already in the previous table (Figure 5.3.c), none of the clones generated from the 4 donors overlapped the peptide specificity. Similar to Tfh-Th1, ROM clones (**Figure 5.5 c**) presented a wide range of peptide specificity and only 3 peptides (225-242, 265-282, 433-450) were recognized by more than 2 donors. Overall there was no single peptide that was recognized by all the 5 donors. Peptide 433-450 was the most universally recognised

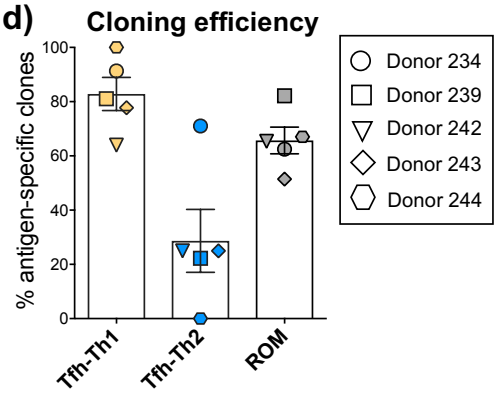
by Tfh-Th1 clones from 4/5 donors (239, 242, 243, 244) and by ROM clones from 3/5 donors (234, 242, 243).

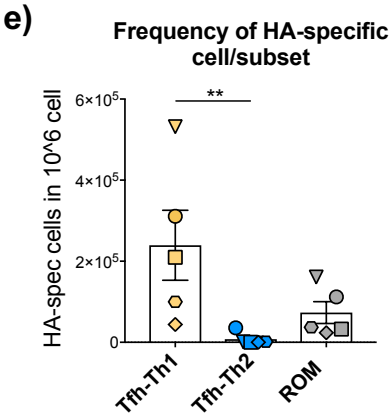




c)

Donor ID	Tfh-Th1	Tfh-Th2	ROM
234	30	11	45
239	42	6	5
242	96	2	85
243	35	1	144
244	4	-	114





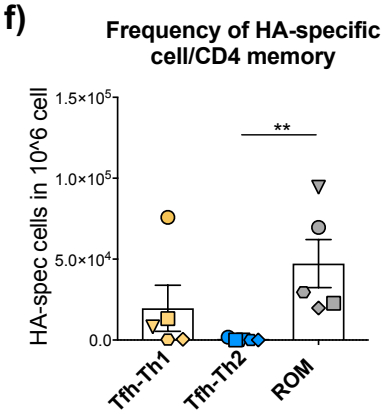
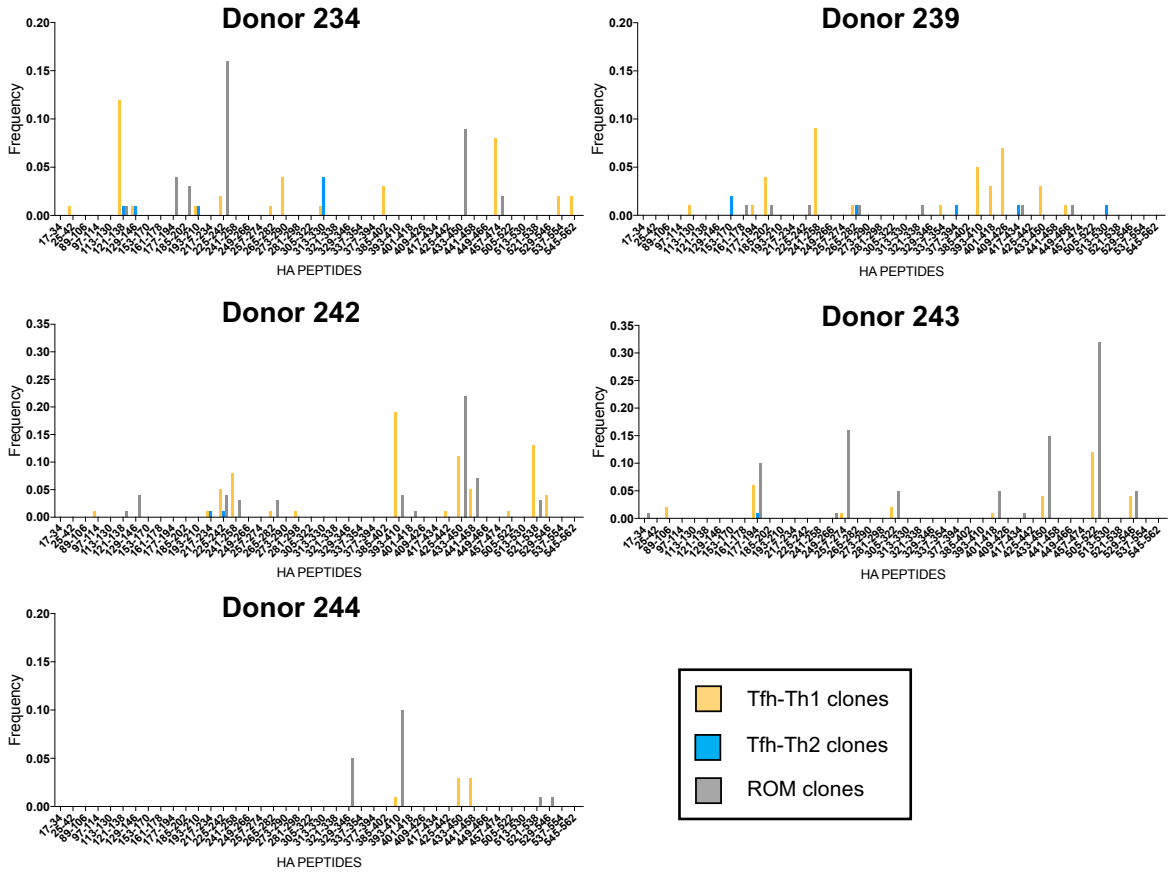


Figure 5.3 HA-specific $CD4^+$ T cell clones generation and Influenza antibody titre detection.

(**a**) IgG anti-HA/California and (**b**) IgG anti-TIV (Trivalent Influenza Vaccine, from 2017) in plasma samples of 5 donors (234, 239, 242, 243, 244) were detected by ELISA and expressed in "ELISA arbitrary units". Data are presented in duplicate, background subtracted (PBS only), with mean and Standard Deviation. Table (**c**) shows the number of HA-specific $CD4^+$ memory T cell clones generated from each of the 5 donors derived from either Tfh-Th1, Tfh-Th2 or ROM populations after *ex vivo* stimulation with overlapping peptides of HA/California and irradiated autologous monocytes. The graph (**d**) represents the cloning efficiency for each subset by percentage of HA-specific clones that confirmed the specificity after expansion. The frequency of HA-specific clones was calculated for each subset based on the percentage of $CD4^+$ T cells $ICOS^+CD25^+$ and the cloning efficiency within (**e**) each subset or within (**f**) total $CD4^+$ memory T cells. Data in graphs **d**, **e** and **f** are presented with mean and SEMn and each donor is represented with a different symbol. *P<0.05, **P<0.01, ***P<0.001, ****P<0.0001.

a)



b)

DONOR ID	A1	A2	B1	B2	Cw1	Cw2
234	11:01	24:02	15:02	51:01	08:01	14:02
239	02:01	25:01	-	-	-	-
242	26:01	26:01	-	-	-	-
243	01:01/04N	02:01	08:01	13:02	06:02	07:01
244	01:01/04N	30:02	08:01	40:01	03:04	07:01

DONOR ID	DRB1-1	DRB1-2	DRB345-1	DRB345-2	DQB1-1	DQB1-2
234	1201	1301	DRB3	DRB3	0301	0602
239	0401	0801	DRB4	-	04	0302
242	0101	1601	DRB5	-	05	05
243	0301	0701	DRB3	DRB4	02	02
244	0301	0401	DRB3	DRB4	02	02

Figure 5.4 Peptide specificity of CD4$^+$ T cell memory clones and HLA type.
HA-specific CD4$^+$ T cell clones were mapped at the peptide level and (**a**) the frequency of peptide-specific clones per subset was normalized throughout the 5 donors. HA peptides, identified as amino acid position in the HA/California protein, are specified on the x-axis. (**b**) HLA genes of class I and class II expressed by the 5 donors are listed in the table.

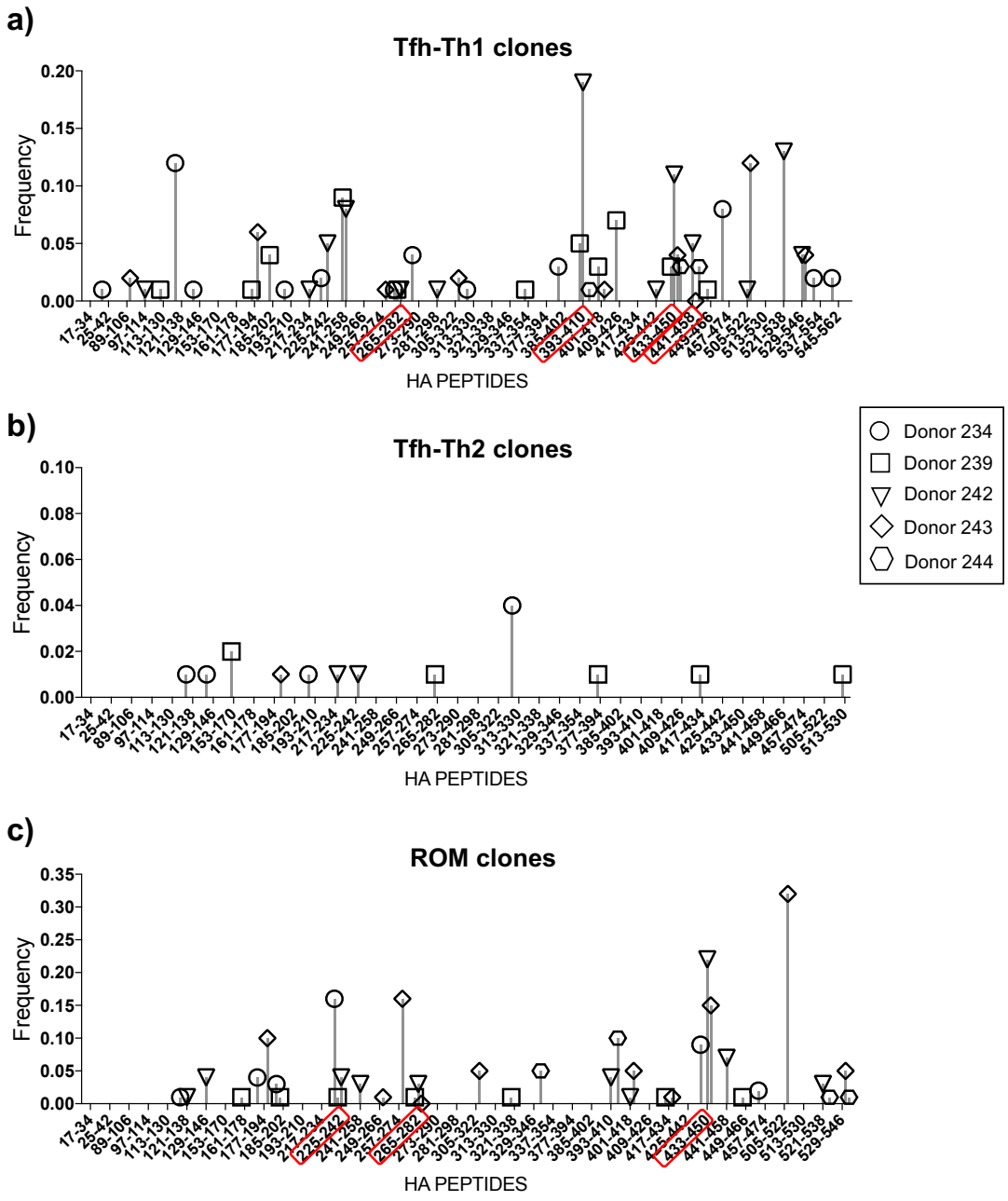


Figure 5.5 Peptide specificity in Tfh-Th1, Tfh-Th2 and ROM clones.

Normalized frequency of HA peptide-specific $CD4^+$ T cell clones were grouped per subset: (**a**) Tfh-Th1, (**b**) Tfh-Th2 and (**c**) ROM. HA peptides, identified as amino acid position in the HA/California protein, are specified on the x-axis. In each subset, peptides recognized by more than 2 donors per subset are highlighted in red.

5.5 T cell receptor sequencing of HA-specific T cell clones and comparison with $CD4^+$ T cell repertoire from tonsil tissue

In addition to the diversity of peptide recognition, mapping data of HA-specific $CD4^+$ T cell clones from the previous section 5.4, showed that few clones derived from different subsets were specific for the same peptide. For instance, in donor 242 the peptide 225-242 was recognized by clones derived from the 3 different subsets: Tfh-Th1, Tfh-Th2 and ROM. The first question was to understand whether clones with the same peptide specificity also shared the same T cell receptor sequence and were therefore primed from the same $CD4^+$ naïve T cell. We decided to sequence the CDR3 region, which is the junction between the V and the J region, since this is the most variable region of the receptor and therefore the region that establishes the identity of a certain T cell clonotype as well as the specificity (Mahe et al., 2018; Nikolich-Zugich et al., 2004). The alpha (α) and beta (β) chains of the TCR from HA-specific clones were sequenced after mRNA extraction (see section 2.10.1). The tables (**Figure 5.6**) list the amino acid (AA) and the nucleotide (Nt) sequences of the CDR3 region for each clone. Sequencing was performed from donors 242 (**Figure 5.6 a**) and 243 (**Figure 5.6 b**). Clones were grouped by peptide specificity and coloured in yellow if derived from Tfh-Th1, in light-blue from Tfh-Th2 or in grey from ROM subset. Sequences of peptides are listed (Supplementary **Figure 8.3**). TCR sequencing data from those tables show that when Tfh-Th1, Tfh-Th2 and ROM clones were specific for the same peptide (for example peptide 225-242 for donor 242 and peptide 177-194 for donor 243), they do not share the same CDR3

region; therefore, those clones belong to different T cell clonotypes. In donor 243 sister clones were identified within the same subsets: for instance, clones Tfh-Th1_07, Tfh-Th1_09, Tfh-Th1_10, Tfh-Th1_29 showed an identical TCR, as well as clones ROM_02, ROM_05, ROM_07, ROM_15. These Tfh-Th1 and ROM clones also presented the same α chain and the same AA sequence of the β chain, nevertheless the Nt sequence of the β chain differed from one nucleotide, indicating that the ROM and Tfh-Th1 clones were derived from different lineages even though their sequences were very similar. In some cases, even if 2 clones were specific for the same peptide and belong to two different lineages, the α or the β chain was related to the same family, showed in the columns of TRAV for the α and TRBV for the β. For instance, in donor 242 clones Tfh-Th1_49, Tfh-Th2_01 and ROM_42 specific for peptide 225-242, despite the different AA sequence, all the 3 α-chains belong to the same TRAV 23/DV6 family. Also in donor 243 clones Tfh-Th1_01 and Tfh-Th2_01 specific for peptide 177-194, despite the different AA sequence, the β chains belong to the same TRBV 2 family.

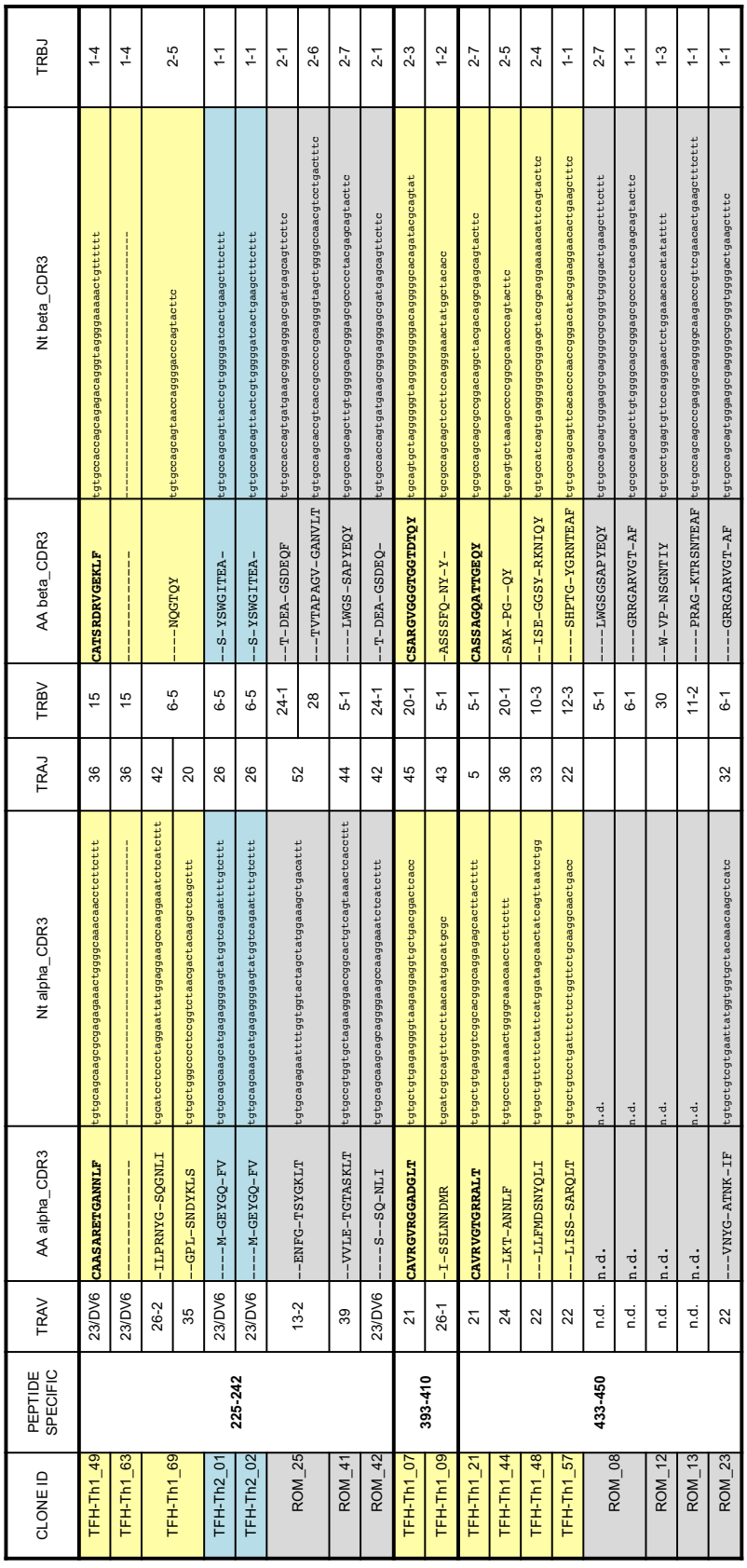
Each TCR sequence was then searched for in the different $CD4^+$ T cell subsets of tonsil (Tfh-GC, Tfh-Th1, Tfh-Th2, ROM) and peripheral blood (Tfh-Th1, Tfh-Th2, ROM), from which the non-paired αβ TCR was deep-sequenced previously from cells in bulk (see section 4). Because both α- and β-chains from T cell clones were sequenced, it was possible to determine the presence or the absence of each clonotype in the subsets analysed. CDR3 regions of HA-specific Tfh-Th1, Tfh-Th2 or ROM clones from donors 242 (**Figure 5.7**) and 243 (**Figure 5.8**) were compared in the tonsil and blood TCR repertoire. Although in few cases either α- or β-chain

were found not to be paired in different subsets (data not shown), for simplicity, the frequency shown on the y-axis is the β-chain frequency that resulted in each subset, and therefore it is related to the number of clonotypes sequenced in the specific subset considered. In donor 242, 3 Tfh-Th1 clones (21, 44, 48) were indeed found in the Tfh-Th1 from tonsil compartment and 2 Tfh-Th1 clones (21, 57) were found in the Tfh-Th1 from peripheral blood (**Figure 5.7 a**). The table shows the frequency of the clonotype of interest for both chains (**Figure 5.7 b**). The vastness of the $CD4^+$ T cell repertoire in tonsil and blood probably made the chances of finding matches very low, but did not impede this correlation in donor 242, although only one ROM clone was found in the ROM population from blood in donor 243 (**Figure 5.8 a**). The table shows the frequency of the ROM clonotype for both chains (**Figure 5.8 b**). Unfortunately, as clone ROM_25 had 2 α- and 2 β-chains (see table in Figure 5.6 b), most probably because it was not a single clone but 2 distinct clones, it was not possible to distinguish whether the α- and the β-chains found in the ROM compartment of the blood repertoire were paired or if they belonged to 2 different clones. Future studies will focus on sorting ROM_25, by using an anti-TRBV 28, generating clones by limiting dilution in culture and sequencing the αβTCR to determine which of the α and β chains sequenced are paired. The low Influenza antibody titre of donor 243 (Figure 5.3 a, b) might explain the absence of correlation between HA-specific $CD4^+$ T cells in tonsil. Tonsil is a secondary lymphoid organ, in which acute responses and antigen priming take place. Even though the level of antibody titre in the blood stream is not the mirror of an acute response because it remains for weeks after the infection, the low value of Influenza IgG antibodies in

donor 243, is in line with the absence of detection of HA-specific $CD4^+$ T cell clones in correlation between tonsils and blood. Moreover, it is very probable that the deep-sequencing analysis of only 100,000 T cells is a limitation due by the size of the wide $CD4^+$ repertoire.

In conclusion, although only few clones were found in the repertoire comparisons, the presence of HA-specific clones isolated first in the PBMC and then found in the same subset of tonsil TCR repertoire, confirmed the direct relationship between circulating and tonsillar Tfh cells.

a) Donor 242



CLONE ID	PEPTIDE SPECIFIC	TRAV	AA alpha_CDR3	Nt alpha_CDR3	TRAJ	TRBV	AA beta_CDR3	Nt beta_CDR3	TRBJ
TFH-Th1_49	225-242	23/DV6	**CAASARETGANNLF**	tgtgcagcaagcgcgagagaaactgggcaaacaacctcttctttt	36	15	**CATSRDRVGEKLF**	tgtgccaccagcagagacaggtagggaaaaactgttttttt	1-4
TFH-Th1_63		23/DV6	-----------	----------	36	15	----------	----------	1-4
TFH-Th1_69		26-2	-ILPRNYG-SQGNLI	tgcatcctccctaggaattatggaggaagccaaggaaatctcatctttt	42	6-5	----NQGTQY	tgtgccagcagtaaccagggacccagtacttc	2-5
		35	--GPL-SNDYKLS	tgtgctggcccctccggtctaacgactacaagctcagctt	20				
TFH-Th2_01		23/DV6	----M-GEYGQ-FV	tgtgcagcaagcatgagagggagtatggtcagaatttgtgtctt	26	6-5	--S-YSWGITEA-	tgtgccagcagttactcgtggggatcactgaagcttctctt	1-1
TFH-Th2_02		23/DV6	----M-GEYGQ-FV	tgtgcagcaagcatgagagggagtatggtcagaatttgtgtctt	26	6-5	--S-YSWGITEA-	tgtgccagcagttactcgtggggatcactgaagcttctctt	1-1
ROM_25		13-2	--ENFG-TSYGKLT	tgtgcagagaaattttgtggtactagctatggaaagctgacattt	52	24-1	--T-DEA-GSDEQF	tgtgccaccagtgatgaagcggaaggagcgatgagcagttctc	2-1
						28	---TVTAPAGY-GANVLT	tgtgccagcaccgtcaccgccccgcagggtagctgggccaacgtcctgacttttc	2-6
ROM_41		39	--VVLE-TGTASKLT	tgtgccgtggtgctagaaggagaccggcactgtcagtaaactcacctttt	44	5-1	----LWGS-SAPYEQY	tgcgccagcagcttgtgggcagcgggagcgccctctagcgagcagtactc	2-7
ROM_42		23/DV6	----S---SQ-NLI	tgtgcagcaagcagcagagggaagccaaggaaatctcatctttt	42	24-1	--T-DEA-GSDEQ-	tgtgccaccagtgatgaagcgggaaggagcgatgagcagttctc	2-1
TFH-Th1_07	393-410	21	**CAVRGVRGGADGLI**	tgtgctgtgagagggtaagaggagtgctgacggactcacc	45	20-1	**CSARGVGGGTGGTDTQY**	tgcagtgctcagggggtagggggggggacagggggcacagatacgcagtat	2-3
TFH-Th1_09		26-1	-I-SSLNNDMR	tgcatcgtcagttctctcttaacaatgacatggc	43	5-1	-ASSSFQ-NY-Y-	tgcgccagcagctcctccagggaaactatggctcacacc	1-2
TFH-Th1_21	433-450	21	**CAVRVGTGRRALT**	tgtgctgtgaggtcggcacgggcaggagagcacttactttt	5	5-1	**CASSAGQATTGEQY**	tgcgccagcagcgccgacaggctacgcaggcgagcgtactc	2-7
TFH-Th1_44		24	--LKT-ANNLF	tgtgccctaaaactgggcaaacacctcttctttt	36	20-1	-SAK-PG---QY	tgcagtgctcaaagccccccggcgcaacccagtacttc	2-5
TFH-Th1_48		22	---LLFMDSNYQLI	tgtgctgttcttcttattcatggatagcaactatcagttaatctgg	33	10-3	--ISE-GGSY-RKNIQY	tgtgccatcagtgaggggcggcggagctacggcaggaaaaactcagtacttc	2-4
TFH-Th1_57		22	---LISS-SARQLT	tgtgctgtcctgatttctttctgttctgcaaggcaactgacc	22	12-3	----SHPTG-YGRNTEAF	tgtgccagcagttccacacccaaccggacatacggaaggaacactgaagctttc	1-1
ROM_08		n.d.	n.d.	n.d.		5-1	----LWGSGSAPYEQY	tgtgccagcagtgggagcgaggggcgcggtgggactgaagcttctctt	2-7
		n.d.	n.d.	n.d.		6-1	----GRRGARVGT-AF	tgcgccagcagcttgtgggcagcgggagcgccctctacgagcagtactc	1-1
ROM_12		n.d.	n.d.	n.d.		30	-W-VP-NSGNTIY	tgtgcctgaagtgttccaggaaactctggaaacaccatatatttt	1-3
ROM_13		n.d.	n.d.	n.d.		11-2	----PRAG-KTRSNTEAF	tgtgccagcagcccgagggcaggggcgaaggcccgttcgaacactgaagcttttctttt	1-1
ROM_23		22	---VNYG-ATNK-IF	tgtgctgtcgtgaatatggtggtgctacaaacaagctcatc	32	6-1	----GRRGARVGT-AF	tgtgccagcagtgggagcgaggggcgcgggtgggactgaagctttc	1-1

b) Donor 243

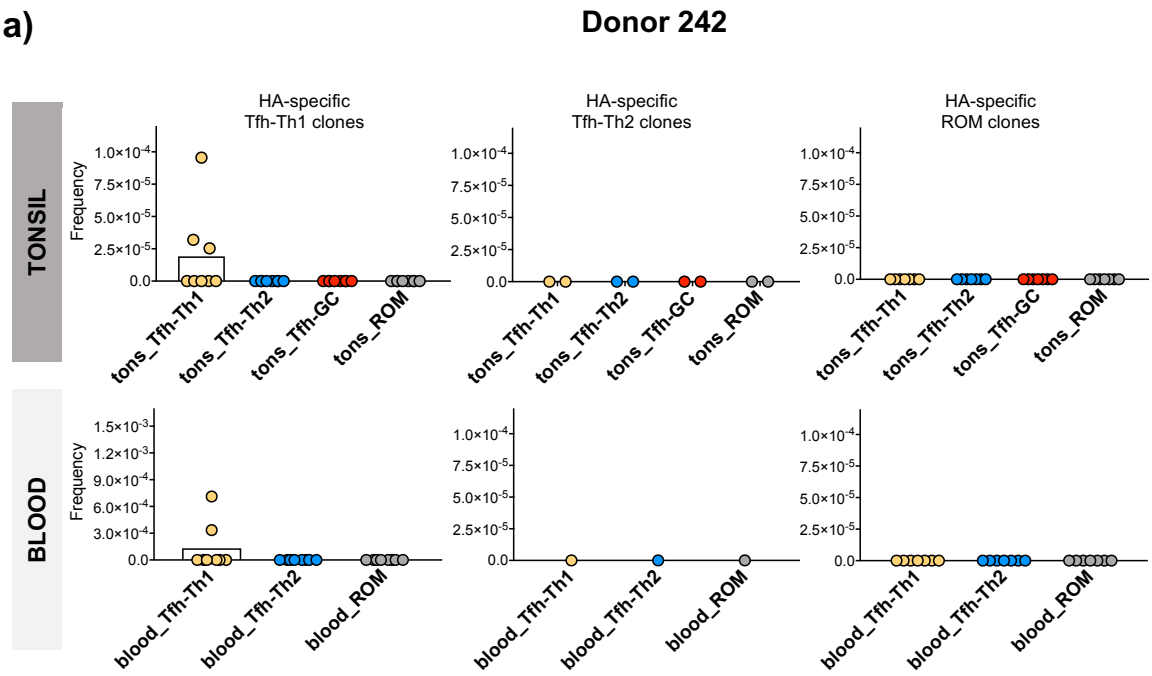
CLONE ID	PEPTIDE SPECIFIC	TRAV	AA alpha_CDR3	Nt alpha_CDR3	TRAJ	TRBV	AA beta_CDR3	Nt beta_CDR3	TRBJ
TFH-Th1_01	177-194	35	**CAGDRDDKII**	tgtgctgcggacgaagatgacaagatcatctt	30	2	**CASRSGAYNEQF**	tgtgccagccgtagcgggggcctacaatgagccagttcttc	2-1
TFH-Th1_18		35	----------	----------	30	2	----------	----------	2-1
TFH-Th1-19		35	----------	----------	30	2	----------	----------	2-1
TFH-Th1-24		35	----------	----------	30	2	----------	----------	2-1
TFH-Th1_31		35	----------	----------	30	2	----------	----------	2-1
TFH-Th2_01		9-2	--LFDTGRRALT	tgtgctctgttcgacacggcaggagagcactatttt	5	2	---WGQGKVRNQPQH	tgtgccagcagttgggcgcaaggaaggtgaaatcagccccagcatttt	1-5
ROM-22		22	--VEGAGGSY-PT	tgtgctgtggagggggcaggagaagctacatacctacaattt	6	9	---SV-VGTNNEKLF	tgtgccagcagcgtagagagttggacgaacaatgaaaaactgttttt	1-4
TFH-Th1_04	257-274	3	**CAVRAYTGRRALT**	tgtgctgtggagagcctacacggcgcaggaagcactacttttt	5	10-1	**CASSEGGSNNEQF**	tgcgccagcagtgaggggggatccgaacaatgagccagttcttc	2-1
ROM-12		9-2	--LSDRVMS-LT	tgtgctctgagatgatcggttcatgtctagttgacttt	58	11-3	---RTLERRKGNSNQPQH	tgtgccagcagccgaacttggagcggaggaaaggaatagcaatcagcccagatttt	1-5
						20-1	-SARV-ENI-YGYT	tgcagtgctagagtcggcgagaacattaactatggctacacctc	1-2
ROM-20		9-2	--LSDRVMS-LT	tgtgctctgagatgatcgggttcatgtctagttgacttt	58	11-3	---RTLERRKGNSNQPQH	tgtgccagcagccgaacttggagcggaggaaaggaatagcaatcagcccagatttt	1-5
						20-1	-SARV-ENI-YGYT	tgcagtgctagagtcggcgagaacattaactatggctacacctc	1-2
TFH-Th1_05	305-322	4	**CLVGANNNAGNMLT**	tgcctcgtgggtgcgaataatgcaggcaacatgctcacttt	39	6-2/6-3	**CASSRELRSSPLH**	tgtgccagcagccgggagctcaggagttcacccctccacttt	1-6
TFH-Th1_06	433-450	8-4	**CAVRLYGNNRLA**	tgtgctgtgagattgtatgggaacaacagactcgctttt	7	13	**CASSSRDRGAAF**	tgtgccagctcccgggacagggggcagcttctttt	1-1
TFH-Th1_23		8-4	----------	----------	7	13	----------	----------	1-1
TFH-Th1_32		8-4	----------	----------	7	13	----------	----------	1-1
ROM_19		35	--GQ--R-TGNQFY	tgtgctggcagctatagagaacacggtaaccagtctctatttt	49	5-4	----P-PGSSTDTQY	tgtgccagcagtcccgactggctctagcacagatacgcagtatttt	2-3
ROM_25		3	---DYT-TASKLT	tgtgctgtgagagactataccggcactgccagtaaactcacctttt	44	12-4	--KRQGLAGDEQY	tgtgccagcaagcgacaagagactagcgggagatgagcagtacttc	2-7
		41	---SGGS-YKLT	tgtgctgtcagtggaagtagcaactataaactgacatttt	53	9	----VSTVGWGARGGELF	tgtgccagcagcgttctccactgttgggtgggggcgcgggggagctgttttttt	2-2
ROM_39		8-1	---NAR---ARLM	tgtgccgtgaatgcgcgggtaacaatgccgactcatgttt	31	3-1	----QLAGDNEQF	tgtgccagcagcacagctagcgaggggacaatgagcagttctc	2-1
		41	---WG-GTSYGKLT	tgtggctgtcagatgggtggtggtactacgtgaaagctgacatttt	52	15	--T-PGGLAGGGKQY	tgtgccacagcccgcgggattagcgggagtgagcgagaaagcagtacttc	2-7
TFH-Th1_07	505-522	13-1	**CAGGGADGLT**	tgtgcagggaggtgctgacggactcacttt	45	6-6	**CASRTGQGASYEQY**	tgtgccagcagaacggacagggggcctcctacgagcagtacttc	2-7
TFH-Th1_09		13-1	----------	----------	45	6-6	----------	----------	2-7
TFH-Th1_10		13-1	----------	----------	45	6-6	----------	----------	2-7
TFH-Th1_29		13-1	----------	----------	45	6-6	----------	----------	2-7
ROM_02		13-1	----------	----g----------	45	6-1	-----L--N---	tgtgccagcagaacaggctagggctaacttatggctacaccttc	1-2
ROM_05		13-1	----------	----g----------	45	6-1	-----L--N---	tgtgccagcagaacaggctagggctaacttatggctacaccttc	1-2
ROM_07		13-1	----------	----g----------	45	6-1	-----L--N---	tgtgccagcagaacaggctagggctaacttatggctacaccttc	1-2
ROM_15		13-1	----------	----g----------	45	6-1	-----L--N---	tgtgccagcagaacaggctagggctaacttatggctacaccttc	1-2

Figure 5.6 αβTCR sequencing of HA-specific clones from donors 242 and 243.

The mRNA of TCR from HA-specific $CD4^+$ memory Tfh-Th1 (yellow), Tfh-Th2 (light-blue) and ROM (grey) was sequenced. Sequences of alpha (α) and beta (β) chains of the CDR3 region are listed in the tables for donors (**a**) 242 and (**b**) 243. The columns showed the clone identity (ID), peptide specificity, amino acid (AA) and nucleotide (Nt) sequences, the family classification of the J region (TRAJ and TRBJ) and of the V region (TRAV and TRBV) for both α and beta β chains. Clones are grouped based on the peptide specificity and AA alignment was made considering the first Tfh-Th1 clone from each group.

n.d.= not determined.

a)



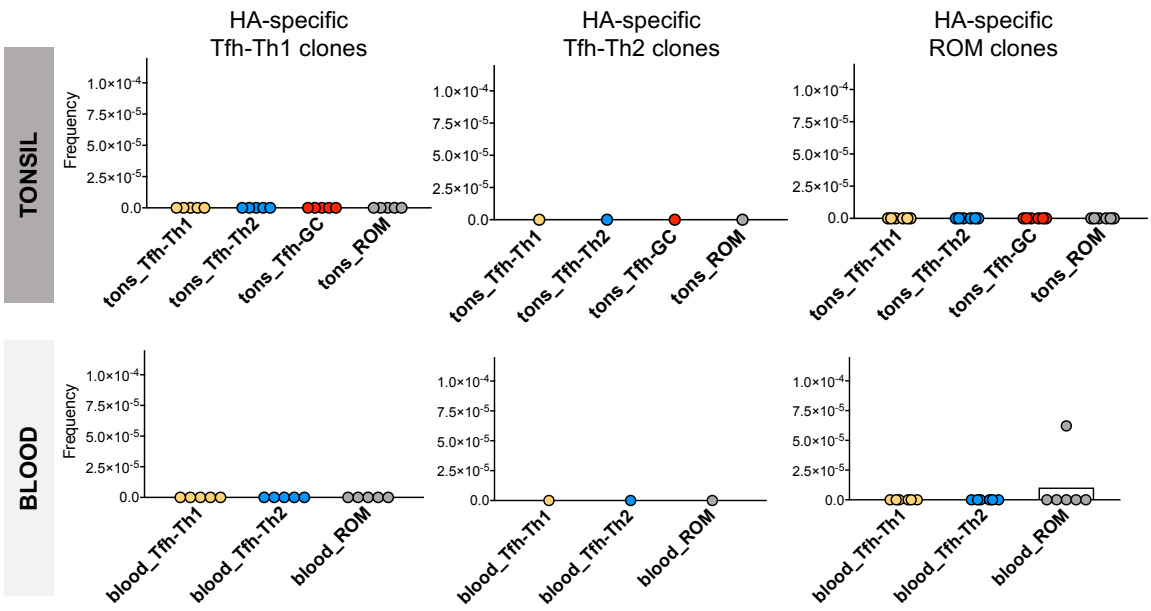
b)

CLONE ID	PEPTIDE SPECIFIC	tons_Tfh-Th1		blood_Tfh-Th1	
		α-chain	β-chain	α-chain	β-chain
Tfh-Th1_21	433-450	7.42E-05	1.17E-04	1.35E-04	5.35E-04
Tfh-Th1_44		2.47E-05	3.91E-05	n.d.	n.d.
Tfh-Th1_48		2.47E-05	2.61E-05	n.d.	n.d.
Tfh-Th1_57		n.d.	n.d.	6.76E-04	7.49E-04

Figure 5.7 Comparison of αβTCR sequences from HA-specific T cell clones with tonsil and blood repertoire in donor 242.

(**a**) α and β TCR chains from HA-specific $CD4^+$ memory isolated Tfh-Th1, Tfh-Th2 and ROM clones, were sought in the TCR repertoires of tonsil (Tfh-Th1, Tfh-Th2, Tfh-GC, ROM) and blood (Tfh-Th1, Tfh-Th2, ROM) $CD4^+$ memory T cell populations. Each dot is a clonotype from an HA-specific clone that appeared in the tonsil or blood populations of interest, listed on the x-axis. The frequency shown on the y-axis is the β-chain frequency that resulted in each subset. The table (**b**) lists the peptide specificity and the frequency values of α and β TCR chains for the clones from which only both chains have been found.

a)



b)

CLONE ID	PEPTIDE SPECIFIC	blood_ROM	
		α-chain	β-chain
ROM_25	**433-450**	7.22E-05	5.20E-05

Figure 5.8 Comparison of αβTCR sequences from HA-specific T cell clones with tonsil and blood repertoire from donor 243.

(**a**) α and β TCR chains from HA-specific $CD4^+$ memory isolated Tfh-Th1, Tfh-Th2 and ROM clones, were sought into TCR repertoire of tonsil (Tfh-Th1, Tfh-Th2, Tfh-GC, ROM) and blood (Tfh-Th1, Tfh-Th2, ROM) populations. Each dot is a clonotype from an HA-specific clone that appeared in the tonsil or blood populations of interest, listed on the x-axis. The frequency shown on the y-axis is the β-chain frequency that resulted in each subset. The table (**b**) lists the peptide specificity and the frequency values of α and β TCR chains for the clone from which only both chains have been found.

5.6 Conclusions

In this section I described how Influenza-specific $CD4^+$ memory T cells were enriched in Tfh-Th1 and ROM subsets in the PBMC of non-infected individuals. Both the peptide specificity and the TCR sequencing results described a wide epitope recognition and a distinct repertoire in each of the 3 subsets analysed. Moreover, the correlation between circulating and tonsillar Tfh cells was confirmed in an antigen-specific context.

Influenza-specific $CD4^+$ T cells were identified using Haemagglutinin (HA) from 2 different strains: Wisconsin/2005 (protein) and California/2009 (overlapping peptides). From the T cell library in section 5.3 was possible to calculate the precursor frequency, which despite the variability between the donors, showed a consistent enrichment of antigen-specific cells per million in both Tfh-Th1 and ROM subsets. Also, the number of HA-specific clones generated from PBMC of 5 donors in section 5.4, showed higher frequencies in Tfh-Th1 and ROM cells compared to Tfh-Th2 cells, from which only few clones were found. The specificity for Influenza in the Tfh-Th2 cells was very low, similar with the canonical $CD4^+$ Th2 subset for any viral antigen (Sallusto and Lanzavecchia, 2009). Moreover, the poor cloning efficiency of Tfh-Th2 cells likely mirrors the low frequency of HA-specific cells in this subset. The peptide specificity of HA-specific T cell clones, showed a wide and diverse epitope response that spanned the entire HA molecule and was not shared amongst donors of similar HLA class II type. No particular peptide was enriched in either Tfh-Th1, Tfh-Th2 or ROM compartments of all the 5 donors but 5 peptides were shown to be recognized by clones derived from 2 or more different T cell populations. Preliminary TCR sequencing data from 2 donors (section 5.4) showed

a distinction between Tfh-Th1, Tfh-Th2 and ROM clonotypes with the same peptide specificity and suggested that those populations derived from 3 different lineages. Finally, a comparison of the entire $CD4^+$ T cell TCR repertoire from tonsil and blood in section 5.5, showed a correlation between HA-specific Tfh-Th1 clonoypes with Tfh-Th1 from both tonsil and blood compartments, from one of the donors. Current experiments are focusing on sequence the TCR of HA-specific clones from donor 234 and a correlation with tonsil and blood $CD4^+$ T cell repertoire will be performed.

6 Results IV: T and B cell contact and observation of immunological synapses

6.1 Background and rational

The *ex vivo* $CD4^+$ T cell repertoire comparison and the antigen-specific cloning analysis of the T cell receptor in the previous sections have highlighted not only the relationship between tonsil and blood Tfh cells, but have also distinguished the unique repertoire and specificity of Tfh populations compared with non-Tfh $CD4^+$ T cell populations.

Several studies have described the characteristic features of cTfh cells from peripheral blood, which are similar to Tfh-GC cells, and their ability to help B cell class-switching and plasmablast formation in co-culture assays *in vitro* (Bentebibel et al., 2013; He et al., 2013; Locci et al., 2013; Morita et al., 2011). However, a direct functional comparison of cTfh and follicular Tfh cells from blood and tonsil of the same donor has yet to be described.

There have been several speculations on why Tfh are circulating. cTfh cells might represent the memory reservoir of previous effector Tfh-GC cells generated during an acute immune response, and/or they might still be important during the effector response by improving the connection between lymph nodes and the site of infections or between secondary lymphoid organs (Schmitt and Ueno, 2013; Vinuesa and Cook, 2011), therefore improved understanding of the cTfh cell function would help in determining their role. One means by which to address the functionality of

cTfh would be to examine the immunological synapse formation of Tfh-GC and cTfh with B cells.

The immunological synapse is the unique event at the contact between T cells and antigen-presenting cells (APC). In the B cell follicle, this contact happens between antigen-specific $CD4^+$ T and cognate B cells and it is a necessary and critical process for the formation of germinal centres, B cell proliferation and selection events occurring from it, such as production of high-affinity and neutralizing antibodies (Bannard and Cyster, 2017). Due to the scarce technology available, it has always been difficult to study this topic, however recent artificial models based on high-resolution imaging technology have helped the visualization of immune synapses (Dustin, 2014a).

Although TCR recognition to peptide:MHC is the most specific interaction during this contact, adhesion molecules (such as LFA-1 on the T cells and ICAM-1 on the B cell), as well as co-stimulatory and co-inhibitory signals, strongly influence immune synapse formation (Dustin, 2014a). The cognate signal between T and B cells is enhanced by CD40L-CD40 in addition to ICOS-ICOSL and CD80/CD86-CD28 interactions and regulated by PD-1-PD-1L signals (see section 1.7) (Casamayor-Palleja et al., 1995; Linterman et al., 2014; Noelle et al., 1992). During a T cell-APC interaction, the phosphatases CD45 on the surface of the T cell segregate passively due by the steric effects of the APC size. The absence of phosphatases allows the phosphorylation of TCR-associated kinases followed by the trigger of TCR signalling inside the T cell (Davis and van der Merwe, 2006). T follicular helper cells are the main players in this particular T-B cell interaction, which is a very localized contact and leads to the formation of T cell receptor (TCR)

microclusters on the membrane of the T cells, binding the MHC peptide complex (pMHC) on the B cells (Dustin, 2014b). Consequently, microvesicles of 1000 nm in diameter containing TCR-pMHC are generated and internalized by the B cells (Choudhuri et al., 2014). In this study Choudhuri et al. described the formation of extracellular microvesicles from either murine $CD4^+$ T cells or human $CD4^+$ T cell lines using an artificial supported lipid bilayer (SLB) technique and total internal reflection fluorescent microscopy (TIRFM) to observe the formation of immunological synapse. SLB technique consists on anchoring molecules such as CD40, ICOSL and ICAM-1 on an artificial lipid bilayer to mimic the B cell surface. More recently, post-doctoral fellow researchers, Dr David Saliba and Dr Pablo Cespedes in the Dustin laboratory, optimised a novel methodology to isolate microvesicles in a simpler way, using flow cytometry (Saliba et al., unpublished personal communication). $CD4^+$ T cells are incubated with silica beads supported lipid bilayer (BSLB), which contain selected receptors to mimic the B cells, CD40, ICOSL and ICAM-1. This method allows the detection not only of the TCR-enriched microvesicles already described, but also a variety of different markers that are important for T and B cell contact, which can be analysed by flow cytometry (see section 2.12).

During priming with DCs, $CD4^+$ T cell fate is influenced by the quality and quantity of the TCR signalling and therefore by the strength and the affinity of the TCR for the antigen (Germain and Stefanová, 1999; Malherbe et al., 2004; Tubo and Jenkins, 2016). Several previous studies have showed how TCR signalling and antigen dose affects Th1 and Th2 cell differentiation *in vitro* and *in vivo* and the strict dependence on the nature of the antigen (Constant et al., 1995; Hosken et al., 1995; VanPanhuys

et al., 2014). There is controversy regarding the role of TCR affinity in Tfh cell differentiation: studies using pigeon cytochrome C (PCC) in a mouse model showed that high affinity TCR are preferentially selected for residential follicular T effector function (Tfh-GC) during acute response (Fazilleau et al., 2007, 2009), however this observation was not confirmed in a persistent viral infection model (Ploquin et al., 2011). Defining affinity as the molecular parameter of the strength of TCR–peptide binding is difficult to measure in studies with whole cells. Therefore, the measure of the TCR avidity, the overall strength of a TCR–peptide binding complex which depends on antigen availability, multivalent binding and influenced by simultaneous co-receptor binding, is often studied rather than the real affinity. In general Tfh-GC differentiation is promoted by a persistent peptide:MHC presentation by germinal centre B cells, but different experimental models still leave open discussions regarding the nature of the antigen in question (Tubo and Jenkins, 2016).

Uncertainties remain about how Tfh cell avidity influences the function and the signals in the immune synapses. Does a high avidity Tfh cell provide a better help to a B cell? Could this influence an immune synapse? The combination of knowledge of the human primary circulating and tonsillar Tfh subsets together with cutting-edge high-resolution technology could contribute to a better understanding of Tfh-B cell immune synapses process in an antigen-specific context. Here we established a collaboration with the Dustin group, focusing on the microvesicles released by different subsets of Tfh cells after a general stimulus, as well as evaluating the role of T cell avidity in an antigen-specific T and B cell contact, using antigen-specific T cell clones.

The aims of this chapter are therefore:

- To evaluate the feasibility of the silica-beads supported lipid bilayer (BSLB) technique to describe the synaptic transfer of vesicles to B cells by different subsets of circulating Tfh and non-Tfh cells.
- To generate high and low avidity Tfh and non-Tfh clones, determine their HLA restriction and optimise the microvesicles transfer using peptide-HLA monomer constructs.
- To optimise T and B cell co-culture for a parallel investigation of the role of T cell avidity in a cognate synapse.

6.2 Synaptic microvesicle transfers on silica bead lipid bilayer from circulating Tfh and non-Tfh cells

The involvement of T follicular helper cells in the immune synapses with B cells is a fundamental process during an immune response (Dustin, 2014b),but the quality of the signal between T and B cells is still not entirely described. An open question is whether different populations of Tfh, such as Tfh-Th1 or Tfh-Th2, can transfer different molecules, contained in microvesicles, to the B cells and whether this transfer can also be quantified. To address this question, the silica beads-SLB technique was optimised in primary $CD4^+CXCR5^+$ T cells from the peripheral blood of healthy blood donors. Before the incubation with silica beads, T cells were expanded in culture for 10 days after a stimulation of anti-CD3/anti-CD28 and complete media with 50 U/mL of IL-2 (CM IL-2, see Figure 2.1). The function of $CD4^+$ T cells *ex vivo* and after expansion was comparable (data not shown). The

detection of microvesicles using this technique requires a large number of cells (250,000 cell/condition) and considering the low cTfh frequency in the blood (0.5-1 % of the total PBMC), it was not feasible to obtain this number from a single blood draw, therefore it was necessary to expand cTfh cells first before using them in the silica beads-SLB assay. Increasing IL-2 concentration in culture could improve cTfh expansion *in vitro*. During a repertoire investigation, such as the T cell library method, it is not fundamental if the phenotype of the T cells changes during expansion because the element in question is the TCR, which does not vary *in vitro*. In case of a functionality assay, it is important that the phenotype of the T cells does not changes drastically during expansion, since the phenotype is directly responsible for the function of T cells.

For these reasons $CD4^+$ memory T cells from 2 healthy blood donors were sorted with the FACS Aria, to a purity of >90 %, into Tfh-Th1 ($CXCR5^+CXCR3^+$), Tfh-Th2 ($CXCR5^+CXCR3^-$) and ROM ($CXCR5^-$), (panel A, see Figure 2.5). The PD-1 surface marker was not considered for isolation of Tfh cells in any synaptic transfer assay because preliminary experiments showed it interfered with silica bead read-out (data not shown, personal communication). Triggering PD-1 with antibodies activates the phosphatases SHP-1 and SHP-2, which lead to a TCR suppressive state of the cells and might not form synapses in response to antigen (Bardhan et al., 2016; Hui et al., 2017).

Each subset of sorted cells was seeded at 10^6 cell/mL (1,000 cell/well) and expanded with anti-CD3/anti-CD28 and CM with either 50 or 100 U/mL of IL-2 (**Figure 6.1**). The number of viable T cells in culture was quantified at day 0, 5, 8 and 12 (**Figure 6.1 a**) and the graphs illustrated the notable expansion detected with 100 U/mL of

IL-2 in culture until day 12 compared with the previously used 50 U/mL condition. The higher concentration of IL-2 allowed cTfh subsets to reach a number of 3-4 $x10^6$ cell/well and 2 $x10^7$ cell/well for the ROM (3-4 and 20 folds greater respectively), compared with the 0.2-0.4 $x10^6$ cell/well and 1 $x10^7$ cell/well in the 50 U/mL condition. Previous experiments have shown the phenotype of $CD4^+$ T cell surface markers changes in culture after expansion with 500 U/mL of IL-2 (see section 3.4). To check that the function of the populations in question did not vary during expansion, the cytokine production profile after 12 days of culture with either 50 or 100 U/mL of IL-2 was evaluated by intracellular cytokine staining after 5h PMA/Ionomycin stimulation (**Figure 6.1 b**). With the caveat that this type of stimulation is often used to observe the unbiased ability of specific subsets of T cells to produce certain cytokines, independently of the antigen (Ai et al., 2013), no significant differences were detected on the IFN-γ, IL-21 and IL-17A production after 12 days of 100 U/mL IL-2 expansion, compared with the 50 U/mL condition, while IL-4 production by ROM cells was greater when expanded with 100 U/mL of IL-2. As expected IFN-γ production was enriched in ROM and Tfh-Th1, IL-4 in ROM and Tfh-Th2 and IL-17A in Tfh-Th2 (Morita et al., 2011; Sallusto and Lanzavecchia, 2009). IL-21-producing cells were found in each of the 3 subsets considered, consistent with previous literature (Raeber et al., 2018; Sallusto, 2016). Although the samples were unavailable to detect and therefore compare the cytokine profile of the same T cell subsets from the same donors *ex vivo*, the results of 100 U/mL IL-2 expansion were encouraging and showed a similar phenotype profile of $CD4^+$ memory T cells in culture with IL-2 at 50 U/mL, expansion conditions that were previously optimised for microvesicle transfer (data not shown, personal

communication), as well as reliable cytokine profiles for the different subsets of $CD4^+$ memory T cells analysed.

To analyse whether different populations of Tfh (Tfh-Th1 or Tfh-Th2) and non-Tfh cells, such as canonical Th1 and Th2 cells, can transfer differently molecules contained in extracellular microvesicles, $CD4^+$ memory T cells from 6 different healthy blood donors were sorted by FACS Aria, with a purity of >90 %, into Tfh-Th1 ($CXCR5^+CXCR3^+$), Tfh-Th2 ($CXCR5^+CXCR3^-$), Th1 ($CXCR5^-CXCR3^+$) and Th2 ($CXCR5^-CXCR3^-$) populations (panel A, Figure 2.5) (**Figure 6.2 a**). Each subset of sorted cells was seeded at 10^6 cell/mL (1,000 cell/well) and expanded with anti-CD3/anti-CD28 and complete media (CM) with 100 U/mL of IL-2 for 12 days. After expansion T cells were washed from IL-2 and rested for 3 hours before incubation at a 1:1 ratio with silica beads, previously coated with lipid solution, ICAM-1, CD40 and ICOSL (see section 2.12). Together with B cell markers and lipid bilayers, silica beads were also coated with a general T cell stimulating antibody, anti-CD3 (UCHT1-Fab) at different concentrations (0, 50, 500 Mol/μm^2). A schematic view of silica beads-supported lipid bilayer (BSLB) methodology is illustrated in **Figure 6.2 b**: silica beads (5 μm) coated with a lipid bilayer, ICAM-1, CD40 and ICOSL are incubated with T cells to stimulate microvesicle release and facilitate the adhesion of the latter onto the beads. EDTA reagent was then added to release the silica beads from the T cell blasts so that the analysis of the beads would include only markers released in the microvesicles rather than on the T cell surface. The surface marker detection is possible by flow cytometry because molecules carried in the microvesicle are expressed on their membrane. Each sample was stained for a panel of different markers (panel E, see Figure 2.5) then acquired at the

flow cytometer LSR-Fortessa. To identify the molecules transferred into the immune synapses, the silica beads were gated and the percentage of protein transferred was calculated (**Figure 6.2 c**). The markers of interest for this first analysis were: TCR αβ, for its importance in previously described TCR-enriched microvesicles (Choudhuri et al., 2014); CD40L and ICOS for their role in T and B cell contact (Casamayor-Palleja et al., 1995; Choi et al., 2011); BST2 (CD317 or Theterin), retroviral restriction factor described to be involved on the formation of extracellular bodies (Edgar et al., 2016; Gould et al., 2003). From each marker is clear the augment of the response with the increase of the anti-CD3 concentration. No significant difference was detected between Tfh and non-Tfh cell populations for any of the molecules considered, although TCR αβ and BST2 transfer was slightly higher from non-Tfh (11% and 8%) compared to Tfh (7% and 5%) cells, with no difference between Th1 and Th2 (**Figure 6.2 c**). The background ($ICOSL^{-}CD40^{-}$) evaluated for each condition, was higher for both TCR αβ and BST2, which suggests that those molecules can be released after a T cell general stimulus independently on the B cell presence.

Since no difference between Tfh and non-Tfh cells was detected after expansion and circulating Tfh cells from peripheral blood are known to gain a follicular behaviour (higher IL-21 and Bcl-6 production and upregulation of PD-1 and ICOS) only in co-culture with B cells (He et al., 2013; Locci et al., 2013; Morita et al., 2011), the same subsets of Tfh and non-Tfh cells were co-cultured with autologous B cells before microvesicle transfer detection. $CD4^{+}$ memory T cells from 2 different healthy blood donors were sorted into Tfh-Th1, Tfh-Th2, Th1 and Th2 cells and incubated at 1:1 ratio with total autologous B cells ($CD19^{+}$), previously stimulated for 2 hours with

SEB (1μg/mL) (see section 2.11). After being in co-culture for 12 days T and B cells were washed and rested in CM for 2 hours before being incubated at 1:1 ratio with BSLB. Molecules transferred were analysed by flow cytometry (**Figure 6.3**) and although no statistical difference was reported due to the low sample number, at the highest concentration of anti-CD3 Tfh-Th2 cells in co-culture with B cells produced a higher CD40L transfer (42%), compared with Tfh-Th1 (28%), Th1 (26%) and Th2 (22%) and also a higher ICOS transfer (5%), compared with Tfh-Th1 (3.8%), Th1 (3.5%) and Th2 (4%) (**Figure 6.3 a**). TCR αβ showed a general higher transfer from canonical Th1 and Th2 rather than Tfh-Th1 and Tfh-Th2, while BST2 showed no differences between Tfh and non-Tfh transfers. TCR αβ and BST2 transferred resulted with a high background, most of the time higher than with CD40+ICOSL+ presence, for both 50 and 500 Mol/μm^2 anti-CD3 condition. Future experiments will focus on clarifying whether the high background for those molecules is caused by a technical issue (for example T cells needed to be rested for longer time or B cells interfere with the transfer read-out and needed to be removed from the co-culture at a certain point) or whether this release is physiologically B cell independent.

Preliminary results on microvesicle transfers showed the BSLB technique to be an interesting means by which to detect microvesicles trafficking in artificial immune synapses with primary Tfh cells from peripheral blood. General T cell stimuli, such as anti-CD3 and SEB, did not give a striking differentiation between cTfh and non-Tfh cells *in vitro*, only partially detected for CD40L and ICOS after a co-culture with B cells. A comparison of the Mean Fluorescent Intensity (MFI) instead of the percentage expression, might better highlight any difference, if present. Future experiments will focus on performing a microvesicle transfer profile from matched

Tfh cells from tonsil with or without co-culture with autologous B cells to study in more detail functional differentiations and/or similarities of circulating and tonsillar Tfh.

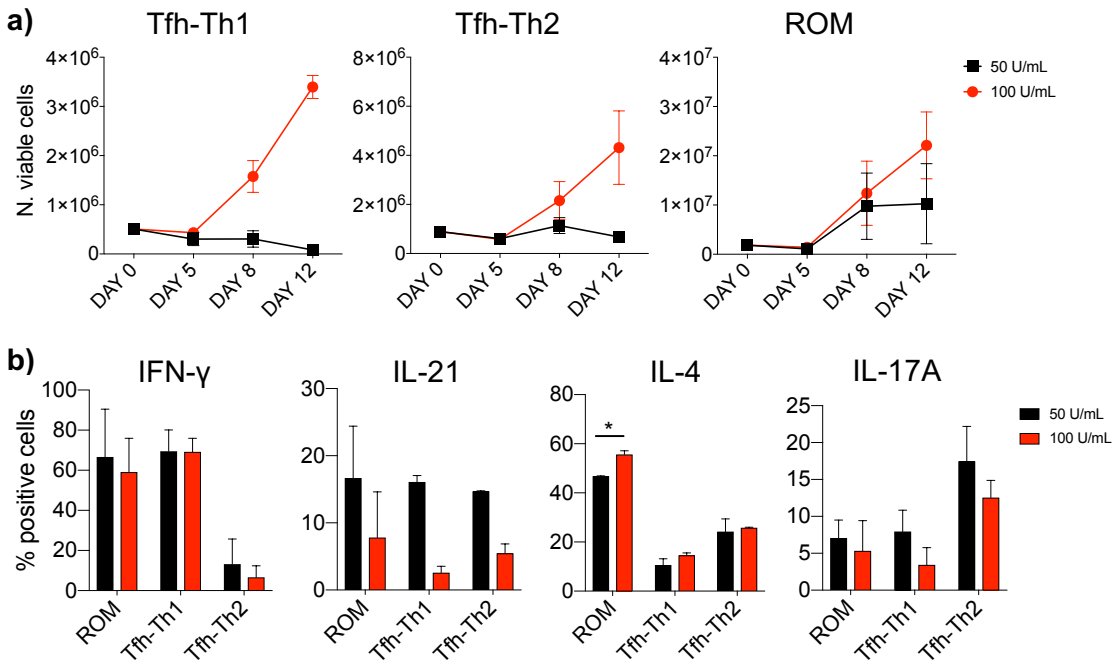


Figure 6.1 Cell culture growth and cytokine profile during culture.

Three different subsets of $CD4^+$ memory T cells (Tfh-Th1, Tfh-Th2 and ROM) were sorted and expanded in culture for 12 days with either 100 U/mL (red) or 50 U/mL (black) of IL-2. (**a**) The number of viable cells in culture was evaluated at day 0, 5, 8 and 12 in 2 wells per condition. (**b**) At day 12 each T cell population was checked for the ability to produce cytokines (IFN-γ, Il-21, IL-4 and IL-17A) after 5 hours of PMA/Ionomycin stimulation and intracellular cytokine staining. In each graph mean and SEM are indicated, *P<0.05, **P<0.01, ***P<0.001, ****P<0.0001.

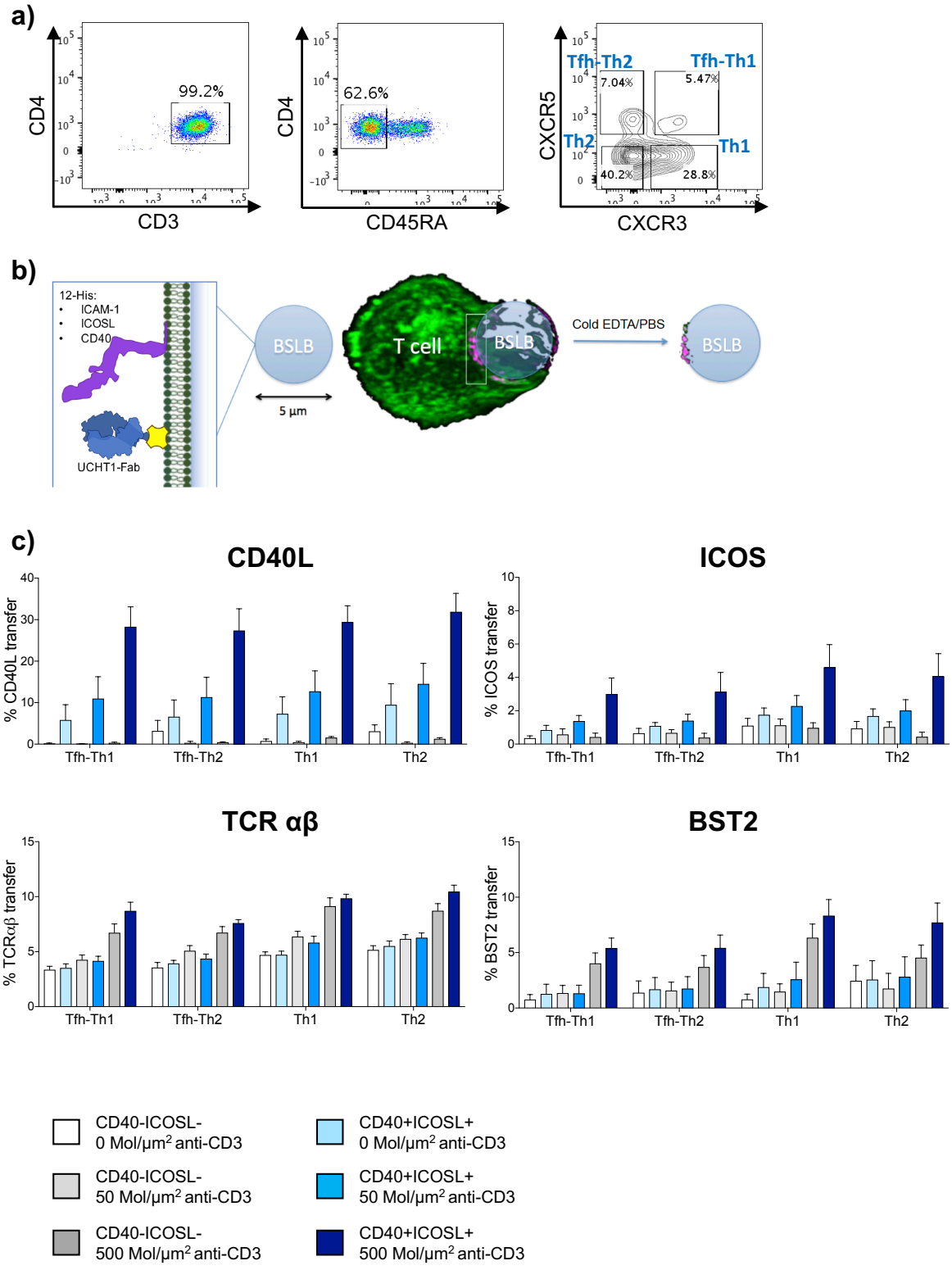

a)
CD4
CD3
99.2%
CD4
CD45RA
62.6%
CXCR5
CXCR3
Tfh-Th2
Tfh-Th1
Th2
Th1
7.04%
5.47%
40.2%
28.8%
b)
12-His:
ICAM-1
ICOSL
CD40
UCHT1-Fab
BSLB
5 µm
T cell
BSLB
Cold EDTA/PBS
BSLB
c)
CD40L
% CD40L transfer
ICOS
% ICOS transfer
TCR αβ
% TCRαβ transfer
BST2
% BST2 transfer
Tfh-Th1
Tfh-Th2
Th1
Th2
CD40-ICOSL-
0 Mol/µm² anti-CD3
CD40+ICOSL+
0 Mol/µm² anti-CD3
CD40-ICOSL-
50 Mol/µm² anti-CD3
CD40+ICOSL+
50 Mol/µm² anti-CD3
CD40-ICOSL-
500 Mol/µm² anti-CD3
CD40+ICOSL+
500 Mol/µm² anti-CD3

Figure 6.2 Microvesicle transfer of Tfh and non-Tfh cells after anti-CD3/anti-CD28 expansion.

(**a**) The sorting strategy illustrated $CD3^+CD4^+$ memory T cells sorted into Tfh-Th1 ($CXCR5^+CXCR3^+$), Tfh-Th2 ($CXCR5^+CXCR3^-$), Th1 ($CXCR5^-CXCR3^+$) and Th2 ($CXCR5^-CXCR3^-$). T cells were then expanded for 12 days in the presence of soluble beads anti-CD3/antiCD28 and 100 U/mL of IL-2. (**b**) A schematic view of silica beads-supported lipid bilayer (BSLB) methodology is illustrated. (**c**) At day 12 the molecules analysed (CD40L, ICOS, TCR αβ and BST2), transferred on silica beads, were measured in percentage (%) after flow cytometry staining. BSLB were previously coated with lipid bilayer, CD40 and ICOSL, and different concentration of anti-CD3 (0, 50, 500 Mol/μm^2). The background is visible in the condition of $CD40^-ICOSL^-$. Mean and SEM are indicated.

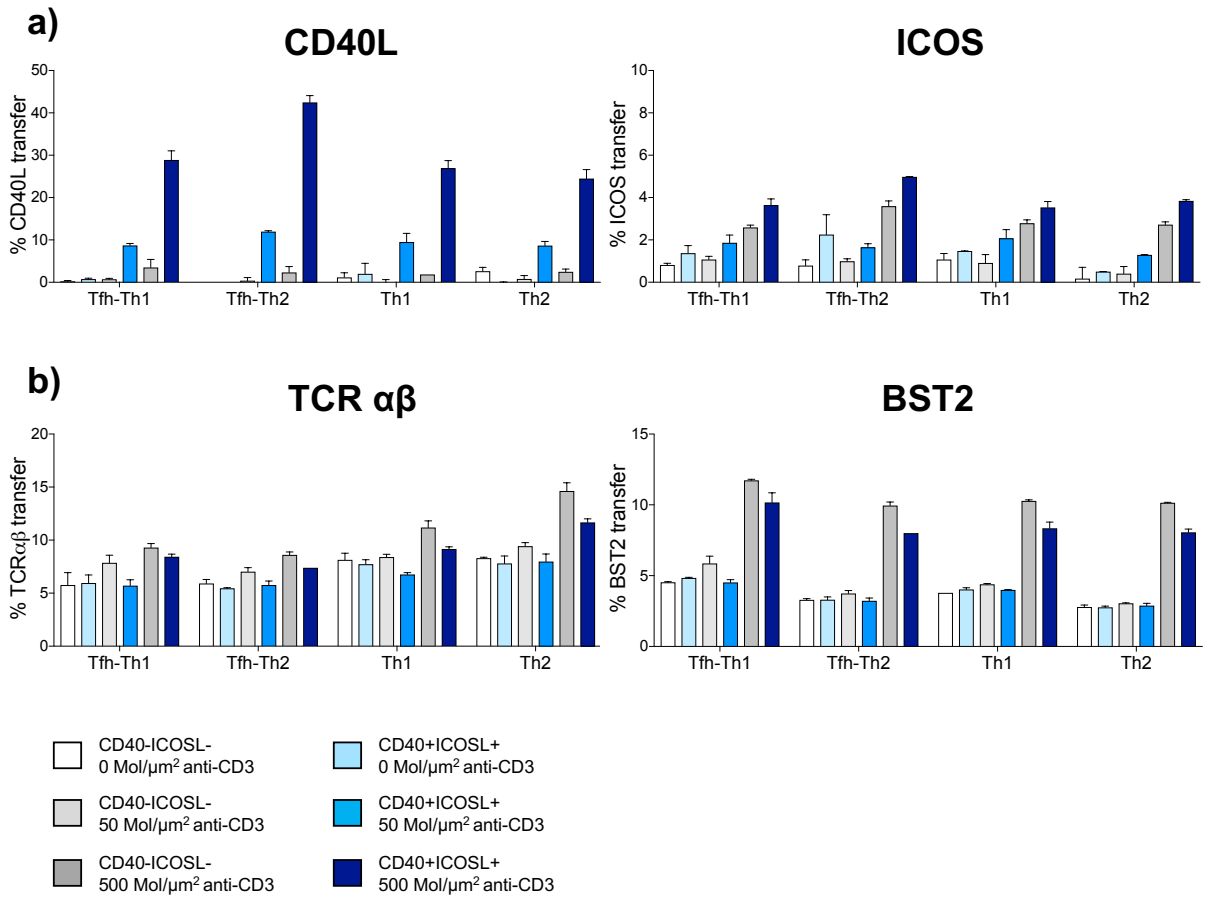


Figure 6.3 Microvesicle transfer of Tfh and non-Tfh cells after co-culture with autologous B cells.

$CD4^+$ memory T cells were sorted into Tfh-Th1, Tfh-Th2, Th1 and Th2 and expanded for 12 days in the presence of autologous B cells stimulated with 1 μg/mL of SEB. At day 12 the transfer of (**a**) CD40L and ICOS and (**b**) TCR αβ and BST2 on silica beads, were measured in percentage (%) after flow cytometry staining. BSLB were previously coated with lipid bilayer, CD40 and ICOSL, and different concentration of anti-CD3 (0, 50, 500 Mol/μm^2). The background is visible in the condition of $CD40^-ICOSL^-$. Mean and SEM are indicated.

6.3 Determination of avidity and HLA restriction of antigen-specific Tfh and non-Tfh cell clones generation

Microvesicle transfer experiments described in the previous section were performed after general stimuli such as anti-CD3 and SEB stimulations. The BSLB optimisation was fundamental to consider the feasibility of this technique in an antigen-specific system. Antigen-specific Tfh and non-Tfh cells could behave differently and the peptide avidity of different clonotypes could also play a role in the generation of immunological synapses. For these reasons, we aim to compare microvesicle trafficking in immunological synapses formed with either high or low avidity antigen-specific Tfh and non-Tfh clones. We opted to use Haemagglutinin protein (HA) as antigen from Influenza virus Wisconsin/67/2005, which is one of the most frequent seasonal infections and to pursue the study on Tfh-Th1 enrichment showed in the previous sections. The stimulus anchored in the lipid bilayer would then be a peptide-HLA monomer, rather than anti-CD3 (UCHT1), that would stimulate only TCR-specific clonotypes. For these reasons, circulating antigen-specific Tfh and non-Tfh clones were generated, from which the peptide avidity was evaluated and the HLA class II restriction determined.

Having shown in previous sections that influenza-specific Tfh are readily identifiable in the circulating and germinal centre Tfh populations we kept with influenza as a model antigen for this study. HA/Wisconsin-specific $CD4^+$ memory T cells Tfh-Th1, Tfh-Th2 and ROM were detected and calculated with the T cell library method in 4 healthy blood donors from previous section (see section 5.3). HA-specific T cell clones were generated from HA-specific T cell lines isolated with the library

technique, using the same approach already explained in detail in section 5.4: T cell lines were stimulated with irradiated autologous monocytes, pulsed with HA/Wisconsin peptides. After 7 days, activated $CD4^+$ T cells were identified as $ICOS^+CD25^+$, FACS sorted (panel D, Figure 2.5) and seeded at 0.4 cell/well. T cell clones were expanded in culture with irradiated allogeneic feeder cells, IL-2 and PHA and after 10 days were re-screened for their specificity to the same pool of peptides in order to exclude T cell clones selected for the initial bio-standard activation. The table (**Figure 6.4 a**) shows the number of HA-specific $CD4^+$ T cell clones generated from each donor (A, B, C and D) derived from Tfh-Th1 or ROM subsets. Unfortunately, the low number of HA-specific Tfh-Th2 clones, mainly detected from donor B, did not grow well in culture and did not survive for any further analysis. The graph (**Figure 6.4 b**) illustrates the cloning efficiency, so the percentage of T cell clones that confirmed the specificity after cloning expansion. The low number of HA-specific Tfh-Th1 clones generated from donor A and the low number of ROM clones for both donors A and D was in line with a poor Tfh-Th1 and ROM cloning efficiency respectively. HA-specific Tfh-Th1 and ROM clones from donors B and C, which had the highest viability in culture, were then mapped at the peptide level using a 3-dimensional matrix from HA/Wisconsin overlapping peptides and either the proliferative (3H-thymidine) or a IFN-γ response (ELISpot) was measured to determine the peptide specificity (see section 2.5 and Supplementary **Figure 8.2** for peptide sequences). To evaluate the avidity, mapped Tfh-Th1 clones in orange (**Figure 6.4 c, e**) and ROM clones in grey (**Figure 6.4 d, f**) were stimulated with different concentrations of peptide and the proliferative response was measured with [3H]-thymidine incorporation. Each graph visualizes

the response of exemplify T cell clones specific for the same peptide in donor B (**Figure 6.4 c, d**) and donor C (**Figure 6.4 e, f**). The peptide responses are standardized on the maximum response per clone. From all the four graphs is clear the exponential augment of the response (on the y-axis) with the increase of the peptide concentration (on the x-axis). 85 % of the clones analysed showed a curve which reached a plateau of response at different concentration of peptide tested. For a few of the clones it was not possible to evaluate whether the response was maximum, since they did not reach the plateau (eg ROM_2 and ROM_3 in donor C) so further experiments will focus on stimulate clones with a broader range of peptide concentration, however care will need to be taken that DMSO toxicity does not affect results from higher concentrations. For the clones that reached a saturated response, it was possible to calculate the effective concentration related to the 50% of the maximum response (EC50, μMol), which was higher for clones with low avidity to the peptide and lower for clones with higher avidity (**Figure 6.4 g**). The EC50 was determined from mapped Tfh-Th1 and ROM clones in donors B and C and in particular for clones specific for the same peptide. We identified Tfh-Th1 clones which responded differently at the different range of the same peptide concentration and so generated a different EC50 (eg peptide 11). Moreover, the EC50 was compared between Tfh-Th1 and ROM clones specific for the same peptide and although the difference was not significant due by the low number of clones tested, the comparison suggested a trend of 5 ROM clones out of 7 with higher EC50 compared with Tfh-Th1 clones, and so a lower avidity for ROM clones compared with Tfh-Th1 specific for the same peptide.

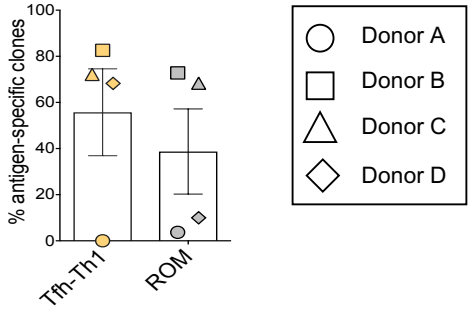
Based on the HLA type profile of the donors considered (**Figure 6.5 a**), we determined the HLA restriction of HA-specific $CD4^+$ memory T cell clones from donors B and C using fibroblast cell lines transfected with a single HLA-DR molecule to present peptide (see sections 2.9.1 and 2.9.2). For donor B, who carried the alleles *HLA-DRB1-1 15:01* and *DRB1-2 03:01*, T cell clones were stimulated with fibroblast expressing either *HLA-DR 15:01* or *03:01*, previously pulsed with the peptide (**Figure 6.5 b**), while for donor C, who carried the alleles *HLA-DRB1-1 15:01* and *DRB1-2 07:01*, clones were stimulated with fibroblast expressing either *HLA-DR 15:01* or *07:01* (**Figure 6.5 c**). T cell responses were detected by ELISpot and for each experiment, a positive control with PHA and a negative control with DMSO was performed. The bar graphs (**Figure 6.5 b, c**) show an example of the 25 clones analysed per donor. In donor B, 5 Tfh-Th1 clones specific for peptide 47 were restricted by HLA-DRB1 03:01 and 5 Tfh-Th1 clones specific for peptide 55 were restricted by HLA-DRB1 15:01. In donor C, 11 Tfh-Th1 clones specific for peptide 74 were restricted by HLA-DRB1 15:01 and 5 Tfh-Th1 clones specific for peptide 82 were restricted by HLA-DRB1 07:01. The clones tested for the restriction are only few of the clones generated per donor and mainly Tfh-Th1 clones have been tested because these were the clones that expanded best in culture and so sufficient cell numbers were available for analysis. In the future by using frozen PBMC remaining from those donors or from other donors with similar HLA profile, it will be possible to generate and screen more clones specific for those peptides. Identifying the molecule of HLA class II involved in the presentation of specific peptides was necessary for the production of peptide-HLA monomer constructs by the NIH Tetramer Core Facility. In the table (**Figure 6.5 d**) are listed the monomers that were

produced and the respective clip peptide as the control peptide. One of the monomers, HLA-DRB15-p74, was tested with a peptide 74-specific Tfh-Th1 clone to validate the feasibility of the BSLB assay with a T cell clone (**Figure 6.5 e**). The transfer of TCR αβ was evaluated using different ratios of beads:cells (2:1, 1:1, 1:2) coated with CD40 and ICOSL, and different concentrations of molecules on the surface (0, 50, 500 Mole/μm^2). The clip peptide (class-II associated invariant chain peptide) and anti-CD3 (UCHT1) were used as negative and positive controls respectively. The transfer background was performed with beads coated with ICAM-1 only, CD40–ICOSL–. The optimisation showed the 1:2 ratio of beads:cells as the best condition for microvesicles transfer (7 %) and a lower background with the clip peptide too. Future experiments will focus on testing high and low avidity T cell clones using the same assay and describing the microvesicle trafficking of different molecules, such as TCR αβ, CD40L, ICOS and BST2. An interesting aspect will also be the comparison of microvesicle release between antigen-specific clones from different $CD4^+$ T cell subsets and from different compartments, for instance tonsil and blood.

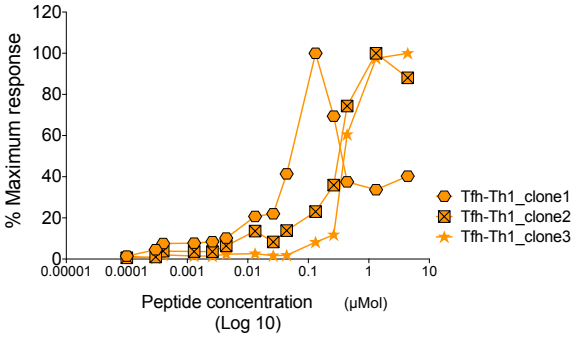
a)

DONOR ID	Tfh-Th1	ROM
A	1	27
B	202	103
C	183	98
D	85	10

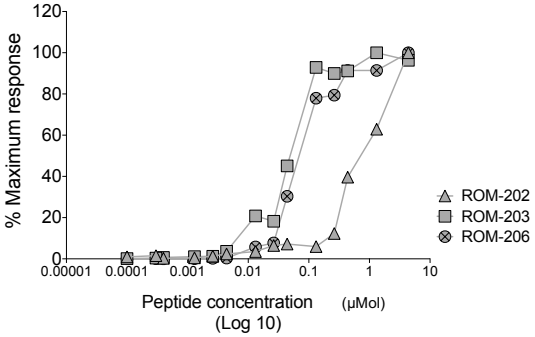
b) Cloning efficiency



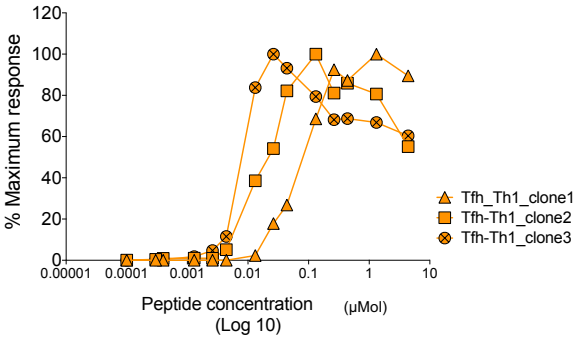
c) Donor B



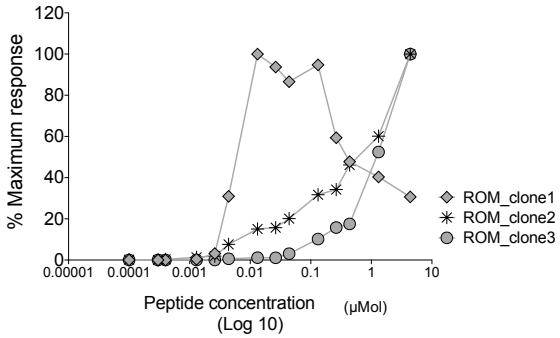
d)



e) Donor C



f)



g)

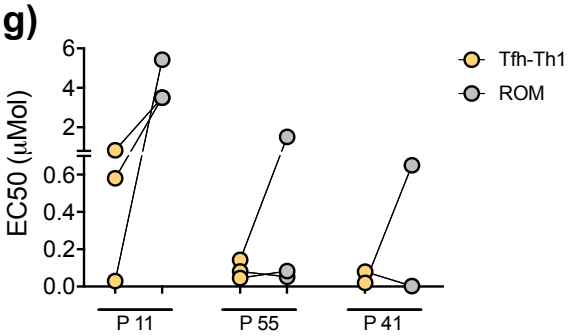


Figure 6.4 Generation of HA-specific T cell clones and determination of the peptide avidity.

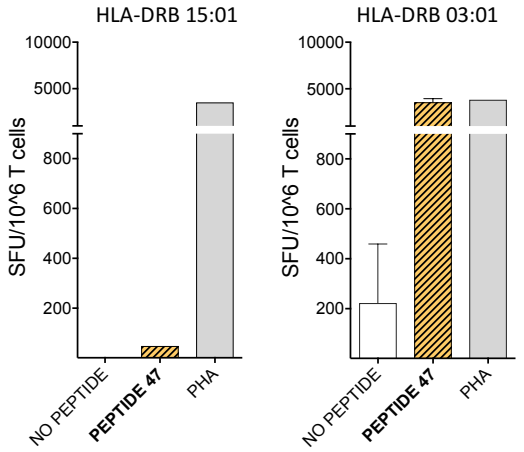
HA-specific Tfh-Th1 and ROM clones were generated from HA- positive lines derived from the T cell library method of 4 healthy blood donors. The table (**a**) shows the number of HA-specific $CD4^+$ memory T cell clones generated from each of the 4 donors derived from either Tfh-Th1 or ROM populations after stimulation with overlapping peptides of HA/Wisconsin and irradiated autologous monocytes. The graph (**b**) represents the cloning efficiency for each subset by percentage of HA-specific clones that confirmed the specificity after expansion. Data are presented with mean and SEM and each donor is represented with a different symbol. HA-specific clones are stimulated with different concentration of the peptide. From donor B, (**c**) 3 of Tfh-Th1 clones specific for peptide 55 and (**d**) 3 ROM clones specific for peptide 55 are shown. From donor C, (**e**) 3 of Tfh-Th1 clones specific for peptide 74 and (**f**) 3 ROM clones specific for peptide 74 are shown. The peptide responses are standardized on the maximum response per clone. The EC50 (μMol) was calculated and clones with the same peptide specificity, Tfh-Th1 (yellow) and ROM (grey), were plotted in correlation to each other. On the x-axis are listed the peptides recognized by the clones (peptides 11, 55, 41).

a)

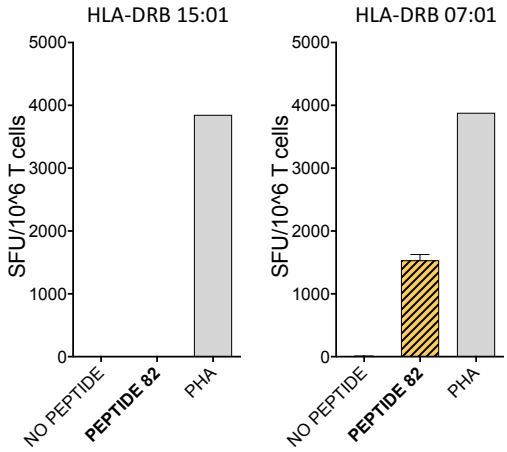
DONOR ID	A1	A2	B1	B2	Cw1	Cw2
A	01:01/04N	03:01	07:02	08:01	07:01	7:02
B	01:01/04N	03:01	27:05	56:01	07:01	7:02
C	03:01	24:02	07:02	08:01	07:01	7:02
D	01:01	68:02	08:01	27:03	02:02	7:02

DONOR ID	DRB1-1	DRB1-2	DRB345-1	DRB345-2	DQB1-1	DQB1-2
A	15:01	03:01	DRB3	DRB5	02	06:02
B	15:01	03:01	DRB3	DRB5	02	06:02
C	15:01	07:01	DRB5	DRB4	02	06:02
D	03:01	07:01	DRB3	DRB4	02	02

b) Donor B: Tfh-Th1 clone



c) Donor C: Tfh-Th1 clone



d)

MONOMER	PEPTIDE SEQUENCE	PEPTIDE ID
HLA-DRB1 03:01	**SGKSSIMRSDAPIGKCN**	**47**
HLA-DRB1 03:01	PVSKMRMATPLLMQA	clip
HLA-DRB1 07:01	**GCFKIYHKCDNACIGSI**	**82**
HLA-DRB1 07:01	PVSKMRMATPLLMQA	clip
HLA-DRB1 15:01	**KIDLWSYNAELLVALEN**	**74**
HLA-DRB1 15:01	PVSKMRMATPLLMQA	clip

e)

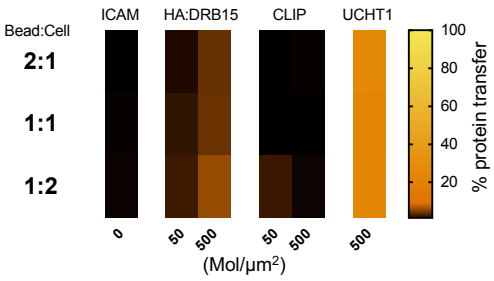


Figure 6.5 HLA restriction of HA-specific T cell clones and monomer check.
(**a**) HLA genes of class I and class II expressed by the 4 donors are listed in the table. The HLA-DR restriction of mapped HA-specific $CD4^+$ T cell clones was determined using fibroblast cell lines transfected with a single HLA-DR molecule, pulsed with the peptide and the T cell response was detected by ELISpot (SFU=spot forming units). Two examples of (**b**) HLA-DR03-restricted Tfh-Th1 clone from donor B and a (**c**) HLA-DR07-restricted Tfh-Th1 clone C are shown. PHA and DMSO were used as positive and negative controls respectively. Bars represent the mean and SEM. The table lists the monomers received from the NIH Tetramer Core Facility (**d**): HLA-DR, peptide sequence and peptide ID are shown. (**e**) The monomer HLADR15-peptide74 was tested using a p74-specific-Tfh-Th1 clone from donor C at different ratios of beads:cells and the transfer of TCR αβ was measured. BSLB was coated with CD40 and ICOSL, and different concentrations of molecules on the surface (Mol/μm^2). The clip peptide and anti-CD3 (UCHT1) were used as negative and positive controls respectively. ICAM-1 only, CD40–ICOSL– was considered as background.

6.4 T and B cell co-culture

For a more comprehensive analysis of Tfh cell function, in parallel with the microvesicle trafficking, the activity of a cTfh cell in the presence of B cells was evaluated using *in vitro* co-culture assays. Although the capacity of circulating Tfh cells ($CXCR5^+$) to help B cell class switched antibodies and to sustain B cell survival has already been studied in detail (He et al., 2013; Locci et al., 2013; Morita et al., 2011), the aim of this study build upon these observations was to compare different populations of circulating and tonsillar Tfh cells function in an antigen specific environment.

Co-culture experiments needed to be optimised for conditions and for the markers of interest. For this reason, $CD4^+$ memory T cells from 2 healthy blood donors were sorted into Tfh ($CXCR5^+$) and non-Tfh ($CXCR5^-$). T cells were co-cultured at a 1:1 ratio with sorted autologous naïve ($CD19^+CD27^-$) and memory ($CD19^+CD27^+$) B cells stimulated with 1μg/mL of SEB (see section 2.11). For each co-culture condition, a negative control was included of Tfh cells in the absence of SEB, with SEB pulsed B cells. B and T cell activation was checked at days 2 and 5 of co-culture. CD40, ICOSL and CD86 expression were checked by flow cytometry (panel I, Figure 2.5) and at day 2 the upregulation of all the 3 markers was observed when both naïve and memory B cells were in co-culture with Tfh cells; naïve B cells were only activated after co-culture with non-Tfh cells (**Figure 6.6 a**). A similar scenario was observed for T cell activation ($ICOS^+CD38^+$): Tfh cells in co-culture with both naïve (80 %) and memory (50 %) B cells expressed a high level of ICOS and CD38, while non-Tfh were activated (with 60 % of $ICOS^+CD38^+$ cells) only in the presence of naïve B cells (**Figure 6.6 b**). Tfh cells co-stimulatory signals and cytokine production are essential elements for B cell survival in the germinal centre (Liu et al., 1989; Okada et al., 2005). Both T and B cell activation could be explained by the cell survival, monitored at day 5 by using Absolute Counting Beads (TermoFisher) from the live cells gated in either B cells or T cells at the flow cytometry (**Figure 6.6 c**). Naïve B cells showed a better viability in co-culture with both Tfh and non-Tfh compared to memory B cells. Viable memory B cells were only detected in co-culture with Tfh cells and notably not with non-Tfh $CD4^+$ T cells. Moreover, in the absence of T cells (either Tfh or non-Tfh cells) naïve B cells survived for longer in culture than memory B cells. Although no significant difference was reported for this

preliminary experiment, Tfh cells showed a higher viability (4400 cell/well) compared to non-Tfh cells (2200 cell/well) also in co-culture with naive B cells. As described already in the introduction of this chapter (section 6.1), during the formation of an immunological synapses molecules are transferred between the contacting T and B cells (Choudhuri et al., 2014; Dustin, 2014a). This transfer of molecules is therefore a relevant aspect to monitor during an *in vitro* T and B cell co-culture experiment and we focused upon the transfer of TCR, CD40L and ICOS, which are commonly considered as molecules present of the T cell surface. Using flow cytometry both the intracellular and the extracellular detection of these molecules were analysed on naïve and memory B cells (**Figure 6.6 d**). The molecule transfer for all the 3 markers considered, confirmed the synapses between naïve cells and either Tfh or non-Tfh cells. ICOS was mainly found in memory B cells in co-culture with Tfh cells, in line with microvesicle trafficking from section 6.2, while TCR showed a notable transfer also during non-Tfh and B cells co-culture (4,000-12,000 MFI). CD40L showed a trend similar to CD40 expression: the molecule transfer was observed for in both naïve and memory B cells co-cultured with Tfh cells, but with non-Tfh cells co-culture CD40L was found only in naïve B cells. One of the most important properties of Tfh cells, confirmed also for circulating Tfh, is to induce class-switch to B cells (Vinuesa and Cook, 2011). To assess this, levels of IgG, IgA and IgM were then evaluated by ELISA in the supernatant of T and B cell co-cultures at days 7 and 10 (**Figure 6.6 e**). This experiment confirmed the unique capacity of Tfh cells to activate B cells, since a higher level of IgG, IgA and IgM was detected for B cells only in co-cultured with Tfh cells. Memory B cells were producing higher level of antibodies, IgG (2,400 pg/ml) and IgA (1,600 pg/ml) after

7 days of co-culture, compared to naïve B cells (IgG=90 pg/ml and IgA=34 pg/ml). A similar level of IgM was detected at day 7 from Tfh cells in co-culture with naïve (IgM= 460 pg/ml) or memory B cells (IgM= 1930 pg/ml), underlying the difficulties to discriminate between class switch or rather a general B cell activation event. This first co-culture experiment tested the feasibility of using T and B cell co-culture techniques and future experiments will go on to evaluate the differences between different subsets of circulating and tonsillar Tfh cells using this system.

In order to apply the co-culture system in an antigen-specific context and to evaluate whether TCR avidity could play a role for the quality of B cell contact, influenza-specific T cell clones of known avidity were co-culture with autologous B cells. Two Tfh-Th1 clones with different avidity (EC50) for peptide 55 (from HA/Wisconsin protein), Tfh-Th1_118=0.15 μMol and Tfh-Th1_121=4.2 μMol respectively from donor B, were co-cultured with sorted autologous total B cells ($CD19^+$) at a 1:1 ratio (**Figure 6.7**). B cells were pulsed with either 0.5 μg/mL or 10 μg/mL of the whole HA/Wisconsin protein and a condition with no antigen was used as negative control. B cell (CD40, ICOSL and CD86, **Figure 6.7 a**) and T cell (ICOS and CD38, **Figure 6.7 b**) activation marker expression was evaluated after 4 days of co-culture by flow cytometry (panel L, Figure 2.5). The activation of both B and T cells was slightly raised with the increasing of HA protein concentration, but no statistical difference was detected between co-culture with either the high or low avidity clone. Intracellular cytokine staining showed that the transfer of TCR and ICOS to B cells at day 6 of co-culture increased as the concentration of HA increased, but there was no statistical difference on the quantity of the signal between the two different clones analysed (**Figure 6.7 c**). This is a pilot study and further experiments with higher

numbers of clones with a greater range of avidities are required to confirm this result. Finally, level of IgG, IgA and IgM was evaluated in the supernatant after 7 and 10 days of co-culture (**Figure 6.7 d**). Interestingly B cells in co-culture with high avidity Tfh-Th1 clone produced a higher level of the 2 class-switched Ig antibodies analysed at day 7 (IgG= 900 pg/mL, IgA= 1750 pg/mL) as well as a higher level of IgM= 1100 pg/mL, compared with low avidity clone (IgG= 75 pg/mL, IgA= 90 pg/mL, IgM= 190 pg/mL). To better evaluate the T cell competition during B cell help and because there was no difference on the T and B cell activation between the 2 clones at the lowest concentration of HA (0.5 μg/mL), Ig detection was only performed for the condition with HA at 0.5 μg/mL. Although the B cells considered were not selected to be HA-specific, B cell activation could be attributed to a BCR-specific recognition and so to the actual antigen processing rather than to the help received from the T cell side.

To better define B cell survival and activation due by the T cell role, future co-culture experiments will focus on performing similar T and B cell system using directly peptides rather than HA protein, and therefore avoid the antigen process from the B cell. Experiments are in progress to titrate down the concentration of peptide presented by the B cells to create an antigen competition environment.

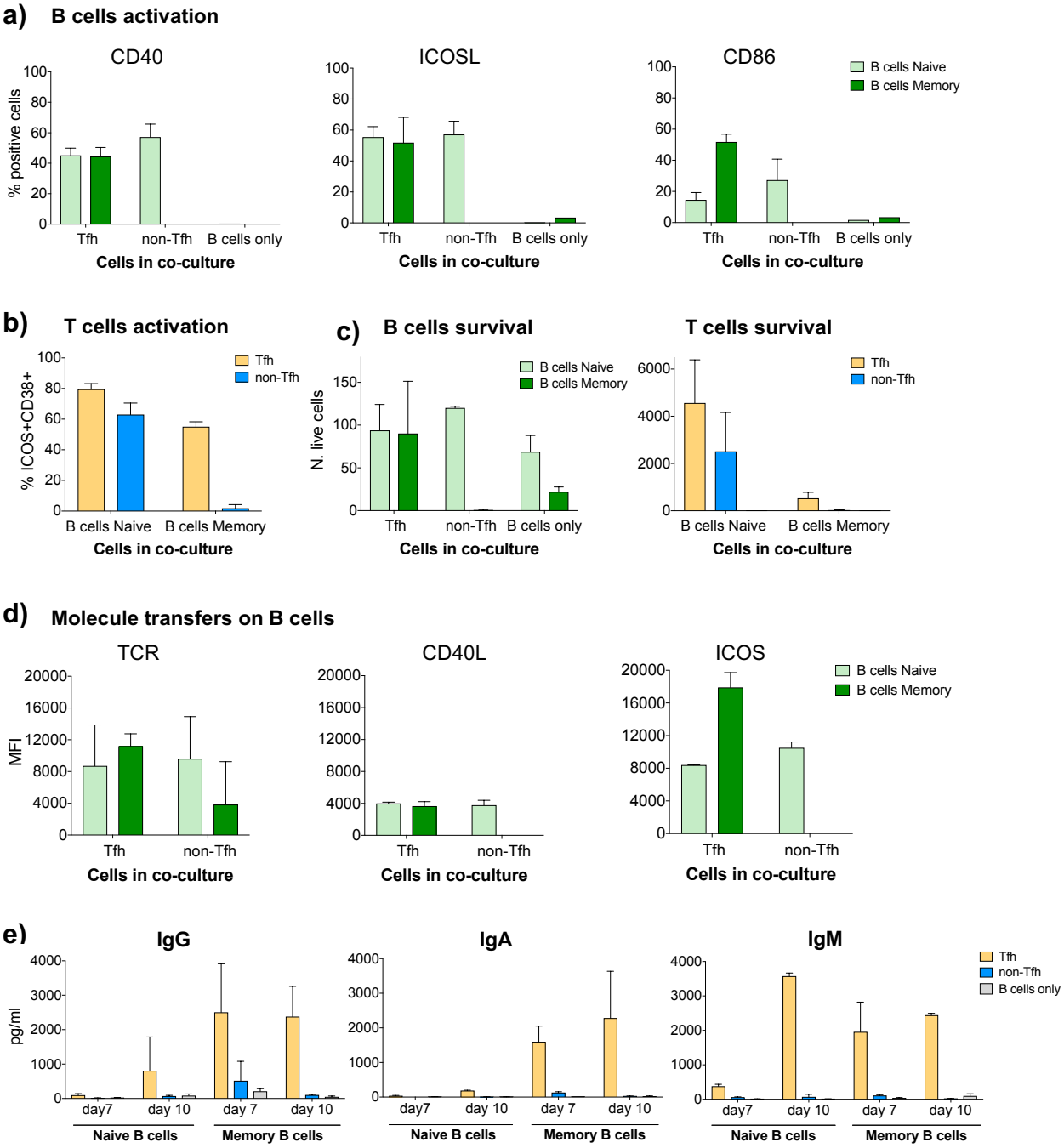

a) B cells activation
CD40
ICOSL
CD86
% positive cells
B cells Naive
B cells Memory
Tfh
non-Tfh
B cells only
Cells in co-culture
b) T cells activation
% ICOS+CD38+
Tfh
non-Tfh
B cells Naive
B cells Memory
Cells in co-culture
c) B cells survival
N. live cells
T cells survival
d) Molecule transfers on B cells
TCR
CD40L
ICOS
MFI
e)
IgG
IgA
IgM
pg/ml
day7
day 10
day 7
Naive B cells
Memory B cells

Figure 6.6 Tfh and non-Tfh cell co-culture with naïve and memory B cells.
$CD4^+$ memory T cells from 2 healthy blood donors were sorted into Tfh ($CXCR5^+$) and non-Tfh ($CXCR5^-$) cells and co-culture at 1:1 ratio with sorted autologous naïve ($CD19^+CD27^-$) and memory ($CD19^+CD27^+$) B cells, pulsed with 1μg/mL of SEB. (**a**) B cell (CD40, ICOSL, CD86) and (**b**) T cell (ICOS, CD38) activation markers were detected by flow cytometry at day 2 and expressed in percentage of positive cells (%).(**c**) Number of live cells were counted at day 5 by using Absolute Counting Beads from the live cells gate in either B cells or T cells at the flow cytometry. (**d**) T cell molecule transferred (TCR, CD40L and ICOS) at day 5 on the B cells were identified after both surface and intracellular staining and analysed as Mean Fluorescence Intensity (MFI). (**e**) IgG, IgA and IgM production (pg/mL) was detected by ELISA in the supernatant after 7 and 10 days of co-culture. Bar graphs represent the mean and SEM.

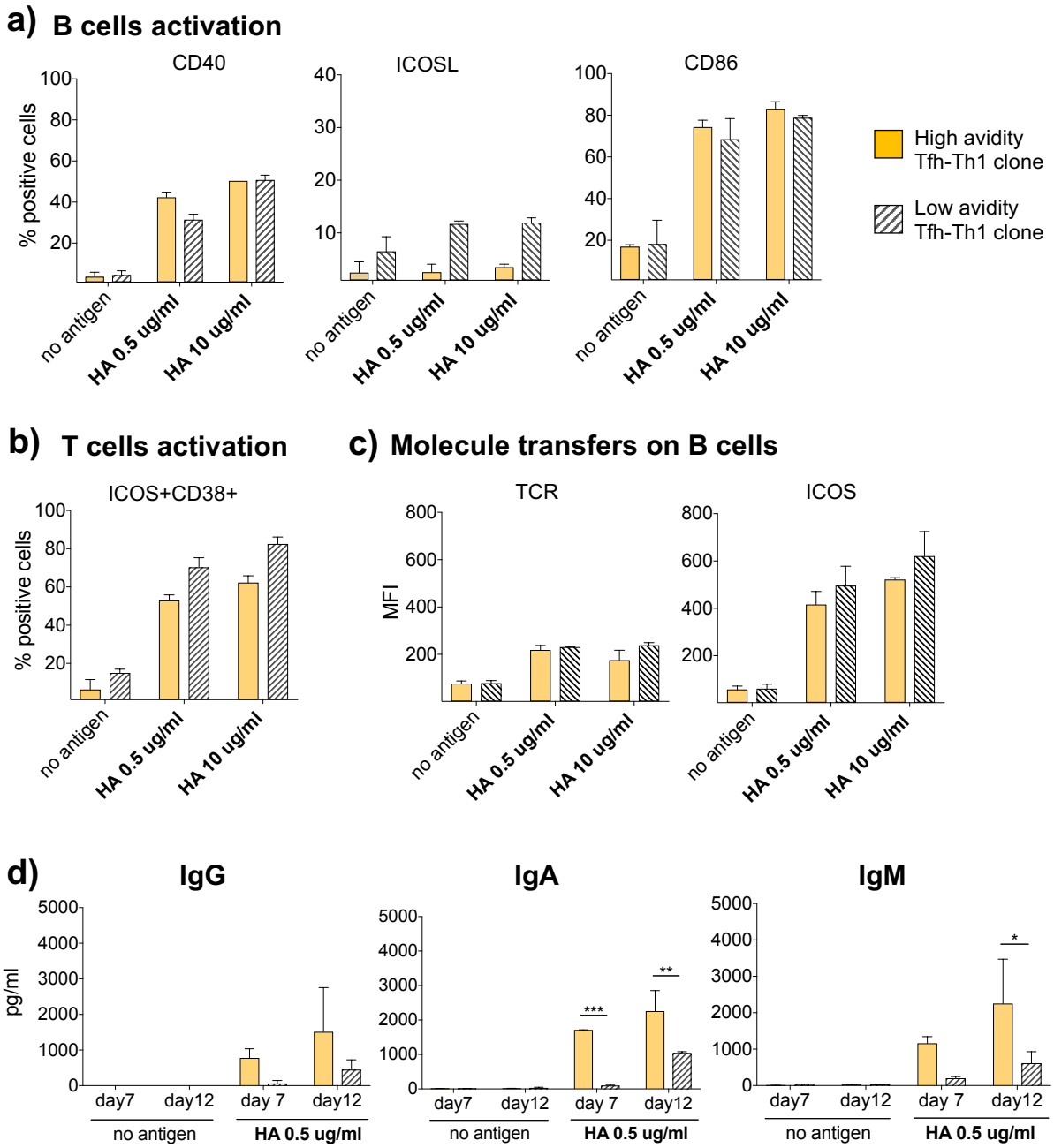

a) B cells activation
CD40
ICOSL
CD86
% positive cells
High avidity Tfh-Th1 clone
Low avidity Tfh-Th1 clone
no antigen
HA 0.5 ug/ml
HA 10 ug/ml
b) T cells activation
ICOS+CD38+
c) Molecule transfers on B cells
TCR
ICOS
MFI
d)
IgG
IgA
IgM
pg/ml
day7
day12
day 7
day12
no antigen
HA 0.5 ug/ml
***
**
*

Figure 6.7 High and low avidity Tfh-Th1 clones provide different help to total B cells in co-culture.

Two Tfh-Th1 clones from donor B, with different avidity to the same peptide 55 (high avidity clone=0.15 μMol and low avidity clone=4.2 μMol) were co-cultured with sorted autologous B cells ($CD19^+$). B cells were pulsed with either 0.5 or 10 μg/mL of the whole HA/Wisconsin protein, a condition with no antigen was used as negative control. (**a**) B cell (CD40, ICOSL, CD86) and (**b**) T cell (ICOS, CD38) activation markers were detected by flow cytometry at day 4 and expressed in percentage of positive cells (%).(**c**) T cell molecules (TCR and ICOS) transferred at day 6 on the B cells were identified after both surface and intracellular staining and analysed as Mean Fluorescence Intensity (MFI). (**d**) IgG, IgA and IgM production (pg/mL) was detected by ELISA in the supernatant after 7 and 12 days of co-culture for the 0.5 μg/mL HA protein condition only. Bar graphs represent the mean and SEM.

6.5 Conclusions

Data shown in this section were important to evaluate the feasibility of different techniques that will help the understanding of the quality and the quantity of Tfh signals during an immune synapse.

Preliminary studies demonstrated the possible application of the beads-supported lipid bilayer (BSLB) methodology, developed by Professor Michael Dustin and his team (Saliba et al., unpublished personal communication), to study primary circulating Tfh and non-Tfh cells. The trafficking of different molecules, such as CD40L, ICOS, TCR and BST2, in artificial immune synapses is a unique and informative way to study the function of different subsets of Tfh cells. Although in this model T cells alone with multiclonal TCR stimulation with anti-CD3 did not reveal a significant difference between Tfh and non-Tfh cell populations, it is

encouraging that in co-culture with B cells Tfh-Th2 cells showed a better release of CD40L- and ICOS-enriched microvesicles during an immune synapse (section 6.2). Future experiments will focus on molecule trafficking comparisons between blood cTfh and matched tonsillar Tfh cells, with or without co-culture with autologous B cells.

There is however some artificiality of this *in vitro* technology and it will be necessary to study a more natural TCR-peptide:MHC synapse, by investigating the same phenomenon in an antigen-specific system. Further applications of the BSLB in an antigen-specific manner, could clarify the poorly understood role of the Tfh avidity in the T-B cell contact. Tfh-GC cells differentiation is promoted by persistent peptide:MHC presentation by B cells, but how Tfh cell avidity influences the function and the signals in the immune synapses is still unknown (Tubo and Jenkins, 2016). Rather than a general anti-CD3 stimulus, a peptide-HLA monomer anchored in the lipid bilayer would induce a more specific signal. It would then be possible to study how extracellular microvesicles release is influenced by different peptide TCR affinities. For these reasons, circulating HA-specific Tfh and non-Tfh clones with different avidity were generated and the HLA class II restriction was determined (section 6.3). Unfortunately, it was beyond the scope of this thesis to directly evaluate the role of avidity in the immune synapses, but preliminary experiments confirmed the feasibility of this approach with primary antigen-specific Tfh clones with different avidity. Parallel preliminary experiments on T and B cell co-culture did reveal an interesting and unique help coming from a high avidity Tfh-Th1 clone (EC50=0.15 μMol), compared with a low avidity clone (EC50= 4.2 μMol). A Tfh-Th1 clone with a higher avidity activated better autologous B cells on producing

IgG, IgA and IgM. In contrast, detection of activation markers and molecule transfer by flow cytometry was not sensitive enough to distinguish a different quality of help between the two clones. The high level of B cell activation in fact might have been induced not only by the T cells, but mainly by the antigen processing, since the whole HA protein was used as antigen. Peptides, instead of whole protein, will not need to be processed by B cells and do not need an antigen-specific BCR to be loaded on the MHC-class II. Therefore, using peptides in future experiments will help to restrict the B cell read out on the T cell help.

Although most of the results presented in this section were preliminary, it was very important to evaluate the feasibility of different techniques to study the immune synapses with primary Tfh cells and the interesting role of avidity using antigen-specific *in vitro* system will need more investigations.

7 Discussion

The work presented in this thesis describes the repertoire and function of follicular and circulating Tfh and non-Tfh cells in a human cohort, from which donor-matched tonsillar adult tissues and peripheral blood samples were available. Different populations of effector and memory Tfh cells have been previously described in tonsils and blood (Chevalier et al., 2011; He et al., 2013; Locci et al., 2013), but a direct comparison between lymphoid Tfh and peripheral blood Tfh is lacking from the literature, because it is both ethically and technically challenging to obtain lymphoid tissue in human studies.

Using donor-matched tonsil and blood samples, my first aim was to evaluate the composition and the phenotype of memory $CD4^+$ T cells focusing on T follicular markers in both compartments. Using surface phenotyping and functional analysis of circulating and tonsillar mononuclear cells I identified heterogeneous populations of memory $CD4^+$ T cells: effector follicular helper T cells, also called germinal centre Tfh (Tfh-GC) that were only present in tonsil samples; Tfh-like cells with an intermediate follicular phenotype that were present in both tonsils and blood; and a $CXCR5^-$ population that I termed "rest of memory" (ROM) that showed similar features in both tonsil and blood (**section 3.2**). The Tfh-GC cells, identified as $PD\text{-}1^{hi}CXCR5^{hi}$, showed high expression of factors that are characteristic for a follicular helper cell phenotype, and are known to be involved in Tfh cell differentiation, development and function including Bcl-6, ICOS, CCR6, IL-21 and IL-4. None of the circulating Tfh or non-Tfh subsets from peripheral blood of the same donor

showed such a polarized follicular helper phenotype. Tfh-GC cells have been previously described in human tonsil samples. These cells were also found in mouse and macaque lymph nodes as part of the effector germinal centre reaction during an ongoing immune response (Baumjohann et al., 2013; Hansen et al., 2016; Havenar-Daughton et al., 2016). Although donors from our cohort had not received a recent vaccination and had not had an acute severe infection in the weeks immediately prior to surgery, the presence of effector Tfh-GC cells in tonsils suggested a probable ongoing immune response in this tissue. This may have been a recent or an ongoing low grade upper respiratory tract infection. Tonsillectomy is often the therapeutic surgical solution for recurrent chronic viral and bacterial infections. Therefore it was not surprising to detect evidence of an ongoing immune response (Grivel and Margolis, 2009; Rao, 2018).

Intermediate phenotypes of Tfh cells were characterized and identified in both tonsil and blood: Tfh-Th1 (PD-1^{lo}CXCR5^{lo}CXCR3^{+}) and Tfh-Th2 (PD-1^{lo}CXCR5^{lo}CXCR3^{-}). For simplicity I termed the latter Tfh-Th2 in this thesis, although it comprised both Tfh-Th2 (PD-1^{lo}CXCR5^{lo}CXCR3^{-}CCR6^{-}) and Tfh-Th17 (PD-1^{lo}CXCR5^{lo}CXCR3^{-}CCR6^{+}) as previously described (Boswell et al., 2014; Morita et al., 2011). Both surface marker expression (CXCR3^{+}CCR6^{-}) and cytokine secretion (IFN-γ^{+}) highlighted similarities between the Tfh-Th1 cells from tonsil and blood. However, only intermediate Tfh-like Th1 cells from tonsils showed a follicular profile based on the intermediate level of Bcl-6 and ICOS expression.

The phenotypic profiling revealed a variety of Tfh cell phenotypes from different compartments in the same donor, that was fundamental for identifying the populations of interest for this study. The observed heterogeneity of phenotypic

analysis supports findings from previous studies where Tfh-GC and circulating Tfh (cTfh) cell function and profile were compared in non-matched donor samples (Chevalier et al., 2011; He et al., 2013). Together, these data support the notion that Tfh cells have specific phenotypes and functions in different compartments, and that these are driven by stimuli that are present in the respective local environments (Wong et al., 2016). Although cTfh cells show a less pronounced Tfh phenotype, these cells possess similarities to germinal centre Tfh cells since they have the ability to re-acquire a Tfh function in the presence of B cells and to promote class-switching of B cells in *in vitro* assays (**section 6.4**) (Bentebibel et al., 2013; Boswell et al., 2014).

The heterogeneous phenotypes observed in different compartments do not contradict a relationship between the two tissues, but the findings suggested that a different approach was required to directly compare Tfh cells from tonsils and blood. It was therefore necessary to consider a parameter of T cells that does not change with the location, namely the T cell antigen specificity repertoire, which is based on the unalterable expression of the T cell receptor (TCR). The T cell library technique, a well-established method for analysis of circulating $CD4^+$ T cell subsets from PBMC (Campion et al., 2014; Geiger et al., 2009; Lindestam Arlehamn et al., 2013; Mele et al., 2017), was chosen to analyse the Tfh and non-Tfh cell repertoire and specificity after a 20 days polyclonal expansion *in vitro*. I confirmed that the technique was suitable to evaluate the specificity of different subsets of cTfh cells (**sections 3.3** and **5.3**) (Bruno et al., 2016). Unlike peripheral blood cells, tonsillar cells did not survive well in culture. Efforts were made to optimise culture conditions for tonsillar cells, however although improvements were made, these were insufficient to make the T

cell library an appropriate assay to address a repertoire comparison between the two tissues (**sections 3.4**).

General spectratyping of 24 Vβ families of the human TCR repertoire using monoclonal flow cytometry antibodies lacked sufficient sensitivity to compare blood and tonsils $CD4^+$ memory T cell populations and therefore it was not suitable to address our initial question (**section 4.2**). Also, the measurement of the Vβ chain usage would miss important differences in TCR sequence in the CDR3 region that profoundly influence the specificity of T cells. Therefore, a targeted sequence-based high-resolution analysis of the T cell receptor was undertaken to generate a more comprehensive and precise analysis.

In a collaborative effort with Professor Dmitriy Chudakov and his team, TCR deep-sequencing of different subsets of Tfh and non-Tfh cells, highlighted not only a correlation between tonsil and blood, but also that this correlation was found in populations with similar features (**section 4.3**).

Before discussing the major findings, several observations and limiting aspects regarding this part of the project need to be highlighted. First, the absence of any known or planned acute or chronic immune response with different time points of sampling before and after immune response are clear limitations that preclude the study of Tfh cells during an acute and subsequent memory response. Secondly, since the repertoire comparison was performed in selected subsets of T cells defined on the basis of subset-specific markers identified in prior studies, it was not an unbiased analysis. In the future, single cell TCR sequencing might be a better unbiased approach, since no well-established high-throughput techniques for performing this were available at the start of this project. Finally, the size of the sample and the

number of cells sequenced is always a constraint for TCR repertoire studies in humans and therefore poses a caveat requiring technical replicates to help interpret correctly whether a correlation is relevant or not.

Exciting findings from the TCR sequencing analysis revealed that effector Tfh-GC cells from tonsil, together with Tfh-Th2 from the same compartment, showed a small but consistent repertoire overlap with Tfh-Th2 cells from blood. Although a Tfh-GC/Tfh-Th2 relationship between tonsil and blood has been previously observed in terms of gene expression (Locci et al., 2013), this is the first time that it was confirmed at a clonal level using a systemic study of tissues derived from the same donor. That the overlap between Tfh-Th2 cells from blood and both Tfh-GC and Tfh-Th2 cells from tonsils was not more substantial is difficult to explain, but a few hypotheses can be outlined. The poor correlation might be explained by the specific and localized role of Tfh-GC cells during their effector phase of an ongoing local infection and therefore a lower ability to circulate. This hypothesis was supported by the scarcity of IFN-γ production and CXCR3 expression from both Tfh-GC and Tfh-Th2 cells, while in contrast, effector T cells that aim to migrate to inflamed tissues do express these markers (Groom and Luster, 2011b). It is also possible that the peripheral blood Tfh CXCR3^{-} (Tfh-Th2) population has a promiscuous role and therefore resembles and includes circulating T cell populations from different origins: a few antigen-experienced Tfh-GC cells (differentiated in either Th1 or Th2 environments) that during an acute response escape from the germinal centre and may be transiting to another lymphoid structure; antigen-experienced Tfh-like cells with a Th2 phenotype in tonsils before or after becoming effector Tfh-GC (suggested by clonotype sharing between Tfh-GC and Tfh-Th2 cells from tonsil, **section 4.4**);

or memory Tfh cells that are recruited from the periphery in response to local chronic infection (**Figure 7.1**).

The highest clonotype sharing detected from TCR sequencing data was observed between $CXCR5^{-}PD\text{-}1^{-}$ cells from tonsils and $CXCR5^{-}$ cells from blood (both populations also called ROM); and between the antigen-experienced Tfh-Th1 population from tonsils and Tfh-Th1 from blood. These correlations were confirmed in the antigen-specific T cell data where blood derived HA-specific clones were compared with tonsil samples (**section 5.5**). A probable chronic inflammation of tonsil tissues might have favoured the retention or the recruitment of antigen-experienced Tfh and non-Tfh cells after priming by DCs, or after performing an effector function in the same or another germinal centre, that then resulted in a high frequency of those memory cells in the tonsil tissue (Rao, 2018).

ROM cells showed a relatively high level of TCR sequence sharing between the two investigated compartments confirming the communication between tonsil and blood. This suggests a different but not mutually exclusive hypothesis: antigen-experienced $CD4^{+}$ T cells primed in secondary lymphoid organs that differentiate into T helper cells exit to the inflamed tissues into the periphery to pursue their effector function first and then acquire memory function. ROM cells could have also been recruited from the circulation to the tonsil because of a suspected ongoing chronic infection and might be retained in the tissue for this reason.

Tfh-Th1 cells from tonsils, which have an intermediate follicular phenotype just like the Tfh-Th2 cells, might have been primed in a Th1 environment and therefore express CXCR3 and become IFN-γ-producers before entering the effector Tfh-GC phase, whereupon they downregulate CXCR3 and upregulate PD-1, CXCR5 and

ICOS (suggested by clonotype sharing between Tfh-GC and Tfh-Th1 cells from tonsil, **section 4.4**). Antigen-experienced Tfh-Th1 cells in tonsils might also represent memory cells differentiated from effector Tfh-GC, which have been primed initially in a Th1 environment (**Figure 7.1**). As happens with canonical T helper cell differentiation, and in Tfh cell development, it is likely that a Th1 environment promotes the generation of a dominant Tfh-Th1 phenotype but also heterogeneous Tfh-Th2 and Tfh-Th17 phenotypes at lower frequency. This hypothesis might explain the correlation we observed between Tfh-Th1 and Tfh-Th2 from tonsils (**section 4.4**). It would be interesting to study samples from donors with a known immune response that is predominately Th1 or Th2 to further explore this hypothesis.

Having described the TCR repertoire relationships between tonsil and blood, further investigation of antigen specificity was an important element to consider, because peptide specificity in combination with TCR sequences are remarkable tools that can be used to determine whether two T cell populations are related to each other or whether they belong to different lineages.

Analysis of T cells specific for influenza virus haemagglutinin (HA) antigen showed an expected Th1-skewing in the memory response (Palladino et al., 1991; Sallusto and Lanzavecchia, 2009; Valkenburg et al., 2018; Yang et al., 2013; Zielinski et al., 2011) and therefore a higher precursor frequency in Tfh-Th1 and ROM (which contains Th1 cells), compared to Tfh-Th2 cells (**sections 5.3** and **5.4**). Further confirming this, the number of HA-specific clones generated was higher for Tfh-Th1 and ROM compartments, compared to Tfh-Th2. These data showed that Tfh-Th1

cells from peripheral blood not only have a Th1 phenotype ($CXCR3^{+}IFN\text{-}\gamma^{+}$) but also recognize an antigen that usually promotes a Th1 response (Valkenburg et al., 2018; Wilkinson et al., 2012). The presence of circulating memory Tfh-Th1 cells is still debatable, especially since several studies have described a correlation between an increased frequency of these cells and poor generation of effective antibody responses (Bowyer et al., 2018; Cubas et al., 2015; Obeng-Adjei et al., 2015; Ryg-Cornejo et al., 2016) and a pathogenic accumulation of Tfh cells in autoimmune diseases is driven by excessive IFN-γ production (Lee et al., 2012). It is thought that effector Tfh cells, even if primed in a Th1 environment and differentiated into a Tfh-like Th1 phenotype at the follicle border, need to downregulate CXCR3 and stop producing IFN-γ to become part of the GC reaction (Crotty, 2018; He et al., 2013). In parallel the same antigen can promote differentiation of effector Th1 cells that express CXCR3 to migrate to inflamed tissues and produce IFN-γ to help pathogen clearance (Groom and Luster, 2011a; Hale et al., 2013; Schmitt et al., 2016; Velu et al., 2016). Whether a few Tfh-GC cells, originally primed in a Th1 environment, are surviving to become memory Tfh-Th1 in the lymphoid organs and later in the periphery is not clear (Crotty, 2018). In simpler words, why Tfh-Th1 cells are needed if viral antigens promote a dual differentiation of Th1 effector cells to migrate to the periphery and of Tfh-GC to help the production of neutralizing antibodies remains to be clarified (**Figure 7.1**).

An arguably simple answer to this question might be that IFN-γ-producing T cells are still needed at the B cell border to induce specific class-switched antibodies (Reinhardt et al., 2009; Stavnezer, 1996) and that CXCR3 acquisition may be carried out through a conserved pathway involving a Th1-differentiation driving factor, but

it is not required for these cells to migrate into inflamed tissues. Alternatively, expression of CXCR3 on Tfh cells, which is especially increased during chronic viral infections (Boyden et al., 2012), might direct those cells to promote help to extrafollicular B cells. Recent studies in *Salmonella typhimurium* infection (Di Niro et al., 2015), rabies vaccines (Haley et al., 2017) and other antigen-specific models (Lee et al., 2018, 2011; Odegard et al., 2008) demonstrated functional extrafollicular Tfh help in chronic infection, where the structure of secondary lymphoid organs may become compromised and T and B cell zone delimitations are less clear (Rao, 2018). Extrafollicular Tfh cell help might then be crucial to help B cells that are unable to form germinal centres and therefore promote antibody production, although extrafollicular plasmablasts produce lower affinity antibodies that are often insufficient to provide protection (MacLennan et al., 2003). Tfh-Th1 cells might have different roles in diverse acute or chronic diseases and memory Tfh-Th1 cells could re-acquire a faster follicular function after antigen re-exposure, without excluding a possible extrafollicular role (Fazilleau et al., 2007; Hale et al., 2013; Herati et al., 2017).

I have discussed Tfh-Th1 cells in particular because the HA protein model used here principally involves Th1 responses, but these are interesting observations that may apply to other Tfh cells with different phenotypes, similarly to canonical T helper cell subsets. Future work focusing on different pathogens that drive Th2 and Th17 responses is needed to elucidate this.

The concept that T follicular helper cells are a separate lineage and that they have a unique program of differentiation is still open to debate. Separate research groups'

investigations support the idea that Tfh cells are in a transient activation state from the memory compartment and that non-Tfh memory cells can revert their phenotype depending on the persistence of the antigen and the presence of co-stimulatory signals in the environment (Baumjohann et al., 2013; Weber et al., 2015). A recent study by Herati et al. demonstrated that after influenza vaccination, expanded antigen-specific clones within cTfh ($CXCR5^+ICOS^+CD38^+$) can be found years later in the cTfh memory ($CXCR5^+ICOS^-CD38^-$) but not in the non-Tfh $CXCR5^-$ cells, suggesting that the memory Tfh subset is distinct from the rest of memory non-Tfh cells (Herati et al., 2017). However, the identity of memory cTfh cells in comparison to follicular memory Tfh cells is still unclear. Also, it is not known whether cTfh and effector Tfh-GC cells originate from rest of memory cells or whether they represent a well-defined separate population.

Both TCR sequencing of bulk memory $CD4^+$ cells and clonotyping of HA-specific T cell clones showed a distinction between Tfh and non-Tfh cells within $CD4^+$ memory cells in both the compartments considered. Tonsil and blood TCR deep-sequencing clearly highlighted the absence of a correlation between either Tfh-Th1 or Tfh-Th2 cells and ROM from blood; and between either Tfh-Th1, Tfh-Th2 or Tfh-GC cells and ROM from tonsils (**section 4.4**). Expanding on these observations by looking at the peptide specificity of HA-specific T cell clones from either circulating Tfh-Th1, Tfh-Th2 or ROM compartments showed the wide diversity of specificities in both Tfh-Th1 and ROM cell clones and surprisingly small overlap in the peptides recognised (**section 5.4**). In collaboration with Professor David Price, Tfh and non-Tfh distinction in peripheral blood was also elegantly and uniquely confirmed by the combination of TCR sequencing and peptide-specificity testing of Tfh-Th1, Tfh-Th2

and ROM HA-specific clones: clones specific for the same peptide but derived from different lineages utilised different TCRs. This suggested that these cells were generated from different naïve clones (**section 5.5**). ROM is the major $CD4^+$ T cell population in blood and predominates in clinical trial assays on unseparated blood $CD4^+$ T cells. Therefore, this finding indicates the necessity to purify circulating $CXCR5^+$ T cells in order to investigate true Tfh responses after immune challenge; measurement of total $CD4^+$ T cells could be uninformative or misleading.

The last part of this thesis focused on improving the understanding of cTfh cell function by studying immunological synapses with B cells. Preliminary data showed the feasibility of applying the bead-supported lipid bilayer (BSLB) methodology, developed by Professor Michael Dustin and his team, to study microvesicle trafficking in an artificial B cell system using circulating Tfh and non-Tfh cells (**section 6.2**). Supported lipid bilayer systems have successfully been used recently to describe the release of secretory granules containing dopamine from Tfh-GC from tonsils (Papa et al., 2017), and have confirmed the feasibility of microvesicle trafficking detection from primary tonsillar Tfh-GC cells. However, a comparison between circulating and follicular Tfh and non-Tfh cells has not previously been performed.

Tfh-GC cell differentiation is promoted by a persistent peptide:MHC presentation by germinal centre B cells, but different experimental models still leave open discussion regarding the nature of the antigen in question and uncertainties regarding the role of T cell avidity in the immune synapses (Fazilleau et al., 2007, 2009; Ploquin et al., 2011; Tubo and Jenkins, 2016). Generation and avidity

characterization of HA-specific T cell clones from circulating Tfh and non-Tfh cells was fundamental to optimise an antigen-specific system for future evaluation of the impact of TCR avidity in immune synapses (**section 6.3**). Preliminary experiments on T and B cell co-cultures revealed an interesting and unique activation coming from a high avidity clone compared to a low avidity Tfh-Th1 clone in regards to IgG, IgA and IgM production (**section 6.4**) and successfully demonstrated that Tfh clones expanded *in vitro* maintain their "B-cell-helper" function. These experiments establish the necessary techniques for future studies that focus on the immune synapse signal comparison between high and low avidity clones and between Tfh and non-Tfh cells from blood and tonsils and work is ongoing to build upon the preliminary data outlined herein.

In conclusion, the work presented in this thesis elucidated novel methodologies and concepts regarding the relationship and function of T follicular helper cells in circulation and in secondary lymphoid tissues and their distinctiveness from the rest of memory $CD4^+$ T cells. Considering the crucial role of Tfh cells in contributing to the generation of high affinity neutralizing antibodies in secondary lymphoid organs, these novel insights support the concept that circulating Tfh cells reflect the repertoire of effector and memory follicular Tfh cells. Importantly the work presented here shows that analysis of these cells in the periphery in human studies and vaccine trials can be used to gain insight into responses occurring in germinal centres after an immune challenge.

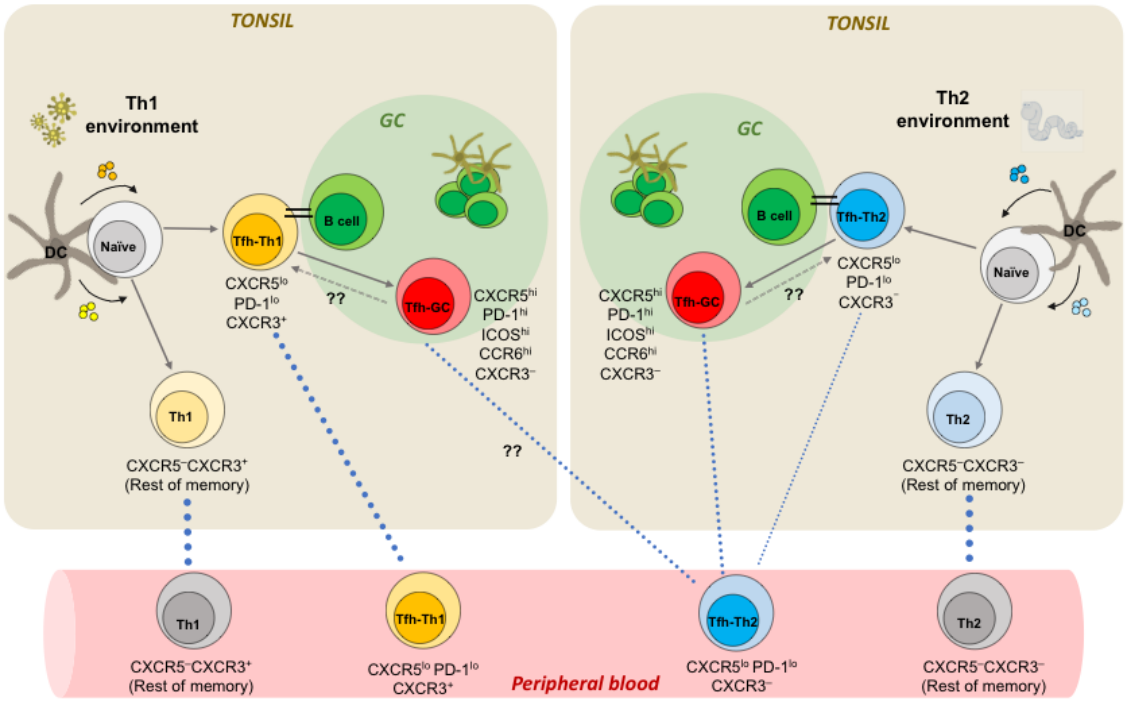


Figure 7.1 Graphical abstract.

Upon priming with DCs (dendritic cells) in either a Th1 or Th2 environment, naïve T cells differentiate into effector Th1 and Th2 cells respectively, or into a Tfh-like phenotype by expressing low level of CXCR5 and PD-1 in combination with Th1 or Th2 features. Expression of CXCR5 allows Tfh-like cells to migrate to the B cell border where they encounter cognate B cells and differentiate to effector Tfh-GC cells, to take part in the germinal centre (GC) reaction, where these cells express high levels of CXCR5, PD-1, ICOS, CCR6 and downregulate CXCR3. Tfh-GC cells show restricted re-circulation to the periphery during an acute response, but can resemble peripheral Tfh-Th2 cells that show lower expression of follicular surface markers. It is not clear whether Tfh-GC cells revert into a memory Tfh-like intermediate phenotype. Both antigen-experienced Tfh-Th1 and Tfh-Th2 cells re-circulate in the periphery as Tfh-Th1 and Tfh-Th2 respectively. Rest of memory, effector Th1 and effector Th2 cells are probably retained and recruited to the tonsils during chronic infection and can be detected in periphery as rest of memory $CXCR5^{-}$ cells.

8 Supplemental material

8.1 Flow cytometry antibody list

The table (**Figure 8.1**) contains the complete list of anti-human antibodies used along different experiments and the respective fluorocrome, manufacture, clone and titration optimised (Brodie et al., 2013).

Antibody	Fluorocrome	Supplier and clone	Dilution
Anti-dead cells	Aqua	Invitrogen, L34957	1:1000
Anti-CD3	BV605 (Brilliant Violet 605)	BD, UCHT1	1:50
Anti-CD3	PETR (R-phycoerythtin Texas Red)	Invitrogen, 7D6	1:50
Anti-CD3	PerCp (Peridinin Chlorophyll Protein Complex)	BD, SK7	1:50
Anti-CD4	APC Cy7 (Allophycocyanin cyanine 7)	BD, RPA-T4	1:40
Anti-CD4	PerCP/Cy 5.5 (Peridinin Chlorophyll Protein Complex cyanine 5.5)	Biolegend, A161A1	1:60
Anti-CD8	PE Cy7 (R-phycoerythrin cyanine 7)	BD, SK1	1:50
Anti-CD8	A700 (Alexa 700)	eBioscience, OKT8	1:40
Anti-CD14	PE (R-phycoerythrin)	BD, M5E2	1:50
Anti-CD14	PE Cy7 (R-phycoerythrin cyanine 7)	BD, M5E2	1:50
Anti-CD14	FITC Fluorescein isothiocyanate	BD, M5E2	1:50
Anti-CD16	PE Cy7 (R-phycoerythrin cyanine 7)	BD, 3G8	1:50
Anti-CD19	PE Cy7 (R-phycoerythrin cyanine 7)	BD, SJ25C1	1:50
Anti-CD19	APC Cy7 (Allophycocyanin cyanine 7)	BD, SJ25C1	1:50
Anti-CD19	BV 650 (Brilliant Violet 650)	Biolegend, H1B19	1:50
Anti-CD19	BV 605 (Brilliant Violet 605)	BD, SJ25C1	1:100
Anti-CD25	PE Cy7 (R-phycoerythrin cyanine 7)	BD, 243	1:50
Anti-CD27	APC Fire (Allophycocyanin Fire)	Biolegend, M-T271	1:100
antiCD38	BV785 (Brilliant Violet 785)	Biolegend, HIT2	1:40
Anti-CD40	A700 (Alexa Fluor ™ 700)	Biolegend, 5C3	1:40

Anti-CD45RA	PETR (R-phycoerythtin Texas Red)	Invitrogen, MEM-56	1:100
Anti-CD56	PE Cy7 (R-phycoerythrin cyanine 7)	BD, B159	1:50
Anti-CD86	PE Cy5 (R-phycoerythrin cyanine 5)	Biolegend, IT2.2	1:100
Anti-CD127 (IL7R)	BV785 (Brilliant Violet 758)	Biolegend, A019D5	1:100
Anti-CD154 (CD40L)	PE (R-phycoerythrin)	BD, TRAP1	1:50
Anti-CD154 (CD40L)	A647 (Alexa Fluor ™ 647)	Biolegend, 24-31	1:60
Anti-CD183 (CXCR3)	PE Cy5 (R-phycoerythrin cyanine 5)	BD, 1C6/CXCR3	1:20
Anti-CD185 (CXCR5)	A488 (Alexa 488)	BD, RF8B2	1:20
Anti-CD185 (CXCR5)	PerCP/Cy 5.5 (Peridinin Chlorophyll Protein Complex cyanine 5.5)	BD, RF8B2	1:20
Anti-CD185 (CXCR5)	A647 (Alexa 647)	BD, RF8B2	1:50
Anti-CD196 (CCR6)	BV605 (Brilliant Violet 605)	BD, 11A9	1:50
Anti-CD275 (ICOSL)	BV421 (Brilliant Violet 421)	BD, 2D/B7-H2	1:20
Anti-CD278 (ICOS)	PE (R-phycoerythrin)	Biolegend, C398.4A	1:40
Anti-CD278 (ICOS)	BV650 (Brilliant Violet 650)	BD, DX29	1:50
Anti-CD278 (ICOS)	BV785 (Brilliant Violet 785)	Biolegend, C398.4A	1:60
Anti-CD279 (PD-1)	BV 421 (Brilliant Violet 421)	BD, EH12.1	1:40
Anti-CD317 (BST2)	PE (R-phycoerythrin)	eBioscience, RS38E	1:60
Anti-αβ T cell Receptor (αβTCR)	A700 (Alexa Fluor ™ 700)	Biolegend, IP-26	1:30
Anti-αβ T cell Receptor (αβTCR)	Biotin	Biolegend, IP-26	1:50
Streptavidin	BV711 (Brilliant Violet 711)	Biolegend	1:80
Anti-interleukin-21 (IL-21)	A647 (Alexa 647)	BD, 3A3-N2.1	1:40
Anti-interleukin-4 (IL-4)	PE (R-phycoerythrin)	BD, MP4-25D2	1:80
Anti-interleukin-10 (IL-10)	BV785 (Brilliant Violet 785)	BD, JES3-9D7	1:30
Anti-interleukin-17A (IL-17A)	eFluor 450	eBioscience,eBio17B7	1:100
Anti-Interferon-Gamma (IFN-γ)	A700 (Alexa 700)	BD, 4S.B3	1:150
Anti-Bcl-6	PE (R-phycoerythrin)	BD, K112-91	1:80
Anti-Foxp3	A647 (Alexa 647)	eBioscience, PCH101	1:50

Figure 8.1 Flow cytometry antibody list.

Complete list of flow cytometry antibodies used for multiple experiments, optimised at the LSR-Fortessa (BD). The columns list the antibody name, the fluorocrome, the manufacture and clone, the titration used.

8.1 Overlapping peptides

Overlapping peptides of HA/Wisconsin/67/2005 H3N2 were provided by BEI (Biodefence and Emerging Infection Research Resources Repository) and the purity

defined using mass spectrometry (QC the peptide of interest must be one of the 3 major peaks). Peptides are 13- to 17- amino acids long with 7 to 12 amino acids overlap spanning the entire Haemagglutinin protein and the sequence in shown (**Figure 8.2**).

Overlapping peptides of HA/California/04/2009 H1N1 were commercially synthetized from GenScript and the purity defined using mass spectrometry (QC the peptide of interest must be one of the 3 major peaks). Peptides are 14- to 18- amino acids long with 12 amino acids overlap spanning the entire Haemagglutinin protein and the sequence in shown (**Figure 8.3**).

Peptide ID	Length	AA position	Sequence
1	17	1-17	AQKLPGNDNSTATLCLG
2	17	7-23	NDNSTATLCLGHHAVPN
3	17	13-29	TLCLGHHAVPNGTIVKT
4	17	19-35	HAVPNGTIVKTITNDQI
5	17	25-41	TIVKTITNDQIEVTNAT
6	15	31-45	TNDQIEVTNATELVQ
7	17	35-51	IEVTNATELVQSSSTGG
8	17	41-57	TELVQSSSTGGICDSPH
9	17	47-63	SSTGGICDSPHQILDGE
10	17	53-69	CDSPHQILDGENCTLID
11	16	59-74	ILDGENCTLIDALLGD
12	17	64-80	NCTLIDALLGDPQCDGF
13	17	70-86	ALLGDPQCDGFQNKKWD
14	17	75-91	PQCDGFQNKKWDLFVER
15	16	80-95	FQNKKWDLFVERSKAY
16	17	85-101	WDLFVERSKAYSNCYPY
17	17	91-107	RSKAYSNCYPYDVPDYA
18	17	97-113	NCYPYDVPDYASLRSLV
19	17	103-119	VPDYASLRSLVASSGTL
20	16	109-124	LRSLVASSGTLEFNDE
21	17	114-130	ASSGTLEFNDESFNWTG
22	17	119-135	LEFNDESFNWTGVTQNG
23	17	125-141	SFNWTGVTQNGTSSACK
24	16	131-146	VTQNGTSSACKRRSNN
25	17	136-152	TSSACKRRSNNSFFSRL
26	17	142-158	RRSNNSFFSRLNWLTHL
27	17	148-164	FFSRLNWLTHLKFKYPA
28	16	154-169	WLTHLKFKYPALNVTM
29	17	159-175	KFKYPALNVTMPNNEKF
30	17	165-181	LNVTMPNNEKFDKLYIW
31	17	171-187	NNEKFDKLYIWGVHHPG
32	17	177-193	KLYIWGVHHPGTDNDQI
33	17	183-199	VHHPGTDNDQIFLHAQA
34	17	189-205	DNDQIFLHAQASGRITV
35	17	195-211	LHAQASGRITVSTKRSQ
36	17	201-217	GRITVSTKRSQQTVIPN
37	17	207-223	TKRSQQTVIPNIGSRPR
38	15	213-227	TVIPNIGSRPRIRNI
39	17	217-233	NIGSRPRIRNIPSRISI
40	17	223-239	RIRNIPSRISIYWTIVK
41	17	229 -245	SRISIYWTIVKPGDILL
42	17	235-251	WTIVKPGDILLINSTGN
43	17	241-257	GDILLINSTGNLIAPRG
44	16	247-262	NSTGNLIAPRGYFKIR
45	17	252 -268	LIAPRGYFKIRSGKSSI
46	16	258-273	YFKIRSGKSSIMRSDA
47	17	263-279	SGKSSIMRSDAPIGKCN

Peptide ID	Length	AA position	Sequence
48	16	269-284	MRSDAPIGKCNSECIT
49	16	274-289	PIGKCNSECITPNGSI
50	17	279-295	NSECITPNGSIPNDKPF
51	17	285-301	PNGSIPNDKPFQNVNRI
52	15	291- 305	NDKPFQNVNRITYGA
53	17	295-311	FQNVNRITYGACPRYVK
54	17	301-317	ITYGACPRYVKQNTLKL
55	17	307-323	PRYVKQNTLKLATGMRN
56	17	313-329	NTLKLATGMRNVPEKQT
57	17	319 -335	TGMRNVPEKQTRGIFGA
58	17	325-341	PEKQTRGIFGAIAGFIE
59	17	331-347	GIFGAIAGFIENGWEGM
60	17	337-353	AGFIENGWEGMVDGWYG
61	16	343-358	GWEGMVDGWYGFRHQN
62	17	348 -364	VDGWYGFRHQNSEGIGQ
63	16	354-369	FRHQNSEGIGQAADLK
64	17	359-375	SEGIGQAADLKSTQAAI
65	17	365-381	ADLKSTQAAINQINGK
66	17	371 -387	TQAAINQINGKLNRLIG
67	17	376-392	NQINGKLNRLIGKTNEK
68	17	382-398	LNRLIGKTNEKFHQIEK
69	17	388-404	KTNEKFHQIEKEFSEVE
70	17	394-410	HQIEKEFSEVEGRIQDL
71	17	400-416	FSEVEGRIQDLEKYVED
72	17	406-422	RIQDLEKYVEDTKIDLW
73	17	412-428	KYVEDTKIDLWSYNAEL
74	17	418-434	KIDLWSYNAELLVALEN
75	17	424-440	YNAELLVALENQHTIDL
76	17	430 -446	VALENQHTIDLTDSEMN
77	17	436 -452	HTIDLTDSEMNKLFERT
78	17	442 - 458	DSEMNKLFERTKKQLRE
79	17	448-464	LFERTKKQLRENAEDMG
80	17	454-470	KQLRENAEDMGNGCFKI
81	17	460-476	AEDMGNGCFKIYHKCDN
82	17	466-482	GCFKIYHKCDNACIGSI
83	17	472-488	HKCDNACIGSIRNGTYD
84	17	478-494	CIGSIRNGTYDHDVYRD
85	17	484 -500	NGTYDHDVYRDEALNNR
86	17	490-506	DVYRDEALNNRFQIKGV
87	17	496-512	ALNNRFQIKGVELKSGY
88	17	501-517	FQIKGVELKSGYKDWIL
89	17	506-522	VELKSGYKDWILWISFA
90	17	512 -528	YKDWILWISFAISCFLL
91	13	518 -530	WISFAISCFLLCV
92	16	524-539	SCFLLCVALLGFIMWA
93	17	529-545	CVALLGFIMWACQKGNI
94	17	535-551	FIMWACQKGNIRCNICI

Figure 8.2 List of peptides overlapping the entire HA/Wisconsin protein.

Peptides provided by BEI spanning the entire HA/Wisconsin/67/2005 protein are listed in the table. Each column refers to peptide identification, amino acids length position and sequence.

Peptide ID	Length	AA position	Sequence
1	18	1-18	MKAILVVLLYTFATANAD
2	18	9-26	LYTFATANADTLCIGYHA
3	18	17-34	ADTLCIGYHANNSTDTVD
4	18	25-42	HANNSTDTVDTVLEKNVT
5	18	33-50	VDTVLEKNVTVTHSVNLL
6	18	41-58	VTVTHSVNLLEDKHNGKL
7	18	49-66	LLEDKHNGKLCKLRGVAP
8	18	57-74	KLCKLRGVAPLHLGKCNI
9	18	65-82	APLHLGKCNIAGWILGNP
10	18	73-90	NIAGWILGNPECESLSTA
11	18	81-98	NPECESLSTASSWSYIVE
12	18	89-106	TASSWSYIVETPSSDNGT
13	18	97-114	VETPSSDNGTCYPGDFID
14	18	105-122	GTCYPGDFIDYEELREQL
15	18	113-130	IDYEELREQLSSVSSFER
16	18	121-138	QLSSVSSFERFEIFPKTS
17	18	129-146	ERFEIFPKTSSWPNHDSN
18	18	137-154	TSSWPNHDSNKGVTAACP
19	18	145-162	SNKGVTAACPHAGAKSFY
20	18	153-170	CPHAGAKSFYKNLIWLVK
21	18	161-178	FYKNLIWLVKKGNSYPKL
22	18	169-186	VKKGNSYPKLSKSYINDK
23	18	177-194	KLSKSYINDKGKEVLVLW
24	18	185-202	DKGKEVLVLWGIHHPSTS
25	18	193-210	LWGIHHPSTSADQQSLYQ
26	18	201-218	TSADQQSLYQNADTYVFV
27	18	209-226	YQNADTYVFVGSSRYSKK
28	18	217-234	FVGSSRYSKKFKPEIAIR
29	18	225-242	KKFKPEIAIRPKVRDQEG
30	18	233-250	IRPKVRDQEGRMNYYWTL
31	18	241-258	EGRMNYYWTLVEPGDKIT
32	18	249-266	TLVEPGDKITFEATGNLV
33	18	257-274	ITFEATGNLVVPRYAFAM
34	18	265-282	LVVPRYAFAMERNAGSGI
35	18	273-290	AMERNAGSGIIISDTPVH

Peptide ID	Length	AA position	Sequence
36	18	281-298	GIIISDTPVHDCNTTCQT
37	18	289-306	VHDCNTTCQTPKGAINTS
38	18	297-314	QTPKGAINTSLPFQNIHP
39	18	305-322	TSLPFQNIHPITIGKCPK
40	18	313-330	HPITIGKCPKYVKSTKLR
41	18	321-338	PKYVKSTKLRLATGLRNI
42	18	329-346	LRLATGLRNIPSIQSRGL
43	18	337-354	NIPSIQSRGLFGAIAGFI
44	18	345-362	GLFGAIAGFIEGGWTGMV
45	18	353-370	FIEGGWTGMVDGWYGYHH
46	18	361-378	MVDGWYGYHHQNEQGSGY
47	18	369-386	HHQNEQGSGYAADLKSTQ
48	18	377-394	GYAADLKSTQNAIDEITN
49	18	385-402	TQNAIDEITNKVNSVIEK
50	18	393-410	TNKVNSVIEKMNTQFTAV
51	18	401-418	EKMNTQFTAVGKEFNHLE
52	18	409-426	AVGKEFNHLEKRIENLNK
53	18	417-434	LEKRIENLNKKVDDGFLD
54	18	425-442	NKKVDDGFLDIWTYNAEL
55	18	433-450	LDIWTYNAELLVLLENER
56	18	441-458	ELLVLLENERTLDYHDSN
57	18	449-466	ERTLDYHDSNVKNLYEKV
58	18	457-474	SNVKNLYEKVRSQLKNNA
59	18	465-482	KVRSQLKNNAKEIGNGCF
60	18	473-490	NAKEIGNGCFEFYHKCDN
61	18	471-498	CFEFYHKCDNTCMESVKN
62	18	479-506	DNTCMESVKNGTYDYPKY
63	18	497-514	KNGTYDYPKYSEEAKLNR
64	18	505-522	KYSEEAKLNREEIDGVKL
65	18	513-530	NREEIDGVKLESTRIYQI
66	18	521-538	KLESTRIYQILAIYSTVA
67	18	529-546	QILAIYSTVASSLVLVVS
68	18	537-554	VASSLVLVVSLGAISFWM
69	18	545-562	VSLGAISFWMCSNGSLQC
70	14	553- 566	WMCSNGSLQCRICI

Figure 8.3 List of peptides overlapping the entire HA/California protein.

Peptides provided synthetized from GenScript spanning the entire HA/California/04/2009 protein are listed in the table. Each column refers to peptide identification, amino acid length position in the HA molecule and sequence.

Bibliography

Abbas, A.K., and Lichtman, A.H. (2001). Basic immunology : functions and disorders of the immune system.

Acosta-Rodriguez, E. V., Rivino, L., Geginat, J., Jarrossay, D., Gattorno, M., Lanzavecchia, A., Sallusto, F., and Napolitani, G. (2007). Surface phenotype and antigenic specificity of human interleukin 17-producing T helper memory cells. Nat. Immunol. *8*, 639–646.

Aderem, A., and Underhill, D.M. (1999). Mechanism of Phagocytosis in Macrophages. Annu. Rev. Immunol. *17*, 593–623.

Ai, W., Li, H., Song, N., Li, L., and Chen, H. (2013). Optimal Method to Stimulate Cytokine Production and Its Use in Immunotoxicity Assessment. Int. J. Environ. Res. Public Health *10*, 3834–3842.

Alam, S., and Sant, A.J. (2011). Infection with Seasonal Influenza Virus Elicits CD4 T Cells Specific for Genetically Conserved Epitopes That Can Be Rapidly Mobilized for Protective Immunity to Pandemic H1N1 Influenza Virus. J. Virol. *85*, 13310–13321.

Alberts, B., Johnson, A., Lewis, J., Raff, M., Roberts, K., and Walter, P. (2008). Molecular Biology of The Cell.

Allen, J.E., and Sutherland, T.E. (2014). Host protective roles of type 2 immunity: Parasite killing and tissue repair, flip sides of the same coin. Semin. Immunol. *26*, 329–340.

Altin, J.G., and Sloan, E.K. (1997). The role of CD45 and CD45-associated molecules in T cell activation. Immunol. Cell Biol. *75*, 430–445.

Andaloussi, S. EL, Mäger, I., Breakefield, X.O., and Wood, M.J.A. (2013). Extracellular vesicles: Biology and emerging therapeutic opportunities. Nat. Rev. Drug Discov. *12*, 347–357.

Annunziato, F., Cosmi, L., Santarlasci, V., Maggi, L., Liotta, F., Mazzinghi, B., Parente, E., Filì, L., Ferri, S., Frosali, F., et al. (2007). Phenotypic and functional features of human Th17 cells. J. Exp. Med. *204*, 1849–1861.

Ansel, K.M., Ngo, V.N., Hyman, P.L., Luther, S.A., Förster, R., Sedgwick, J.D., Browning, J.L., Lipp, M., and Cyster, J.G. (2000). A chemokine-driven positive feedback loop organizes lymphoid follicles. Nature *406*, 309–314.

Armitage, R.J., Fanslow, W.C., Strockbine, L., Sato, T.A., Clifford, K.N., Macduff, B.M., Anderson, D.M., Gimpel, S.D., Davis-Smith, T., Maliszewski, C.R., et al. (1992). Molecular and biological characterization of a murine ligand for CD40.

Nature *357*, 80–82.

Arpin, C., Dechanet, J., Van Kooten, C., Merville, P., Grouard, G., Briere, F., Banchereau, J., and Liu, Y. (1995). Generation of memory B cells and plasma cells in vitro. Science (80-.). *268*, 720–722.

Arstila, T.P., Casrouge, A., Baron, V., Even, J., Kanellopoulos, J., and Kourilsky, P. (1999). A direct estimate of the human alpha beta T cell receptor diversity. Science *286*, 958–961.

Aschenbrenner, D., Foglierini, M., Jarrossay, D., Hu, D., Weiner, H.L., Kuchroo, V.K., Lanzavecchia, A., Notarbartolo, S., and Sallusto, F. (2018). An immunoregulatory and tissue-residency program modulated by c-MAF in human TH17 cells. Nat. Immunol. *10*.

Avery, D.T., Bryant, V.L., Ma, C.S., de Waal Malefyt, R., and Tangye, S.G. (2008). IL-21-Induced Isotype Switching to IgG and IgA by Human Naive B Cells Is Differentially Regulated by IL-4. J. Immunol. *181*, 1767–1779.

Ballesteros-Tato, A., León, B., Graf, B.A., Moquin, A., Adams, P.S., Lund, F.E., and Randall, T.D. (2012). Interleukin-2 Inhibits Germinal Center Formation by Limiting T Follicular Helper Cell Differentiation. Immunity *36*, 847–856.

Bannard, O., and Cyster, J.G. (2017). Germinal centers: programmed for affinity maturation and antibody diversification. Curr. Opin. Immunol.

Bardhan, K., Patsoukis, N., Weaver, J., Freeman, G., Li, L., and Boussiotis, V.A. (2016). PD-1 inhibits the TCR signaling cascade by sequestering SHP-2 phosphatase, preventing its translocation to lipid rafts and facilitating Csk-mediated inhibitory phosphorylation of Lck. J. Immunol. *196*, 128.15 LP-128.15.

Baumjohann, D., Preite, S., Reboldi, A., Ronchi, F., Ansel, K.M., Lanzavecchia, A., and Sallusto, F. (2013). Persistent Antigen and Germinal Center B Cells Sustain T Follicular Helper Cell Responses and Phenotype. Immunity *38*, 596–605.

Becattini, S., Latorre, D., Mele, F., Foglierini, M., De Gregorio, C., Cassotta, A., Fernandez, B., Kelderman, S., Schumacher, T.N., Corti, D., et al. (2014). Functional heterogeneity of human memory CD4+ T cell clones primed by pathogens or vaccines. Science (80-.). *347*, 400–406.

Belz, G.T., Wodarz, D., Diaz, G., Martin, a, Doherty, P.C., and Nowak, M. a (2002). Compromised Influenza Virus-Specific CD8 + -T-Cell Memory in CD4+ -T-Cell-Deficient Mice. J. Virol. *76*, 12388–12393.

Bender, B.S., Croghan, T., Zhang, L., and Small, P.A.J. (1992). Transgenic Mice Lacking Class I Major Histocompatibility Complex-restricted T Cells Have Delayed Viral Clearance and Increased Mortality after Influenza Virus Challenge. J. Exp. Med. *157*, 1360–1365.

Bentebibel, S., Lopez, S., Obermoser, G., Schmitt, N., Mueller, C., Harrod, C., Flano, E., Mejias, A., Albrecht, R. a, Blankenship, D., et al. (2013). Induction of ICOS+CXCR3+CXCR5+ TH cells correlates with antibody responses to influenza vaccination. Sci. Transl. Med. *5*, 176–232.

Bentebibel, S.-E., Khurana, S., Schmitt, N., Kurup, P., Mueller, C., Obermoser, G., Palucka, A.K., Albrecht, R.A., Garcia-Sastre, A., Golding, H., et al. (2016). ICOS+PD-1+CXCR3+ T follicular helper cells contribute to the generation of high-avidity antibodies following influenza vaccination. Sci. Rep. *6*, 26494.

Birnbaum, M.E., Mendoza, J.L., Sethi, D.K., Dong, S., Glanville, J., Dobbins, J., Özkan, E., Davis, M.M., Wucherpfennig, K.W., and Garcia, K.C. (2014). Deconstructing the Peptide-MHC Specificity of T Cell Recognition. Cell *157*, 1073–1087.

Blum, J.S., Wearsch, P.A., and Cresswell, P. (2013). Pathways of antigen processing. Annu Rev Immunol *31*, 443–473.

Von Boehmer, H. (2005). Unique features of the pre-T-cell receptor aα-chain: Not just a surrogate. Nat. Rev. Immunol. *5*, 571–577.

Von Boehmer, H., Aifantis, I., Azogui, O., Feinberg, J., Saint-Ruf, C., Zober, C., Garcia, C., and Buer, J. (1998). Crucial function of the pre-T-cell receptor (TCR) in TCR beta selection, TCR beta allelic exclusion and alpha beta versus gamma delta lineage commitment. Immunol. Rev. *165*, 111–119.

Bolotin, D.A., Poslavsky, S., Mitrophanov, I., Shugay, M., Mamedov, I.Z., Putintseva, E. V., and Chudakov, D.M. (2015). MiXCR: Software for comprehensive adaptive immunity profiling. Nat. Methods *12*, 380–381.

Bone, A., Guthmann, J.P., Assal, A., Rousset, D., Degeorges, A., Morel, P., Valette, M., Enouf, V., Jacquot, E., Pelletier, B., et al. (2012). Incidence of H1N1 2009 virus infection through the analysis of paired plasma specimens among blood donors, France. PLoS One *7*, 1–9.

Borowski, C., Li, X., Aifantis, I., Gounari, F., and von Boehmer, H. (2004). Pre-TCRα and TCRα Are Not Interchangeable Partners of TCRβ during T Lymphocyte Development. J. Exp. Med. *199*, 607–615.

Boswell, K.L., Paris, R., Boritz, E., Ambrozak, D., Yamamoto, T., Darko, S., Wloka, K., Wheatley, A., Narpala, S., McDermott, A., et al. (2014). Loss of circulating CD4 T cells with B cell helper function during chronic HIV infection. PLoS Pathog. *10*, 1–14.

Botta, D., Fuller, M.J., Marquez-Lago, T.T., Bachus, H., Bradley, J.E., Weinmann, A.S., Zajac, A.J., Randall, T.D., Lund, F.E., León, B., et al. (2017). Dynamic regulation of T follicular regulatory cell responses by interleukin 2 during influenza infection. Nat. Immunol. *18*, 1249–1260.

Bowyer, G., Grobbelaar, A., Rampling, T., Venkatraman, N., Morelle, D., Ballou, R.W., Hill, A.V.S., and Ewer, K.J. (2018). CXCR3+ T Follicular Helper Cells Induced by Co-Administration of RTS,S/AS01B and Viral-Vectored Vaccines Are Associated With Reduced Immunogenicity and Efficacy Against Malaria. Front. Immunol. *9*, 1–15.

Boyden, A.W., Legge, K.L., and Waldschmidt, T.J. (2012). Pulmonary infection with influenza A virus induces site-specific germinal center and T follicular helper cell responses. PLoS One *7*.

Breitfeld, D., Ohl, L., Kremmer, E., Ellwart, J., Sallusto, F., Lipp, M., and Förster, R. (2000). Follicular B helper T cells express CXC chemokine receptor 5, localize to B cell follicles, and support immunoglobulin production. J. Exp. Med. *192*, 1545–1552.

Brodie, T., Brenna, E., and Sallusto, F. (2013). OMIP-018: Chemokine receptor expression on human T helper cells. Cytom. Part A *83A*, 530–532.

Bruno, F., Fornara, C., Zelini, P., Furione, M., Carrara, E., Scaramuzzi, L., Cane, I., Mele, F., Sallusto, F., Lilleri, D., et al. (2016). Follicular helper T-cells and virus-specific antibody response in primary and reactivated human cytomegalovirus infections of the immunocompetent and immunocompromised transplant patients. J. Gen. Virol. *97*, 1928–1941.

Burke, D.F., and Smith, D.J. (2014). A Recommended numbering scheme for influenza A HA Subtypes. PLoS One *9*.

Cabaniols, J.-P., Fazilleau, N., Casrouge, A., Kourilsky, P., and Kanellopoulos, J.M. (2001). Most α/β T Cell Receptor Diversity Is Due to Terminal Deoxynucleotidyl Transferase. J. Exp. Med. *194*, 1385–1390.

Campbell, J.J., Murphy, K.E., Kunkel, E.J., Brightling, C.E., Soler, D., Shen, Z., Boisvert, J., Greenberg, H.B., Vierra, M.A., Goodman, S.B., et al. (1997). CCR7 Expression and Memory T Cell Diversity in Humans. J. Immunol. *166*, 877–884.

Campion, S.L., Brodie, T.M., Fischer, W., Korber, B.T., Rossetti, A., Goonetilleke, N., McMichael, A.J., and Sallusto, F. (2014). Proteome-wide analysis of HIV-specific naive and memory CD4(+) T cells in unexposed blood donors. J. Exp. Med. *211*, 1273–1280.

Casamayor-Palleja, M., Khan, M., and MacLennan, I.C. (1995). A subset of CD4+ memory T cells contains preformed CD40 ligand that is rapidly but transiently expressed on their surface after activation through the T cell receptor complex. J. Exp. Med. *181*, 1293–1301.

Caza, T., and Landas, S. (2015). Functional and Phenotypic Plasticity of CD4(+) T Cell Subsets. Biomed Res Int *2015*, 521957.

Chen, W., Jin, W., Hardegen, N., Lei, K., Li, L., Marinos, N., McGrady, G., and

Wahl, S.M. (2003). Conversion of Peripheral CD4 $^{+}$ CD25 $^{-}$ Naive T Cells to CD4 $^{+}$ CD25 $^{+}$ Regulatory T Cells by TGF-β Induction of Transcription Factor *Foxp3*. J. Exp. Med. *198*, 1875–1886.

Chen, Z., Tato, C.M., Muul, L., Laurence, A., and O'Shea, J.J. (2007). Distinct regulation of interleukin-17 in human T helper lymphocytes. Arthritis Rheum. *56*, 2936–2946.

Chevalier, N., Jarrossay, D., Ho, E., Danielle, T., Ma, C.S., Yu, D., Sallusto, F., Stuart, G., and Mackay, C.R. (2011). CXCR5 Expressing Human Central Memory CD4 T Cells and Their Relevance for Humoral Immune Responses. J. Immunol. *186*, 5556–5568.

Cho, H., Kang, H., Lee, H.H., and Kim, C.W. (2017). Programmed cell death 1 (PD-1) and cytotoxic T lymphocyte-associated antigen 4 (CTLA-4) in viral hepatitis. Int. J. Mol. Sci. *18*, 1–20.

Choi, Y.S., Kageyama, R., Eto, D., Escobar, T.C., Johnston, R.J., Monticelli, L., Lao, C., and Crotty, S. (2011). ICOS Receptor Instructs T Follicular Helper Cell versus Effector Cell Differentiation via Induction of the Transcriptional Repressor Bcl6. Immunity *34*, 932–946.

Choi, Y.S., Eto, D., Yang, J.A., Lao, C., and Crotty, S. (2013). Cutting edge: STAT1 is required for IL-6-mediated Bcl6 induction for early follicular helper cell differentiation. J. Immunol. *190*, 3049–3053.

Choudhuri, K., Llodrá, J., Roth, E.W., Tsai, J., Gordo, S., Wucherpfennig, K.W., Kam, L.C., Stokes, D.L., and Dustin, M.L. (2014). Polarized release of T-cell-receptor-enriched microvesicles at the immunological synapse. Nature *507*, 118–123.

Chtanova, T., Tangye, S.G., Newton, R., Frank, N., Hodge, M.R., Rolph, M.S., and Mackay, C.R. (2004). T Follicular Helper Cells Express a Distinctive Transcriptional Profile, Reflecting Their Role as Non-Th1/Th2 Effector Cells That Provide Help for B Cells. J. Immunol. *173*, 68–78.

Chung, Y., Tanaka, S., Chu, F., Nurieva, R.I., Martinez, G.J., Rawal, S., Wang, Y.H., Lim, H., Reynolds, J.M., Zhou, X.H., et al. (2011). Follicular regulatory T cells expressing Foxp3 and Bcl-6 suppress germinal center reactions. Nat. Med. *17*, 983–988.

Ci, W., Polo, J., and Melnick, A. (2008). B-cell lymphoma 6 and the molecular pathogenesis of diffuse large B-cell lymphoma. Curr Opin Hematol *15*, 381–390.

Ciofani, M., Madar, A., Galan, C., Sellars, M., Mace, K., Pauli, F., Agarwal, A., Huang, W., Parkhurst, C.N., Muratet, M., et al. (2013). A validated regulatory network for Th17 cell specification. Cell *151*, 289–303.

Cirelli, K.M., and Crotty, S. (2017). Germinal center enhancement by extended

antigen availability. Curr. Opin. Immunol. *47*, 64–69.

Claman, H., Chaperon, E., and Triplett, R. (1966). Thymus-marrow cell combinations. Synergism in antibody production. Proc Soc Exp Biol Med *122*, 1167–1171.

Clark, E.A., and Ledbetter, J.A. (1986). Activation of human B cells mediated through two distinct cell surface differentiation antigens, Bp35 and Bp50. Proc. Natl. Acad. Sci. U. S. A. *83*, 4494–4498.

Constant, S., Pfeiffer, C., Woodard, A., Pasqualini, T., and Bottomly, K. (1995). Extent of T Cell Receptor Ligation Can Determine the Functional Differentiation of Naive CD4 + T Cells. J Exp Med *182*, 0–5.

Corti, D., Voss, J., Gamblin, S.J., Codoni, G., Macagno, A., Jarrossay, D., Vachieri, S.G., Pinna, D., Minola, A., Vanzetta, F., et al. (2011). A Neutralizing Antibody Selected from Plasma Cells That Binds to Group 1 and Group 2 Influenza A Hemagglutinins. Science (80-.). *333*, 850–856.

Crotty, S. (2011). Follicular helper CD4 T cells (TFH). Annu. Rev. Immunol. *29*, 621–663.

Crotty, S. (2014). T Follicular Helper Cell Differentiation, Function, and Roles in Disease. Immunity *41*, 529–542.

Crotty, S. (2015). A brief history of T cell help to B cells. Nat. Rev. Immunol. *15*, 185–189.

Crotty, S. (2018). Complexities of Interpretation due to the Heterogeneity of Memory CD4 T Cells, Including T Follicular Helper Cells. Cold Spring Harb. Perspect. Biol.

Cubas, R., van Grevenynghe, J., Wills, S., Kardava, L., Santich, B.H., Buckner, C.M., Muir, R., Tardif, V., Nichols, C., Procopio, F., et al. (2015). Reversible Reprogramming of Circulating Memory T Follicular Helper Cell Function during Chronic HIV Infection. J. Immunol.

Cubas, R. a, Mudd, J.C., Savoye, A.-L., Perreau, M., van Grevenynghe, J., Metcalf, T., Connick, E., Meditz, A., Freeman, G.J., Abesada-Terk, G., et al. (2013). Inadequate T follicular cell help impairs B cell immunity during HIV infection. Nat. Med. *19*, 494–499.

Cupedo, T., and Papazian, N. (2012). Isolation of mononuclear cells from human tonsil using the gentleMACS™ Dissociator. MiltenyiBiotec 1–2.

Cyster, J.G. (2000). Leukocyte migration: Scent of the T zone. Curr. Biol. *10*, 30–33.

D'Souza, M., Fontenot, A.P., Mack, D.G., Lozupone, C., Dillon, S., Meditz, A.,

Wilson, C.C., Connick, E., and Palmer, B.E. (2007). Programmed Death 1 Expression on HIV-Specific CD4+ T Cells Is Driven by Viral Replication and Associated with T Cell Dysfunction. J. Immunol. *179*, 1979–1987.

Davis, M.M., and Bjorkman, P.J. (1988). T-cell antigen receptor genes and T-cell recognition. Nature *334*, 395–402.

Davis, S.J., and van der Merwe, P.A. (2006). The kinetic-segregation model: TCR triggering and beyond. Nat. Immunol. *7*, 803–809.

Day, C.L., Kaufmann, D.E., Kiepiela, P., Brown, J.A., Moodley, E.S., Reddy, S., Mackey, E.W., Miller, J.D., Leslie, A.J., DePierres, C., et al. (2006). PD-1 expression on HIV-specific T cells is associated with T-cell exhaustion and disease progression. Nature *443*, 350–354.

Deenick, E.K., Chan, A., Ma, C.S., Gatto, D., Schwartzberg, P.L., Brink, R., and Tangye, S.G. (2010). Follicular Helper T Cell Differentiation Requires Continuous Antigen Presentation that Is Independent of Unique B Cell Signaling. Immunity *33*, 241–253.

Derhovanessian, E., Maier, A.B., Hähnel, K.H., Beck, R., de Craen, A.J.M., Slagboom, E.P., Westendorp, R.G.J., and Pawelec, G. (2011). Infection with cytomegalovirus but not herpes simplex virus induces the accumulation of latedifferentiated CD4 + and CD8 + T-cells in humans. J. Gen. Virol. *92*, 2746–2756.

Diamantis, A., Magiorkinis, E., and Koutselini, H. (2009). Fine-needle aspiration (FNA) biopsy: Historical aspects. Folia Histochem. Cytobiol. *47*, 191–197.

DiToro, D., Winstead, C.J., Pham, D., Witte, S., Andargachew, R., Singer, J.R., Wilson, C.G., Zindl, C.L., Luther, R.J., Silberger, D.J., et al. (2018). Differential IL-2 expression defines developmental fates of follicular versus nonfollicular helper T cells. Science (80-.). *361*, 1–13.

Djuretic, I.M., Levanon, D., Negreanu, V., Groner, Y., Rao, A., and Ansel, K.M. (2007). Transcription factors T-bet and Runx3 cooperate to activate Ifng and silence Il4 in T helper type 1 cells. *2007*, 1–10.

Dorfman, D.M., Brown, J.A., Shahsafaei, A., and Freeman, G.J. (2006). Programmed Death-1 (PD-1) is a Marker of Germinal Center- associated T Cells and Angioimmunoblastic T-Cell Lymphoma. Am. J. Surg. Pathol. *30*, 802–810.

Douek, D.C., Betts, M.R., Brenchley, J.M., Hill, B.J., Ambrozak, D.R., Ngai, K.-L., Karandikar, N.J., Casazza, J.P., and Koup, R.A. (2002). A Novel Approach to the Analysis of Specificity, Clonality, and Frequency of HIV-Specific T Cell Responses Reveals a Potential Mechanism for Control of Viral Escape. J. Immunol. *168*, 3099–3104.

Dudley, E.C., Petrie, H.T., Shah, L.M., Owen, M.J., and Hayday, A.C. (1994). T

cell receptor beta chain gene rearrangement and selection during thymocyte development in adult mice. Immunity *1*, 83–93.

Duhen, T., Geiger, R., Jarrossay, D., Lanzavecchia, A., and Sallusto, F. (2009). Production of interleukin 22 but not interleukin 17 by a subset of human skin-homing memory T cells. Nat. Immunol. *10*, 857–863.

Dustin, M. (2014a). The immunological synapse. Cancer Immunol Res *2*, 1023–1033.

Dustin, M.L. (2008). T-cell activation through immunological synapses and kinapses. Immunol. Rev. *221*, 77–89.

Dustin, M.L. (2014b). What counts in the immunological synapse? Mol. Cell *54*, 255–262.

Edgar, J.R., Manna, P.T., Nishimura, S., Banting, G., and Robinson, M.S. (2016). Tetherin is an exosomal tether. Elife *5*, 1–19.

Egorov, E.S., Merzlyak, E.M., Shelenkov, A.A., Britanova, O. V., Sharonov, G. V., Staroverov, D.B., Bolotin, D.A., Davydov, A.N., Barsova, E., Lebedev, Y.B., et al. (2015). Quantitative Profiling of Immune Repertoires for Minor Lymphocyte Counts Using Unique Molecular Identifiers. J. Immunol. *194*, 6155–6163.

Fazilleau, N., Eisenbraun, M.D., Malherbe, L., Ebright, J.N., Pogue-Caley, R.R., McHeyzer-Williams, L.J., and McHeyzer-Williams, M.G. (2007). Lymphoid reservoirs of antigen-specific memory T helper cells. Nat. Immunol. *8*, 753–761.

Fazilleau, N., McHeyzer-Williams, L.J., Rosen, H., and McHeyzer-Williams, M.G. (2009). The function of follicular helper T cells is regulated by the strength of T cell antigen receptor binding. Nat. Immunol. *10*, 375–384.

Förster, R., Schubel, A., Breitfeld, D., Kremmer, E., Renner-Müller, I., Wolf, E., and Lipp, M. (1999). CCR7 coordinates the primary immune response by establishing functional microenvironments in secondary lymphoid organs. Cell *99*, 23–33.

Fujita, T. (2002). Evolution of the lectin - Complement pathway and its role in innate immunity. Nat. Rev. Immunol. *2*, 346–353.

Garcia, K.C., Degano, M., Stanfield, R.L., Brunmark, A., Jackson, M.R., Peterson, P.A., Teyton, L., and Wilson, I.A. (1996). An αβ T Cell Receptor Structure at 2 . 5 Å and Its Orientation in the TCR-MHC Complex. Science (80-.). *274*, 209–219.

Gatto, D., Wood, K., and Brink, R. (2011). EBI2 Operates Independently of but in Cooperation with CXCR5 and CCR7 To Direct B Cell Migration and Organization in Follicles and the Germinal Center. J. Immunol. *187*, 4621–4628.

Gaya, M., Barral, P., Burbage, M., Aggarwal, S., Montaner, B., Warren Navia, A.,

Aid, M., Tsui, C., Maldonado, P., Nair, U., et al. (2018). Initiation of Antiviral B Cell Immunity Relies on Innate Signals from Spatially Positioned NKT Cells. Cell *172*, 517–533.

Geiger, R., Duhen, T., Lanzavecchia, A., and Sallusto, F. (2009). Human naive and memory CD4+ T cell repertoires specific for naturally processed antigens analyzed using libraries of amplified T cells. J. Exp. Med. *206*, 1525–1534.

Germain, R.N., and Stefanová, I. (1999). The dynamics of T cell receptor signaling: Complex Orchestration and the Key Roles of Tempo and Cooperation. Annu. Rev. Immunol. *17*, 467–522.

Gillis, S., and Watson, J. (1980). Biochemical and biological characterization of lymphocyte regulatory molecules. V. Identification of an interleukin 2-producing human leukemia T cell line. J. Exp. Med. *152*, 1709–1719.

Gillis, S., Ferm, M.M., Ou, W., and Smith, K. a (1978). T cell growth factor: parameters of production and a quantitative microassay for activity. J. Immunol. *120*, 2027–2032.

Gong, Y.N., Chen, G.W., and Shih, S.R. (2012). Characterization of subtypes of the influenza A hemagglutinin (HA) gene using profile hidden Markov models. J. Microbiol. Immunol. Infect. *45*, 404–410.

González, P.A., Carreño, L.J., Céspedes, P.F., Bueno, S.M., Riedel, C.A., and Kalergis, A.M. (2013). Modulation of tumor immunity by soluble and membrane-bound molecules at the immunological synapse. Clin. Dev. Immunol. *2013*, 22–26.

Gonzalo, J.-A., Delaney, T., Corcoran, J., Goodearl, A., Gutierrez-Ramos, J.C., and Coyle, A.J. (2001). Cutting Edge: The Related Molecules CD28 and Inducible Costimulator Deliver Both Unique and Complementary Signals Required for Optimal T Cell Activation. J. Immunol. *166*, 1–5.

Gould, S.J., Booth, A.M., and Hildreth, J.E.K. (2003). The Trojan exosome hypothesis. Proc. Natl. Acad. Sci. *100*, 10592–10597.

Graham, M.B., Braciale, V.L., and Braciale, T.J. (1994). Influenza Virus-specific CD4+ T Helper Type 2 T Lymphocytes Do Not Promote Recovery from Experimental Virus Infection. J Exp Med *179*.

Grant, E.J., Chen, L., Quinones-Parra, S., Pang, K., Kedzierska, K., and Chen, W. (2014). T-Cell Immunity to Influenza A Viruses. Crit. Rev. Immunol. *34*, 15–39.

Grivel, J.-C., and Margolis, L. (2009). Use of human tissue explants to study human infectious agents. Nat. Protoc. *4*, 256–269.

Groom, J.R., and Luster, A.D. (2011a). CXCR3 ligands: redundant, collaborative and antagonistic functions. Immunol. Cell Biol. *89*.

Groom, J.R., and Luster, A.D. (2011b). CXCR3 in T cell function. Exp Cell Res *317*, 620–631.

Hale, J.S., and Ahmed, R. (2015). Memory T follicular helper CD4 T cells. Front. Immunol. *6*, 1–9.

Hale, J.S., Youngblood, B., Latner, D.R., Mohammed, A.U.R., Ye, L., Akondy, R.S., Wu, T., Iyer, S.S., and Ahmed, R. (2013). Distinct memory CD4+ T cells with commitment to T follicular helper- and Thelper 1-cell lineages are generated after acute viral infection. Immunity *38*, 805–817.

Haley, S.L., Tzvetkov, E.P., Meuwissen, S., Plummer, J.R., and McGettigana, J.P. (2017). Targeting Vaccine-Induced Extrafollicular Pathway of B Cell Differentiation Improves Rabies Postexposure Prophylaxis. J. Virol. *91*, 1–13.

Hamada, H., Bassity, E., Flies, A., Strutt, T.M., Garcia-Hernandez, M. d. L., McKinstry, K.K., Zou, T., Swain, S.L., and Dutton, R.W. (2013). Multiple Redundant Effector Mechanisms of CD8+ T Cells Protect against Influenza Infection. J. Immunol. *190*, 296–306.

Hammarlund, E., Lewis, M.W., Hansen, S.G., Strelow, L.I., Nelson, J.A., Sexton, G.J., Hanifin, J.M., and Slifka, M.K. (2003). Duration of antiviral immunity after smallpox vaccination. Nat. Med. *9*, 1131–1137.

Hansen, D.S., Obeng-adjei, N., Ly, A., Ioannidis, L.J., and Crompton, P.D. (2016). Emerging concepts in T follicular helper cell responses to malaria. Int. J. Parasitol.

Hansen, D.S., Obeng-adjei, N., Ly, A., Ioannidis, L.J., and Crompton, P.D. (2017). Emerging concepts in T follicular helper cell responses to malaria. Int. J. Parasitol. *47*, 105–110.

Hansen, S.G., Sacha, J.B., Hughes, C.M., Ford, J.C., Burwitz, B.J., Scholz, I., Gilbride, R.M., Lewis, M.S., Gilliam, A.N., Ventura, A.B., et al. (2013). Cytomegalovirus Vectors Violate CD8+ T Cell Epitope Recognition Paradigms. Science (80-.). *340*, 1–17.

Hargreaves, D.C., Hyman, P.L., Lu, T.T., Ngo, V.N., Bidgol, A., Suzuki, G., Zou, Y., Littman, D.R., and Cyster, J.G. (2001). A Coordinated Change in Chemokine Responsiveness Guides Plasma Cell Movements. *194*.

Harrell, F.E. (2013). Regression Modeling Strategies: With Applications to Linear Models, Logistic Regression, and Survival Analysis.

Hataye, J., Moon, J.J., Khoruts, A., Reilly, C., and Jenkins, M.K. (2006). Naive and Memory CD4+ T cell survival controlled by clonal abundance. Science (80-.). *312*, 114–117.

Havenar-daughton, C., Carnathan, D.G., Sanders, R.W., Silvestri, G., Pauthner, M., and Briney, B. (2016). Direct Probing of Germinal Center Responses Reveals

Immunological Features and Bottlenecks for Neutralizing Antibody Responses to HIV Env Trimer Article Direct Probing of Germinal Center Responses Reveals Immunological Features and Bottlenecks for Neutral. 2195–2209.

Havenar-Daughton, C., Carnathan, D.G., Torrents, A., Peña, D., Gils, M.J. Van, Rosales, S., Woude, P. Van Der, Locci, M., Khoa, M., Gumber, S., et al. (2016). Direct probing of germinal center responses reveals immunological features and bottlenecks for neutralizing antibody responses to HIV Env trimer. Cell Rep. *17*, 2195–2209.

Havenith, S.H.C., Remmerswaal, E.B.M., Idu, M.M., van Donselaar-van der Pant, K. a M.I., Van der Bom, N., Bemelman, F.J., Van Leeuwen, E.M.M., Ten Berge, I.J.M., and Van Lier, R. a W. (2014). CXCR5+CD4+ follicular helper T cells accumulate in resting human lymph nodes and have superior B cell helper activity. Int. Immunol. *26*, 183–192.

Hayday, A.C., Barber, D.F., Douglas, N., and Hoffman, E.S. (1999). Signals involved in gamma/delta T cell versus alpha/beta T cell lineage commitment. Semin. Immunol. *11*, 239–249.

Haynes, N.M., Allen, C.D.C., Lesley, R., Ansel, K.M., Killeen, N., and Cyster, J.G. (2007). Role of CXCR5 and CCR7 in Follicular Th Cell Positioning and Appearance of a Programmed Cell Death Gene-1 ^{High} Germinal Center-Associated Subpopulation. J. Immunol. *179*, 5099–5108.

He, J., Tsai, L.M., Leong, Y.A., Hu, X., Ma, C.S., Chevalier, N., Sun, X., Vandenberg, K., Rockman, S., Ding, Y., et al. (2013). Circulating precursor CCR7loPD-1hi CXCR5+ CD4+ T cells indicate tfh cell activity and promote antibody responses upon antigen reexposure. Immunity *39*, 770–781.

Heath, W.R., Carbone, F.R., Walter, T., Hall, E., and Royal, P.O. (2001). Cross-presentation in viral immunity and self-tolerance. Nat. Rev. Immunol. *1*, 126–135.

Heesters, B.A., Myers, R.C., and Carroll, M.C. (2014). Follicular dendritic cells: dynamic antigen libraries. Nat. Rev. Immunol. *14*, 495–504.

Heesters, B.A., Poel, C.E. Van Der, Das, A., and Carroll, M.C. (2016). Antigen Presentation to B Cells. Trends Immunol. *37*, 844–854.

Hegazy, A.N., Peine, M., Helmstetter, C., Panse, I., Fröhlich, A., Bergthaler, A., Flatz, L., Pinschewer, D.D., Radbruch, A., and Löhning, M. (2010). Interferons Direct Th2 Cell Reprogramming to Generate a Stable GATA-3+T-bet+ Cell Subset with Combined Th2 and Th1 Cell Functions. Immunity *32*, 116–128.

Heissmeyer, V., and Vogel, K.U. (2013). Molecular control of Tfh-cell differentiation by Roquin family proteins. Immunol. Rev. *253*, 273–289.

Heit, A., Schmitz, F., Gerdts, S., Flach, B., Moore, M.S., Perkins, J.A., Robins, H.S., Aderem, A., Spearman, P., Tomaras, G.D., et al. (2017). Vaccination

establishes clonal relatives of germinal center T cells in the blood of humans. J. Exp. Med. *214*, 2139–2152.

Herati, R.S., Muselman, A., Vella, L., Bengsch, B., Parkhouse, K., Alcazar, D. Del, Kotzin, J., Doyle, S.A., Tebas, P., Hensley, S.E., et al. (2017). Successive annual influenza vaccination induces a recurrent oligoclonotypic memory response in circulating T follicular helper cells. *2152*.

Hess, C., Sadallah, S., Hefti, A., Landmann, R., and Jurg-Alfred, S. (1999). Ectosomes Released by Human Neutrophils ar Specialized Functional Units. J. Immunol. *163*, 4564–4573.

Heyman, B. (2000). Regulation of antibody responses via antibodies, complement, and Fc receptors. Annu. Rev. Immunol. *18*, 709–737.

Hornef, M.W., Wick, M.J., Rhen, M., and Normark, S. (2002). Bacterial strategies for overcoming host innate and adaptive immune responses. Nat Immunol *3*, 1033–1040.

Hosken, N.A., Shibuya, K., Heath, A.W., Murphy, K.M., and O'Garra, A. (1995). The Effect of Antigen Dose on CD4 + T Helper Cell Phenotype Development in a T Cell Receptor-AlphaBeta-transgenic Model. J. Exp. Med. *184*, 0–5.

Hui, E., Cheung, J., Zhu, J., Su, X., Taylor, M.J., Wallweber, H.A., Sasmal, D.K., Huang, J., Kim, J.M., Mellman, I., et al. (2017). T cell costimulatory receptor CD28 is a primary target for PD-1 – mediated inhibition. Sci. Rep. *4*, 1428–1433.

Ikawa, T. (2010). An Essential Developmental Checkpoint for Production of the T Cell Lineage Tomokatsu Ikawa,. *93*, 93–97.

Influenza Research Database (2018). www.fludb.org.

Ise, W., Fujii, K., Shiroguchi, K., Ito, A., Kometani, K., Takeda, K., Kawakami, E., Yamashita, K., Suzuki, K., Okada, T., et al. (2018). T Follicular Helper Cell-Germinal Center B Cell Interaction Strength Regulates Entry into Plasma Cell or Recycling Germinal Center Cell Fate. Immunity *48*, 702–715.e4.

Itano, A.A., and Jenkins, M.K. (2003). Antigen presentation to naive CD4 T cells in the lymph node. Nat. Immunol. *4*, 733–739.

Izraelson, M., Nakonechnaya, T.O., Moltedo, B., Egorov, E.S., Kasatskaya, S.A., Putintseva, E. V, Mamedov, I.Z., Staroverov, D.B., Shemiakina, I.I., Zakharova, M.Y., et al. (2017). Comparative analysis of murine T-cell receptor repertoires. Immunology *140*, 874–888.

Johnston, R.J., Poholek, A.C., DiToro, D., Yusuf, I., Eto, D., Barnett, B., Dent, A.L., Craft, J., and Crotty, S. (2009). Bcl6 and Blimp-1 are reciprocal and antagonistic regulators of T follicular helper cell differentiation. Science *325*, 1006–1010.

Johnston, R.J., Choi, Y.S., Diamond, J. a., Yang, J. a., and Crotty, S. (2012). STAT5 is a potent negative regulator of TFH cell differentiation. J. Exp. Med. *209*, 243–250.

Josefowicz, S.Z., Lu, L.-F., and Rudensky, A.Y. (2012). Regulatory T Cells: Mechanisms of Differentiation and Function. Annu. Rev. Immunol. *30*, 531–564.

Jung, S., Rajewsky, K., and Radbruch, A. (1993). Shutdown of class switch recombination by deletion of a switch region control element. Science. *259*, 984–987.

Kaplan, M.H., Schindler, U., Smiley, S.T., and Grusby, M.J. (1996). Stat6 is required for mediating responses to IL-4 and for the development of Th2 cells. Immunity *4*, 313–319.

Katz, D., Hamaoka, T., and Benacerraf, B. (1973). Cell interactions between histoincompatible T and B lymphocytes. II. Failure of physiologic cooperative interactions between T and B lymphocytes from allogeneic donor strains in humoral response to hapten-protein conjugates. J. Exp. Med. *137*, 1405–1418.

Kavaler, J., Davis, M., and Chien, Y. (1984). Localization of a T-cell receptor diversity-region element. Nature *310*, 421–423.

Kim, C.H., Rott, L.S., Clark-Lewis, I., Campbell, D.J., Wu, L., and Butcher, E.C. (2001). Subspecialization of CXCR5+ T cells: B helper activity is focused in a germinal center-localized subset of CXCR5+ T cells. J. Exp. Med. *193*, 1373–1381.

Kim, C.H., Lim, H.W., Kim, J.R., Rott, L., Hillsamer, P., and Butcher, E.C. (2017). Unique gene expression program of human germinal center T helper cells. Blood *104*, 1952–1961.

Kim, Y., Ponomarenko, J., Zhu, Z., Tamang, D., Wang, P., Greenbaum, J., Lundegaard, C., Sette, A., Lund, O., Bourne, P.E., et al. (2012). Immune Epitope Database and Analysis Resource. Nucleic Acids Res. *40*, 525–530.

Kitano, M., Moriyama, S., Ando, Y., Hikida, M., Mori, Y., Kurosaki, T., and Okada, T. (2011). Bcl6 Protein Expression Shapes Pre-Germinal Center B Cell Dynamics and Follicular Helper T Cell Heterogeneity. Immunity *34*, 961–972.

Klein, U., and Dalla-Favera, R. (2008). Germinal centres: Role in B-cell physiology and malignancy. Nat. Rev. Immunol. *8*, 22–33.

Klein, U., Rajewsky, K., and Küppers, R. (1998). Human Immunoglobulin (Ig)M $^{+}$ IgD $^{+}$ Peripheral Blood B Cells Expressing the CD27 Cell Surface Antigen Carry Somatically Mutated Variable Region Genes: CD27 as a General Marker for Somatically Mutated (Memory) B Cells. J. Exp. Med. *188*, 1679–1689.

Koch, U., and Radtke, F. (2011). Mechanisms of T Cell Development and Transformation. Annu. Rev. Cell Dev. Biol. *27*, 539–562.

Koh, A.S., Kuo, A.J., Park, S.Y., Cheung, P., Abramson, J., Bua, D., Carney, D., Shoelson, S.E., Gozani, O., Kingston, R.E., et al. (2008). Aire employs a histone-binding module to mediate immunological tolerance, linking chromatin regulation with organ-specific autoimmunity. Proc. Natl. Acad. Sci. *105*, 15878–15883.

Kong, F.K., Chen, C.L., Six, a, Hockett, R.D., and Cooper, M.D. (1999). T cell receptor gene deletion circles identify recent thymic emigrants in the peripheral T cell pool. Proc. Natl. Acad. Sci. U. S. A. *96*, 1536–1540.

Kreijtz, J.H.C.M., Fouchier, R.A.M., and Rimmelzwaan, G.F. (2011). Immune responses to influenza virus infection. Virus Res. *162*, 19–30.

Kroenke, M.A., Eto, D., Locci, M., Cho, M., Davidson, T., Haddad, E.K., and Crotty, S. (2012). Bcl6 and Maf cooperate to instruct human follicular helper CD4 T cell differentiation. J. Immunol. *188*, 3734–3744.

Kurosawa, Y., Von Boehmer, H., Haas, W., Sakano, H., Trauneker, A., and Tonegawa, S. (1981). Identification of D segments of immunoglobulin heavy-chain genes and their rearrangement in T lymphocytes. Nature *290*, 565–570.

Lanzavecchia, A. (1999). Three Signals and a Master Switch in the Regulation of T-cell Immunity. Cold Spring Harb Symp Quant Biol *64*, 253–258.

Lanzavecchia, A., and Sallusto, F. (2009). Human B cell memory. Curr. Opin. Immunol. *21*, 298–304.

Lee, J.G., Jang, J.Y., Fang, T., Xu, Y., Yan, J.J., Ryu, J.H., Jeon, H.J., Koo, T.Y., Kim, D.K., Oh, K.H., et al. (2018). Identification of human B-1 helper T cells with a Th1-like memory phenotype and high integrin CD49d expression. Front. Immunol. *9*, 1–13.

Lee, S.K., Rigby, R.J., Zotos, D., Tsai, L.M., Kawamoto, S., Marshall, J.L., Ramiscal, R.R., Chan, T.D., Gatto, D., Brink, R., et al. (2011). B cell priming for extrafollicular antibody responses requires Bcl-6 expression by T cells. J. Exp. Med. *208*, 1377–1388.

Lee, S.K., Silva, D.G., Martin, J.L., Pratama, A., Hu, X., Chang, P.P., Walters, G., and Vinuesa, C.G. (2012). Interferon-γ Excess Leads to Pathogenic Accumulation of Follicular Helper T Cells and Germinal Centers. Immunity *37*, 880–892.

Lefranc, M.P., Giudicelli, V., Kaas, Q., Duprat, E., Jabado-Michaloud, J., Scaviner, D., Ginestoux, C., Clement, O., Chaume, D., and Lefranc, G. (2003). IMGT, the international ImMunoGeneTics database®. Nucleic Acids Res. *33*, 307–310.

Li, X., Wu, Z., Ding, J., Zheng, Z., Li, X., Chen, L., and Zhu, P. (2012). Role of the frequency of blood CD4 + CXCR5 + CCR6 + T cells in autoimmunity in patients with Sjögren ' s syndrome. Biochem. Biophys. Res. Commun. *422*, 238–244.

Lindestam Arlehamn, C.S., Gerasimova, A., Mele, F., Henderson, R., Swann, J., Greenbaum, J.A., Kim, Y., Sidney, J., James, E.A., Taplitz, R., et al. (2013). Memory T Cells in Latent Mycobacterium tuberculosis Infection Are Directed against Three Antigenic Islands and Largely Contained in a CXCR3+CCR6+Th1 Subset. PLoS Pathog. *9*.

Linsley, P.S., Greene, J.L., Brady, W., Bajorath, J., Ledbetter, J.A., and Peach, R. (1994). Human B7-1 (CD80) and B7-2 (CD86) bind with similar avidities but distinct kinetics to CD28 and CTLA-4 receptors. Immunity *1*, 793–801.

Linterman, M.A., Beaton, L., Yu, D., Ramiscal, R.R., Srivastava, M., Hogan, J.J., Verma, N.K., Smyth, M.J., Rigby, R.J., and Vinuesa, C.G. (2010). IL-21 acts directly on B cells to regulate Bcl-6 expression and germinal center responses. J. Exp. Med. *207*, 353–363.

Linterman, M.A., Denton, A.E., Divekar, D.P., Zvetkova, I., Kane, L., Ferreira, C., Veldhoen, M., Clare, S., Dougan, G., Espéli, M., et al. (2014). CD28 expression is required after T cell priming for helper T cell responses and protective immunity to infection. Elife *3*, 1–21.

Linterman, M. a, Pierson, W., Lee, S.K., Kallies, A., Kawamoto, S., Rayner, T.F., Srivastava, M., Divekar, D.P., Beaton, L., Jennifer, J., et al. (2012). Foxp3 + follicular regulatory T cells control T follicular helper cells and the germinal center response. Nat. Med. *17*, 975–982.

Liu, X., Yan, X., Zhong, B., Nurieva, R.I., Wang, A., Wang, X., Martin-orozco, N., Wang, Y., Chang, S.H., Esplugues, E., et al. (2012). Bcl6 expression specifies the T follicular helper cell program in vivo. J. Exp. Med. *209*, 1841–1852.

Liu, X., Chen, X., Zhong, B., Wang, A., Wang, X., Chu, F., Nurieva, R.I., Yan, X., Chen, P., van der Flier, L.G., et al. (2014). Transcription factor achaete-scute homologue 2 initiates follicular T-helper-cell development. Nature *507*, 513–518.

Liu, Y., Yang, B., Zhou, M., Li, L., Zhou, H., Zhang, J., Chen, H., and Wu, C. (2009). Memory IL-22-producing CD4+T cells specific for Candida albicans are present in humans. Eur. J. Immunol. *39*, 1472–1479.

Liu, Y.J., Joshua, D.E., Williams, G.T., Smith, C.A., Gordon, J., and MacLennan, I.C.M. (1989). Mechanism of antigen-driven selection in germinal centres. Nature *342*, 929–931.

Locci, M., Havenar-daughton, C., Landais, E., Wu, J., Mark, A., Arlehamn, C.L., Su, L.F., Cubas, R., and Davis, M.M. (2013). Human Circulating PD-1+ CXCR3– CXCR5+ Memory Tfh Cells Are Highly Functional and Correlate with Broadly Neutralizing HIV Antibody Responses. Immunity *39*, 758–769.

Locci, M., Wu, J.E., Arumemi, F., Mikulski, Z., Dahlberg, C., Miller, A.T., and Crotty, S. (2016). Activin A programs the differentiation of human TFH cells. Nat.

Immunol. *17*, 976–984.

Lorenz, U. (2009). SHP-1 and SHP-2 in T cells: two phosphatases functioning at many levels. Immunol. Rev. *46*, 26–29.

Ma, C.S., Suryani, S., Avery, D.T., Chan, A., Nanan, R., Santner-Nanan, B., Deenick, E.K., and Tangye, S.G. (2009). Early commitment of naive human CD4+T cells to the T follicular helper (Tfh) cell lineage is induced by IL-12. Immunol. Cell Biol. *87*, 590–600.

Maceiras, A.R., Almeida, S.C.P., Mariotti-Ferrandiz, E., Chaara, W., Jebbawi, F., Six, A., Hori, S., Klatzmann, D., Faro, J., and Graca, L. (2017). T follicular helper and T follicular regulatory cells have different TCR specificity. Nat. Commun. *8*, 1–12.

MacLennan, I.C.M., Toellner, K.-M., Cunningham, A.F., Serre, K., Sze, D.M.-Y., Zuniga, E., Cook, M.C., and Vinuesa, C.G. (2003). Extrafollicular antibody responses. Immunol. Rev. *194*, 8–18.

Macleod, M.K.L., David, A., Mckee, A.S., Crawford, F., Kappler, J.W., Marrack, P., Macleod, M.K.L., David, A., Mckee, A.S., Crawford, F., et al. (2011). Memory CD4 T Cells That Express CXCR5 Provide Accelerated Help to B Cells. J. Immunol. *186*, 2889–2896.

Mahe, E., Pugh, T., and Kamel-Reid, S. (2018). T cell clonality assessment: past, present and future. J. Clin. Pathol. *71*, 195–200.

Malherbe, L., Hausl, C., Teyton, L., and McHeyzer-Williams, M.G. (2004). Clonal selection of helper T cells is determined by an affinity threshold with no further skewing of TCR binding properties. Immunity *21*, 669–679.

Mamedov, I.Z., Britanova, O. V., Zvyagin, I. V., Turchaninova, M.A., Bolotin, D.A., Putintseva, E. V., Lebedev, Y.B., and Chudakov, D.M. (2013). Preparing unbiased T-cell receptor and antibody cDNA libraries for the deep next generation sequencing profiling. Front. Immunol. *4*, 1–10.

Marinov, G.K., Williams, B.A., McCue, K., Schroth, G.P., Gertz, J., Myers, R.M., and Wold, B.J. (2014). From single-cell to cell-pool transcriptomes: Stochasticity in gene expression and RNA splicing. Genome Res. *24*, 496–510.

Marrack, P., Scott-Browne, J.P., Dai, S., Gapin, L., and Kappler, J.W. (2008). Evolutionarily Conserved Amino Acids That Control TCR-MHC Interaction. Annu. Rev. Immunol. *26*, 171–203.

Mason, D. (1998). A very high level of crossreactivity is an essential feature of the T- cell receptor. Immunol. Today *19*, 395–404.

McHeyzer-Williams, M.G., and Davis, M.M. (1995). Antigen-specific development of primary and memory T cells in vivo. Science (80-.). *268*.

McHeyzer-Williams, L.J., Panus, J.F., Mikszta, J.A., and McHeyzer-Williams, M.G. (1999). Evolution of Antigen-specific T Cell Receptors In Vivo: Preimmune and Antigen-driven Selection of Preferred Complementarity-determining Region 3 (CDR3) Motifs. J. Exp. Med. *189*, 1823–1838.

McKinney, D.M., Southwood, S., Hinz, D., Oseroff, C., Arlehamn, C.S.L., Schulten, V., Taplitz, R., Broide, D., Hanekom, W.A., Scriba, T.J., et al. (2013). A strategy to determine HLA class II restriction broadly covering the DR, DP, and DQ allelic variants most commonly expressed in the general population. Immunogenetics *65*, 357–370.

Mcvernon, J., Laurie, K., Faddy, H., Irving, D., Nolan, T., Barr, I., and Kelso, A. (2014). Seroprevalence of antibody to influenza A(H1N1)pdm09 attributed to vaccination or infection, before and after the second (2010) pandemic wave in Australia. Influenza Other Respi. Viruses *8*, 194–200.

Mele, F., Fornara, C., Jarrossay, D., Furione, M., Arossa, A., Spinillo, A., Lanzavecchia, A., Gerna, G., Sallusto, F., and Lilleri, D. (2017). Phenotype and specificity of T cells in primary human cytomegalovirus infection during pregnancy: IL-7Rpos long-term memory phenotype is associated with protection from vertical transmission. PLoS One *12*, e0187731.

Mesin, L., Ersching, J., and Victora, G.D. (2016). Germinal Center B Cell Dynamics. Immunity *45*, 471–482.

Michie, C.A., McLean, A., Alcock, C., and Beverley, P.C.L. (1992). Lifespan of human lymphocyte subsets defined by CD45 isoforms. Nature *360*, 264–265.

Mitchell, B.Y.G.F., and Miller, J.F.A.P. (1968a). Cell to cell interaction in the immune response. II. The source of hemolysin-forming cells in irradiated mice given bone marrow and thymus or thoracic duct lymphocytes. J.Exp.Med. 821–837.

Mitchell, G.F., and Miller, J.F.A.P. (1968b). Cell to cell interaction in the immune response. I. Hemolysin-forming cells in neonatally thymectomized mice reconstituted with thymus or thoracic duct lymphocytes. J.Exp.Med. *128*, 801–820.

Mittelbrunn, M., Gutiérrez-Vázquez, C., Villarroya-Beltri, C., González, S., Sánchez-Cabo, F., González, M.Á., Bernad, A., and Sánchez-Madrid, F. (2011). Unidirectional transfer of microRNA-loaded exosomes from T cells to antigen-presenting cells. Nat. Commun. *2*.

Mittrücker, H.-W., Visekruna, A., and Huber, M. (2014). Heterogeneity in the Differentiation and Function of CD8+ T Cells. Arch. Immunol. Ther. Exp. (Warsz). *62*, 449–458.

Miura, K., Orcutt, A.C., Muratova, O. V., Miller, L.H., Saul, A., and Long, C.A. (2008). Development and characterization of a standardized ELISA including a reference serum on each plate to detect antibodies induced by experimental malaria

vaccines. Vaccine *26*, 193–200.

Moore, A., McGuirk, P., Adams, S., Jones, W.C., Paul McGee, J., O'Hagan, D.T., and Mills, K.H.G. (1995). Immunization with a soluble recombinant HIV protein entrapped in biodegradable microparticles induces HIV-specific CD8+cytotoxic T lymphocytes and CD4+Th1 cells. Vaccine *13*, 1741–1749.

Morita, R., Schmitt, N., Bentebibel, S.-E., Ranganathan, R., Bourdery, L., Zurawski, G., Foucat, E., Dullaers, M., Oh, S., Sabzghabaei, N., et al. (2011). Human Blood CXCR5+CD4+ T Cells Are Counterparts of T Follicular Cells and Contain Specific Subsets that Differentially Support Antibody Secretion. Immunity *34*, 108–121.

Moseman, E.A., Iannacone, M., Bosurgi, L., Tonti, E., Chevrier, N., Tumanov, A., Fu, Y.X., Hacohen, N., and von Andrian, U.H. (2012). B Cell Maintenance of Subcapsular Sinus Macrophages Protects against a Fatal Viral Infection Independent of Adaptive Immunity. Immunity *36*, 415–426.

Murali-Krishna, K., Altman, J.D., Suresh, M., Sourdive, D.J.D., Zajac, A.J., Miller, J.D., Slansky, J., and Ahmed, R. (1998). Counting antigen-specific CD8 T cells: A reevaluation of bystander activation during viral infection. Immunity *8*, 177–187.

Murphy, K. (2012). Janeway's Immunobiology.

Murray, R., Suda, T., Wrighton, N., Lee, F., and Zlotnik, A. (1989). IL-7 is a growth and maintenance factor for mature and immature thymocyte subsets. Int. Immunol. *1*, 526–531.

Nikolich-Zugich, J., Slifka, M.K., and Messaoudi, I. (2004). The many important facets of T-cell repertoire diversity. Nat. Rev. Immunol. *4*, 123–132.

Di Niro, R., Lee, S.J., Vander Heiden, J.A., Elsner, R.A., Trivedi, N., Bannock, J.M., Gupta, N.T., Kleinstein, S.H., Vigneault, F., Gilbert, T.J., et al. (2015). Salmonella Infection Drives Promiscuous B Cell Activation Followed By Extrafollicular Affinity Maturation. Immunity *43*, 120–131.

Noelle, R.J., Roy, M., Shepherd, D.M., Stamenkovic, I., Ledbetter, J.A., and Aruffo, A. (1992). A 39-kDa protein on activated helper T cells binds CD40 and transduces the signal for cognate activation of B cells. Proc. Natl. Acad. Sci. U. S. A. *89*, 6550–6554.

Nograles, K.E., Zaba, L.C., Shemer, A., Fuentes-Duculan, J., Cardinale, I., Kikuchi, T., Ramon, M., Bergman, R., Krueger, J.G., and Guttman-Yassky, E. (2009). IL-22-producing "T22" T cells account for upregulated IL-22 in atopic dermatitis despite reduced IL-17-producing TH17 T cells. J. Allergy Clin. Immunol. *123*, 1244–1252.e2.

Nossal, G.J., Cunningham, A., Mitchell, B.Y.G.F., and Miller, J.F.A.P. (1968).

Cell to cell interaction in the immune response. 3. Chromosomal marker analysis of single antibody-forming cells in reconstituted, irradiated, or thymectomized mice. J.Exp.Med. *128*, 839–853.

Nurieva, R., Chung, Y., Hwang, D., Yang, X., Kang, H., Ma, L., Wang, Y., Watowich, S., Jetten, A.M., Tian, Q., et al. (2008). Generation of T Follicular Helper Cells Is Mediated by Interleukin-21 but Independent of T Helper 1, 2, or 17 Cell Lineages. Immunity *29*, 138–149.

Nurieva, R.I., Chung, Y., Martinez, G.J., Yang, X.O., Tanaka, S., Matskevitch, T.D., Wang, Y., and Dong, C. (2009). Bcl6 mediates the development of T follicular helper cells. Science (80-.). *325*, 1001–1005.

O'Shea, J.J.O., Cells, C.D.T., and Paul, W.E. (2010). Commitment and Plasticity of Helper. Science (80-.). *327*, 1098–1102.

Obeng-Adjei, N., Portugal, S., Tran, T.M., Yazew, T.B., Skinner, J., Li, S., Jain, A., Felgner, P.L., Doumbo, O.K., Kayentao, K., et al. (2015). Circulating Th1-Cell-type Tfh Cells that Exhibit Impaired B Cell Help Are Preferentially Activated during Acute Malaria in Children. Cell Rep. 1–15.

Obst, R., van Santen, H.-M., Mathis, D., and Benoist, C. (2005). Antigen persistence is required throughout the expansion phase of a CD4 $^{+}$ T cell response. J. Exp. Med. *201*, 1555–1565.

Odegard, J.M., Marks, B.R., DiPlacido, L.D., Poholek, A.C., Kono, D.H., Dong, C., Flavell, R.A., and Craft, J. (2008). ICOS-dependent extrafollicular helper T cells elicit IgG production via IL-21 in systemic autoimmunity. J. Exp. Med. *205*, 2873–2886.

Okada, T., Miller, M.J., Parker, I., Krummel, M.F., Neighbors, M., Hartley, S.B., O'Garra, A., Cahalan, M.D., and Cyster, J.G. (2005). Antigen-engaged B cells undergo chemotaxis toward the T zone and form motile conjugates with helper T cells. PLoS Biol. *3*, 1047–1061.

Okazaki, T., and Honjo, T. (2006). The PD-1-PD-L pathway in immunological tolerance. Trends Immunol. *27*, 195–201.

Okazaki, H., Ito, M., Sudo, T., Hattori, M., Kano, S., Katsura, Y., and Minato, N. (1989). IL-7 promotes thymocyte proliferation and maintains immunocompetent thymocytes bearing alpha beta or gamma delta T-cell receptors in vitro: synergism with IL-2. J Immunol *143*, 2917–2922.

Org, T., Chignola, F., Hetényi, C., Gaetani, M., Rebane, A., Liiv, I., Maran, U., Mollica, L., Bottomley, M.J., Musco, G., et al. (2008). The autoimmune regulator PHD finger binds to non-methylated histone H3K4 to activate gene expression. EMBO Rep. *9*, 370–376.

Padovan, E., Casorati, G., Dellabona, P., Meyer, S., Brockhaus, M., and

Lanzavecchia, A. (1993). Expression of Two T Cell Receptor α Chains : Dual Receptor T Cells. Science *262*, 422–424.

Palladino, G., Scherle, P.A., and Gerhard, W. (1991). Activity of CD4+ T-cell clones of type 1 and type 2 in generation of influenza virus-specific cytotoxic responses in vitro. J. Virol. *65*, 6071–6076.

Papa, I., Saliba, D., Ponzoni, M., Bustamante, S., Canete, P.F., Gonzalez-Figueroa, P., McNamara, H.A., Valvo, S., Grimbaldeston, M., Sweet, R.A., et al. (2017). TFH-derived dopamine accelerates productive synapses in germinal centres. Nature *547*, 318–323.

Paul, S., Dillon, M.B.C., Lindestam Arlehamn, C.S., Huang, H., Davis, M.M., McKinney, D.M., Scriba, T.J., Sidney, J., Peters, B., and Sette, A. (2015). A Population Response Analysis Approach To Assign Class II HLA-Epitope Restrictions. J. Immunol. *194*, 6164–6176.

Pedersen, G.K., Sjursen, H., Nøstbakken, J.K., Jul-Larsen, A., Hoschler, K., and Cox, R.J. (2014). Matrix M^{TM} adjuvanted virosomal H5N1 vaccine induces balanced Th1/Th2 CD4+T cell responses in man. Hum. Vaccines Immunother. *10*, 2408–2416.

Pepper, M., and Jenkins, M. (2011). Origins of CD4(+) effector and central memory T cells. Nat. Immunol. *12*, 467–471.

Petrie, H.T., Livak, F., Schatz, D.G., Strasser, A., Crispe, I.N., and Shortman, K. (1993). Multiple Rearrangements in T Cell Receptor alpha Chain Genes Maximize the Production of useful Thymocytes. J. Exp. Med. *178*, 615–622.

Pico de Coaña, Y., Choudhury, A., and Kiessling, R. (2015). Checkpoint blockade for cancer therapy: Revitalizing a suppressed immune system. Trends Mol. Med. *21*, 482–491.

Pilzer, D., Gasser, O., Moskovich, O., Schifferli, J.A., and Fishelson, Z. (2005). Emission of membrane vesicles: Roles in complement resistance, immunity and cancer. Springer Semin. Immunopathol. *27*, 375–387.

Plank, M.W., Kaiko, G.E., Maltby, S., Weaver, J., Tay, H.L., Shen, W., Wilson, M.S., Durum, S.K., and Foster, P.S. (2017). Th22 Cells Form a Distinct Th Lineage from Th17 Cells In Vitro with Unique Transcriptional Properties and Tbet-Dependent Th1 Plasticity. J. Immunol. *198*, 2182–2190.

Ploquin, M.J.-Y., Eksmond, U., and Kassiotis, G. (2011). B Cells and TCR Avidity Determine Distinct Functions of CD4+ T Cells in Retroviral Infection. J. Immunol. *187*, 3321–3330.

Poholek, A.C., Hansen, K., Hernandez, S.G., Eto, D., Chandele, A., Weinstein, J.S., Dong, X., Odegard, J.M., Kaech, S.M., Dent, A.L., et al. (2010a). In Vivo

Regulation of Bcl6 and T Follicular Helper Cell Development. J. Immunol. *185*, 313–326.

Poholek, A.C., Hansen, K., Hernandez, S.G., Eto, D., Chandele, A., Weinstein, J.S., Dong, X., Odegard, J.M., Kaech, S.M., Dent, A.L., et al. (2010b). In vivo regulation of Bcl6 and T follicular helper cell development. J. Immunol. *185*, 313–326.

Prasad, R., Narasimhan, R., Sankaran, V., and Veliath, A. (1996). Fine-needle aspiration cytology in the diagnosis of superficial lymphadenopathy: an analysis of 2,418 cases. Diagn. Cytopathol. *15*, 382–386.

Precopio, M.L., Butterfield, T.R., Casazza, J.P., Little, S.J., Richman, D.D., Koup, R.A., and Roederer, M. (2008). Optimizing peptide matrices for identifying T-cell antigens. Cytometry. A *73*, 1071–1078.

Puel, A., Cypowyj, S., Bustamante, J., Wright, J.F., Liu, L., Kyung Lim, H., Migaud, M., Israel, L., Chrabieh, M., Audry, M., et al. (2011). Chronic Mucocutaneous Candidiasis in Humans with Inborn Errors of Interleukin-17 Immunity. Science (80-.). 65–69.

Quigley, M.F., Almeida, J.R., Price, D.A., and Douek, D.C. (2011). Unbiased Molecular Analysis of T Cell Receptor Expression Using Template-Switch Anchored RT-PCR. Curr. Protoc. Immunol. 1–16.

Raeber, M.E., Zurbuchen, Y., Impellizzieri, D., and Boyman, O. (2018). The role of cytokines in T-cell memory in health and disease. Immunol. Rev. *283*, 176–193.

Rao, D.A. (2018). T Cells That Help B Cells in Chronically Inflamed Tissues. Front. Immunol. *9*.

Reimer, D., Lee, A.Y.S., Bannan, J., Fromm, P., Kara, E.E., Comerford, I., Mccoll, S., Wiede, F., Mielenz, D., and Körner, H. (2017). Early CCR6 expression on B cells modulates germinal centre kinetics and efficient antibody responses. 33–41.

Reinhardt, R.L., Khoruts, A., Merica, R., Zell, T., and Jenkins, M.K. (2001). Visualizing the generation of memory CD4 T-cells in the whole body. Nature *410*, 101–105.

Reinhardt, R.L., Liang, H., and Locksley, R.M. (2009). Cytokine-secreting follicular T cells shape the antibody repertoire. Nat. Immunol. *10*, 385–393.

Revy, P., Muto, T., Levy, Y., Geissmann, F., Plebani, A., Sanal, O., Catalan, N., Forveille, M., Dufourcq-Lagelouse, R., Gennery, A., et al. (2000). Activation-induced cytidine deaminase (AID) deficiency causes the autosomal recessive form of the hyper-IgM syndrome (HIGM2). Cell *102*, 565–575.

Rivino, L., Messi, M., Jarrossay, D., Lanzavecchia, A., Sallusto, F., and Geginat, J. (2004). Chemokine Receptor Expression Identifies Pre–T Helper (Th)1, Pre–Th2,

and Nonpolarized Cells among Human CD4 + Central Memory T Cells. J. Exp. Med. *200*, 725–735.

Rogge, L., Barberis-Maino, L., Biffi, M., Passini, N., Presky, D.H., Gubler, U., and Sinigaglia, F. (1997). Selective expression of an interleukin-12 receptor component by human T helper 1 cells. J. Exp. Med. *185*, 825–831.

Rosati, E., Dowds, C.M., Liaskou, E., Henriksen, E.K.K., Karlsen, T.H., and Franke, A. (2017). Overview of methodologies for T-cell receptor repertoire analysis. BMC Biotechnol. *17*, 1–16.

Rothenberg, E. V. (2014). Transcriptional Control of Early T and B Cell Developmental Choices. Annu. Rev. Immunol. *32*, 283–321.

Rothenberg, E. V, Moore, J.E., and Yui, M. a (2008). Launching the T-Lineage Developmental Programme. Nat. Rev. Immunol. *8*, 9–21.

Rush, J., and Hodgkin, P. (2001). B cells activated via CD40 and IL-4 undergo a division burst but require continued stimulation to maintain division, survival and differentiation. Eur. J. Immunol. *31*, 1150–1159.

Ryg-Cornejo, V., Ioannidis, L.J., Ly, A., Chiu, C.Y., Tellier, J., Hill, D.L., Preston, S.P., Pellegrini, M., Yu, D., Nutt, S.L., et al. (2016). Severe Malaria Infections Impair Germinal Center Responses by Inhibiting T Follicular Helper Cell Differentiation. Cell Rep. *14*, 68–81.

Sada-Ovalle, I., Talayero, a., Chavéz-Galán, L., Barrera, L., Castorena-Maldonado, a., Soda-Merhy, a., and Torre-Bouscoulet, L. (2012). Functionality of CD4 + and CD8 + T cells from tonsillar tissue. Clin. Exp. Immunol. *168*, 200–206.

Sage, P.T., and Sharpe, A.H. (2016). T follicular regulatory cells. Immunol. Rev. *271*, 246–259.

Sakano, H., Maki, R., Kurosawa, Y., Roeder, W., and Tonegawa, S. (1980). Two types of somatic recombination are necessary for the generation of complete immunoglobulin heavy-chain genes. Nature *286*, 676–683.

Sakano, H., Kurosawa, Y., Weigert, M., and Tonegawa, S. (1981). Identification and nucleotide sequence of a diversity DNA segment (D) of immunoglobulin heavy-chain genes. Nature *290*, 562–565.

Sallusto, F. (2016). Heterogeneity of Human CD4 + T Cells Against Microbes. Annu. Rev. Immunol. *34*, 317–334.

Sallusto, F., and Lanzavecchia, A. (2009). Heterogeneity of CD4+ memory T cells: Functional modules for tailored immunity. Eur. J. Immunol. *39*, 2076–2082.

Sallusto, F., Lanzavecchia, A., and MacKay, C.R. (1998). Chemokines and chemokine receptors in T-cell priming and Th1/Th2- mediated responses. Immunol.

Today *19*, 568–574.

Sallusto, F., Lenig, D., Förster, R., Lipp, M., and Lanzavecchia, A. (1999). Two subsets of memory T lymphocytes with distinct homing potential and effector functions. Nature *401*, 708–712.

Sallusto, F., Geginat, J., and Lanzavecchia, A. (2004). Central Memory and Effector Memory T Cell Subsets : Function, Generation, and Maintenance. Annu. Rev. Immunol. *22*, 745–763.

Sallusto, F., Lanzavecchia, A., Araki, K., and Ahmed, R. (2010). From Vaccines to Memory and Back. Immun. Rev. *33*, 451–463.

Sallusto, F., Cassotta, A., Hoces, D., Foglierini, M., and Lanzavecchia, A. (2018). T-Cell Heterogeneity, Plasticity, and Selection in Humans. Cold Spring Harb. Perspect. Biol. 1–10.

Samji, T., and Khanna, K.M. (2017). Understanding memory CD8+T cells. Immunol. Lett. *185*, 32–39.

Sant, A.J., DiPiazza, A.T., Nayak, J.L., Rattan, A., and Richards, K.A. (2018). CD4 T cells in protection from influenza virus: Viral antigen specificity and functional potential. Immunol. Rev. *284*, 91–105.

Schaerli, P., Willimann, K., Lang, A.B., Lipp, M., Loetscher, P., and Moser, B. (2000). CXC chemokine receptor 5 expression defines follicular homing T cells with B cell helper function. J. Exp. Med. *192*, 1553–1562.

Schatz, D., and Spanopoulou, E. (2005). Biochemistry of V(D)J recombination. Curr. Top. Microbiol. Immunol. *290*, 49–85.

Schmitt, N., and Ueno, H. (2013). Blood Tfh cells come with colors. Immunity *39*, 629–630.

Schmitt, N., Liu, Y., Bentebibel, S.-E., Munagala, I., Bourdery, L., Venuprasad, K., Banchereau, J., and Ueno, H. (2014). The cytokine TGF-β co-opts signaling via STAT3-STAT4 to promote the differentiation of human TFH cells. Nat. Immunol.

Schmitt, N., Liu, Y., Bentebibel, S.E., and Ueno, H. (2016). Molecular Mechanisms Regulating T Helper 1 versus T Follicular Helper Cell Differentiation in Humans. Cell Rep. *16*, 1082–1095.

Selin, L.K., Cornberg, M., Brehm, M.A., Kim, S.K., Calcagno, C., Ghersi, D., Puzone, R., Celada, F., and Welsh, R.M. (2004). CD8 memory T cells: Cross-reactivity and heterologous immunity. Semin. Immunol. *16*, 335–347.

Sheppard, K.A., Fitz, L.J., Lee, J.M., Benander, C., George, J.A., Wooters, J., Qiu, Y., Jussif, J.M., Carter, L.L., Wood, C.R., et al. (2004). PD-1 inhibits T-cell receptor induced phosphorylation of the ZAP70/CD3ζ signalosome and downstream

signaling to PKCθ. FEBS Lett. *574*, 37–41.

Shi, J., Hou, S., Fang, Q., Liu, X., Liu, X., and Qi, H. (2018). PD-1 Controls Follicular T Helper Cell Positioning and Function. Immunity 1–11.

Shugay, M., Bolotin, D.A., Putintseva, E. V., Pogorelyy, M. V., Mamedov, I.Z., and Chudakov, D.M. (2013). Huge overlap of individual TCR beta repertoires. Front. Immunol. *4*, 9–11.

Sinigaglia, F., and Hammer, J. (1994). Defining rules for the peptide-MHC class II interaction. Curr. Opin. Immunol. *6*, 52–56.

Six, A., Mariotti-Ferrandiz, M.E., Chaara, W., Magadan, S., Pham, H.P., Lefranc, M.P., Mora, T., Thomas-Vaslin, V., Walczak, A.M., and Boudinot, P. (2013). The past, present, and future of immune repertoire biology - the rise of next-generation repertoire analysis. Front. Immunol. *4*, 1–16.

Snell, L.M., Osokine, I., Yamada, D.H., De la Fuente, J.R., Elsaesser, H.J., and Brooks, D.G. (2016). Overcoming CD4 Th1 Cell Fate Restrictions to Sustain Antiviral CD8 T Cells and Control Persistent Virus Infection. Cell Rep. *16*, 3286–3296.

Soghoian, D.Z., and Streeck, H. (2010). Cytolytic CD4 $^{+}$ T cells in viral immunity. Expert Rev. Vaccines *9*, 1453–1463.

Spillane, K.M., and Tolar, P. (2018). Mechanics of antigen extraction in the B cell synapse. Mol. Immunol. *101*, 319–328.

Stavnezer, J. (1996). Immunoglobulin class switching. Curr. Opin. Immunol. *8*, 199–205.

Su, K., Watanabe, A., Yeh, C., Kelsoe, G., and Masayuki, K. (2016). Efficient Culture of Human Naive and Memory B Cells for Use as APCs. J. Immunol.

Su, L.F., Kidd, B.A., Han, A., Kotzin, J.J., and Davis, M.M. (2013). Virus-specific CD4(+) memory-phenotype T cells are abundant in unexposed adults. Immunity *38*, 373–383.

Suan, D., Kräutler, N.J., Maag, J.L.V., Butt, D., Bourne, K., Hermes, J.R., Avery, D.T., Young, C., Statham, A., Elliott, M., et al. (2017). CCR6 Defines Memory B Cell Precursors in Mouse and Human Germinal Centers, Revealing Light-Zone Location and Predominant Low Antigen Affinity. Immunity *47*, 1142–1153.e4.

Sui, J., Hwang, W.C., Perez, S., Wei, G., Aird, D., Chen, L.M., Santelli, E., Stec, B., Cadwell, G., Ali, M., et al. (2009). Structural and functional bases for broad-spectrum neutralization of avian and human influenza A viruses. Nat. Struct. Mol. Biol. *16*, 265–273.

Summers, K.L., Hock, B.D., McKenzie, J.L., and Hart, D.N. (2001). Phenotypic

characterization of five dendritic cell subsets in human tonsils. Am. J. Pathol. *159*, 285–295.

Sun, J., and Bevan, M. (2003). Defective CD8 T Cell Memory Following Acute Infection Without CD4 T Cell Help. Science (80-.). *300*, 339–342.

Szabo, S.J., Kim, S.T., Costa, G.L., Zhang, X., Fathman, C.G., and Glimcher, L.H. (2000). A novel transcription factor, T-bet, directs Th1 lineage commitment. Cell *100*, 655–669.

Tamura, S., Miyata, K., Matsuo, K., Asanuma, H., Takahashi, H., Nakajima, K., Suzuki, Y., Aizawa, C., and Kurata, T. (1996). Acceleration of influenza virus clearance by Th1 cells in the nasal site of mice immunized intranasally with adjuvant-combined recombinant nucleoprotein. J. Immunol. *156*, 3892–3900.

Tanaka, S., Suto, A., Iwamoto, T., Kashiwakuma, D., Kagami, S., Suzuki, K., Takatori, H., Tamachi, T., Hirose, K., Onodera, A., et al. (2014). Sox5 and c-Maf cooperatively induce Th17 cell differentiation via RORγt induction as downstream targets of Stat3. J. Exp. Med. *211*, 1857–1874.

Tatovic, D., Young, P., Kochba, E., Levin, Y., Wong, F.S., and Dayan, C.M. (2015). Fine-Needle Aspiration Biopsy of the Lymph Node: A Novel Tool for the Monitoring of Immune Responses after Skin Antigen Delivery. J. Immunol. *195*, 386–392.

Topham, D.J., Tripp, R. a, and Doherty, P.C. (1997). CD8+ T cells clear influenza virus by perforin or Fas-dependent processes. J. Immunol. *159*, 5197–5200.

Trifari, S., Kaplan, C.D., Tran, E.H., Crellin, N.K., and Spits, H. (2009). Identification of a human helper T cell population that has abundant production of interleukin 22 and is distinct from TH-17, TH1 and TH2 cells. Nat. Immunol. *10*, 864.

Tripathi, S.K., and Lahesmaa, R. (2014). Transcriptional and epigenetic regulation of T-helper lineage specification. Immunol. Rev. *261*, 62–83.

Tubo, N.J., and Jenkins, M.K. (2016). TCR signal quantity and quality in CD4+ T cell differentiation. Trends Immunol *35*, 591–596.

Tuomela, S., Salo, V., Tripathi, S.K., Chen, Z., Laurila, K., Gupta, B., Äijö, T., Oikari, L., Stockinger, B., Lähdesmäki, H., et al. (2012). Identification of early gene expression changes during human Th17 cell differentiation. Blood *119*.

Valkenburg, S.A., Li, O.T.W., Li, A., Bull, M., Waldmann, T.A., Perera, L.P., Peiris, M., and Poon, L.L.M. (2018). Protection by universal influenza vaccine is mediated by memory CD4 T cells. Vaccine *36*, 4198–4206.

Valmori, D., Scheibenbogen, C., Dutoit, V., Effector, C.C.C.R., Exerting, S., Nagorsen, D., Asemissen, A.M., Rubio-godoy, V., Rimoldi, D., Guillaume, P., et

al. (2002). Circulating Tumor-reactive CD8 + T Cells in Melanoma Patients Contain a CD45RA + CCR7 – Effector Subset Exerting ex Vivo Tumor-specific Cytolytic Activity. Cancer Res. *62*, 1743–1750.

VanDePavert, S.A., and Mebius, R.E. (2010). New insights into the development of lymphoid tissues. Nat. Rev. Immunol. *10*, 664–674.

Vandermerwe, P.A., Bodian, D.L., Daenke, S., Linsley, P., and Davis, S.J. (1997). CD80 (B7-1) binds both CD28 and CTLA-4 with a low affinity and very fast kinetics. J. Exp. Med. *185*, 393–403.

VanKempen M.J.P., G.T., R., and P.B., van C. (2007). The immune response in Adenoids and Tonsils. Int. Arch. Allergy Immunol. 621–636.

VanPanhuys, N., Klauschen, F., and Germain, R. (2014). T-Cell-Receptor-Dependent Signal Intensity Dominantly Controls CD4+T Cell Polarization InVivo. Immunity *41*, 63–74.

Vantourout, P., and Hayday, A. (2013). Six-of-the-best: Unique contributions of γδ T cells to immunology. Nat. Rev. Immunol. *13*, 88–100.

Veldhoen, M., Uyttenhove, C., van Snick, J., Helmby, H., Westendorf, A., Buer, J., Martin, B., Wilhelm, C., and Stockinger, B. (2008). Transforming growth factor-β "reprograms" the differentiation of T helper 2 cells and promotes an interleukin 9-producing subset. Nat. Immunol. *9*, 1341–1346.

Velu, V., Mylvaganam, G.H., Gangadhara, S., Hong, J.J., Iyer, S.S., Gumber, S., Ibegbu, C.C., Villinger, F., and Amara, R.R. (2016). Induction of Th1-Biased T Follicular Helper (Tfh) Cells in Lymphoid Tissues during Chronic Simian Immunodeficiency Virus Infection Defines Functionally Distinct Germinal Center Tfh Cells. J. Immunol. *197*, 1832–1842.

Victora, G.D., and Nussenzweig, M.C. (2012). Germinal Centers. Annu. Rev. Immunol. *30*, 429–457.

Victora, G.D., Schwickert, T.A., Fooksman, D.R., Kamphorst, A.O., Meyer-Hermann, M., Dustin, M.L., and Nussenzweig, M.C. (2010). Germinal center dynamics revealed by multiphoton microscopy with a photoactivatable fluorescent reporter. Cell *143*, 592–605.

Vinuesa, C.G., and Cook, M.C. (2011). Blood Relatives of Follicular Helper T Cells. Immunity *34*, 10–12.

Vinuesa, C.G., Tangye, S.G., Moser, B., and Mackay, C.R. (2005). Follicular B helper T cells in antibody responses and autoimmunity. Nat. Rev. Immunol. *5*, 853–865.

Vogel, T.U., Horton, H., Fuller, D.H., Carter, D.K., Vielhuber, K., O'Connor, D.H., Shipley, T., Fuller, J., Sutter, G., Erfle, V., et al. (2002). Differences between

T cell epitopes recognized after immunization and after infection. J. Immunol. *169*, 4511–4521.

Vogelzang, A., McGuire, H.M., Yu, D., Sprent, J., Mackay, C.R., and King, C. (2008). A Fundamental Role for Interleukin-21 in the Generation of T Follicular Helper Cells. Immunity *29*, 127–137.

Wang, C.J., Heuts, F., Ovcinnikovs, V., Wardzinski, L., Bowers, C., Schmidt, E.M., Kogimtzis, A., Kenefeck, R., Sansom, D.M., and Walker, L.S.K. (2015). CTLA-4 controls follicular helper T-cell differentiation by regulating the strength of CD28 engagement. Proc. Natl. Acad. Sci. *112*, 524–529.

Wang, T.T., Bournazos, S., and Ravetch, J. V. (2018). Immunological responses to influenza vaccination: lessons for improving vaccine efficacy. Curr. Opin. Immunol. *53*, 124–129.

Weber, J.P., Fuhrmann, F., Feist, R.K., Lahmann, A., Al Baz, M.S., Gentz, L.-J., Vu Van, D., Mages, H.W., Haftmann, C., Riedel, R., et al. (2015). ICOS maintains the T follicular helper cell phenotype by down-regulating Krüppel-like factor 2. J. Exp. Med. *212*, 217–233.

Weidmann, E., Logan, T.F., Yasumura, S., Kirkwood, J.M., Trucco, M., and Whiteside, T.L. (1993). Evidence for Oligoclonal T-Cell Response in a Metastasis of Renal Cell Carcinoma Responding to Vaccination with Autologous Tumor Cells and Transfer of in Vitro-sensitized Vaccine-draining Lymph Node Lymphocytes. Cancer Res. *53*, 4745–4749.

Wiede, F., Fromm, P.D., Comerford, I., Kara, E., Bannan, J., Schuh, W., Ranasinghe, C., Tarlinton, D., Winkler, T., McColl, S.R., et al. (2013). CCR6 is transiently upregulated on B cells after activation and modulates the germinal center reaction in the mouse. Immunol. Cell Biol. *91*, 335–339.

Wilkinson, T.M., Li, C.K.F., Chui, C.S.C., Huang, A.K.Y., Perkins, M., Liebner, J.C., Lambkin-Williams, R., Gilbert, A., Oxford, J., Nicholas, B., et al. (2012). Preexisting influenza-specific CD4+T cells correlate with disease protection against influenza challenge in humans. Nat. Med. *18*, 274–280.

Willinger, T., Freeman, T., Hasegawa, H., McMichael, A.J., and Callan, M.F.C. (2005). Molecular Signatures Distinguish Human Central Memory from Effector Memory CD8 T Cell Subsets. J. Immunol. *175*, 5895–5903.

Wilson, N.J., Boniface, K., Chan, J.R., McKenzie, B.S., Blumenschein, W.M., Mattson, J.D., Basham, B., Smith, K., Chen, T., Morel, F., et al. (2007). Development, cytokine profile and function of human interleukin 17-producing helper T cells. Nat. Immunol. *8*, 950–957.

Wolk, K., Witte, E., Wallace, E., Döcke, W.D., Kunz, S., Asadullah, K., Volk, H.D., Sterry, W., and Sabat, R. (2006). IL-22 regulates the expression of genes

responsible for antimicrobial defense, cellular differentiation, and mobility in keratinocytes: A potential role in psoriasis. Eur. J. Immunol. *36*, 1309–1323.

Wollenberg, I., Agua-Doce, A., Hernandez, A., Almeida, C., Oliveira, V.G., Faro, J., and Graca, L. (2011). Regulation of the Germinal Center Reaction by Foxp3+ Follicular Regulatory T Cells. J. Immunol. *187*, 4553–4560.

Wong, M.T., Eng, D., Ong, H., Sheau, F., Lim, H., Ginhoux, F., Alicia, M., Lafaille, C. De, Wong, M.T., Eng, D., et al. (2016). A High-Dimensional Atlas of Human T Cell Diversity Reveals Tissue-Specific Trafficking and Cytokine Signatures. Immunity *45*, 442–456.

World Health Organization (2011). Influenza N°211, Fact sheet.

World Health Organization (2018).
www.who.it/influenza/vaccines/virus/reccomendations.

Wrammert, J., Koutsonanos, D., Li, G.-M., Edupuganti, S., Sui, J., Morrissey, M., McCausland, M., Skountzou, I., Hornig, M., Lipkin, W.I., et al. (2011). Broadly cross-reactive antibodies dominate the human B cell response against 2009 pandemic H1N1 influenza virus infection. J. Exp. Med. *208*, 181–193.

Xiong, N., and Raulet, D.H. (2007). Development and selection of gammadelta T cells. Immunol Rev *215*, 15–31.

Xu, H., Li, X., Liu, D., Li, J., Zhang, X., Chen, X., Hou, S., Peng, L., Xu, C., Liu, W., et al. (2013). Follicular T-helper cell recruitment governed by bystander B cells and ICOS-driven motility. Nature *496*.

Yang, J., James, E., Gates, T.J., DeLong, J.H., LaFond, R.E., Malhotra, U., and Kwok, W.W. (2013). CD4+ T cells recognize unique and conserved 2009 H1N1 influenza hemagglutinin epitopes after natural infection and vaccination. Int. Immunol. *25*, 447–457.

Yang, Y., Zhang, M., Ye, Y., Ma, S., Fan, L., and Li, Z. (2017). High frequencies of circulating Tfh-Th17 cells in myasthenia gravis patients. Neurol. Sci. *38*, 1599–1608.

Yarke, C.A., Dalheimer, S.L., Zhang, N., Catron, D.M., Jenkins, M.K., and Mueller, D.L. (2008). Proliferating CD4+ T Cells Undergo Immediate Growth Arrest upon Cessation of TCR Signaling In Vivo. J. Immunol. *180*, 156–162.

Yoon, S.W., Wong, S.S., Zhu, H., Chen, R., Li, L., Zhang, Y., Guan, Y., and Webby, R.J. (2017). Dysregulated T-Helper Type 1 (Th1):Th2 Cytokine Profile and Poor Immune Response in Pregnant Ferrets Infected with 2009 Pandemic Influenza A(H1N1) Virus. J. Infect. Dis. *217*, 438–442.

Yu, D., Rao, S., Tsai, L.M., Lee, S.K., He, Y., Sutcliffe, E.L., Srivastava, M., Linterman, M., Zheng, L., Simpson, N., et al. (2009). The Transcriptional Repressor

Bcl-6 Directs T Follicular Helper Cell Lineage Commitment. Immunity *31*, 457–468.

Yusuf, I., Kageyama, R., Monticelli, L., Johnston, J., Ditoro, D., Hansen, K., Barnett, B., and Crotty, S. (2010). Germinal Center T Follicular Helper Cell IL-4 Production Is Dependent on Signaling Lymphocytic Activation Molecule Receptor (CD150). J. Immunol. *185*, 190–202.

Zander, R.A., Vijay, R., Pack, A.D., Guthmiller, J.J., Graham, A.C., Lindner, S.E., Vaughan, A.M., Kappe, S.H.I., and Butler, N.S. (2017). Th1-like Plasmodium - Specific Memory CD4 + T Cells Support Humoral Immunity. Cell Rep. *21*, 1839–1852.

Zerrahn, J., Held, W., and Raulet, D.H. (1997). The MHC reactivity of the T cell repertoire prior to positive and negative selection. Cell *88*, 627–636.

Zheng, W., and Flavell, R. (1997). The transcription factor GATA-3 is necessary and sufficient for Th2 cytokine gene expression in CD4 T cells. Cell *16*, 587–596.

Zheng, Y., and Rudensky, A.Y. (2007). Foxp3 in control of the regulatory T cell lineage. Nat. Immunol. *8*, 457–462.

Zielinski, C.E., Corti, D., Mele, F., Pinto, D., Lanzavecchia, A., and Sallusto, F. (2011). Dissecting the human immunologic memory for pathogens. Immunol. Rev. *240*, 40–51.

Zielinski, C.E., Mele, F., Aschenbrenner, D., Jarrossay, D., Ronchi, F., Gattorno, M., Monticelli, S., Lanzavecchia, A., and Sallusto, F. (2012). Pathogen-induced human TH17 cells produce IFN-γ or IL-10 and are regulated by IL-1β. Nature *484*, 514–518.

Zotos, D., Coquet, J.M., Zhang, Y., Light, A., D'Costa, K., Kallies, A., Corcoran, L.M., Godfrey, D.I., Toellner, K.-M., Smyth, M.J., et al. (2010). IL-21 regulates germinal center B cell differentiation and proliferation through a B cell–intrinsic mechanism. J. Exp. Med. *207*, 365–378.

Acknowledgements

This 4 years of DPhil would have never been possible without the constant and precious supports of my three supervisors, each of them contributing in a unique way. I have always felt the privilege to have had Andrew McMichael as my mentor, from whom I have learnt the endless enthusiasm of doing research and the idea that Knowledge is for definition a continuous ongoing process. My co-supervisor Seph Borrow was fundamental to actively sustain and guide together with Andrew all the research projects and to constantly suggest the right thing at the right time. The brilliant mind of Suzanne Campion, who introduced me first to the Oxford's world, was my light throughout these years inside and outside the lab and I have always felt very lucky to have had such a great scientific support.

I would like to acknowledge the NDM, that funded this project.

Many of the lab members contributed to make this work possible: Gerry, Simon, Nicky, Mike, Gemma, Matt and Dimitra. A particular thank goes to Elaine and her positivity that accompanied me in the last two years. I also wanted to acknowledge the fantastic support from the building facility (Omar, Ross, Chris, Tiph, Darren, Andrea and Diana) and the salsa flavour in the air.

The ethics cohort and the sample collections would have not been possible without the collaboration with Professor Sarah Gilbert, Mr James Ramsden, the incredible effort and support of Teresa Lambe and the fantastic team work of the research nurses from the John Radcliffe Hospital in Oxford, especially Dawn and Debbie. I would also like to thank all the patients who consented to participate to this study. I particular thank the FACS facility, especially Jonathan Webber and Drew Worth.

I gratefully acknowledge Professor David Price and his team with Kristin and James in Cardiff, where I learnt the clonotyping technique. I discovered the world of the

TCR with them and I thank them for all their useful scientific discussions. TCR sequencing was performed thank to the special collaboration with Professor Dmitriy Chudakov and Alexey Davydov and their precious help with analyses and discussions. I would also like to thank Professor Michael Dustin to have given me the opportunity to learn the microvesicle technique together with David and Pablo and I wish that this collaboration, together with Professor Garnett Kelsoe, will be even more consolidated in the future.

I am thankful in particular to Isabela for her magic harmony inside and outside the lab and to the "Tfh girls" Isa and Ane and their fruitful late evening discussions. I wanted to thank the exceptional people like Wayne, Tom, Elaine, Suzanne and Kathie and the true friendship that we have built during these years.

Special thanks go to Julia, Rebecca, Cynthia, and Christina, exceptional friends met in Oxford, with whom everything started. Thank to Rosy for her incessant and indispensable presence and for everything we have shared, I hope there will more to come.

I am particularly grateful for the impressive geographically long-distance support, never so close, from my inseparable friends Lazza, Matti, Gio', Lalla, Schatzy and Ste. I wanted to thank my family and in particular my cousin Pilo, never tired to help and sustain me as well as my sister Dani, to be how she is. A special thank goes to my fairies Allice, Giue, Vale and Simo. This work would have never been possible without thinking that they were with me.

I am deeply thankful to the incredible and natural support from my parents: to my dad and for his tremendous helpful scientific discussions and his incessant desire of knowledge; to my wonderful mum because without her sincere and constant encouragements I would had not considered to pursue with a PhD.

Finally, I would like to thank "la mia dolce metá" Dominik for walking next to me.